Investigating mechanisms of odontogenic pain
the role of odontoblasts, trigeminal ganglion neurons, and their interaction

Gaurilcikaite, Egle

Awarding institution:
King's College London

Investigating mechanisms of odontogenic pain: the role of odontoblasts, trigeminal ganglion neurons, and their interaction

Thesis submitted for the degree of

Doctor of Philosophy

Egle Gaurilcikaite

Wolfson Centre for Age-Related Diseases

Institute of Psychiatry, Psychology, and Neuroscience

King's College London

2014-2018

Abstract

Despite the prevalence of pain originating from the teeth (dental, or odontogenic, pain) and its impact on patients' lives, the cellular and molecular mechanisms of odontogenic pain are still not completely understood. The teeth are unique structures, innervated by sensory neurons that originate in the trigeminal ganglia. Factors that increase the sensitivity of these neurons, such as inflammatory cytokines, may contribute to odontogenic pain associated with dental pulp inflammation. To address this, a calcium imaging-based mouse trigeminal ganglion (TG) neuron sensitisation assay was established as part of this project. Short-term exposure to tumour necrosis factor alpha (TNFα), but not to interleukin 1 beta (IL-1β), was found to sensitise the transient receptor potential (TRP) ion channels TRPA1 and TRPV1 on TG neurons. This assay provides the opportunity to test other molecules relevant to odontogenic pain for their ability to sensitise TG neurons.

Previous research suggests that initiation of dentine hypersensitivity, a type of odontogenic pain evoked by thermal, osmotic, chemical, evaporative, or mechanical stimuli to the exposed dentine, might involve both neurons and odontoblasts, the specialised mineralising cells in the teeth. In this project, mouse odontoblast-like (OB) cells were used as a cellular model to study the sensory function of odontoblasts *in vitro*. OB cells were demonstrated to express functional TRPV4 ion channels, known to be involved in thermal, osmotic, and mechanosensation. TRPV4 activation was also found to stimulate ATP release from OB cells, highlighting a potential means for odontoblast communication with dental afferent fibres.

In addition, this study was the first to demonstrate the odontoblast ability to detect biologically relevant acids. Both an acid-induced increase in OB cell intracellular calcium concentrations and subsequent ATP release were detected. These processes were found to be independent of TRPV4 activity.

Finally, to address the ability of odontoblasts to transmit sensory information to adjacent neurons, a co-culture approach was used to directly study intercellular communication between mouse OB cells and TG neurons. Pharmacological activation of TRPV4 was chosen as an odontoblast-selective stimulus, based on the functional expression of TRPV4 ion channels in OB cells, but not in mouse TG neurons. Blocking purinergic signalling disrupted the interaction between stimulated OB cells and TG neurons, demonstrating the importance of ATP as a primary mediator.

Taken together, the findings described in this thesis support the ability of odontoblasts to detect physiologically-relevant stimuli and respond with a release of ATP to modulate the activity of adjacent sensory neurons. Thus, this interaction may play an important role in the initiation of odontogenic pain *in vivo*.

Acknowledgements

First and foremost, I would like to thank my primary supervisor, Dr Andy Grant, for his scientific expertise as well as guidance and support throughout these four years. His willingness to give his time so generously has been very much appreciated. To my second supervisor, Professor Stephen McMahon, for providing both feedback on my PhD work and insight into the wider area of pain research. I would also like to thank the members of his lab who kindly offered their help whenever I needed it.

In addition, I would like to thank Professor Peter McNaughton and his lab members for the friendly research environment and advice. Also, to BSc project students Navneet Dhaliwal and Arauthy Gnanasampanthan (Gina) who have helped out along the way.

A special thanks to my parents and my brother Vaidas for their continued encouragement. Lastly, I would like to thank Audrius, for his patience and all-round support, especially during the final stages of this journey.

Table of contents

Table of figures

Table of tables

Abbreviations

2-APB	2-aminoethoxydiphenyl borate
2-ThioUTP	2-thiouridine-5'-triphosphate
4α-PDD	4α-phorbol 12,13-didecanoate
αMEM	Minimum Essential Medium Eagle - alpha modification
AITC	Allyl isothiocyanate
ALP	Alkaline phosphatase
AMPA	α-amino-3-hydroxy-5-methyl-4-isoxazolepropionic acid
ARS	Alizarin red S
ASIC	Acid-sensing ion channel
ATP	Adenosine-5'-triphosphate
BAPTA-AM	Bis(2-aminophenoxy)ethane-N,N,N',N'-tetraacetic acid tetrakis(acetoxymethyl ester)
BCIP	5-bromo-4-chloro-3-indolyl phosphate
BDNF	Brain-derived neurotrophic factor
BGP	Bone gamma-carboxyglutamic acid-containing protein
BSA	Bovine serum albumin
BSP2	Bone sialoprotein 2
CALHM1	Calcium homeostasis modulator 1
cAMP	3',5'-cyclic adenosine monophosphate
CAPS	Capsaicin
CaSR	Calcium-sensing receptor
CGRP	Calcitonin gene-related peptide
COL1α1	Collagen type I, alpha 1
Ct	Cycle threshold
DAG	Diacylglycerol
DLX3	Distal-less homeobox 3
DMEM	Dulbecco's Modified Eagle Medium
DMP1	Dentine matrix protein 1
DMSO	Dimethyl sulfoxide
DPBS	Dulbecco's phosphate-buffered saline
DPP	Dentine phosphoprotein
DSP	Dentine sialoprotein
DSPP	Dentine sialophosphoprotein

DTT	1,4-dithiothreitol
E1A	Early transcription unit 1A
ECS	Extracellular solution
ED	Embryonic day
EDTA	Ethylenediaminetetraacetic acid
EGTA	Ethylene glycol-bis(β-aminoethyl ether)-N,N,N′,N′-tetraacetic acid
ENaC	Epithelial sodium channel
ERK	Extracellular signal-regulated kinase
F12	Ham's F12 nutrient mixture
Fura-2AM	Fura-2-acetoxymethyl ester
GABA	γ-aminobutyric acid
GDNF	Glial cell line-derived neurotrophic factor
GFP	Green fluorescent protein
GFRα-1	GDNF receptor alpha-1
GSK101	GSK1016790A
HBSS	Hank's balanced salt solution
HCl	Hydrochloric acid
HEPES	4-(2-Hydroxyethyl)piperazine-1-ethanesulfonic acid
IB4	Isolectin B4
IL-1R	Interleukin 1 receptor
IL-1β	Interleukin 1 beta
IP_3	Inositol 1,4,5-trisphosphate
IP_3R	Inositol 1,4,5-trisphosphate receptor
JNK	cJun NH_2-terminal kinases
K_{2P}	Two-pore domain potassium channels
K_a	Acid dissociation constant
K_{Ca}	Calcium-activated potassium channels
KCl	Potassium chloride
K_v	Voltage-gated potassium channels
LHX	LIM homeobox protein
LPS	Lipopolysaccharide
LTA	Lipoteichoic acid
LTM	Low-threshold mechanoreceptive
MAPK	Mitogen-activated protein kinases
MES	2-(*N*-morpholino)ethanesulfonic acid
mGluR	Metabotropic glutamate receptor
MrgprD	Mas-related G protein-coupled receptor member D
MRS2365	(N)-methanocarba-2-MeSADP
Na_v	Voltage-gated sodium channel
NBT	Nitro blue tetrazolium
NF-κB	Nuclear factor kappa-light-chain-enhancer of activated B cells
NF200	Neurofilament 200
NGF	Nerve growth factor
NK_1	Neurokinin 1 receptor
NMDA	N-methyl-D-aspartic acid
NSAIDs	Nonsteroidal anti-inflammatory drugs

NTPDase2	Nucleoside triphosphate diphosphohydrolase 2
OB	Odontoblast-like
OPN	Osteopontin
OSX	Osterix
P2X	Purinergic ionotropic P2X receptor
P2Y	Purinergic metabotropic P2Y receptor
p38 MAPK	p38 mitogen-activated protein kinases
PAMP	Pathogen-associated molecular pattern
PBS	Phosphate-buffered saline
PGE_2	Prostaglandin E_2
PIP_2	Phospholipid phosphatidylinositol-4,5-bisphosphate
PKA	Protein kinase A
PKC	Protein kinase C
PKD2L1	Polycystic kidney disease 2-like 1
PLC	Phospholipase C
PLG	Phase lock gel
PPADS	Pyridoxalphosphate-6-azophenyl-2′,4′-disulfonic acid
PRR	Pattern recognition receptor
qPCR	Quantitative PCR
RFU	Relative fluorescence units
RLU	Relative luminescence units
RNA-seq	RNA sequencing
rRNA	Ribosomal RNA
RT-PCR	Reverse transcription polymerase chain reaction
RUNX2	Runt-related transcription factor 2
S1P	Sphingosine 1-phosphate
SEM	Standard error of the mean
SIBLING	Small integrin-binding ligand *N*-linked glycoproteins
SV40	Simian virus 40
Ta	Annealing temperature
TBE	Tris/borate/EDTA
TG	Trigeminal ganglion
TLR	Toll-like receptor
TMC	Transmembrane channel-like
TNFR	Tumour necrosis factor receptor
TNFα	Tumour necrosis factor alpha
TRAAK	Potassium two pore domain channel subfamily K member 4
TREK-1/2	Potassium two pore domain channel subfamily K member 2/10
TrkA	Tropomyosin receptor kinase A
TRP	Transient receptor potential
V-ATPase	Vacuolar-type H^+ -ATPase
VEGF	Vascular endothelial growth factor
VNUT	Vesicular nucleotide transporter
VSOR	Volume-sensitive outwardly rectifying
WDR	Wide dynamic range

Chapter 1

General introduction

1.1 Orofacial pain

Pain localised to the face and oral cavity (orofacial pain) represents a major problem at an individual and public health level. Cross-sectional population-based studies in the United Kingdom estimated the prevalence of orofacial pain to be 26-30% over a one-month period, with a significant associated negative impact on daily life (Macfarlane *et al.*, 2002; Joury *et al.*, 2018).

Orofacial pain is caused by a broad range of acute and chronic conditions, such as temporomandibular disorders, burning mouth syndrome, dental pain, and trigeminal neuralgia. The overlap in the clinical presentation of many conditions with such different origins (Shephard *et al.*, 2014) arises from a shared sensory system, where the trigeminal (5th cranial) nerve acts as the principal sensory nerve (Huff & Daly, 2018). The trigeminal system is separate from the spinal nociceptive system and has some unique characteristics, including distinct responses to injury (Hargreaves, 2011). Most importantly, from the patient's perspective, pain from the head is generally perceived to be worse than from other regions in the body and is associated with more intense negative emotions, such as fear (Meier *et al.*, 2014; Schmidt *et al.*, 2015; Schmidt *et al.*, 2016; Rodriguez *et al.*, 2017).

The high prevalence and impact on the quality of patients' lives, combined with a comparatively limited mechanistic knowledge, encouraged us to investigate the mechanisms underlying the most common type of orofacial pain – dental, or odontogenic, pain. Before focusing on research efforts to identify the mechanisms of odontogenic pain, the trigeminal sensory system and the structure and innervation of the teeth will be briefly discussed.

1.2 Trigeminal sensory system

A wide variety of tissues and structures in the orofacial region (e.g. facial skin, cornea, oral mucosa, tongue, dental pulp, temporomandibular joint, masticatory muscles) are innervated by the three major branches of the trigeminal nerve (ophthalmic, maxillary, and mandibular), illustrated in Figure 1.1 (Huff & Daly, 2018). Sensory information from these tissues is primarily carried by afferent fibres with cell bodies located in two trigeminal ganglia (TG), except for proprioceptive fibres, which have their cell bodies in the mesencephalic trigeminal nucleus within the brainstem (Lazarov, 2007).

Primary TG neurons synapse with second-order (projection) neurons in the spinal trigeminal nucleus and adjacent spinal dorsal horns (C1-C2) or, in the case of non-nociceptive mechanosensory information, mainly in the principal sensory nucleus of the trigeminal brainstem nuclear complex (Iwata *et al.*, 2017). Based on the observations of distinct anatomical structures by Olszewski (1950), the spinal trigeminal nucleus is further subdivided into the subnuclei oralis, interporalis, and caudalis (see Figure 1.2). Most nociceptive orofacial inputs travel through the subnucleus caudalis, also called the medullary dorsal horn due to its structural and functional similarities with the spinal dorsal horn (Sessle, 2000). However, as argued by Bereiter and colleagues (2000), the distinct properties of the subnucleus caudalis, such as substantial interconnection with other areas within the trigeminal brainstem complex, means it should not be viewed simply as an extension of the spinal dorsal horn. Moreover, convergence of sensory inputs from different target areas onto the same projection neurons in the subnucleus caudalis is thought to underlie the pain referral and poor localisation often observed with orofacial pain conditions (Sessle *et al.*, 1986; Sessle, 2000).

The axons of the trigeminal second-order neurons ascend via the trigeminothalamic tract to the thalamus and synapse with third-order neurons that relay the signal to the cerebral cortex. For pain perception to occur, sensory-discriminative information is integrated with affective-motivational and cognitive-evaluative elements in a process involving not just the somatosensory cortex but also other cortical and limbic systems (Melzack, 2001; Chichorro *et al.*, 2017).

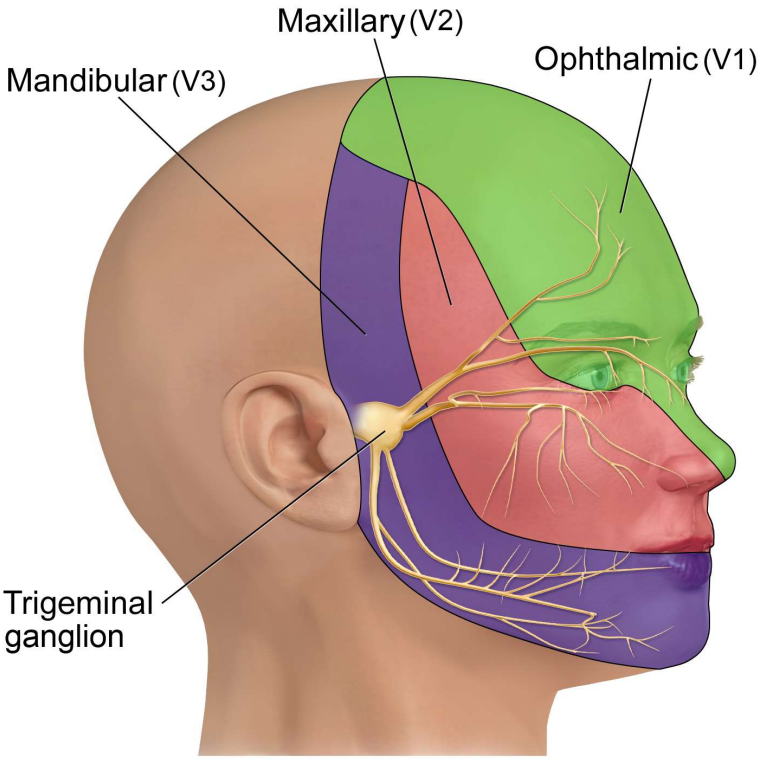

Figure 1.1 Schematic representation of the trigeminal nerve and its dermatome distribution

At trigeminal ganglia, the trigeminal nerve divides into three main peripheral branches: ophthalmic (V1), maxillary (V2), and mandibular (V3). Each branch innervates a non-overlapping area of the head and face. Illustration adapted from Blausen Medical Gallery, CC BY-SA 4.0 (Blausen, 2014).

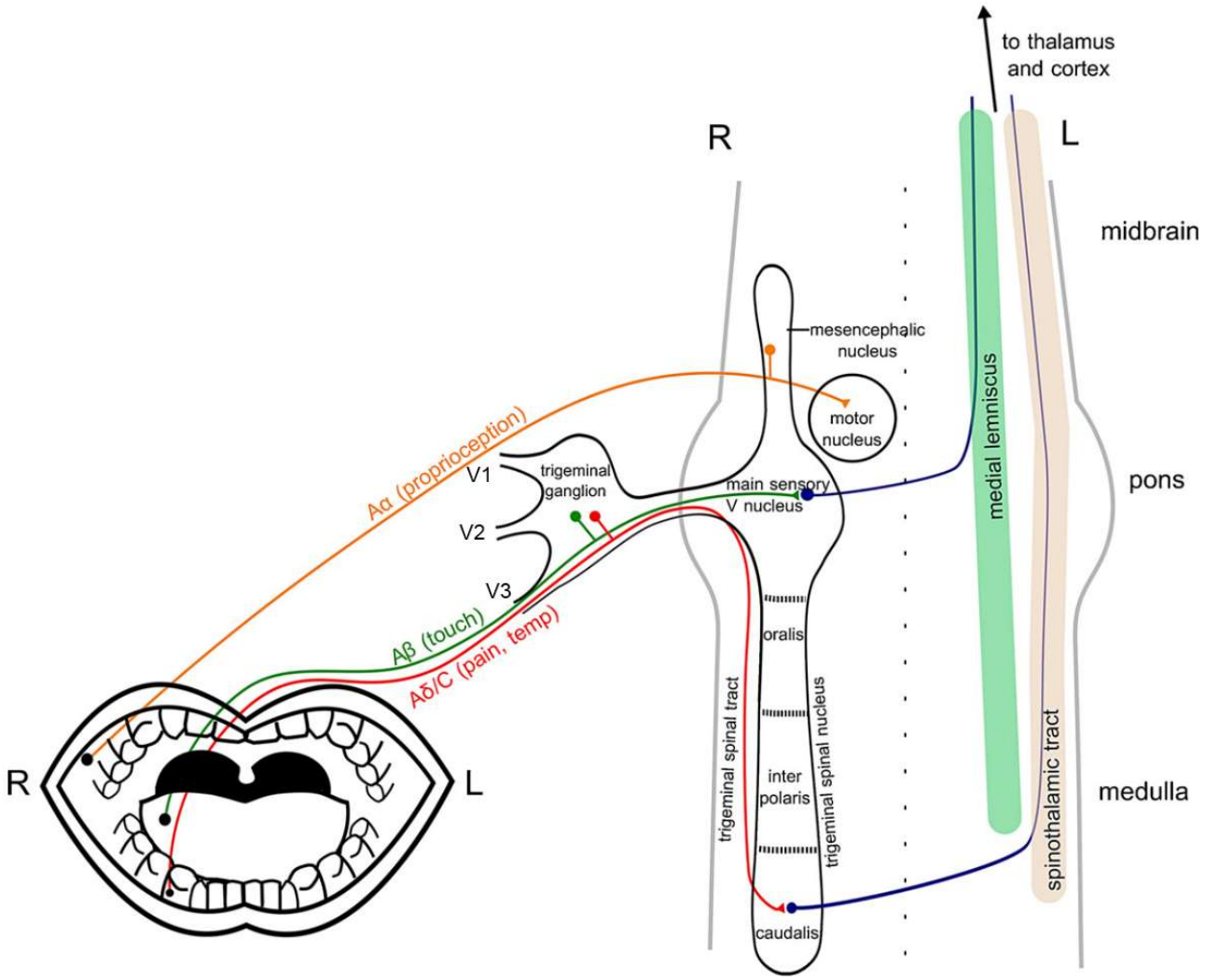

Figure 1.2 Illustration of the trigeminal sensory pathways from the oral cavity

Examples of three different sensory nerve fibre types are shown. Proprioceptive signals from the masticatory muscle spindles are carried by Aα-type afferent fibres to the brainstem via a minor peripheral branch of the trigeminal nerve. These fibres have their cell bodies in the mesencephalic nucleus and send projections to the trigeminal motor nucleus. In addition, some mesencephalic nucleus neurons innervate periodontal mechanoreceptors. Mechanoreceptive Aβ fibres and thermoreceptive and nociceptive Aδ/C-fibres that innervate the tongue and the lower teeth belong to the mandibular branch of the trigeminal nerve and have their cell bodies in the trigeminal ganglion. While mechanoreceptive fibres provide input to the second-order neurons in the main (principal) sensory nucleus, thermal/nociceptive fibres descend along the spinal trigeminal tract and synapse with secondary neurons primarily in the spinal trigeminal nucleus, especially subnucleus caudalis, of the trigeminal brainstem nuclear complex. The second-order neuronal axons cross to the opposite side and ascend to the thalamus either via the medial lemniscus or via the trigeminothalamic or spinothalamic tracts, as indicated. Third-order neurons from the thalamus relay the signal to the cortical structures. The diagram was adapted from (Haggard & de Boer, 2014), CC BY 3.0.

1.2.1 PRIMARY SENSORY TRIGEMINAL NEURONS AND PERIPHERAL SENSITISATION

Trigeminal primary afferents terminate in orofacial tissues either as free nerve endings, detecting thermal and noxious stimuli, or as specialised mechanoreceptors. Moreover, peripheral nerve fibres have been historically classified based on their diameter, myelination, as well as conduction velocities, as summarised in Table 1.1.

Table 1.1 Classification of sensory nerve fibres

Morphological and functional characteristics of different classes of primary afferents. Adapted from (Nair, 1995; Julius & Basbaum, 2001; Haggard & de Boer, 2014).

Fibre type	Receptor morphology	Function/sensory modality	Axon diameter (μm)	Myelin	Conduction velocity (m/s)	Threshold of activation
Aα	Muscle spindles, Golgi tendon organs, Palisade endings	Proprioception	12–22	Yes (thick)	70–120	Low
Aβ	Meissner's, Pacinian corpuscles Ruffini endings, Merkel's disks	Light touch, pressure, vibration	5–12	Yes	30–70	Low
Aδ	Free nerve endings	Nociception (sharp pain), heat, crude touch	2–5	Yes (thin)	3–30	High
C	Free nerve endings	Nociception (dull pain), heat, cold, itch	0.2–1.5	No	0.5–2	High

Table 1.1 represents the dogma that large, myelinated, and fast-conducting Aα and Aβ axons carry non-nociceptive information, whereas medium-diameter, thinly-myelinated Aδ and small-diameter, unmyelinated C-fibres carry signals about thermal and noxious stimuli. In the case of nociceptors, Aδ and C fibres are known to convey acute and well-localised "first" pain, and slow and poorly localised "second" pain, respectively (Basbaum et al., 2009). However, it should be noted that sensory modality

is not consistently related to the nerve fibre type, as there is evidence for the existence of Aα/β-fibre nociceptive neurons, as well as Aδ and C-fibre low-threshold mechanoreceptors (Lawson, 2002; Djouhri & Lawson, 2004). In addition to classification based on histological and electrophysiological properties, further heterogeneity of sensory nerve fibres arises from their cytochemical profile. For example, C-type nociceptors are often subdivided into peptidergic and non-peptidergic fibres. Peptidergic fibres produce neuropeptides calcitonin gene-related peptide (CGRP) and substance P and express TrkA neurotrophin receptor, rendering them responsive to nerve growth factor (NGF). On the other hand, non-peptidergic C-fibres tend to bind isolectin B4 (IB4), express purinergic ligand-gated $P2X_3$ and G protein-coupled MrgprD receptors, and respond to GDNF due to the expression of GDNF receptor alpha-1 (GFRα-1) and c-Ret (Basbaum et al., 2009). However, as with the attempts to link nerve fibre histology to a particular function, cytochemical properties also do not clearly define functional nerve subsets. Technical advancement enabled recent efforts to classify sensory neurons in an unbiased way, based on their transcriptome (Usoskin et al., 2014; Nguyen et al., 2017). Nonetheless, these classifications have not been widely adopted by the time of writing this thesis. Therefore, references will be made to the classical A and C types of sensory nerve fibres in subsequent sections, as the vast majority of relevant literature uses this terminology.

Conversion of thermal, mechanical, and chemical stimuli into electrical signals in sensory neurons depends on the specialised membrane proteins present on the peripheral terminals of primary afferents. The transient receptor potential (TRP) family represents a major group of such sensory transducers. The first to be identified and the most extensively studied so far is TRPV1 – a polymodal receptor activated by noxious temperatures above 43°C, low pH, and capsaicin, the pungent compound in chilli peppers (Caterina *et al.*, 1997). While initially described as another heat-sensitive (>52°C) ion channel, TRPV2 is unlikely to play a role in thermodetection, based on the normal thermosensory phenotype of TRPV2 knock-out mice (Park *et al.*, 2011). Instead, TRPV2 might be involved in sensing osmotic stimuli (Muraki et al., 2003). Another example is TRPV4, which displays sensitivity to innocuous warmth as well as playing a role in osmotic/mechanotransduction (Strotmann et al., 2000; Guler et al., 2002; Mochizuki et al., 2009). TRPA1 has been proposed to be involved in sensing cold and

mechanical stimuli and is activated by a range of natural compounds, such as allyl isothiocyanate in mustard, allicin in garlic, and cinnamaldehyde in cinnamon oil (Bandell et al., 2004; Macpherson et al., 2005; Vilceanu & Stucky, 2010). However, TRPM8 was identified as the main detector of low (<25°C) temperatures and is also activated by menthol (Bautista et al., 2007).

In addition to some of the TRPs, other channels have been proposed as potential mechanotransducers, including acid-sensing ion channels (ASICs), primarily known for their ability to detect extracellular acidification, two-pore domain potassium channels (K_{2P}), such as TREK-1, TREK-2 and TRAAK, and Piezo channels (Ranade *et al.*, 2015). In fact, Piezo2 was recently identified as the principal mechanotransducer protein in mammalian proprioceptors and low-threshold mechanoreceptors (Ranade *et al.*, 2014; Woo *et al.*, 2015). However, the receptor(s) involved in the transduction of noxious mechanical stimuli have not been conclusively identified.

Activation of sensory transducers, such as TRPs and ASICs, leads to cation (Na^+, Ca^{2+}, and/or Mg^{2+}, depending on the channel type) influx, depolarisation of sensory peripheral terminals, and generation of action potentials, which then propagate along the axons. Critical for the initiation and propagation of action potentials are voltage-gated sodium (Na_v) and potassium channels. Sensory information encoded as an action potential discharge pattern (e.g. frequency, duration) is then sent for central processing via the release of neurotransmitters, such as the excitatory amino acid glutamate, and the neuropeptides CGRP and substance P, from the central terminals of primary afferents (Basbaum *et al.*, 2009).

Tissue injury and inflammation can lead to peripheral sensitisation, i.e. enhanced excitability of primary sensory neurons, by affecting the local microenvironment of their peripheral endings. The mediators of this process are produced by local non-neuronal cells, infiltrating immune cells, or neurons, and include a broad range of molecules, such as bradykinin, histamine, various pro-inflammatory cytokines and chemokines, prostaglandins, neurotrophins, neuropeptides, lipids, proteases, ATP, and extracellular protons (Hucho & Levine, 2007). By acting on their respective receptors on the peripheral terminals of primary sensory neurons, these mediators can activate a multitude of signalling cascades. Subsequent changes to gene transcription, translation,

post-translational modifications, stability, and surface presentation affect the number of available ion channels or their activity (Bhave & Gereau, 2004). Sensitisation of nociceptors can ultimately lead to 1) action potential discharge in response to a normally innocuous stimulus to their receptive field, which can manifest as lowered pain threshold (allodynia), 2) hyperresponsiveness, e.g. increased rate of action potential firing to a suprathreshold stimulus, manifesting as hyperalgesia, or 3) spontaneous action potential discharge leading to spontaneous pain, although central mechanisms have also been implicated in these pain states (Schaible et al., 2011).

1.2.2 Second-order sensory neurons and central modulation of pain

Based on their response properties, second-order neurons in both trigeminal and spinal sensory systems are classified into three main types: low-threshold mechanoreceptive (LTM), nociceptive-specific (NS), and wide dynamic range (WDR) neurons. The LTM projection neurons receive tactile and proprioceptive information from non-nociceptive (mainly Aα and Aβ) primary afferents. On the other hand, both NS and WDR second-order neurons are activated by nociceptive inputs, mostly from Aδ and C-fibre primary afferents. However, unlike NS, WDR second-order neurons can also receive synaptic inputs from Aβ and Aδ fibres activated by non-noxious stimulation in their receptive fields (Chichorro *et al.*, 2017).

The activity of NS and WDR projection neurons is key in the processing of peripheral nociceptive signals and is subject to complex excitatory and inhibitory modulation by primary afferent neurons, local interneurons, glia, and descending neurons. Enhanced responsiveness of nociceptive second-order trigeminal neurons (and other nociceptive neurons in the central nervous system) to their normal or subthreshold afferent input is known as central sensitisation, as defined by the International Association for the Study of Pain (Loeser & Treede, 2008). Some of the main mechanisms of central sensitisation include an increase in excitatory inputs, loss of inhibitory connections (disinhibition), or interaction between neuronal and glial cells (Iwata *et al.*, 2017). Second-order neurons express receptors, such as AMPA and NMDA, that enable the detection of neurotransmitters (in this case, glutamate), released from the central terminals of primary sensory neurons. Only AMPA glutamate receptors can be activated under normal conditions. However, persistent injury and inflammation leads to

enhanced nociceptor activity and, consequently, depolarisation of post-synaptic neurons (Basbaum *et al.*, 2009). Sufficient depolarisation dislodges magnesium ions that block NMDA channels at resting membrane potentials, enabling ion, including Ca^{2+}, flow into the post-synaptic neurons, which can ultimately lead to central sensitisation (Vanegas & Schaible, 2007). The second mechanism, disinhibition, can arise from the loss of inhibitory (GABAergic or glycinergic) interneurons. Finally, glial cells contribute to central sensitisation by switching to an "activated" state in response to peripheral or central injury or inflammation, resulting in the release of various mediators, capable of modulating the activity of second-order neurons (Chiang *et al.*, 2011).

Although central processing is crucial for the perception of pain, this thesis will focus on the peripheral mechanisms that underlie the development of odontogenic pain.

1.3 Structure and innervation of the teeth

The main anatomic parts of the tooth are a crown (visible portion that projects into the mouth) and a root (the part of the tooth that is embedded in the jaw bone; Figure 1.3). Enamel is a highly mineralised substance forming the outermost layer of the crown, whereas cementum is an analogous but less calcified layer covering the root (Zhang *et al.*, 2014). Underlying these structures is a layer of dentine, which encapsulates the soft dental pulp tissue and forms the bulk of the tooth.

Dentine is a mineralised connective tissue with approximately 70% inorganic, 20% organic, and 10% water content by weight (Goldberg *et al.*, 2011). The inorganic phase of dentine consists of calcium phosphate biomineral hydroxyapatite [$Ca_{10}(PO_4)_6(OH)_2$] with multiple substitutions (e.g. carbonate or fluoride) in its crystalline structure (Featherstone & Lussi, 2006). The organic matrix of dentine primarily contains collagen (90%), particularly type I, and a range of non-collagenous proteins (10%). These include typical bone matrix proteins (e.g. osteocalcin) as well as members of a small integrin-binding ligand, N-linked glycoprotein (SIBLING) family, such as bone sialoprotein 2 (BSP2), dentine matrix protein 1 (DMP1), osteopontin (OPN), and dentine sialophosphoprotein (DSPP) (Goldberg *et al.*, 2011). The latter gets cleaved post-translationally into dentine sialoprotein (DSP) and dentine phosphoprotein (DPP) (MacDougall *et al.*, 1997). While initially thought to be specific to dentine, DMP1 and

DSPP were also later detected in other tissues like bone (D'Souza *et al.*, 1997; Fen *et al.*, 2002; Qin *et al.*, 2002; Feng *et al.*, 2003).

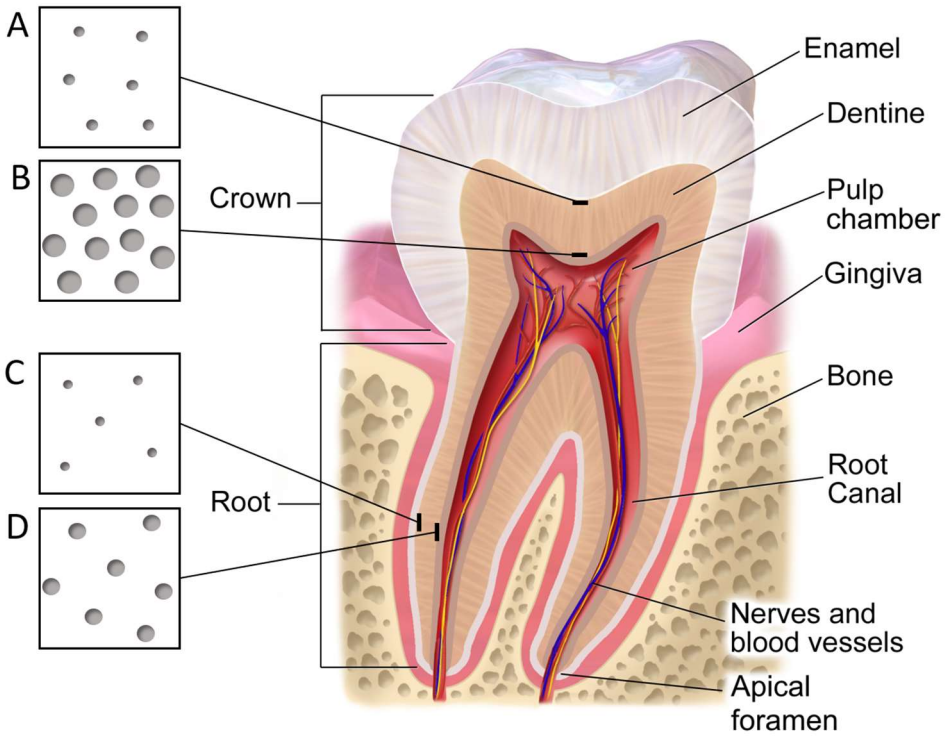

Figure 1.3 Tooth anatomy

Schematic diagram of a tooth cross-section, illustrating the major anatomic parts and layers of the tooth and the variation in dentinal tubule morphology. Dentinal tubule density and diameter increase from the dentine-enamel junction (A) to the dentine-pulp border (B) and from the dentine-cementum junction (C) to the root canal wall (D), with higher density and diameter in the crown, compared with the root. Adapted from Blausen Medical Gallery, CC BY 3.0 (Blausen, 2014) and (Marshall *et al.*, 1998).

An important structural feature of dentine is the presence of millions of microscopic channels, known as dentinal tubules, that connect the pulp with the outer enamel and cementum layers. Multiple studies have demonstrated the variability in tubule density and diameter throughout the tooth. As illustrated in Figure 1.3, the highest density and diameter of dentinal tubules is in deep dentine (closest to the pulp chamber) in the crown of the tooth (Forssell-Ahlberg *et al.*, 1975; Schilke *et al.*, 2000). The number and diameter of open dentinal tubules in human teeth tends to decrease with age (Kontakiotis *et al.*, 2015).

In a healthy tooth, dentinal tubules are filled with dentinal fluid that is similar in ionic composition to interstitial fluid (Coffey *et al.*, 1970), although others reported higher potassium and lower sodium and calcium ion concentrations compared with serum (Larsson *et al.* (1988), as cited by Magloire *et al.* (2010)). Moreover, each dentinal tubule contains an extension of an odontoblast cell (odontoblast process). Odontoblasts are the cells that secrete the unmineralised organic matrix, known as pre-dentine, as well as producing the mineralised dentine throughout the life of the tooth (Goldberg *et al.*, 2011). While some research groups found that odontoblast processes do not extend beyond the inner dentine (Tsuchiya *et al.*, 2002), recently Li and colleagues (2018) clearly visualised odontoblast processes spanning the whole length of dentinal tubules, containing multiple small branches, and depositing minerals along the entire process. Odontoblast morphology and function will be discussed in more detail in section 1.3.1.

The cell bodies of odontoblasts are located at the junction between the dentine and the dental pulp, which due to developmental and functional links are sometimes referred to as the dentine-pulp complex (Pashley, 1996). The pulp itself is a soft connective tissue, containing a heterogeneous population of cells, with fibroblasts being the most abundant cell type (Goldberg & Smith, 2004). The pulp provides nutrition and immune defence to the tooth (About, 2014; Goldberg, 2014). Moreover, the low-compliance environment combined with an extensive vasculature and dense sensory innervation (discussed in section 1.3.2), led to the status of dental pulp as a unique sensory organ (Yu & Abbott, 2007).

1.3.1 ODONTOBLASTS

Odontoblasts located at the dentine-pulp junction are mature cells, differentiated from cranial neural crest-derived mesenchymal cells (Chai *et al.*, 2000). Terminal differentiation of odontoblasts involves the cessation of mitosis, cellular elongation, and cytological polarisation, with the nucleus located in the proximal part of the cell body, away from the odontoblast process (see Figure 1.4) (Ruch *et al.*, 1995). The appearance of the mature odontoblast layer differs between the tooth crown, where the cell bodies are tall, columnar, and tightly packed, and the root, where they appear cuboidal or globular and more disjoined (Marion *et al.*, 1991). In addition, the cell bodies of differentiated odontoblasts become interconnected via gap junctions, formed by

connexin 43 channels, as well as tight and desmosome-like junctions, with proposed roles in intercellular communication, regulation of molecule and ion transport, and cellular adhesion (Turner *et al.*, 1989; Ushiyama, 1989; Arana-Chavez & Katchburian, 1997; Murakami *et al.*, 2001; About *et al.*, 2002; Ikeda & Suda, 2013).

Upon differentiation, odontoblasts become functional, i.e. able to synthesise and secrete collagen and various non-collagenous extracellular matrix components found in pre-dentine and dentine, as mentioned earlier (Goldberg *et al.*, 2011; Kawashima & Okiji, 2016). In line with their mineralising function, they also exhibit high activity of enzymes, such as tissue non-specific alkaline phosphatase (ALP), required for the deposition of hydroxyapatite in dentine matrix (Larmas & Thesleff, 1980; Hotton *et al.*, 1999; Orimo, 2010). In addition to the formation of primary dentine during tooth development and secretion of secondary dentine throughout the life of the tooth, under pathological conditions odontoblasts also produce tertiary dentine, which can be either reactionary or reparative (Smith *et al.*, 1995). Reactionary dentine is secreted by the same pre-existing odontoblasts in response to mild noxious stimuli. On the other hand, reparative dentine production is initiated when the damage is severe enough to compromise the viability of mature odontoblasts. In that case, reparative dentine is secreted by new odontoblast-like cells, potentially differentiated from progenitors, dental pulp stem cells, or sub-odontoblastic Höhl cells (Ricucci *et al.*, 2014).

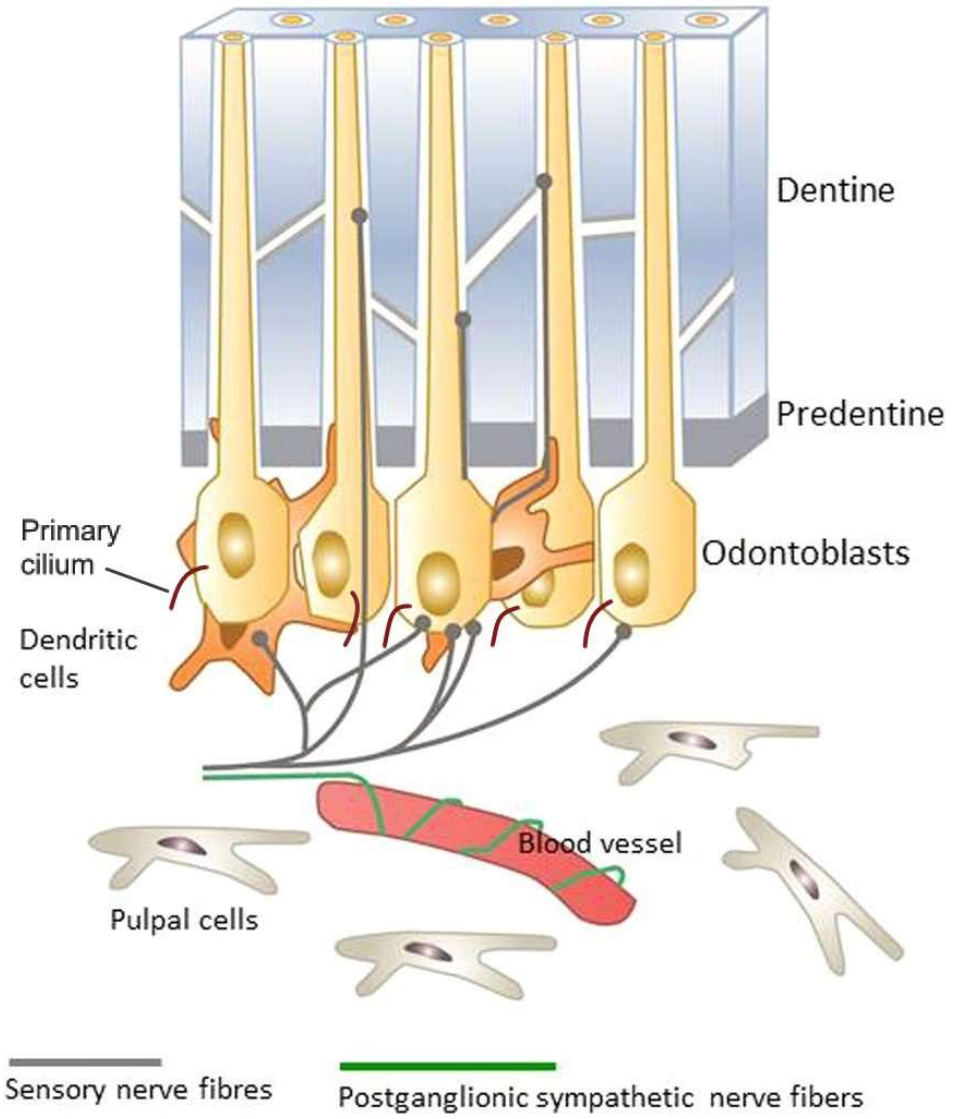

Figure 1.4 Schematic representation of the odontoblast cell layer

Odontoblasts form a continuous layer at the junction between the dentine and the pulp, with their processes extending throughout the diameter of pre-dentine and dentine. Odontoblast primary cilia tend to point towards the pulp. A dense network of sensory nerve fibres is located subjacent to the odontoblast cell layer, with free nerve endings extending into pre-dentine and the inner part of dentine in some dentinal tubules. Intradental postganglionic sympathetic nerve fibres primarily innervate the blood vessels. Dendritic cells are present near or within the odontoblast layer and redistribute in response to injury/inflammation. The diagram is adapted from (Solé-Magdalena et al., 2018) with permission from Elsevier.

While the apical odontoblast process is an important membrane structure for both dentinogenesis and detection of pathogens, an antenna-like primary cilium (see Figure 1.4) is also present near the odontoblast cell nucleus, mainly oriented towards the tooth pulp (Thivichon-Prince *et al.*, 2009; Hisamoto *et al.*, 2016). The primary cilium is an organelle ubiquitously present in mammalian cells (Wheatley *et al.*, 1996).

In the case of a carious lesion, odontoblasts are positioned as the first cells to encounter invading oral bacteria and their products. In fact, odontoblasts have been proposed to play a role in innate immunity, as they express multiple pattern recognition receptors (PRRs), such as Toll-like receptors 2 and 4 (TLR2 and TLR4), enabling the detection of pathogen-associated molecular patterns (PAMPs) (Durand *et al.*, 2006; Veerayutthwilai *et al.*, 2007). Activators of these receptors were demonstrated to modulate the gene expression and/or production of pro-inflammatory mediators and antimicrobial molecules by odontoblasts (Durand *et al.*, 2006; Jiang *et al.*, 2006; Veerayutthwilai *et al.*, 2007; Staquet *et al.*, 2008; Horst *et al.*, 2011; Farges *et al.*, 2015).

Furthermore, mediators released in response to odontoblast stimulation with lipoteichoic acid (LTA), a cell wall component of Gram-positive bacteria and known TLR2 activator, induced the recruitment of immature dendritic cells (Durand *et al.*, 2006). This is relevant, as dendritic cells were detected in the sub-odontoblastic layer or dispersed among the odontoblasts in intact human teeth. They also congregate in areas of inflammation or underneath new deep cavities, with some dendritic processes observed in the dentinal tubules (Yoshiba *et al.*, 2003). Enhanced pro-inflammatory cytokine, chemokine, and growth factor expression in the odontoblast layer was also observed in decayed teeth, when compared with healthy teeth (Veerayutthwilai *et al.*, 2007; Horst *et al.*, 2011). Moreover, pro-inflammatory cytokines, such as tumour necrosis factor alpha (TNFα) and interleukin 1 beta (IL-1β), were also detected in the dentinal fluid, although no significant difference was observed between sound and carious teeth (Geraldeli *et al.*, 2012).

The fact that multiple genetic ciliopathies, such as oral-facial-digital syndrome and cranioectodermal dysplasia, have a dental phenotype recently brought attention to the role of cilia in tooth development (Hampl *et al.*, 2017). Moreover, the primary cilium acts as a fluid shear-stress mechanosensor in various organs in the body (Nauli *et al.*,

2013), which led to suggestions that it might be involved in sensing changes in the tooth microenvironment by odontoblasts (Magloire *et al.*, 2004; Magloire *et al.*, 2010). The molecular basis of odontoblast sensory function will be explored in Chapter 3.

1.3.2 Dental primary afferents

The teeth are densely innervated, with average reported values of 2300 axons at the apex of human pre-molars (Nair, 1995). However, the density of nerve fibres seems to vary depending on the tooth type, its health status and the location of measurement within the tooth (Johnsen & Johns, 1978; Rodd & Boissonade, 2001).

Primary afferents generally enter the teeth via the apical foramina and display extensive branching in the sub-odontoblastic region, forming a network called the plexus of Raschkow. Some nerve endings originating from the plexus also extend into dentinal tubules, reaching pre-dentine or the inner part of dentine (Byers *et al.*, 1982; Byers, 1985). The highest density of intradentinal fibres, in up to a half of all tubules, was detected near the roof of the pulp chamber, whereas less than 1% of tubules contained nerve fibres in the root (Fearnhead, 1957; Gunji, 1982; Byers & Dong, 1983).

Overall, the axons in human dental pulps were found to be primarily unmyelinated C-fibres (70-90%) as well as myelinated Aβ and Aδ fibres, with the majority (>90%) of myelinated axons being Aδ (Johnsen & Johns, 1978; Nair *et al.*, 1992; Nair & Schroeder, 1995). The receptive fields for myelinated A-fibres were also demonstrated to be near the pulp-dentine junction, whereas those for C-fibres are located deeper within the pulp (Jyvasjarvi & Kniffki, 1987; Närhi *et al.*, 1994). It should be noted that a small proportion of unmyelinated axons in dental pulps are postganglionic sympathetic efferent fibres from superior cervical ganglion that primarily innervate blood vessels (Uddman *et al.*, 1984; Fried *et al.*, 1988), whereas the presence of parasympathetic tooth innervation is disputed (Sasano *et al.*, 1995; Byers & Narhi, 1999). Nonetheless, the following discussion will focus on sensory primary afferent fibres.

Despite the heterogeneity of dental pulp afferents, multiple studies in humans have demonstrated that activation of dental pulp afferents by application of different types of physiological stimuli produces only pain (Anderson & Matthews, 1967; Edwall &

Olgart, 1977; Ahlquist *et al.*, 1984). Induced pain is either instant and sharp, in line with Aδ fibre activation, or dull, throbbing, and poorly localised, associated with C-fibre activation by high intensity stimuli (Mengel *et al.*, 1993; Hildebrand *et al.*, 1995). However, other studies have also reported a "pre-pain" sensation induced by electrical tooth stimulation (McGrath *et al.*, 1983; Brown *et al.*, 1985; Virtanen *et al.*, 1987). In addition, a magnetoencephalography study demonstrated a response in human primary somatosensory cortex following a non-painful electrical stimulation of a pre-molar dental pulp, with latencies corresponding to fast conduction by Aβ fibres (Kubo *et al.*, 2008). There is also evidence in the literature for the presence of intradental mechanoreceptors, thought to be involved in the detection of vibration and food hardness (Dong *et al.*, 1985; Dong *et al.*, 1993; Paphangkorakit & Osborn, 1998; Robertson *et al.*, 2003) and potentially responsible for jaw reflex activity observed in response to non-painful electrical stimulation (Matthews *et al.*, 1976; McGrath *et al.*, 1981; Boissonade & Matthews, 1993; Cadden *et al.*, 2013). Mechanosensory function of dental primary afferents is still controversial, as it is often attributed to periodontal ligament mechanoreceptors (Trulsson, 2006). Interestingly, recent studies comparing vital and root canal-treated teeth reported significant differences in maximal bite force (Awawdeh *et al.*, 2017), but not in tactile sensitivity of the teeth (Schneider *et al.*, 2014), continuing the debate regarding the presence of intradental mechanoreceptors.

The possibility that dental primary afferents are not all typical nociceptors is supported by experimental animal studies, showing that parent axons of dental pulp afferents are often large in diameter, myelinated, and display fast conduction velocities (Lisney, 1978; Cadden *et al.*, 1983; Johansson *et al.*, 1992; Paik *et al.*, 2009). Furthermore, immunolabelling studies demonstrated prominent expression of myelinated fibre markers (e.g. neurofilament 200 (NF200) and parvalbumin) by unmyelinated dental pulp afferents (Ichikawa *et al.*, 1995; Paik *et al.*, 2010; Fried *et al.*, 2011; Henry *et al.*, 2012). Overall, this suggests the loss of myelination and extensive branching by parent axons upon entering the teeth. A similar phenomenon is also observed in afferent terminals in other tissues, such as the skin (Peng *et al.*, 1999).

Retrograde labelling in rodents has widely been used to further study the properties of dental primary afferents by tracing to their neuronal cell bodies in the TG. Several

research groups reported that only 5-20% of labelled TG neurons were small in diameter (Sugimoto & Takemura, 1993; Kvinnsland *et al.*, 2004; Paik *et al.*, 2009; Kovacic *et al.*, 2013), with the majority being IB4-negative (Fried *et al.*, 1989; Kvinnsland *et al.*, 2004; Gibbs *et al.*, 2011; Kovacic *et al.*, 2013). However, others reported smaller average diameters and more prevalent IB4 binding (Park *et al.*, 2006; Kim *et al.*, 2011). Chung and colleagues (2012) provided further evidence that non-peptidergic sensory neuron population represented only 2.5% of TG neurons innervating dental pulps by performing retrograde labelling in mice expressing green fluorescent protein (GFP) under the control of *Mrgprd* promoter. Such a sparse non-peptidergic innervation is common in deep tissues, such as the knee joint, as opposed to superficial tissues like the skin (Fried & Gibbs, 2014). However, despite very low IB4 binding and *Mrgprd* expression, dental pulp afferent neurons were found to express $P2X_3$, although the reported percentages range widely from 8 to over 60% (Cook *et al.*, 1997; Yang *et al.*, 2006; Kim *et al.*, 2011).

With regard to the peptidergic nociceptor population innervating dental pulps, about 33-87% of labelled neurons were found to express CGRP (Fried *et al.*, 1989; Pan *et al.*, 2003; Yang *et al.*, 2006; Won *et al.*, 2017), but less than 2% were positive for substance P (Fried *et al.*, 1989). A similar trend was observed in a cat dental pulp immunolabelling study, where CGRP was found to be 3-4 times more abundant than substance P (Heyeraas *et al.*, 1993). Moreover, a large proportion (78-86%) of dental primary afferent neurons express the NGF receptor TrkA (Yang *et al.*, 2006; Kovacic *et al.*, 2013) and the GDNF receptor GFRα-1 (72%), whereas 65% express both (Yang *et al.*, 2006). In addition, about 30% express GDNF itself (Kvinnsland *et al.*, 2004). While the above values were obtained from rat molar pulp primary afferent neurons, a much lower TrkA (about 10%) and CGRP (5%) expressing TG neuron population was detected in mouse incisor pulp afferent neurons (Mosconi *et al.*, 2001), supporting differential innervation in continuously growing incisor teeth (Paik *et al.*, 2009) and/or representing species differences. Collectively, these studies demonstrated that dental pulp afferent neurons do not follow the typical patterns of peptidergic and non-peptidergic nociceptor marker expression observed in the spinal nociceptive system.

To explain such an overall unusual profile of dental pulp afferent neurons, Fried *et al.* (2011) proposed an idea that some pulpal afferents are low-threshold "algoneurons" that get activated by weak stimuli, in a similar way to typical low-threshold mechanoreceptors, but they connect to central pain-mediating pathways to evoke the sensation of pain. Indeed, anterograde tracing studies have demonstrated that dental pulp afferents terminate in the subnucleus caudalis, although connections to subnuclei interpolaris and oralis, as well as the main sensory nucleus, have also been detected (Arvidsson & Gobel, 1981; Marfurt & Turner, 1984; Takemura *et al.*, 1993; Sugimoto *et al.*, 1997).

To sum up, rather than representing a typical nociceptive neuronal population that produces exclusively painful sensations, dental pulp innervation demonstrates a unique sensory profile that requires further research. Specific neurochemical properties of dental pulp afferent neurons will be further discussed in section 1.4 and Chapter 5.

1.3.3 Relationship between odontoblasts and dental primary afferent neurons

Given the importance of dentition in vertebrate feeding and, ultimately, survival, it is perhaps not surprising that dental pulps are densely innervated to ensure rapid detection of tissue damage (Fried & Gibbs, 2014). This would suggest that evolution of mineralised structures preceded the adaptation of associated sensory units (Hildebrand *et al.*, 1995). However, an intriguing alternative evolutionary hypothesis suggests the presence of a precursor sensory organ that acquired a biomineral shield for enhanced sensitivity and protection, before providing a masticatory function (Gans & Northcutt, 1983; Farahani *et al.*, 2011).

While both mature odontoblasts and dental primary afferent neurons are terminally differentiated cells with very distinct phenotypes, they share a cranial neural crest origin (Miletich & Sharpe, 2004). Furthermore, tooth maturation and innervation are closely associated during development (Luukko *et al.*, 2008). A developmental link between the two types of cells is also reflected in the expression of neural progenitor cell and neuronal markers, such as nestin, galanin, microtubule-associated proteins 1b and tau, by odontoblasts (About *et al.*, 2000; Maurin *et al.*, 2009; Paakkonen *et al.*, 2009;

Miyazaki *et al.*, 2015). However, the implications of this to odontoblast function are still not fully understood.

In mature teeth, odontoblasts are positioned in a dense network of axons. While no synaptic connections or junctional structures between the odontoblasts and adjacent axons have been identified, a particularly close contact was observed between odontoblast processes and nerve fibres within dentinal tubules, with shortest reported distances of 15-30 nm (Shiromoto, 1984; Ibuki *et al.*, 1996). Moreover, there are some reports in the literature of intercellular adhesion (Frank, 1968; Byers *et al.*, 1982; Allard *et al.*, 2006), odontoblast membrane densification in the vicinity of nerve fibres (Carda & Peydro, 2006), and formation of beaded nerve varicosities near odontoblasts (Shiromoto, 1984). The last observation was also confirmed in odontoblast-like cell and TG neuron co-cultures *in vitro* (Maurin *et al.*, 2004). Interestingly, nerve varicosities in dentinal tubules were also recently demonstrated to contain the protein machinery necessary for exocytosis (Honma *et al.*, 2017). In addition, a close contact between pulpal nerves and odontoblast primary cilia has also been demonstrated (Thivichon-Prince *et al.*, 2009), further supporting the possibility of odontoblast and pulpal afferent interaction.

Odontoblasts and neurons seem to mutually depend on such a close contact. For example, dentinal innervation demonstrates plasticity and is only detected in tubules that contain viable odontoblasts (Byers & Dong, 1983; Byers *et al.*, 1988). Therefore, it was proposed that odontoblasts are involved in dental axonal guidance (Magloire *et al.*, 2010). Indeed, expression of several glycoproteins, known to regulate neuronal migration, axonal guidance, adhesion, and plasticity, such as reelin, laminins, semaphorins, and teneurins, has already been demonstrated (Lesot *et al.*, 1981; Fried *et al.*, 1992; Maurin *et al.*, 2004; Yuasa *et al.*, 2004; Maurin *et al.*, 2005; Torres-da-Silva *et al.*, 2017). In addition, there is some evidence that nerve fibres regulate mature odontoblast function, as decreased sensory innervation significantly reduces dentine formation (Jacobsen & Heyeraas, 1996).

In summary, research suggests evolutionary, developmental, anatomical, and physiological relationship between odontoblasts and neurons in the teeth. It should be noted that the restricted accessibility of mature odontoblasts and intradentinal nerves

due to their location within the dentinal tubules limit attempts to functionally characterise them. A brief overview of the cellular models and methods used to study their individual properties and interactions will be provided in subsequent chapters. Paracrine signalling as a means of intercellular communication between odontoblasts and neurons will be also discussed.

1.4 Odontogenic pain

Dental pain can cause extreme discomfort and is one of the main reasons why people seek dental care. According to the 2009 Adult Dental Health Survey (Steele *et al.*, 2011), as many as 29% of adults in the United Kingdom reported experiencing dental pain in the preceding 12 months. Similarly, around 26% of dentate adults in the United States reported toothache or sensitive teeth within a 6-month period, as found in the National Health Interview Survey, 2008 (Bloom *et al.*, 2012). Despite the prevalence of dental pain, the exact mechanisms involved in its development are still not fully understood. Odontogenic pain of pulpal and dentinal origin will be the focus of the following discussion.

1.4.1 PULPITIS PAIN

Since pain associated with pulpitis is often dull, throbbing, and poorly localised, it has typically been attributed to the activation of C-fibres (Narhi *et al.* (1992), as cited in Magloire *et al.* (2010)). At different stages of the disease, clinical features of pulpitis can include thermal hyperalgesia, spontaneous pain, and thermal allodynia (Rechenberg *et al.*, 2016), indicating neuronal sensitisation in the trigeminal nociceptive system. Some of the main contributing factors include the presence of bacterial plaque on the surface of the tooth, elements of the host immune response to bacteria, and increased intrapulpal pressure in a low-compliance chamber.

1.4.1.1 Bacterial contribution to dental pain

Bacteria have been experimentally demonstrated to be the cause of most pulpal diseases, as germ-free rats with exposed dental pulps do not develop inflammation and subsequent pulp necrosis (Kakehashi *et al.*, 1965). Bacterial plaque is a sticky microbial

biofilm containing bacterial cells that may cause tooth decay (dental caries) due to local acid and proteolytic enzyme generation (Simon-Soro *et al.*, 2013). Even when the integrity of enamel or cementum layers is compromised, vital teeth with healthy dental pulps contain defence mechanisms, such as the outward flow of dentinal fluid, to oppose the diffusion of toxins and bacterial invasion of dentinal tubules (Nagaoka *et al.*, 1995; Love & Jenkinson, 2002).

In the case of extensive destruction of the mineralised layers of the tooth, bacteria may reach the pulp chamber and activate the host innate immune response, causing inflammation and extensive damage to the tissue (Hahn & Liewehr, 2007). However, due to the ability to release diffusible toxic products, bacteria in the carious lesion do not necessarily have to reach the pulp to cause inflammation and pain (Bergenholtz, 1977). In pulpitis, painful symptoms in carious teeth are associated with higher concentrations of endotoxin (a Gram-negative bacterial wall component lipopolysaccharide (LPS)) than asymptomatic cases (Khabbaz *et al.*, 2000; Jacinto *et al.*, 2005).

1.4.1.2 Inflammation-induced molecular changes in the dental pulp

Some well-established inflammatory mediators, including the cytokines TNFα and IL-1ß, are upregulated in inflamed human dental pulps, particularly in the case of irreversible pulpitis (Pezelj-Ribaric *et al.*, 2002; Kokkas *et al.*, 2007; Silva *et al.*, 2009). These results are supported by recent work by Galicia and colleagues (2016), who performed a genome-wide microarray analysis of healthy and irreversibly inflamed human dental pulp tissues. They also detected increased TLR2 and TLR4 expression in pulpitis, as well as a positive correlation between TNFα and IL-1ß expression and the severity of pulpitis pain. The expression of the neuropeptide substance P was similarly found to be increased in human dental pulps in the presence of tooth decay or irreversible pulpitis (Awawdeh *et al.*, 2002; Bowles *et al.*, 2003), with significantly higher levels in painful compared with asymptomatic cases (Rodd & Boissonade, 2000). The inflammation-dependent increase was also detected in substance P receptor NK_1 levels (Caviedes-Bucheli *et al.*, 2007). The levels of other neuropeptides, such as CGRP and neurokinin A, were also found to be elevated in inflamed dental pulps (Awawdeh *et al.*, 2002; Rodd & Boissonade, 2002; Caviedes-Bucheli *et al.*, 2006; Sattari *et al.*, 2010).

Moreover, inflammatory mediators, such as bradykinin and PGE_2 (Nakanishi *et al.*, 1995; Lepinski *et al.*, 2000), and growth factors, including brain-derived neurotrophic factor (BDNF), vascular endothelial growth factor (VEGF), and NGF (Byers *et al.*, 1992; Wheeler *et al.*, 1998; Artese *et al.*, 2002) are increased in inflamed or injured dental pulps.

1.4.1.3 Structural and functional neuronal changes

Consistent with the changes in growth factors in the tooth pulp, the nerve fibres innervating it demonstrate plasticity in response to injury and inflammation (Byers *et al.*, 2003). For example, the sprouting of terminal branches of CGRP-immunoreactive nerve fibres occurred following experimental dentine injury (Taylor *et al.*, 1988). Denervation experiments later demonstrated the importance of this phenomenon in maintaining the viability of the pulp (Byers and Taylor (1993) as cited in Fried and Gibbs (2014)).

Several receptors and ion channels expressed by dental primary afferent neurons have been proposed as integrators of both bacterial and host-derived signals that may modulate neuronal activity and, consequently, contribute to dental pain. The most extensively studied is heat-sensitive TRPV1, which was found to be increased in pulpal nerve fibres from carious dental pulps (Morgan *et al.* (2005), as cited in Fried and Gibbs (2014)). However, the proportion of retrogradely traced dental primary afferent neurons reported to be immunoreactive for TRPV1, or activated by its agonist capsaicin, ranges widely from 8% to over 70% (Park *et al.*, 2006; Gibbs *et al.*, 2011; Kim *et al.*, 2011). The application of LPS to the dentinal surfaces of mice caused an increase in TRPV1 mRNA and protein levels in the TG in mice (Chung *et al.*, 2011). In relation to TRPV1 function, LPS has been reported to indirectly sensitise its activity via TLR4 activation (Diogenes *et al.*, 2011), whereas substance P sensitises TRPV1 via its receptor NK_1 (Zhang *et al.*, 2007).

The involvement of cold/mechanosensitive TRPA1 channel in pulpitis pain has also been considered, as TRPA1 was detected on retrogradely labelled dental primary afferent neurons (Park *et al.*, 2006; Hermanstyne *et al.*, 2008; Kim *et al.*, 2011) and was upregulated in painful human dental pulps (Kim *et al.*, 2012) and in rat TG in response

to experimental tooth injury (Haas *et al.*, 2011). Moreover, LPS was found to directly activate neuronal TRPA1 (Meseguer *et al.*, 2014), which could contribute to pulpitis pain.

Furthermore, purinergic $P2X_3$ receptor immunoreactivity was also detected on the nerve fibres in human dental pulps (Alavi *et al.*, 2001; Renton *et al.*, 2003), and its activation by ATP was shown to evoke action potentials in dental primary afferent neurons (Cook *et al.*, 1997). $P2X_3$ on TG neurons can also be sensitised by substances found in inflamed dental pulps, such as substance P (Park *et al.*, 2010).

In addition, the involvement of TRPV1, TRPA1, and $P2X_3$ in dental pain is supported by the findings that pulpal application of their respective agonists activates second-order neurons in the spinal trigeminal nucleus or induces NMDA receptor-dependent neuroplastic changes (Chiang *et al.*, 1998; Shimizu *et al.*, 2006; Adachi *et al.*, 2010). Moreover, in an *in vivo* electrophysiological experiment, noxious cold stimulation of the mouse dental pulp was demonstrated to activate the primary somatosensory cortex, which was inhibited by a non-selective TRP channel blocker La^{3+} (Jin, 2015), further supporting the involvement of TRP channels. Overall, the knowledge on the processes that occur centrally in response to dental pulp injury or inflammation is expanding. However, the fact that extraction of a painful tooth (or even removal of only the diseased portion of the pulp) generally results in pain relief (Hasselgren & Reit, 1989), encouraged us to focus on the processes affecting dental primary afferent neurons, their cell bodies in the TG, and mechanisms that potentially regulate their sensitivity.

1.4.1.4 Tissue swelling in a low-compliance pulpal compartment

Blood vessel dilation occurred in the areas of inflammation-induced neuronal sprouting in dental pulps (Taylor & Byers, 1990). Both CGRP and substance P, released from the peripheral terminals of peptidergic fibres, are known to cause vasodilation and plasma extravasation, as well as playing a role in the recruitment of immune cells to the site of injury (Caviedes-Bucheli *et al.*, 2008). In human dental pulps, activation of TRPV1 induced CGRP release (Fehrenbacher *et al.*, 2009; Burns *et al.*, 2016). Moreover, bacterial products and inflammatory mediators present in inflamed dental pulps, including LPS, bradykinin, and PGE_2, can further stimulate CGRP release (Goodis *et al.*, 2000; Ferraz *et al.*, 2011). As a result of accumulation of inflammatory exudate, tissue swelling occurs.

The low compliance of the pulpal compartment due to the rigid surrounding layers significantly increases the fluid pressure in the tissue (Heyeraas & Berggreen, 1999), which is likely to contribute to the painful sensation (Kim (1990), as cited in Caviedes-Bucheli *et al.* (2008)).

1.4.1.5 Treatment strategies

Recent review of the best available data supports the use of nonsteroidal anti-inflammatory drugs (NSAIDs) for the management of acute dental pain (Moore *et al.*, 2018), suggesting an involvement of prostaglandins in nociceptor sensitisation. Other strategies are also constantly being explored. For example, NK_1 receptor antagonists have been tested in clinical trials against acute dental pain. However, they demonstrated poor analgesic properties, despite some promising previous pre-clinical data (Dionne *et al.*, 1998; Urban & Fox, 2000). It should be noted that other pre-clinical models of acute dental pain have been developed that more accurately predict the clinical analgesic effect of compounds, including the relative ineffectiveness of the NK_1 receptor antagonist (Worsley *et al.*, 2008). Multiple TRPV1 antagonists have also been developed and tested in clinical trials for dental pain conditions (Mickle *et al.*, 2016). However, the reports published so far revealed hyperthermia as a potentially dangerous side effect (Gavva *et al.*, 2008) and only short-lasting TRPV1 antagonist-dependent analgesia was observed in acute dental pain (molar tooth extraction) studies (Quiding *et al.*, 2013). Novel compounds targeting both TRPA1 and TRPV1 are also described in the literature as being promising due to effectiveness against orofacial allodynia in pre-clinical tests (Gualdani *et al.*, 2015).

1.4.2 Dentine hypersensitivity

Despite extreme fluctuations in the oral environment, such as the temperatures ranging from 0 to 77°C in response to cold and hot drinks (Barclay *et al.*, 2005), healthy teeth generally do not produce pain due to the presence of an intact protective enamel layer with high thermal insulating capacity (Lin *et al.*, 2010). However, normal sensitivity to noxious stimuli is present, as observed during dental pulp sensibility tests (Chen & Abbott, 2009). Although inflammation of the dental pulp can also induce severe and persistent hypersensitivity of the teeth to external stimuli, dentine hypersensitivity is

recognised as a separate clinical condition, characterised by sharp, short-lasting pain that is evoked by thermal (hot or cold foods and drinks), osmotic (sugars), chemical (dietary acids), evaporative (air blast), or tactile/mechanical stimuli (scratching by a probe) to the exposed dentine (Dababneh *et al.*, 1999). Dentine can be exposed following the damage of enamel layer or as a result of gingival recession and subsequent loss of the relatively fragile cementum layer (West *et al.*, 2013). Exposure of dentine is required, but not sufficient, to cause dentine hypersensitivity, as the number of unoccluded, or patent, dentinal tubules and their diameters were found to be key determining factors (Absi *et al.*, 1987; Addy *et al.*, 1987; Rimondini *et al.*, 1995).

Although dentine hypersensitivity is a short-lasting, acute type of pain, it nonetheless considerably impairs the oral health-related quality of life (Bekes & Hirsch, 2013). Therefore, it is of importance to research the underlying mechanisms. The main theories that have been proposed to explain the exaggerated sensitivity of the dentine to different types of external stimuli will be discussed next.

1.4.2.1 Neural theory

Direct activation of the free nerve endings present in dentinal tubules forms the basis of the "neural theory" of dentine hypersensitivity (Chung *et al.* (2013), see Figure 1.5A). Based on the sudden and sharp sensation, dentinal pain has been classically attributed to the activation of Aδ type primary afferents, although the presence of functionally indistinct Aβ fibres has later been recognised (Narhi *et al.* (1992), as cited in Magloire *et al.* (2010)). Some receptors, known to be involved in sensory transduction, are found on the neurons that innervate dental pulps, which supports their potential role in detecting external stimuli. Specifically, studies using retrograde labelling confirmed the expression and/or function of ion channels like TRPA1, TRPM8, TRPV1, and TRPV2, on dental primary afferent neurons (Chaudhary *et al.*, 2001; Park *et al.*, 2006; Hermanstyne *et al.*, 2008; Gibbs *et al.*, 2011; Kim *et al.*, 2011; Kadala *et al.*, 2018).

On the other hand, the neural theory fails to address how the stimulus reaches the nerve endings, as most studies could only detect nerve fibres in the inner part of the pre-dentine and dentine (Byers & Dong, 1983; Carda & Peydro, 2006). Moreover, Lin *et al.* (2014) brought attention to the fact that dental neuron discharge and pain in response

to cold stimulus occurs much faster than temperature changes reach the dentine-pulp junction, as estimated from the thermomechanical properties of the tooth, to directly stimulate the nerve endings. Therefore, the neural theory cannot explain the sudden, sharp pain in response to cold (Mengel *et al.*, 1993). However, in the case of dull, burning dental pain produced by sustained heat stimulus, the latency of neuronal discharge matches the predicted heat transfer across the layers of the tooth (Lin *et al.*, 2017), and could be explained by direct activation of intrapulpal nerve fibres expressing heat-sensitive receptors, such as TRPV1. The difference between hot and cold responses could be further explained using the "hydrodynamic theory".

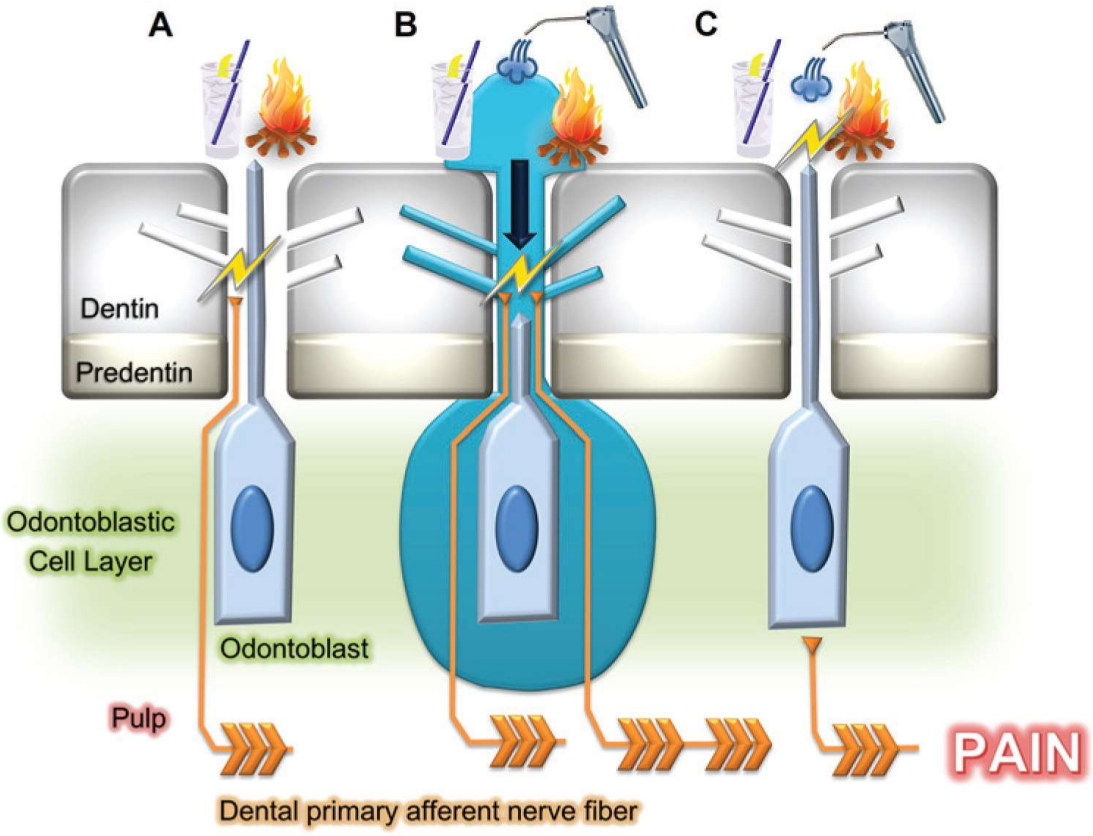

Figure 1.5 Three main hypotheses for dentine hypersensitivity

A) The neural theory proposes direct activation of intradentinal sensory nerves by external (e.g. thermal) stimuli. *B)* The hydrodynamic theory suggests that any stimulation of the exposed dentine causes dentinal fluid movement, which is detected by the free nerve endings. *C)* The odontoblast transducer theory suggests that odontoblasts act as sensory cells, capable of detecting external stimuli and transmitting the signal to the adjacent dental primary afferents. Taken from (Chung *et al.*, 2013) with permission from SAGE Publications.

1.4.2.2 Hydrodynamic theory

The earliest suggestions for the link between dentinal fluid flow and pain date back to 1850-1900 (Cox *et al.*, 2017). However, what is known as the "hydrodynamic theory", one of the most widely accepted theories of dentine hypersensitivity, is primarily based on work by Brännström and colleagues in the 1960s and 1970s (Brannstrom *et al.*, 1967; Johnson & Brannstrom, 1974). They demonstrated that various pain-producing stimuli all cause displacement of fluid within the dentinal tubules, which pointed to an indirect mechanism of external stimuli recognition via detection of fluid flow by dentinal nerve endings (see Figure 1.5B).

Later studies demonstrated a direct correlation between the direction and speed of dentinal fluid flow and dental neuron activity in cats (Andrew & Matthews, 2000; Vongsavan & Matthews, 2007), with higher discharge frequencies in response to outward (away from the pulp chamber) rather than inward flow. Higher sensitivity to outward dentinal fluid flow was also reported in humans (Charoenlarp *et al.*, 2007). This has been proposed to explain the difference between the gradual/dull and sudden/sharp sensations produced by hot and cold stimuli, respectively (Lin *et al.*, 2014). While cold stimulation immediately induces the outward flow capable of activating mechanoreceptors, the inward flow due to high temperatures produces less shear stress, and only the delayed thermal activation of nerve endings is thought to occur (Matthews, 1977; Lin *et al.*, 2011; Lin *et al.*, 2017). Interestingly, mechanical stimulus equivalent to normal chewing was also demonstrated to cause dentinal fluid flow (Paphangkorakit & Osborn, 2000), and a simulation of fast mastication of hard food estimated that the fluid flow velocity can reach the pain threshold values (Su *et al.*, 2014).

Irrespective of the type of initial stimulus, the hydrodynamic mechanism of dentine hypersensitivity requires the presence of mechanoreceptors. Potentially mechanosensitive ion channels detected in dental primary afferent neurons include some of the TRP channels, such as TRPA1, as well as ASIC3 and K_{2P} channels TREK-1 and TREK-2 (Hermanstyne *et al.*, 2008), with the most recent finding of a mechanosensitive Piezo2 (Won *et al.*, 2017). However, even a fast, outward dentinal fluid flow is a relatively mild mechanical stimulus, unlikely to activate classical high-threshold nociceptive nerve fibres. Thermally-induced deformation of the tooth

structure was proposed as an alternative mechanical stimulus (Linsuwanont *et al.*, 2008). However, it is unknown if such temperature-dependent structural changes could directly activate nerve fibres or whether it simply influences the fluid movement. Moreover, it does not explain the painful sensations produced by non-thermal (e.g. chemical or osmotic) stimulation of exposed dentine.

The fact that dentine fluid flow can activate dental primary afferents could potentially also be explained by pre-existing neuronal sensitisation or the aforementioned proposal that pulpal neurons are low-threshold "algoneurons" rather than high-threshold nociceptive neurons (Fried *et al.*, 2011). Nonetheless, given the sparse innervation of dentinal tubules, the involvement of odontoblasts, which have their processes extending further and in all dentinal tubules, should be considered. While it has been suggested that fluid flow-dependent displacement of odontoblast processes in the dentinal tubules might passively affect the amount of shear stress reaching the nerve endings (Lin *et al.*, 2011), the third theory focuses on the active role of odontoblasts in dentine hypersensitivity and will be discussed next.

1.4.2.3 Odontoblast transducer theory

The third hypothesis proposed to explain dentine hypersensitivity, termed the "odontoblast transducer theory", relies on odontoblasts detecting external stimuli and, subsequently, sending the signal to neurons (Figure 1.5C). Their position closest to the external environment and adjacent to the network of nerve fibres (Shiromoto, 1984; Ibuki *et al.*, 1996) supports this role. A more recently proposed working model for dentine hypersensitivity also includes the hydrodynamic component. It suggests that external stimuli-induced dentinal fluid flow produces sufficient shear stress to distort the odontoblast cell membrane, which activates mechanosensitive ion channels on odontoblasts, and this is followed by paracrine signalling to neurons (Shibukawa *et al.*, 2015).

The evidence against the odontoblast transducer theory comes from early studies (e.g. Hirvonen and Narhi (1986)) that used an intensive air-blast stimulation to the exposed dentine to destroy the odontoblast layer. This was repeated for several hours but did not affect the pulpal nerve responses to a light air-blast or probing of exposed dentine.

However, it is likely that the injury produced by the stimulation and other processes involved in the method (e.g. repeated drilling and acid etching of dentine) introduced confounding factors and do not conclusively invalidate the sensory role of odontoblasts. In fact, the evidence in the literature supporting the sensory function of odontoblasts is rapidly increasing and will be discussed in detail in subsequent chapters.

1.5 Hypothesis and general aims

In this study, mouse cellular models and *in vitro* techniques were used to test the hypothesis that 1) the detection of external stimuli relevant in dentine hypersensitivity involves odontoblasts and adjacent dental primary afferent neurons acting as a sensory unit and 2) bacterial products and host-derived inflammatory mediators can modulate the activity of odontoblasts and/or neurons, resulting in increased sensitivity and pulpal pain.

The general aims of this thesis are as follows:

- To investigate the sensitivity of odontoblasts to physiologically-relevant stimuli and the sensory transducers involved in their detection.
- To determine the functional profile of trigeminal ganglion neurons.
- To examine the potential means of odontoblast-neuron intercellular communication.
- To investigate the ability of bacterial wall components and classical inflammatory mediators to sensitise the activities of odontoblasts and/or trigeminal ganglion neurons.

Chapter 2

General materials and methods

2.1 Solutions

Extracellular solution (ECS; complete formulation in Table 2.1) was prepared by adding HEPES to Hank's balanced salt solution (HBSS; Gibco, Life Technologies). ECS lacking Ca^{2+} was prepared using Ca^{2+}/Mg^{2+}-free HBSS (Gibco, Life Technologies), supplemented with 10 mM HEPES, 1 mM Mg^{2+}, and 1 mM EGTA. Solutions were buffered to pH 7.4 using NaOH.

Table 2.1 Composition of extracellular solution (ECS)

Inorganic salts	**Concentration (mM)**
Sodium chloride (NaCl)	137.93
Potassium chloride (KCl)	5.33
Calcium chloride ($CaCl_2$)	1.26
Magnesium chloride ($MgCl_2 \cdot 6H_2O$)	0.49
Potassium phosphate monobasic (KH_2PO_4)	0.44
Magnesium sulphate ($MgSO_4 \cdot 7H_2O$)	0.41
Sodium phosphate dibasic ($Na_2HPO_4 \cdot 7H_2O$)	0.34
Other components	
HEPES	10
D-Glucose	5.56

2.2 Reagents

Allyl isothiocyanate (AITC), capsaicin, GSK1016790A, HC067047 and *N*-ethylmaleimide were all purchased from Sigma, UK. Murine tumour necrosis factor alpha (TNFα) was obtained from PeproTech.

AITC, capsaicin, GSK1016790A, and HC067047 were all dissolved in dimethyl sulfoxide (DMSO; Sigma), whereas *N*-ethylmaleimide and TNFα were dissolved in dH_2O. Compounds were further diluted in either complete culture medium or ECS to achieve appropriate final concentrations, as indicated in the text and figures.

2.3 Cell culture

2.3.1 Mouse 17IA4/OB cells

Mouse dental pulp 17IA4 cell line (Priam *et al.*, 2005) was kindly provided by Professor Paul Sharpe (King's College London). Unless stated otherwise, undifferentiated 17IA4 cells were cultured in αMEM basal medium containing deoxyribonucleosides, ribonucleosides and UltraGlutamine 1 (Lonza), supplemented with heat-inactivated foetal bovine serum (15% (v/v); Sigma), 100 U/ml penicillin, and 100 µg/ml streptomycin (Sigma). Differentiating medium was additionally supplemented with L-ascorbic acid (50 µg/ml; Sigma), β-glycerophosphate (10 mM; Calbiochem), and dexamethasone (100 nM; Sigma), as published elsewhere (Wei *et al.*, 2007). Cells were grown in 75 cm^2 flasks. When the confluency of 80-90% was reached, cells were passaged using a solution of 0.25% Trypsin-0.1% (w/v) EDTA in Ca^{2+}/Mg^{2+}-free Dulbecco's PBS (Sigma) as a dissociation reagent. Cultures were maintained in a humidified incubator at 37°C and 5% CO_2. Culture medium was changed every 2-3 days. 17IA4 cells exposed to differentiating medium before starting the experiments will be referred to in the text and figures as odontoblast-like (OB) cells.

2.3.2 PRIMARY MOUSE TRIGEMINAL GANGLION NEURONS

Trigeminal ganglia (TG) were dissected from adult male and female C57BL/6 mice sacrificed by either intraperitoneal injection of sodium pentobarbital or concussion of the brain by striking the cranium, followed by dislocation of the neck, as approved by the UK Home Office. Collected TG were each cut into several pieces and incubated in Ham's F12 medium (GE Healthcare) with 0.125% (w/v) collagenase (Sigma) for 60 min at 37°C. Subsequently, collagenase solution was carefully removed, and TG pieces were washed with F12. They were then placed in F12 medium containing 1% N2 supplement (Gibco, Life Technologies), 0.3% (v/v) bovine serum albumin (Sigma), 100 U/ml of penicillin, and 100 µg/ml streptomycin (Sigma). This was followed by mechanical dissociation of TG neurons by trituration with fire-polished glass Pasteur pipettes (150 mm in length) of decreasing inside diameter. The collected suspension was filtered through a 70-micrometre cell strainer and centrifuged for 6 minutes at 600 rpm. The pellet containing the neurons was then resuspended in an appropriate volume of the supplemented F12 medium. The cells were plated onto the centre of sterile round glass coverslips (10 µl of cell suspension per coverslip) pre-coated with poly-D-lysine (100 µg/ml at 4°C overnight; Sigma) and laminin (40 µg/ml at 37°C for at least 2 hours; Sigma). After a 30-45-minute incubation at 37°C, each well was flooded with another 490 µl of pre-warmed supplemented F12 medium containing no exogenous nerve growth factor (NGF). TG neurons were maintained in a humidified incubator at 37°C and 5% CO_2.

2.4 Reverse transcription polymerase chain reaction (RT-PCR)

2.4.1 RNA EXTRACTION AND PURIFICATION

QIAzol lysis reagent (Qiagen) was used to extract RNA from both trigeminal ganglion (TG) tissue and cultured 17IA4/OB cells. TG were dissected from BALB/c mice and flash-frozen. Frozen TG were dropped into QIAzol, homogenised using a hand-held homogeniser, and incubated at room temperature for 5 minutes. QIAzol was directly added to 17IA4/OB cell culture dishes after complete aspiration of the culture medium, and the cell monolayer was disrupted using cell scrapers and by pipetting up and down.

TG homogenate and cell lysates (500 µl/sample) were then transferred to pre-spun (12,000 rpm for 2 minutes) phase lock gel (PLG) columns (5PRIME) followed by the addition of chloroform (100 µl/column). The columns were shaken for 15 seconds and incubated at room temperature for 3 minutes, followed by a 15-minute centrifugation (12,000 rpm at 4°C). The aqueous phase was then poured off into RNAse-free tubes before processing the samples using RNeasy Micro kit (Qiagen), according to the manufacturer's protocol for the purification of total RNA. This included on-column digestion of DNA by incubation with DNAse I for 15 minutes at room temperature. The concentration and quality of the resulting RNA samples were tested using NanoDrop spectrophotometer (Thermo Fisher Scientific).

2.4.2 First-strand cDNA synthesis

For each sample, the same amount of RNA (1.5 µg) was diluted in RNAse-free dH_2O in a final volume of 12 µl. Random primers (1 µl of 50 mM; Promega) and dNTPs (1 µl of 10 mM; Promega) were added to each reaction, and the tubes were placed in a thermocycler (GeneAmp PCR System 9700, Applied Biosystems) at 65°C for 5 minutes, then cooled on ice for at least 1 minute. Reverse transcription master mix (4 µl of first strand buffer (5x), 1 µl of 0.1 M DTT, and 1 µl of 200 U/µl Superscript III RT (Invitrogen) per sample) was then added to each reaction, followed by gentle pipetting up and down to mix. No RT control reactions, where Superscript III RT was replaced with RNAse-free water, were also prepared. All tubes were then incubated in a thermocycler at 25°C for 5 minutes, 50°C for 60 minutes, 70°C for 15 minutes, and cooled to 4°C, before storing the cDNA products at -20°C.

2.4.3 Amplification of cDNA by PCR

A PCR master mix was prepared, containing (per reaction): 12.4 µl dH_2O, 4 µl Green GoTaq® reaction buffer (5x) and 0.2 µl of GoTaq® G2 DNA Polymerase (5 U/µl; Promega), 0.4 µl dNTPs (10 mM each; Promega), 1 µl of forward and 1 µl of reverse primer (both pre-diluted in dH_2O to 10 µM). A template (1 µl of cDNA diluted 1:5 in dH_2O to the concentration of 15 ng/µl) was then added to each reaction, to obtain the final volume of 20 µl/tube. No template control reactions, where cDNA was replaced

Table 2.2 Primer pairs used for reverse transcription PCR (RT-PCR)

Mouse gene	Primer sequence (5'-3')	Size (bp)	Ta (°C)
Alpl	F: CGGGACTGGTACTCGGATAA R: TGAGATCCAGGCCATCTAGC	209	60
Asic1	F: GGCTTCCAGACGTTTGTGTC R: TGGTAACAGCATTGCAGGTG	82	60
Asic2	F: TGGAGAACTGTAACTGCCGC R: TTCTGCCAGTAAGCCGAGG	107	60
Asic3	F: GCCCTGTGGACCTGAGAAC R: CCCTTAGGAGTGGTGAGCAG	105	60
Asic4	F: CCTGACATGGTAGACATCCTCA R: CACTTCCCATAGCGAGTATAGACC	128	60
Bglap	F: CCGCCTACAAACGCATCTACG R: GAGAGAGGACAGGGAGGATCAAG	115	63
Cbfa1	F: CTTCGTCAGCATCCTATCAGTTC R: TCAGCGTCAACACCATCATTC	145	60
Col1α1	F: CCTGACGCATGGCCAAGAAGA R: GCATTGCACGTCATCGCACA	145	63
Dlx3	F: GCGACACTCAGGAATCATTG R: CGGTCCATGCATTTGTTATC	108	55
Dmp1	F: CAGTGAGGATGAGGCAGACA R: TCGATCGCTCCTGGTACTCT	175	60
Dspp	F: AACTCTGTGGCTGTGCCTCT R: TATTGACTCGGAGCCATTCC	171	60
Gapdh	F: CAAAGTTGTCATGGATGACC R: CCATGGAGAAGGCTGGGG	195	60
Gja1	F: TTTGACTTCAGCCTCCAAGG R: CGCTCCAGTCACCCATGT	96	60
Ibsp	F: AAAGTGAAGGAAAGCGACGA R: GTTCCTTCTGCACCTGCTTC	215	60
Lhx6	F: AGAAGCTAGCGGACATGACG R: CTCTCAATGTAGCCGTGCAA	220	56
Lhx8	F: TACTTCAGACGGTATGGGAC R: TCCCATTACCGTTCTCCACT	238	56
Panx1	F: GCAGCCAGAGAGTGGAGTTC R: CCATTAGCAGGACGGATTCA	107	60
Panx3	F: AGGCTGCATACGTGGATAGC R: GCCAGAGCCAGTAGAGAGTAGG	127	60
Sp7	F: ACTCATCCCTATGGCTCGTG R: GGTAGGGAGCTGGGTTAAGG	238	56
Spp1	F: TCTGATGAGACCGTCACTGC R: AGGTCCTCATCTGTGGCATC	170	60
Tlr2	F: CTTCCAGGTCTTCAGTCTTCCTA	113	60

	R: GACACATCTCCTGCCAGTGAC		
Tlr4	F: CCCTGCATAGAGGTAGTTCCTA R: TGCCATGCCTTGTCTTCAAT	215	60
Trpa1	F: TCTCTGTCCTCTGCATCACG R: GGGTATTTCCATAACCATCCATT	113	60
TrpC5	F: GCTTCACAGAACGTCATGC R: TTGCAGCCACATATCTCTTGACT	90	60
Trpm7	F: CCTTCGTTCCTGTACCTCCA R: GGCCTAGCTGAGACCATGAA	108	60
Trpm8	F: GCTGTGGCCTCGTATCATTT R: GAGCAGCACATAGGCAAACA	155	60
Trpv1	F: AACCAGGGCAAAGTTCTTCC R: CATCATCAACGAGGACCCAG	109	60
Trpv4	F: TCCTCCCTGGACACATGC R: CTACAGCCAGCATCTCATGG	94	60

with dH_2O, were also prepared. The thermocycler programme used for PCR involved initial heating of the samples to 95°C for 5 minutes, followed by 35 cycles of 30 seconds at 94°C, 30 seconds at an appropriate annealing temperature (Ta) for each primer pair (listed in Table 2.2), and 30 seconds at 72°C, finishing with 5-10 minutes at 72°C. Products were stored at -20°C.

2.4.4 Agarose gel electrophoresis

RT-PCR products or DNA ladder (typically 5 µl/well) were run on agarose gels (2% in standard Tris/Borate/EDTA (TBE) buffer with ethidium bromide) at 80-100V, until sufficient separation of DNA fragments was achieved, as seen from dye-containing DNA ladder bands. DNA ladders used include Quick-Load® 100 bp DNA Ladder (New England Biolabs), 100 bp DNA ladder (Promega), and Quick-Load® Purple 50 bp DNA ladder (New England Biolabs), and are specified in figure captions. The gels were visualised under UV using GelDoc-It imaging system (UVP). Inverted colour images were produced using Picasa 3 software.

2.5 Measurement of intracellular Ca^{2+} concentration

Fura-2AM, one of the most popular ratiometric, cell membrane-permeant intracellular calcium indicators, was used to measure intracellular Ca^{2+} concentrations ($[Ca^{2+}]_i$).

Ratiometric calcium indicators enable accurate quantification of $[Ca^{2+}]_i$, with a signal that is stable, generally not affected by photobleaching and confounding variables, such as differences in dye loading and distribution, dye leakage, or changes in cell volume during the experiment (Paredes *et al.*, 2008). Calcium imaging using ratiometric dyes can be slower, compared with the use of single-wavelength calcium indicators, and might require specialised equipment to enable dual excitation at correct wavelengths. Moreover, some newer generation calcium indicators demonstrate higher signal-to-background ratio than Fura-2AM. However, these potential disadvantages of Fura-2AM did not seem to impact our calcium imaging experiments.

With increasing $[Ca^{2+}]_i$, fluorescence resulting from Fura-2AM excitation at 340 nm increases, but fluorescence resulting from excitation at 380 nm decreases. Therefore, the 340 nm/380 nm Fura-2AM emission intensity ratio (F_{340}/F_{380}) directly correlates with $[Ca^{2+}]_i$. Fura-2AM used in these experiments was purchased either from Teflabs (discontinued) or Invitrogen.

2.5.1 Microplate-based calcium flux assay

OB or 17IA4 cells were seeded into black-walled clear-bottom 96-well plates. When the cells reached confluence, they were washed with pre-warmed ECS and incubated with Fura-2AM (2 μM) in ECS (100 μl/well) for 1 hour at 37°C. Fura-2AM solution was then replaced with ECS only (typically 50 μl/well), followed by the measurement of mean fluorescence (excitation at 340 and 380 nm, emission at 520 nm) from the bottom of each well using a FlexStation 3 microplate reader with integrated programmable liquid handling (Molecular Devices). All experimental runs were performed at 30°C. Unless stated otherwise in specific method sections, each run lasted for 180 seconds, with automatic compound additions performed at 20 seconds, and fluorescence readings made every 6 seconds. F_{340}/F_{380} ratios were calculated in Excel after exporting the fluorescence values from SoftMax Pro software (Molecular Devices). To calculate the amplitude of responses to different compounds, the mean baseline F_{340}/F_{380} (average of recordings from 0 to 20 seconds) was subtracted from the maximum change in F_{340}/F_{380} (maximum values from 20 to 180 seconds). The values from 3 wells of a 96-well plate were averaged to give an n of 1. Independent experiments were performed on different days, using cells from different passages.

2.5.2 MICROSCOPE-BASED SINGLE-CELL CALCIUM IMAGING

Unless stated otherwise, primary TG neurons were used for calcium imaging experiments after 18-24 hours in culture. The cells were incubated with 2 μM Fura-2AM in ECS for 1 hour at 37°C. The coverslips were then mounted in an open bath chamber and washed with ECS. Compounds diluted to appropriate concentrations in ECS (or complete OB medium in some co-culture experiments, as indicated) were applied using gravity-feed perfusion system at a flow rate of 4 ml/min. The temperature of solutions perfused onto the cells was maintained at approximately 30°C using an in-line solution heater/cooler (Warner Instruments). Experimental protocols will be described in specific method sections. However, at the end of every experimental run, the cells were challenged with 50 mM KCl to distinguish healthy TG neurons from low-viability neurons and non-neuronal cells present on the coverslips.

The Fura-2AM fluorescence ratio (excitation at 340 and 380 nm, emission at 510 nm) of a group of cells in the field of view (10x magnification) was measured using an inverted microscope-based imaging system (PTI EasyRatioPro), with images being captured by ORCA Flash 4.0 digital CMOS camera (Hamamatsu) approximately every 2 seconds. Fura-2AM emission intensity ratios (F_{340}/F_{380}) were calculated using EasyRatioPro software (PTI). The average of baseline F_{340}/F_{380} values, typically recorded for 30-60 seconds before the first compound application, was subtracted from the maximal ratio values detected in response to each compound. The amplitude of each response was expressed as a percentage of the corresponding maximum Fura-2AM ratio change detected in response to 50 mM KCl. However, in the experiments where TG neurons were exposed to 1 μM capsaicin just before the application of KCl, capsaicin-sensitive neurons displayed reduced subsequent KCl responses. In those cases, the maximum Fura-2AM ratio change in response to either KCl or capsaicin (whichever was greater) was used for calculations. Only the neurons that responded to 50 mM KCl with an increase in F_{340}/F_{380} of at least 0.1 above baseline were included in the analysis. TG neurons that responded to the treatments with an increase in F_{340}/F_{380} of at least 20% of the maximum (KCl or capsaicin) response were counted as responders. Each experimental run was considered as n = 1.

2.6 Measurement of extracellular ATP concentration

OB cells were seeded into clear 4-well plates and grown in differentiating medium to confluence. On the day of the experiment, culture medium in the wells was replaced with pre-warmed fresh medium or ECS, with or without any added compounds, as specified in the result figures and their captions. Unless stated otherwise in specific method sections, final compounds were diluted in the well at a ratio of 1:10 by careful, dropwise application to prevent any artefacts from mechanical stimulation of the cells due to pipetting. This typically resulted in a final volume of 500 µl/well. Moreover, the medium or ECS from each well were sampled at least 15 minutes after the final treatment, as increases in extracellular ATP concentrations ($[ATP]_o$) induced by a culture medium change were reported to return to baseline by this time point (Egbuniwe *et al.*, 2014). Two 100-microlitre samples of the medium/ECS from each well of a 4-well plate were then transferred into a white opaque 96-well plate. CellTiter-Glo® (Promega) luciferin-luciferase assay was used according to the manufacturer's protocol to measure ATP concentration. First, CellTiter-Glo reagent was prepared by mixing the supplied substrate and buffer solutions. Equal volume (100 µl) of the room-temperature reagent was added into the wells containing the samples or the same volume of ATP standards. The plate was incubated at room temperature away from light for 10 minutes, followed by luminescence detection using FLUOstar Omega microplate reader (BMG Labtech). An average of measurements from duplicate samples from two separate wells of a 4-well plate was considered an n of 1. Comparisons were made with corresponding vehicle-treated wells from the same 4-well plate.

2.6.1 ATP STANDARD CURVES

ATP standards (1 nM, 10 nM, 100 nM, and 1 µM) were freshly prepared in either complete OB medium or ECS, as appropriate, and assayed in duplicate to generate a standard curve for each 96-well assay plate. Mean value of relative luminescence units (RLUs) per 1 nM ATP was then calculated and used for conversion of RLU to $[ATP]_o$. To ensure that any observed differences in luminescence recordings are not due to artefactual effects of added compounds on the luminescence signal or the bioluminescence reaction itself, additional ATP standard curves were generated. These

standards were prepared by adding ATP to solutions representing the final combination of test compounds and vehicles that the cells were exposed to. In cases where these standards were run on a separate 96-well plate from experimental samples, a correction factor for the RLU to $[ATP]_o$ conversion was established from 2-4 sets (OB/ECS *vs.* vehicle or OB/ECS *vs.* test compound) of ATP standard curves.

2.7 Statistical analysis

All quantitative data are represented graphically or in the text as mean values ± standard error of the mean (SEM). GraphPad Prism 7 software was used for data visualisation and statistical analysis. Specific statistical tests used will be indicated in the method and result sections of result chapters. A p-value of less than 0.05 ($p < 0.05$) was considered statistically significant.

Chapter 3

Characterisation of mouse odontoblast-like cells and their sensory function

3.1 Introduction

3.1.1 Current models for studying odontoblasts

Due to their post-mitotic nature and location at the dentine-pulp junction, with cellular processes embedded in pre-dentine and dentine (Goldberg, 2014), studies of mature odontoblasts have often been limited to immunohistochemical and histological analyses of the odontoblast cell layer in extracted teeth. However, several different approaches have been used to overcome this and enable more extensive investigations *in vitro*. Some research groups established tooth slice or organ cultures that preserve the odontoblast morphology in dentine, either with the underlying pulpal soft tissue (e.g. Sloan *et al.* (1998)) or without (Tjaderhane *et al.*, 2001; Veerayutthwilai *et al.*, 2007), relying on odontoblast attachment to the dentine scaffold. Although these strategies provided some useful information about certain gene expression or protein secretion by mature odontoblasts, a lot of functional assays require isolation of the cells. Primary cell cultures enable manipulation and live visualisation, while generally maintaining the *in vivo* phenotype, although they usually have a short life span before senescence occurs

(Vertrees *et al.*, 2008). However, the reports of successful primary mature odontoblast culture in the literature are relatively rare, reflecting the difficulty of their isolation (Guo *et al.*, 2000; Cuffaro *et al.*, 2016). As a result, the majority of researchers studying odontoblast function have relied on odontoblast precursor/progenitor cells and their *in vitro* differentiation into odontoblast-like cells. The species of origin as well as the methods for obtaining the precursor cells vary. For example, dental pulp stem cells can be obtained from pulpal explants (Couble *et al.*, 2000) or by dissociation of dental pulp tissues (Gronthos *et al.*, 2000). The most recent development, reported by Xie and colleagues (2018), is the differentiation of odontoblast-like cells from human induced pluripotent stem cells (iPSCs). In addition, pre-odontoblastic immortalised cell lines, such as MDPC-23, have also been commonly used (Hanks *et al.*, 1998). Therefore, a great variety of methods have been employed to study odontoblast function in the laboratory.

3.1.2 SENSORY ION CHANNELS IN ODONTOBLASTS

The ability of odontoblasts to detect physical and chemical stimuli and convert them into electrical signals, essential for their proposed role in sensation and pain, is supported by numerous studies that demonstrate the expression and/or function of sensory ion channels in odontoblasts or odontoblast-like cells from mice (Table 3.1), rats (Table 3.2), and humans (Table 3.3). These include a wide range of transient receptor potential (TRP) ion channels, epithelial sodium channels (ENaCs), and acid-sensing ion channels (ASICs), known to be involved in sensory transduction, as well as calcium-activated (K_{Ca}) and voltage-gated (K_v) potassium channels, and voltage-gated sodium channels (Na_v), involved in the membrane potential regulation. This provides evidence for the odontoblast sensory function, which supports their involvement in dentine hypersensitivity. Moreover, odontoblast expression of ion channels specifically linked to mechanotransduction, such as TRPP1 and 2, localised to odontoblast primary cilia, as well as TRPV4, Piezo2, transmembrane channel-like 2 (TMC2) and two-pore domain (K_{2P}) potassium channel TREK-1, also suggests that odontoblasts are able to detect the membrane deformation resulting from dentinal fluid movement, which supports the "odontoblast hydrodynamic receptor theory" proposed by Shibukawa and colleagues (2015). Nonetheless, it should be noted that there are a lot of inconsistencies between the species and individual studies on the same species regarding specific ion channel

expression. This prompted us to characterise the expression of some of these sensory ion channels in our chosen cellular model for studying odontoblast function – mouse odontoblast like-cells (described in section 3.1.4).

Table 3.1 Sensory ion channel expression in mouse odontoblasts

Mouse			
Channels present	Channels not present	Evidence for functional expression	References
TRPV1 TRPV2 TRPV3 TRPV4 TRPM3	TRPA1 TRPM8	▪ Increase in $[Ca^{2+}]_i$ in response to hypotonic solution and noxious heat, but not to cold ▪ Increase in $[Ca^{2+}]_i$ and currents induced by capsaicin (TRPV1), 2-APB (TRPV2-3), and 4α-PDD (TRPV4), but not icilin or menthol (TRPM8 and TRPA1)	(Son *et al.*, 2009)
TRPV1 TRPV2 TRPV4	TRPA1# TRPM8#	▪ Increase in $[Ca^{2+}]_i$ in response to capsaicin, probenecid (TRPV2), and RN-1747 (TRPV4). ▪ Increase in $[Ca^{2+}]_i$ and inward currents induced by hypotonic solution were blocked by TRPV1, TRPV2, and TRPV4 antagonists, but not by TRPM8 or TRPA1 antagonists	(Sato *et al.*, 2013)
TRPV1	-	-	(Utreras *et al.*, 2013)
TRPP1 TRPP2	-	-	(Jerman *et al.*, 2014)
TRPV1 TRPV3 TRPV4	-	-	(Tokuda *et al.*, 2015a)
TRPM5 Piezo2	-	-	(Khatibi Shahidi *et al.*, 2015)
TRPM7	-	-	(Nakano *et al.*, 2016; Ogata *et al.*, 2017)

= only functional evidence for the conditions tested, no gene/protein expression data provided

Table 3.2 Sensory ion channel expression in rat odontoblasts

Rat			
Channels present	Channels not present	Evidence for functional expression	References
TRPV1	-	Capsaicin induced inward currents, which were inhibited by capsazepine	(Okumura *et al.*, 2005)
-	TRPV1 TRPV2 TRPM8 TRPA1	No change in $[Ca^{2+}]_i$ in response to heat, cold, capsaicin, menthol, or icilin	(Yeon *et al.*, 2009)
TRPA1 $Na_v1.1$-1.9	-	-	(Byers & Westenbroek, 2011)
TRPV1	-	TRPV1 activation induced an increase in $[Ca^{2+}]_i$ and inward currents	(Tsumura *et al.*, 2012)
TRPM8 TRPA1		Increase in $[Ca^{2+}]_i$ in response to TRPM8 and TRPA1 activation, inhibited by respective antagonists	(Tsumura *et al.*, 2013)
TRPM7 TRPC1 TRPC6* TRPV4*	TRPM3	-	(Kwon *et al.*, 2014)
TRPV1# TRPV2# TRPV4# TRPA1#	TRPM8#	Mechanical stimulation induced an increase in $[Ca^{2+}]_i$, which was inhibited by TRPV1, TRPV2, TRPV4, and TRPA1 antagonists, but not TRPM8 antagonist	(Shibukawa *et al.*, 2015)
TRPM8	-	-	(Tokuda *et al.*, 2015b)
TRPA1#	-	High pH-induced increase in $[Ca^{2+}]_i$ is reduced by TRPA1 antagonist	(Kimura *et al.*, 2016)
TRPA1 TRPV1 TREK-1	-	-	(Cho *et al.*, 2016)
$K_v1.1$# $K_v1.2$# and/or $K_v1.6$#	-	Electrophysiological characterisation of respective slow activating voltage-dependent K^+ currents	(Kojima *et al.*, 2017)
TRPM7 Piezo2* TMC2*	Piezo1 TMC1	Increase in $[Ca^{2+}]_i$ in response to hypotonic solution and naltriben (TRPM7), both inhibited by TRPM7 antagonists	(Won *et al.*, 2018)
TRPV1	-	-	(Ohkura *et al.*, 2018)

* = detected in a small percentage of odontoblasts or expressed at low levels
# = only functional evidence for the conditions tested, no gene/protein expression data provided

Table 3.3 Sensory ion channel expression in human odontoblasts

Human			
Channels present	Channels not present	Evidence for functional expression	References
K_{Ca}	-	K_{Ca} currents activated by negative pressure and osmotic shock	(Allard *et al.*, 2000)
TREK-1	-	-	(Magloire *et al.*, 2003)
TRPP1 TRPP2	-	-	(Thivichon-Prince *et al.*, 2009)
TRPA1 TRPV1 TRPM8	-	▪ Increase in $[Ca^{2+}]_i$ in response to icilin, cinnamaldehyde, capsaicin, and menthol, blocked by non-selective TRP antagonist, TRPA1 antagonist, or capsazepine ▪ Increase in $[Ca^{2+}]_i$ in response to heat and cool temperatures, blocked by capsazepine, and cold, reduced by TRPA1 blocker and TRPA1 siRNA	(El Karim *et al.*, 2011)
β-ENaC γ-ENaC ASIC1* ASIC2 ASIC3* TRPV4	-	-	(Sole-Magdalena *et al.*, 2011)
TRPA1	-	-	(Kim *et al.*, 2012)
K_{Ca}[#] Na_vs (TTX-sensitive)[#]	-	Electrophysiological characterisation of respective currents	(Ichikawa *et al.*, 2012)
TRPA1 TRPV1[&] TRPV4	TRPM8	▪ Increase in $[Ca^{2+}]_i$ in response to GSK1016790A, blocked by selective TRPV4 antagonist ▪ Increase in $[Ca^{2+}]_i$ in response to allyl isothiocyanate and cinnamaldehyde, inhibited by TRPA1 antagonists ▪ No change in $[Ca^{2+}]_i$ in response to capsaicin or icilin	(Egbuniwe *et al.*, 2014)
TRPA1 TRPV4	-	▪ Increase in $[Ca^{2+}]_i$ in response to cinnamaldehyde and GSK1016790A ▪ Increase in $[Ca^{2+}]_i$ in response to hypotonic solution, inhibited by both TRPA1 and TRPV4 antagonists	(El Karim *et al.*, 2015)

TRPC1	-	Increase in $[Ca^{2+}]_i$ in response to thapsigargin, reduced in shRNA-TRPC1 cells	(Song *et al.*, 2017)
TRPC6	-	Increase in $[Ca^{2+}]_i$ in response to 1-oleoyl-2-acetyl-sn-glycerol, reduced in shRNA-TRPC6 cells	(Yang *et al.*, 2017)
TRPV1 TRPV2 TRPV3	-	-	(Wen *et al.*, 2017)
TRPM8	TRPA1	-	(Tazawa *et al.*, 2017)

* = detected in a small percentage of odontoblasts or expressed at low levels
# = only functional evidence for the conditions tested, no gene/protein expression data provided
& = gene expression detected, but no channel function

3.1.3 PARACRINE SIGNALLING FROM ODONTOBLASTS

In addition to the ability to detect external stimuli, a sensory role of odontoblasts in dentine hypersensitivity requires a mechanism to signal from odontoblasts to neurons. Since no synaptic connections could be detected between the two cell types in the teeth (Shiromoto, 1984; Byers *et al.*, 1987), paracrine signalling has been explored as a means of intercellular communication. ATP and glutamate have so far been proposed as potential mediators of this process. Cultured human and rat odontoblasts release ATP in response to TRPA1 and TRPV4 activation (Egbuniwe *et al.*, 2014) and direct mechanical stimulation (Shibukawa *et al.*, 2015), respectively. ATP is also released in human teeth *in vitro* in response to cold and mechanical stimulation to the exposed dentine (Liu *et al.*, 2015). While ATP release via connexin hemichannels, pannexin transmembrane channels, and vesicular exocytosis has been considered in the literature, most evidence point to the involvement of pannexin 1 (Liu *et al.*, 2015; Shibukawa *et al.*, 2015; Ikeda *et al.*, 2016). ATP hydrolysis enzyme nucleoside triphosphate diphosphohydrolase 2 (NTPDase2) has also been detected in the vicinity of odontoblasts and nerve fibres in human dental pulps (Liu *et al.*, 2012), suggesting local degradative regulation of ATP concentrations. Finally, the role of ATP as a mediator of odontoblast-neuron signalling is supported by the presence of purinergic $P2X_3$ receptors on dental pulp primary afferents (Alavi *et al.*, 2001; Jiang & Gu, 2002; Renton *et al.*, 2003).

Recently, two research groups also proposed the involvement of glutamate in the odontoblast-neuron communication. Cho and colleagues (2016) demonstrated the

presence of glutamate near the odontoblasts and their processes, glutamate release from odontoblasts in response to increased intracellular calcium concentrations, and expression of metabotropic glutamate receptor 5 (mGluR5) on the dental pulp primary afferents. Nishiyama and co-workers (2016) provided evidence for glutamate release from mechanically stimulated odontoblasts via glutamate-permeable anion channels and subsequent activation of mGluR receptors on the neighbouring trigeminal ganglion neurons in co-cultures. While we focused our attention on the mechanisms of ATP release from mouse odontoblast-like cells, a preliminary experiment testing if these cells release glutamate when stimulated will also be discussed.

3.1.4 Mouse dental pulp 17IA4 cells and odontoblastic differentiation

Immortalised mouse dental pulp 17IA4 cells were differentiated into odontoblast-like (OB) cells and used in our experiments as a cellular model for studying odontoblasts *in vitro*. These cells were established by Priam and colleagues (2005) by dissociation of first molar tooth germs from embryonic day (ED) 18 mice and subsequent cloning by limiting dilution. The mice used were transgenic for simian virus 40 (SV40) large T antigen under the control of the adenovirus early transcription unit 1A (E1A) promoter. This induces low-level expression of the SV40 oncogene, which causes inhibition of p53 and Rb family tumour suppressors (Ahuja *et al.*, 2005) and potential stimulation of telomerase activity (Yuan *et al.*, 2002), resulting in the immortalisation of the cells. We viewed the immortalised nature of 17IA4 cells as an advantage, as it enables their continuous use for multiple types of *in vitro* experiments, including functional studies, which would be difficult using primary mature odontoblasts. Moreover, mouse cells were favoured over odontoblast-like cells from other species when choosing a cellular model, as our later experimental plans involved co-culturing odontoblast-like cells with mouse trigeminal ganglion neurons (discussed in Chapter 6).

Most importantly, the researchers that established 17IA4 cells (Priam *et al.*, 2005) confirmed their identity as odontoblast precursors by demonstrating gene or protein expression of multiple odontoblastic markers, such as dentine matrix protein 1, dentine sialoprotein, nestin, type I collagen, osteopontin, and the transcription factor Runx2, as well as genes for LIM homeobox proteins 6 and 8, which are thought to be key transcription factors in tooth development (Grigoriou *et al.*, 1998). Further studies

provided some additional information about the odontoblast-like phenotype of these cells. Unlike freshly dissociated ED14 dental mesenchymal cells, but similarly to ED18 primary dental mesenchymal cells, cultured 17IA4 cells were unable to induce tooth formation after *in vitro* re-association with ED14 dental epithelium (Keller *et al.*, 2011). However, this is likely related to the developmental stage difference. On the other hand, even though conventionally cultured 17IA4 cells morphologically do not resemble typical odontoblasts that contain a cellular process (see Figure 3.1), they were demonstrated to form new dentine-like structures when implanted into mouse dental pulps (Lacerda-Pinheiro *et al.*, 2008), supporting their odontoblast-like function.

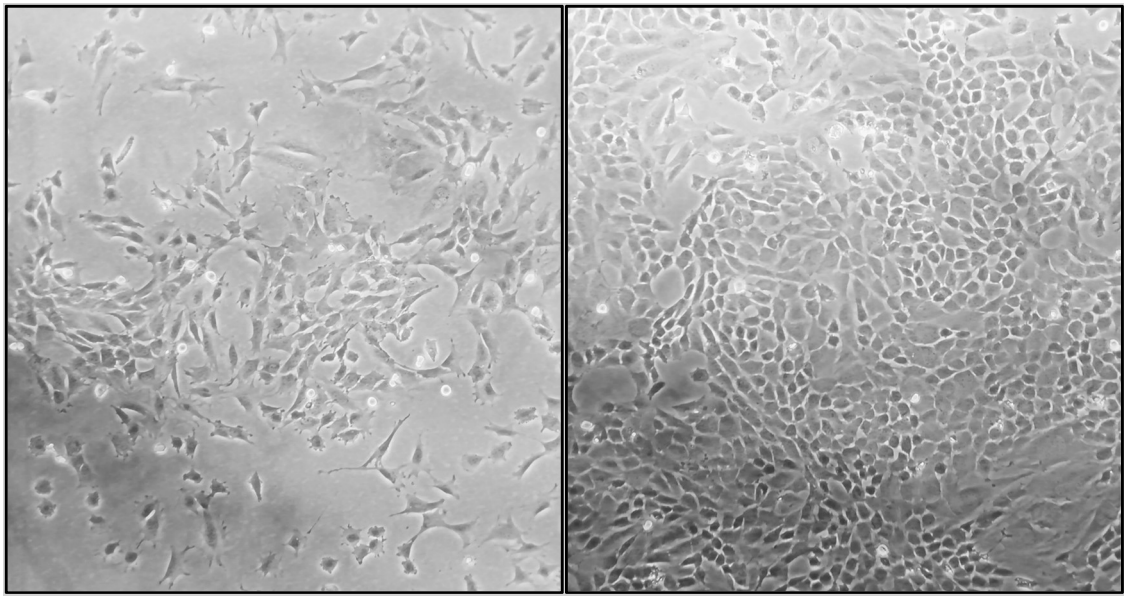

Figure 3.1 Mouse dental pulp 17IA4 cells

Photographs of sub-confluent and near-confluent 17IA4 cells (3 days in culture in both cases), visualised under phase contrast microscope.

To check that 17IA4 cells we obtained demonstrate the reported odontoblastic phenotype, preliminary tests for their *in vitro* odontogenic differentiation potential were performed before starting the main experiments. The details of odontoblastic markers used for gene expression studies can be found in Table 3.4.

3.1.5 OBJECTIVES OF THE PRESENT STUDY

Specific objectives of the experiments described in this chapter are as follows:

- To assess whether cultured mouse dental pulp 17IA4 cells provide an appropriate model for studying odontoblast function by testing their *in vitro* differentiation into odontoblast-like (OB) cells using gene expression and mineralisation assays.
- To determine functional expression of a selection of TRP channels, implicated in sensory transduction, in mouse OB cells using RT-PCR and calcium flux assay.
- To test the ability of bacterial wall components lipopolysaccharide (LPS) and lipoteichoic acid (LTA), and inflammatory mediator TNFα to modulate TRP channel function in mouse OB cells using calcium flux assay.
- To investigate whether activation of TRP channels in mouse OB cells stimulates ATP release and the potential underlying mechanisms, primarily by using pharmacological tools and bioluminescent detection of extracellular ATP concentration.
- To investigate whether stimulated mouse OB cells release glutamate, using bioluminescent detection of extracellular glutamate concentration.

Table 3.4 Odontoblastic markers used in this study

Protein (alternative name)	Symbol	Gene	Relevance to odontoblast function	Reference
Alkaline phosphatase	ALP	*Alpl*	Enzyme involved in dentine mineralisation	(Foster *et al.*, 2013)
Bone gamma-carboxyglutamic acid-containing protein (osteocalcin)	BGP	*Bglap*	Non-collagenous protein synthesised by odontoblasts	(Papagerakis *et al.*, 2002)
Bone sialoprotein 2 (integrin-binding sialoprotein)	BSP2	*Ibsp*	Extracellular matrix protein found in dentine	(Qin *et al.*, 2001)
Collagen type I, alpha 1	COL1α1	*Col1a1*	Major component of collagen present in dentine	(Linde & Goldberg, 1993)
Runt-related transcription factor 2 (core-binding factor subunit alpha 1)	RUNX2	*Cbfa1*	Transcription factor involved in odontoblast differentiation and tooth development	(D'Souza *et al.*, 1999)
Dentine matrix protein 1	DMP1	*Dmp1*	Non-collagenous protein important in odontoblast maturation and mineralisation	(Qin *et al.*, 2007)
Dentine sialophosphoprotein	DSPP	*Dspp*	Precursor for major non-collagenous dentine matrix components, involved in tooth development and mineralisation	(Sreenath *et al.*, 2003)
Distal-less homeobox 3 protein	DLX3	*Dlx3*	Transcription factor important for odontoblast polarisation and dentine formation	(Choi *et al.*, 2010)
LIM homeobox protein 6	LHX6	*Lhx6*	Transcription factors demonstrating restricted expression during tooth development	(Grigoriou *et al.*, 1998)
LIM homeobox protein 8 (7)	LHX8	*Lhx8*		
Secreted phosphoprotein 1 (osteopontin)	OPN	*Spp1*	Extracellular matrix protein that regulates dentine mineralisation	(McKee & Nanci, 1996)
Specificity protein 7 (Osterix)	OSX	*Sp7*	Transcription factor involved in odontoblast maturation and dentine synthesis	(Bae *et al.*, 2018)

3.2 Materials and methods

3.2.1 Reagents

The following reagents have been used in addition to the reagents listed in Chapter 2 (section 2.2). Bafilomycin A1, brilliant blue G, cinnamaldehyde, clodronic acid disodium salt (clodronate), EGTA, flufenamic acid, icilin, lipopolysaccharide (LPS, from *Escherichia coli*), lipoteichoic acid (LTA, from *Streptococcus faecalis*), and probenecid were all purchased from Sigma, UK. BAPTA-AM was obtained from Invitrogen. Carbenoxolone disodium salt was purchased from Alfa Aesar.

Bafilomycin A1, BAPTA-AM, cinnamaldehyde, and probenecid were all dissolved in dimethyl sulfoxide (DMSO; Sigma), whereas brilliant blue G, carbenoxolone, clodronate, and LTA were dissolved in dH_2O. EGTA was dissolved in ECS or cell culture medium, as required, and LPS was dissolved in ECS. Compounds were further diluted on the day of the experiment in either complete culture medium or ECS to achieve appropriate final concentrations (indicated in the text and figures).

3.2.2 Detection of odontoblast marker gene expression in 17IA4/OB cells

3.2.2.1 Reverse transcription polymerase chain reaction (RT-PCR)

RT-PCR and agarose gel electrophoresis were performed using the methods described in Chapter 2 (section 2.4). Where not specified on gel images, samples used were from 17IA4 cells grown in either non-differentiating (labelled '17IA4') or differentiating medium (labelled 'OB') for 7 days. Information on media formulations can be found in section 2.3.1.

3.2.2.2 Quantitative polymerase chain reaction (qPCR)

After the first-strand synthesis, described in section 2.4.2, cDNA from 17IA4/OB cells was diluted 1:15 in dH_2O to obtain 5 ng/µl. For each gene tested, forward and reverse primers (listed in Table 3.5) were freshly diluted to 10 µM in dH_2O in a primer master

mix. A qPCR master mix was then prepared, containing (per sample): 5 µl of LightCycler® 480 SYBR Green I Master (Roche), 0.5 µl of primer master mix, and 3.5 µl of molecular grade water. This was dispensed into a white 384-well plate at 9 µl/well, followed by the addition of 1 µl of cDNA or 1 µl of dH_2O (for no template control samples). All samples were tested in triplicate (technical replicates). The plate was then sealed, centrifuged for 20 seconds, and run using a Lightcycler 480 II (Roche) qPCR machine and a pre-set SYBR Green programme (pre-incubation at 95°C for 5 minutes, followed by 45 cycles of amplification at 95°C, 60°C and 72°C, 10 seconds each, with a single acquisition after each incubation at 72°C). A standard melting curve programme was then performed (95°C for 5 seconds, 65°C for 1 min, and temperature ramp up to 97°C with continuous acquisition). Melting curve analysis and agarose gel electrophoresis of the samples were used to confirm the identity and specificity of amplified products. Moreover, in order to assess primer efficiency, serial 5-fold dilutions of cDNA (from samples found to express highest levels of each gene in the previous run) were performed and tested for each primer pair. Seven-point standard curves (from cDNA being undiluted to diluted 1:15625) were constructed, and primer efficiencies were found to range from 1.84 to 2.00 (Table 3.5; $R^2 = 0.99$ in each case). To account for these differences in primer efficiency, Pfaffl relative quantification method (Pfaffl, 2001) was used to calculate relative fold changes in odontoblast marker gene expression (expressed as differentiated OB *vs.* undifferentiated 17IA4 cells at 1, 3 or 7 days, using *18S rRNA* as a reference gene).

Table 3.5 Primer pairs used for quantitative PCR (qPCR)

Mouse gene	Primer sequence (5'-3')	Size (bp)	Primer efficiency
18S rRNA	F: CTCAACACGGGAAACCTCAC R: CGCTCCACCAACTAAGAACG	110	1.95
Alpl	F: GGCCAGCTACACCACAACA R: CTGAGCGTTGGTGTTATATGTCTT	96	2.00
Col1α1	F: CATGTTCAGCTTTGTGGACCT R: GCAGCTGACTTCAGGGATGT	94	1.91
Dmp1	F: CTGTCCTGTGCTCTCCCAGT R: CTTCTGATGACTCACTGTTCGTG	118	1.84
Ibsp	F: AGTTAGCGGCACTCCAACTG R: TCGCTTTCCTTCACTTTTGG	73	1.92

3.2.3 Alkaline phosphatase activity assay

Undifferentiated 17IA4 cells were seeded in clear 96-well plates at equal density per well for each condition. The cells were grown for 14 days in total, with designated wells on the same plate exposed to either unsupplemented (non-differentiating) culture medium for 14 days, differentiating medium for 14 days, or the medium was switched from non-differentiating to differentiating for the last 1 or 7 days, as indicated. On the day of the assay, the medium was removed from the plate, and the cells were washed with room-temperature 1x Dulbecco's PBS (DPBS) containing no calcium and magnesium ions (Sigma). After removing DPBS, the cells were fixed using ice-cold 75% ethanol for 10 minutes, followed by washing twice with PBS containing 0.05% (v/v) Tween-20® (Santa Cruz Biotechnology). SIGMAFAST™ BCIP®/NBT (Sigma) tablet was dissolved in 10 ml dH_2O to yield a solution containing alkaline phosphatase substrate 5-bromo-4-chloro-3-indolyl phosphate (BCIP; 0.15 mg/ml), nitro blue tetrazolium (NBT, 0.30 mg/ml), Tris buffer (100 mM), and $MgCl_2$ (5 mM), pH 9.25–9.75. The cells were stained using this solution for 5 minutes at room temperature. After removing the substrate solution, the cells were washed again with PBS containing Tween-20. PBS (100 µl/well) was then added onto the cells, and absorbance was measured at a wavelength of 560 nm, corresponding to a blue-purple end-product NBT diformazan. The measurements of absorbance from each well were performed twice using FLUOstar Omega microplate reader (BMG Labtech). Average absorbance from cell-free blank control wells, which were exposed to the same solutions during the experiment, was subtracted from the values from cell-containing wells. An average of 4 wells was considered an $n = 1$. The data represent three independent experiments from different cell passages.

3.2.4 Alizarin red S staining

Undifferentiated 17IA4 cells were seeded in 6-well plates in either non-differentiating or differentiating (supplemented) medium at equal densities per well, and grown for 1-14 days, as indicated. On the day of the procedure, the medium was removed from the wells, and the cells were washed with room-temperature 1x DPBS containing no Ca^{2+} and Mg^{2+} (Sigma). After removing DPBS, the cells were fixed using ice-cold 75% ethanol for 10 minutes, washed twice with dH_2O, and stained with 2% (w/v) alizarin red S (ARS;

Sigma) solution in ddH_2O (pH adjusted to 4.2 using NaOH) for 30-45 minutes (the same amount of time for both conditions to enable direct comparisons). The wells were then washed twice with dH_2O to remove any unincorporated excess dye. The photographs of each well were then taken. The proportion of ARS-positive area in each well was determined using ImageJ software, with a threshold (red) set to 75.

3.2.5 Detection of changes in intracellular calcium concentration

The activity of different transient receptor potential (TRP) ion channels in non-differentiated 17IA4 or differentiated odontoblast-like (OB) cells was investigated using a microplate-based calcium flux assay, as described in section 2.5.1. These experiments involved a final 1:2 dilution of TRP channel agonists or respective vehicles, performed by automated addition of 50 µl of test compound to 50 µl of extracellular solution (ECS) already present in the cell-containing wells of a 96-well plate. In addition to the cells grown in the differentiating or non-differentiating αMEM-based media, 17IA4 cells grown in non-differentiating DMEM/F-12-based culture medium were also tested in the initial experiments, as this medium was used for growing 17IA4 cells by some other research groups (Keller *et al.*, 2011).

TRPV4 antagonist experiments involved pre-treatment of the cells with HC067047 (50 nM-10 µM) or DMSO vehicle for 15 minutes. Antagonist remained in contact with the cells throughout experimental runs. In the experiments involving cell pre-treatment with LPS, LTA, or tumour necrosis factor alpha (TNFα), these agents were either added to the culture medium (24-hour pre-treatments), included in the ECS during cell incubation with Fura-2AM (1-hour pre-treatments), or automatically added during prolonged experimental runs (10-minute pre-treatment with TNFα). LPS, LTA, and TNFα were washed off after the 1-hour pre-treatments but remained in contact with the cells during experimental runs in the case of 24-hour and 10-minute pre-treatments. Calcium chelation experiments involved an initial loading of the cells with a higher concentration of Fura-2AM (4 µM, 50 µl/well) for 30 minutes, followed by the addition of 50 µl/well of BAPTA-AM or DMSO vehicle at appropriate concentrations for another 30 minutes. After washing the cells with ECS, a combination of BAPTA-AM (10-200 µM) and EGTA (1 mM, pH 7.4) or the corresponding vehicle were added onto the cells,

and experimental runs were started 15 minutes later. The duration of calcium chelation experiments was also longer (15 minutes) to match corresponding ATP release assays. In all cases, vehicles used represented the solvent content of experimental compound solutions at the highest concentration tested in that experiment, as specified in result figure captions.

3.2.6 Measurement of ATP release

ATP release from OB cells was detected using the method for measuring extracellular ATP concentrations ($[ATP]_o$) described in section 2.6. In the TRPV4 blocker experiments, the cells were treated with HC067047 (10 μM) or 0.2% (v/v) DMSO vehicle for 15 minutes before adding the TRPV4 agonist GSK1016790A (100 nM). Initial calcium chelation experiments involved pre-treatment of the cells with BAPTA-AM (100 μM) or 0.33% (v/v) DMSO vehicle for 15 minutes before adding EGTA (final concentration of 1 mM, pH 7.4) for another 15 minutes, followed by the 15-minute treatment with GSK1016790A (100 nM). Experiments testing the effects of inhibitors of different ATP release mechanisms involved pre-treatment of the cells for 30 minutes, in the case of bafilomycin A1, brilliant blue G, carbenoxolone, clodronate, and *N*-ethylmaleimide, or 1 hour, in the case of flufenamic acid and probenecid. All blockers and Ca^{2+} chelators remained in contact with the cells during the agonist treatment. Direct effects of the BAPTA-AM (100 μM) and EGTA (1 mM, pH 7.4) combination on $[ATP]_o$, without the subsequent agonist stimulation, were tested after a 45- and 30- minute treatment, respectively, in order to reproduce the overall treatment times from previous calcium chelation experiments. Unlike in the previous experiments, the media samples from the wells treated with BAPTA-AM and EGTA, or from the corresponding vehicle-treated wells in the same 4-well plate, were additionally filtered using centrifuge tube filters (pore size of 0.22 μm; Sigma) before adding the assay reagent to remove any cells that may have detached. No difference was observed in ATP concentrations from samples filtered by fast pulse (20-30 seconds at approximately 6000 rpm) compared to slower spinning at 1000 rpm for 6 minutes. Therefore, all filtered samples were included in the analysis for each treatment.

3.2.7 Measurement of glutamate release

Undifferentiated 17IA4 cells were seeded into clear 4-well plates and grown in the differentiating medium to confluence. On the day of experiment, culture medium in the wells was carefully replaced with pre-warmed solutions of GSK1016790A (1 μM) or vehicle (0.1% (v/v) DMSO) in ECS. Fifteen minutes later, 50-microlitre samples were taken from each well and transferred into a white 96-well plate. Glutamate-Glo™ (Promega) assay was used according to the manufacturer's protocol to measure extracellular glutamate concentration. This involved the addition of equal volumes (50 μl) of glutamate detection reagent into the wells containing the samples, the same volume of glutamate standards, or ECS only (negative control). The plate was shaken for 30 seconds and incubated at room temperature away from light for 35-60 minutes, followed by luminescence detection using FLUOstar Omega microplate reader (BMG Labtech). Glutamate standards (10 nM, 100 nM, 1 μM, and 10 μM) were freshly prepared in ECS, and assayed in duplicate in order to generate a standard curve for each 96-well plate. Luminescence values from the negative control wells represented background luminescence and were subtracted from both experimental and glutamate standard results. Mean value of relative luminescence units (RLUs) per 1 nM glutamate was then calculated and used for conversion of RLUs to extracellular glutamate concentration. An average of measurements from two samples collected from two separate wells of a 4-well plate was considered an n of 1. Comparisons were made with vehicle-treated wells from the same 4-well plate. Data are from three independent experiments from different cell passages.

3.2.8 Statistics

Differences in alkaline phosphatase activity in 17IA4 cells exposed to the differentiating medium for 1-14 days compared with undifferentiated control cells were analysed using a one-way analysis of variance (ANOVA) with Dunnett's multiple comparisons test. Two-way ANOVA with Bonferroni's multiple comparisons test were used to analyse the differences in mean $[ATP]_o$ from experiments comparing the effects of: 1) two different GSK1016790A concentrations (100 nM and 1 μM) to their respective vehicles; 2) a single GSK1016790A concentration to the corresponding vehicle, when performing

experiments in either complete OB culture medium or ECS; or 3) different ATP release blockers to their respective vehicles on 100 nM GSK1016790A-induced responses. Unpaired Student's *t*-test was used to analyse the differences in mean extracellular glutamate concentrations in response to GSK1016790A (1 μM) or vehicle treatment, as well as mean $[ATP]_o$ from experiments comparing the effects of: 1) a single concentration of KCl or AITC to their respective vehicles; 2) TRPV4 antagonist HC067047 or Ca^{2+} chelators BAPTA-AM and EGTA to their respective vehicles on the responses induced by 100 nM GSK1016790A; 3) direct effects of BAPTA-AM and EGTA combination to the corresponding vehicle; or 4) calcium-free to calcium-containing ECS on 100 nM GSK1016790A-induced responses. EC_{50} and IC_{50} values for the agonist and antagonist of TRPV4 response were estimated using GraphPad Prism 7 software, after fitting sigmoidal concentration-response curves. A three-parameter model, which assumes a standard slope (Hill slope = 1.0 for the agonist or -1.0 for the antagonist) was used.

3.3 Results

3.3.1 Differentiated 17IA4 cells display odontoblast-like characteristics

First, RNA samples from 17IA4 cells cultured in either differentiating or non-differentiating medium for 1-7 days were studied by reverse transcription polymerase chain reaction (RT-PCR) and subsequent separation of amplified DNA products by agarose gel electrophoresis. Primers selective for the genes that encode enzymes, extracellular matrix components, and transcription factors found in odontoblasts, such as *Alpl*, *Col1a1*, *Cbfa1*, *Spp1*, *Sp7*, *Lhx6,* and *Lhx8* produced similar intensity bands from all of the samples tested (see Figure 3.2). By contrast, increasing band intensities were observed when using primers selective for *Bglap*, *Dlx3*, *Dmp1*, and *Ibsp* genes. In particular, the greatest band intensities for *Bglap*, *Dlx3*, and *Ibsp* corresponded to the longest 17IA4 cell exposure to the differentiating medium, whereas band intensities for *Dmp1* seemed to increase with time in culture, in both non-differentiating and differentiating media. Since similar transcript levels of *Gapdh*, used as an internal

control, were detected in all of the samples, the observed differences are unlikely to arise from unequal amounts of total cDNA in different RT-PCR products.

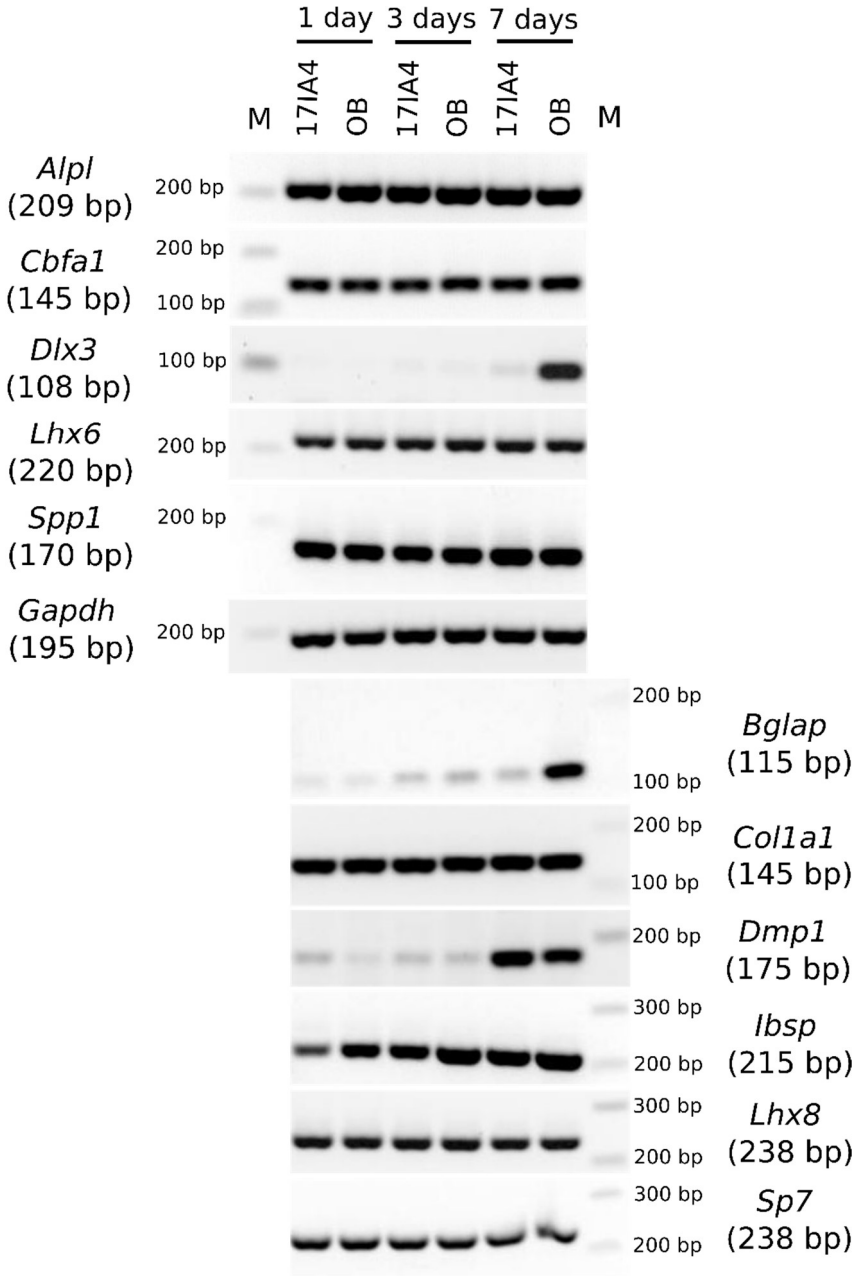

Figure 3.2 Cultured 17IA4 cells express multiple genes typical for odontoblasts

Reverse transcription polymerase chain reaction (RT-PCR) analysis of odontogenic gene expression in mouse dental pulp 17IA4 cells grown in either non-differentiating (17IA4) or differentiating (OB) medium for 1, 3, or 7 days, as indicated above the gels. Inverted colour images of 2% agarose gels are presented in the figure. M – Quick-Load® 100 bp DNA ladder (New England Biolabs).

To further explore the changes in some of the main odontoblast marker gene expression during 17IA4 cell differentiation, the same samples were tested by quantitative PCR (qPCR) using different primer pairs (Table 3.5). Based on low and relatively consistent raw cycle threshold (Ct) values among all of the samples tested, *18S rRNA* was found to be a suitable reference gene, not affected by 17IA4 cell differentiation (see Table 3.6). Among the four odontoblast marker genes tested, *Col1a1* was the most highly expressed, with mean raw Ct values ranging from 16.84 to 18.50. When *Col1a1* expression data from 17IA4 cells exposed to the differentiating medium was normalised to *18S rRNA*, a 1.8 ± 0.6-fold increase in *Col1a1* expression was detected after 7 days in the differentiating medium, compared to the samples from the cells grown in the non-differentiating medium for the same number of days (Figure 3.3). Alkaline phosphatase (ALP) and bone sialoprotein 2 (BSP2) gene expression levels were already increased after 1 day in the differentiating medium, with a considerable 20.5 ± 4.5- and 218.5 ± 45.3-fold respective increase after 7 days in the differentiating medium. By contrast, dentine matrix protein 1 (DMP1) gene expression levels were on average 1.4 to 5.9 times lower in the cells exposed to the differentating medium, compared with those exposed to the non-differentiating medium. However, similarly to the pattern seen in Figure 3.2, based on raw Ct values, an overall increase in DMP1 gene expression levels was observed in 7-day samples, compared to 1-day and 3-day samples.

It should be noted that RT-PCR and qPCR analyses for another odontoblast marker gene *Dspp*, which encodes dentine sialophosphoprotein, are not reported due to issues with the initial primer pairs tested. This is likely related to the long length of the designed primers (22-27 nt), which was supposed to ensure the primer specificity for this gene. However, a different primer pair (listed in Table 2.2), identified from multiple sources in the literature, was included in a later RT-PCR analysis. A faint band produced by these *Dspp* primers from the 17IA4 (7 days in the differentiating medium) sample can be seen in Figure 3.6.

Table 3.6 Raw cycle threshold (Ct) values for 17A4 cell samples tested by qPCR

Mean Ct values ± standard errors of the mean (SEM; 2-3 technical replicates) for 17IA4 cells grown in either non-differentiating or differentiating (supplemented) medium for 1, 3, or 7 days, as quantified by quantitative PCR (qPCR). 18S rRNA, 18S ribosomal RNA used as a reference gene; ALP, alkaline phosphatase; BSP2, bone sialoprotein 2/integrin-binding sialoprotein; COL1α1, collagen, type I, alpha 1; DMP1, dentine matrix protein 1.

Target	Non-differentiating			Differentiating		
	1 day	3 days	7 days	1 day	3 days	7 days
18S rRNA	7.43 ± 0.02	6.76 ± 0.06	7.91 ± 0.11	7.07 ± 0.04	7.83 ± 0.03	7.13 ± 0.05
ALP	26.32 ± 0.07	24.22 ± 0.04	25.27 ± 0.09	24.15 ± 0.08	23.02 ± 0.02	20.20 ± 0.08
BSP2	31.60 ± 0.26	28.76 ± 0.07	27.43 ± 0.06	29.49 ± 0.11	25.69 ± 0.39	18.40 ± 0.03
DMP1	30.75 ± 0.10	30.40 ± 0.11	24.51 ± 0.02	32.51 ± 0.04	32.27 ± 0.45	26.56 ± 0.07
COL1α1	17.57 ± 0.06	17.56 ± 0.03	18.50 ± 0.12	17.42 ± 0.10	18.43 ± 0.07	16.84 ± 0.13

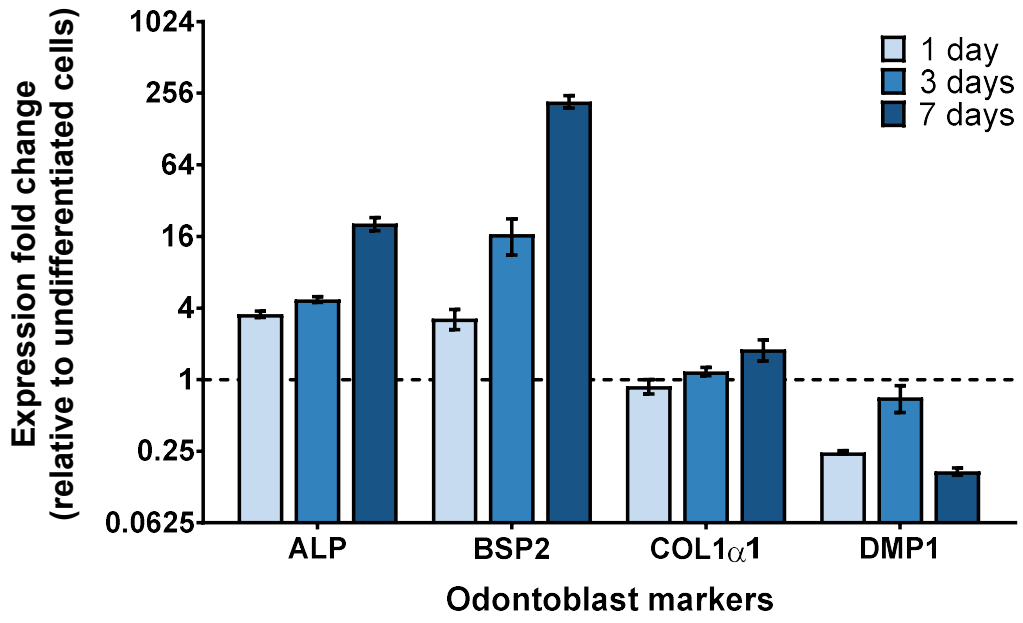

Figure 3.3 Relative quantification of odontoblast marker gene expression changes during 17IA4 cell differentiation

Quantitative PCR analysis of odontoblast marker gene expression in 17IA4 cells exposed to the differentiating medium for 1, 3, or 7 days, normalised using 18S rRNA as a reference gene, and expressed relative to 17IA4 cells grown in the non-differentiating medium for the same amount of time. Data are reported as mean ± SEM from 2-3 technical replicates. Note that *y* axis is on a log2 scale. ALP, alkaline phosphatase; BSP2, bone sialoprotein 2/integrin-binding sialoprotein; COL1α1, collagen, type I, alpha 1; DMP1, dentine matrix protein 1.

An ALP enzyme activity assay was then performed to test if the observed changes in odontoblast marker gene expression correspond to altered 17IA4 cell mineralising ability. Indeed, a gradual increase in ALP activity was detected (Figure 3.4), with levels significantly higher after 7 and 14 (out of 14) days in the differentiating medium, compared with 14 days in the non-differentiating medium (p = 0.010 and 0.001, respectively).

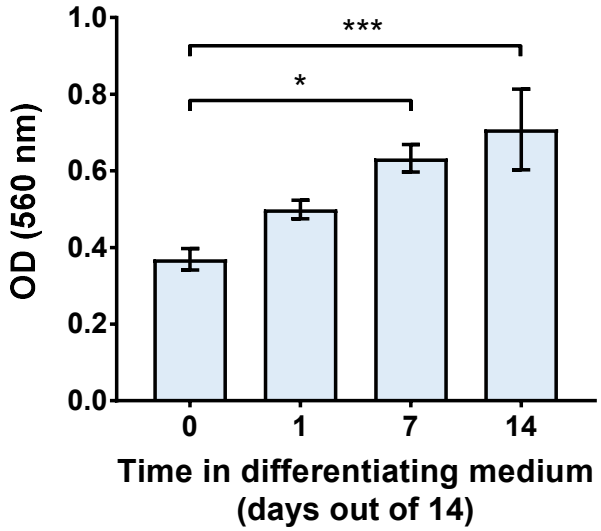

Figure 3.4 Differentiation of 17IA4 cells increases alkaline phosphatase enzyme activity

Optical density corresponding to the amount of alkaline phosphatase reaction product, measured at 560 nm from 17IA4 cells grown in either non-differentiating culture medium for 14 days (0 days in differentiating medium) or for 1, 7, or 14 (out of 14) days in differentiating medium. Data are presented as mean absorbance values per well ± SEM. $^{*}p < 0.05$; $^{***}p < 0.005$ *vs.* 0 days in differentiating medium (one-way ANOVA with Dunnett's *post hoc* test; n = 8 quadruplicate measurements from 3 independent experiments).

The formation of mineralised nodules by cultured 17IA4 cells was also tested by staining with alizarin red S (ARS) dye. Due to its ability to interact with calcium ions, ARS is widely used to detect various calcium-rich deposits in cell culture. As an example, ARS reacts with Ca^{2+} in hydroxyapatite crystals, which are known to be present in the dentine matrix, by both chelation and salt formation (Moriguchi *et al.*, 2003). An increase from 0.42% to 99.85% in the ARS-stained area was observed in the cell-containing wells exposed to the differentiating medium for 1 and 14 days (Figure 3.5). By contrast, only some background staining could be seen in the wells exposed to the non-differentiating medium, with a maximum ARS-stained area of 3.03% at 7 days.

Collectively, these results provided sufficient evidence for the odontoblast-like phenotype of differentiated 17IA4 cells (further referred to as OB cells), supporting their use in further studies.

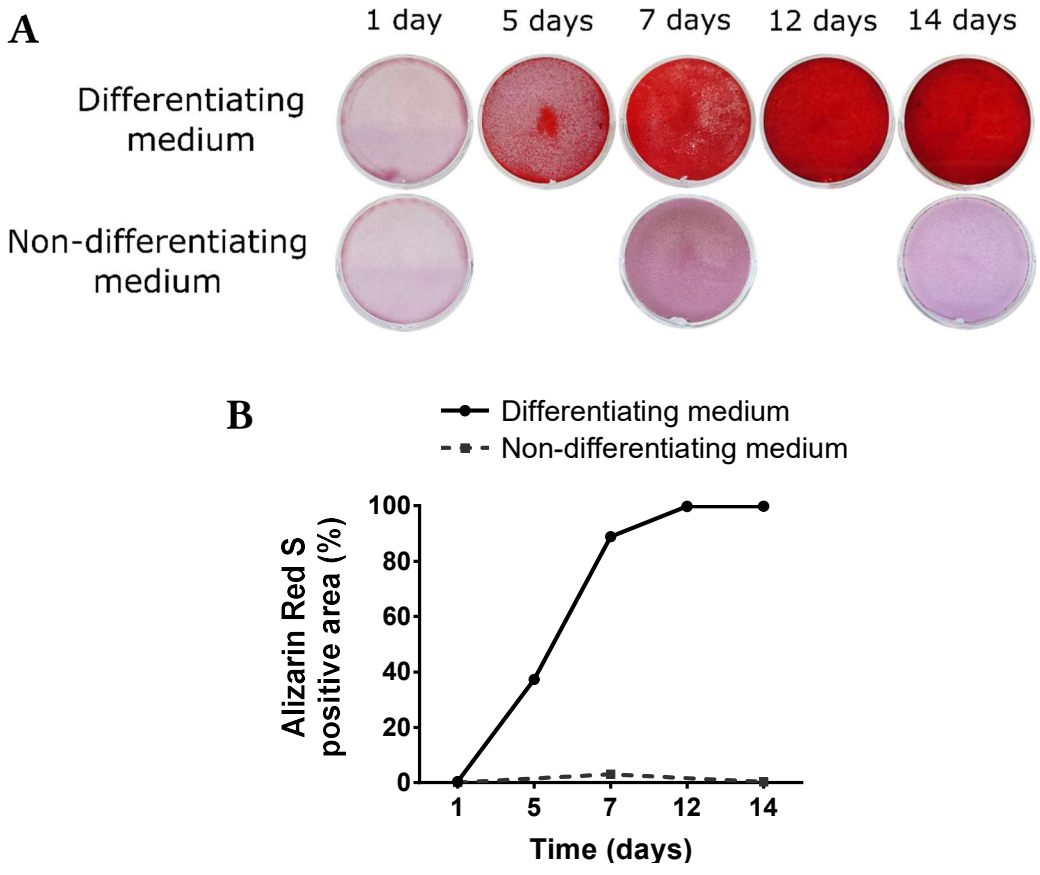

Figure 3.5 Differentiated 17IA4 cells display enhanced mineralisation

A) Alizarin red S staining of calcium minerals deposited by 17IA4 cells grown in either differentiating or non-differentiating medium for 1-14 days. *B)* Quantification of the percentage of alizarin red S-stained area in each well.

3.3.2 Characterisation of transient receptor potential ion channel functional expression in mouse odontoblast-like cells

Given the proposed roles of TRP channels in sensing external stimuli by odontoblasts, the expression of multiple TRP channels in OB cells was examined. Separation of RT-PCR products by agarose gel electrophoresis produced bands for *Trpv4* and *Trpm7* at predicted sizes (see Figure 3.6). A faint band was also produced for *Trpv1*, but not *Trpa1*, *Trpm8*, or *Trpc5*, from the OB sample. Since TRPA1, TRPC5, TRPM8, and TRPV1 channels are known to be expressed in mouse trigeminal ganglia (TG; Manteniotis *et al.* (2013); Vandewauw *et al.* (2013)), mouse TG tissue was used as a positive control for testing the corresponding primer pairs. Intense bands for all these targets were produced from TG tissue at predicted sizes. While two bands were produced for *Trpm8*, suggesting some primer non-specificity, both were completely absent from the OB sample.

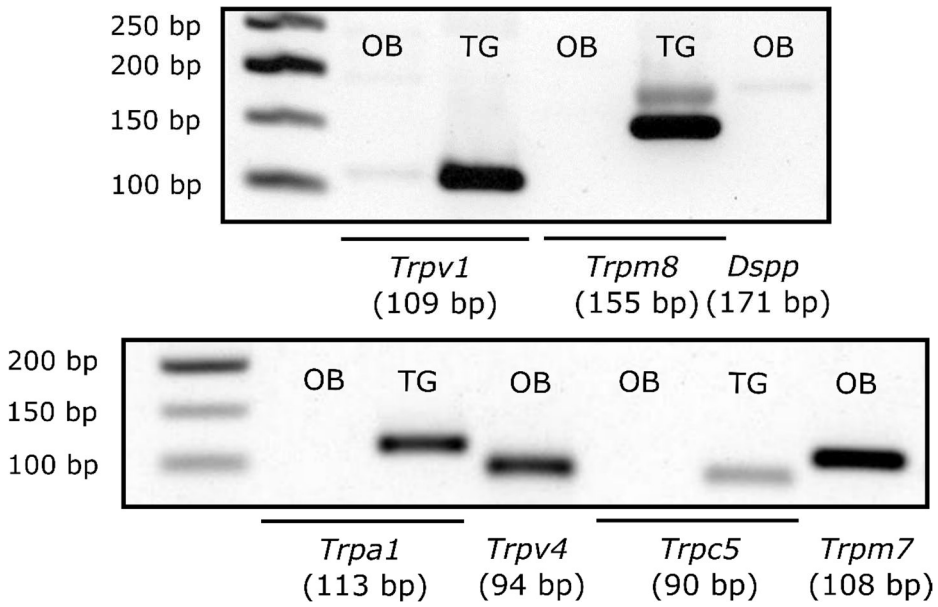

Figure 3.6 Gene expression of DSPP and TRP ion channels in OB cells

Gel electrophoresis of RT-PCR products from odontoblast-like (OB) cell samples produced bands for *Trpv1*, *Dspp*, *Trpv4*, and *Trpm7*, but not for *Trpm8*, *Trpa1*, or *Trpc5*. The same primers for *Trpa1*, *Trpc5*, *Trpv1*, and *Trpm8* produced intense bands from mouse trigeminal ganglion (TG) tissue sample, used as a positive control. Inverted colour images are presented in the figure. First lane of both gels contains Quick-Load® Purple 50 bp DNA Ladder (New England Biolabs).

A microplate-based calcium flux assay was then used to determine whether some of the main TRP channels reported by others to be expressed in odontoblasts, namely TRPA1, TRPM8, TRPV1, and TRPV4, are functional in mouse OB cells. The effects of different formulations of cell culture medium were also tested. This was done by comparing the concentration-response curves for TRP channel agonists between OB cells (grown in the differentiating αMEM-based medium) and undifferentiated 17IA4 cells (grown in either non-differentiating αMEM-based or DMEM/F-12-based culture medium).

The TRPA1 agonists allyl isothiocyanate (AITC) and cinnamaldehyde caused an increase in Fura-2AM emission intensity ratio (F_{340}/F_{380}) above baseline (Figure 3.7A-B), indicating increased intracellular Ca^{2+} concentrations ($[Ca^{2+}]_i$). However, this was only seen at concentrations of 100 μM or higher. Similar increases in F_{340}/F_{380} were observed in the cells grown in all three types of media (see Figure 3.7C-D). By contrast, a TRPM8 agonist icilin, tested at concentrations up to 80 times higher than the reported EC_{50} (Andersson *et al.*, 2004), did not induce any changes in F_{340}/F_{380} (see Figure 3.8). Similarly to the TRPA1 activators, a TRPV1 agonist capsaicin only induced changes in F_{340}/F_{380} above baseline at the highest concentrations tested (5 and 10 μM; Figure 3.9). The greatest ratio increase in response to 10 μM capsaicin application, detected in the cells grown in the differentiating medium, was 0.39 ± 0.17.

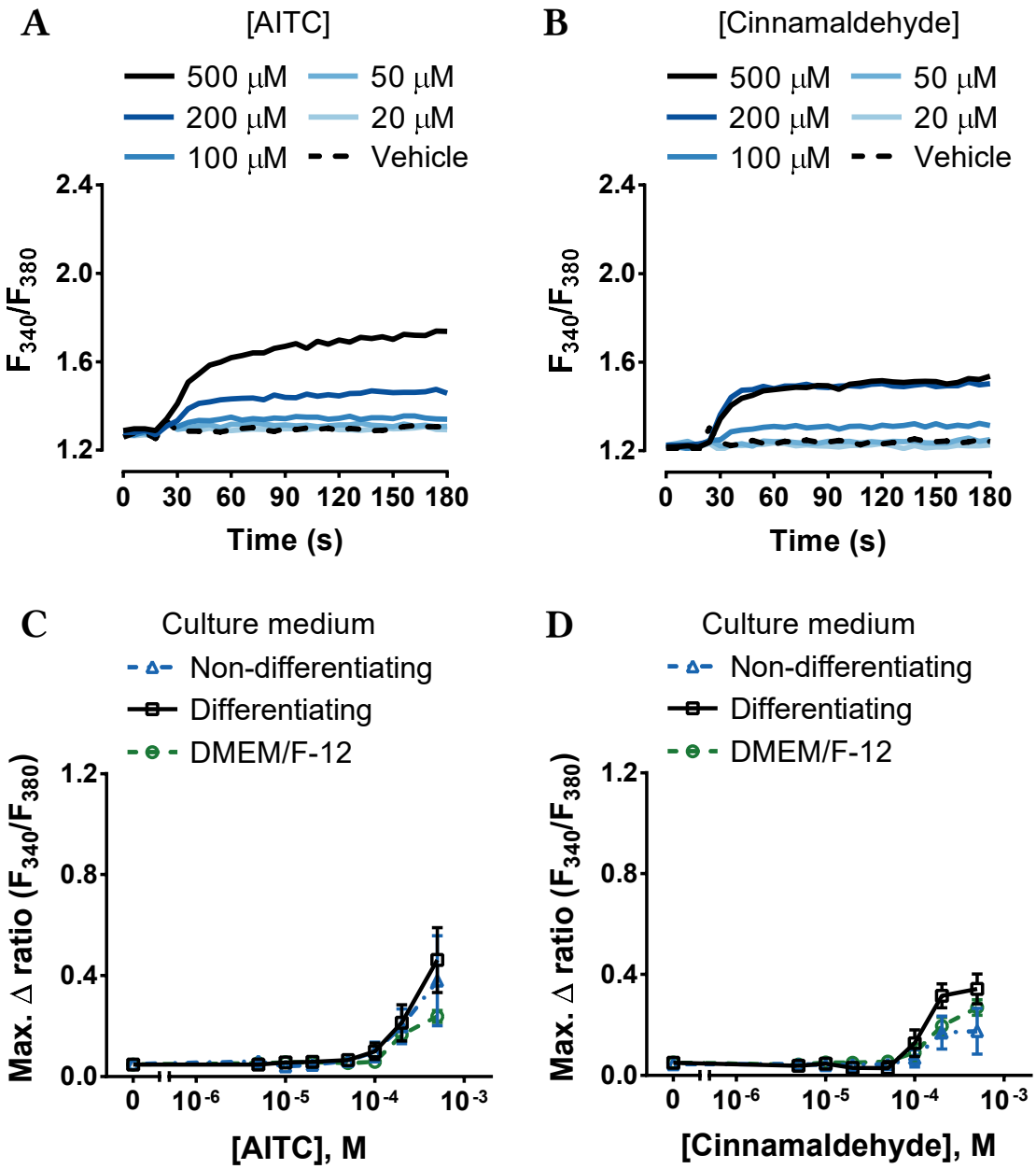

Figure 3.7 High concentrations of TRPA1 agonists increase $[Ca^{2+}]_i$ in OB cells

A-B) Average traces of differentiated (odontoblast-like) cell responses to allyl isothiocyanate (AITC; 20-500 µM), cinnamaldehyde (20-500 µM), or 0.5-0.65% (v/v) DMSO used as a vehicle control. Fura-2AM fluorescence ratios (340 nm/380 nm) were recorded for 3 minutes, with test compound or vehicle addition at 20 seconds. Error bars and traces for the lowest concentrations tested (5 and 10 µM) have been omitted for clarity. *C-D)* Irrespective of the culture medium and differentiation status of 17IA4 cells, both AITC and cinnamaldehyde increased intracellular Ca^{2+} concentration, but only when used at concentrations of 100 µM or higher. Data are presented as mean maximal Fura-2AM ratio changes from baseline ± SEM (n = 3-4 triplicate measurements from 3-4 independent experiments).

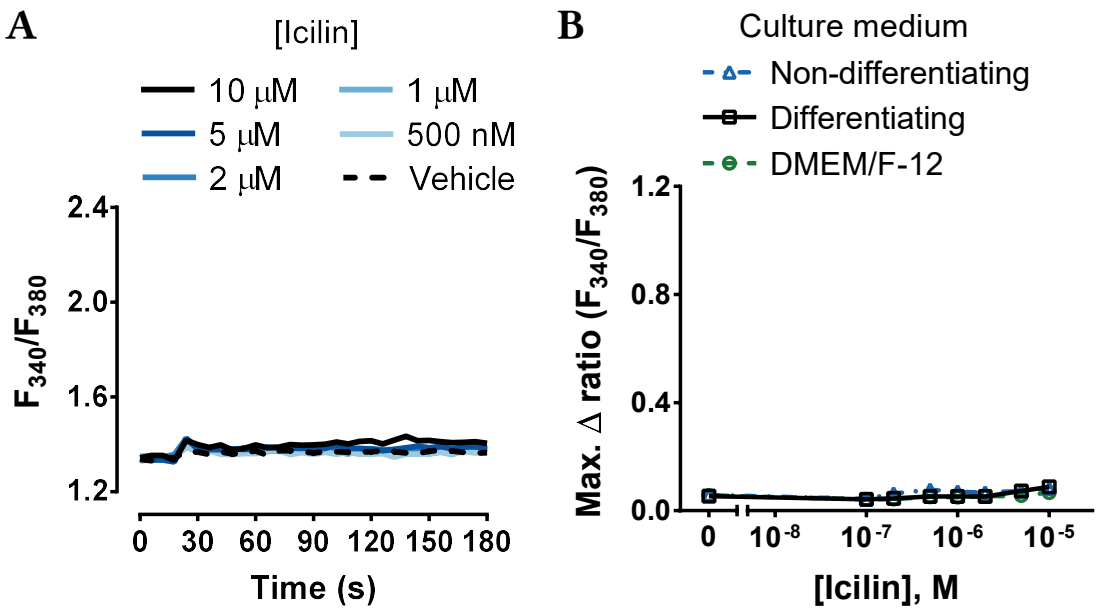

Figure 3.8 TRPM8 agonist does not affect $[Ca^{2+}]_i$ in OB cells

A) Average traces of differentiated (odontoblast-like) cell responses to the TRPM8 agonist icilin or 0.1% (v/v) DMSO used as a vehicle control. Fura-2AM fluorescence ratios (340 nm/380 nm) were recorded for 3 minutes, with icilin or vehicle addition at 20 seconds. Error bars and traces for the lowest concentrations tested (100 and 200 nM) have been omitted for clarity. *B)* Icilin did not affect $[Ca^{2+}]_i$ at the concentrations tested (0.1-10 μM), irrespective of the culture medium and differentiation status of 17IA4 cells. Data are presented as mean maximal Fura-2AM ratio changes from baseline ± SEM (n = 3 triplicate measurements from 3 independent experiments).

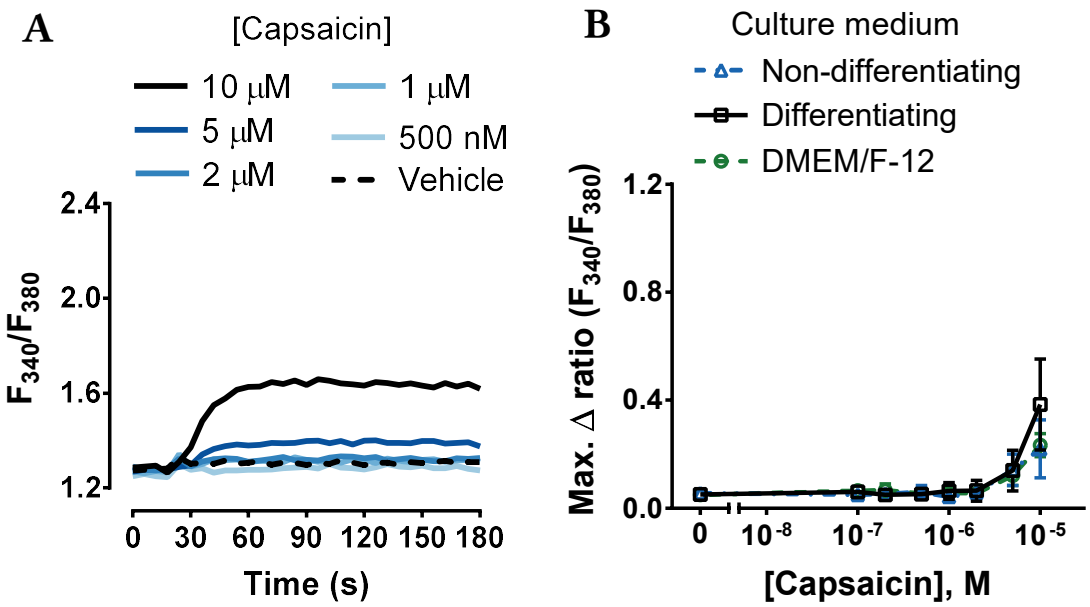

Figure 3.9 High concentrations of TRPV1 agonist capsaicin increase $[Ca^{2+}]_i$ in OBs

A) Average traces of differentiated (odontoblast-like) cell responses to the TRPV1 agonist capsaicin (0.5-10 μM) or 0.1% (v/v) DMSO used as a vehicle control. Fura-2AM fluorescence ratios (340 nm/380 nm) were recorded for 3 minutes, with capsaicin or vehicle addition at 20 seconds. Error bars and traces for the lowest concentrations tested have been omitted for clarity. *B)* Irrespective of the culture medium and differentiation status of 17IA4 cells, capsaicin increased $[Ca^{2+}]_i$, but only when used at concentrations of 5 and 10 μM. Data are presented as mean maximal Fura-2AM ratio changes from baseline ± SEM (n = 3 triplicate measurements from 3 independent experiments).

Finally, a TRPV4 agonist GSK1016790A caused a concentration-dependent increase in $[Ca^{2+}]_i$, with estimated EC_{50} values of 107 ± 59 nM, 69 ± 56 nM, and 265 ± 98 nM for the cells grown in the differentiating, non-differentiating αMEM-based, and DMEM/F12-based culture medium, respectively (see Figure 3.10A-B). The mean maximum Fura-2AM fluorescence ratio changes in response to 1 μM GSK1016790A were 0.84 ± 0.18, 0.76 ± 0.18, and 0.46 ± 0.05, respectively. Based on the greatest EC_{50} and the smallest amplitude of responses to GSK1016790A, DMEM/F12-based culture medium appears to provide suboptimal conditions for 17IA4 cell function. Therefore, only αMEM-based medium was used to culture the cells for further studies. The differentiation process did not seem to affect 17IA4 cell responses to the TRPV4 agonist. However, to ensure the results are most applicable to odontoblasts, only OB cells, which were exposed to the differentiating medium prior to experiments, were subsequently studied.

In order to confirm that the observed OB cell responses to GSK1016790A were exclusively due to TRPV4 activation, in a separate experiment, the cells were pre-treated with a selective TRPV4 inhibitor HC067047 before the application of GSK1016790A (200 nM). HC067047 blocked the GSK1016790A-induced increase in $[Ca^{2+}]_i$ in a concentration-dependent manner (see Figure 3.10C), with mean maximum F_{340}/F_{380} ratio changes of 1.24 ± 0.07 and 0.05 ± 0.01 in the cells pre-treated with vehicle and 10 μM HC067047, respectively. The IC_{50} value for HC067047 was estimated to be 819 ± 62 nM.

Overall, these results demonstrate the presence of functional TRPV4 channels in OB cells, encouraging further investigation into their role in odontoblast sensory mechanisms.

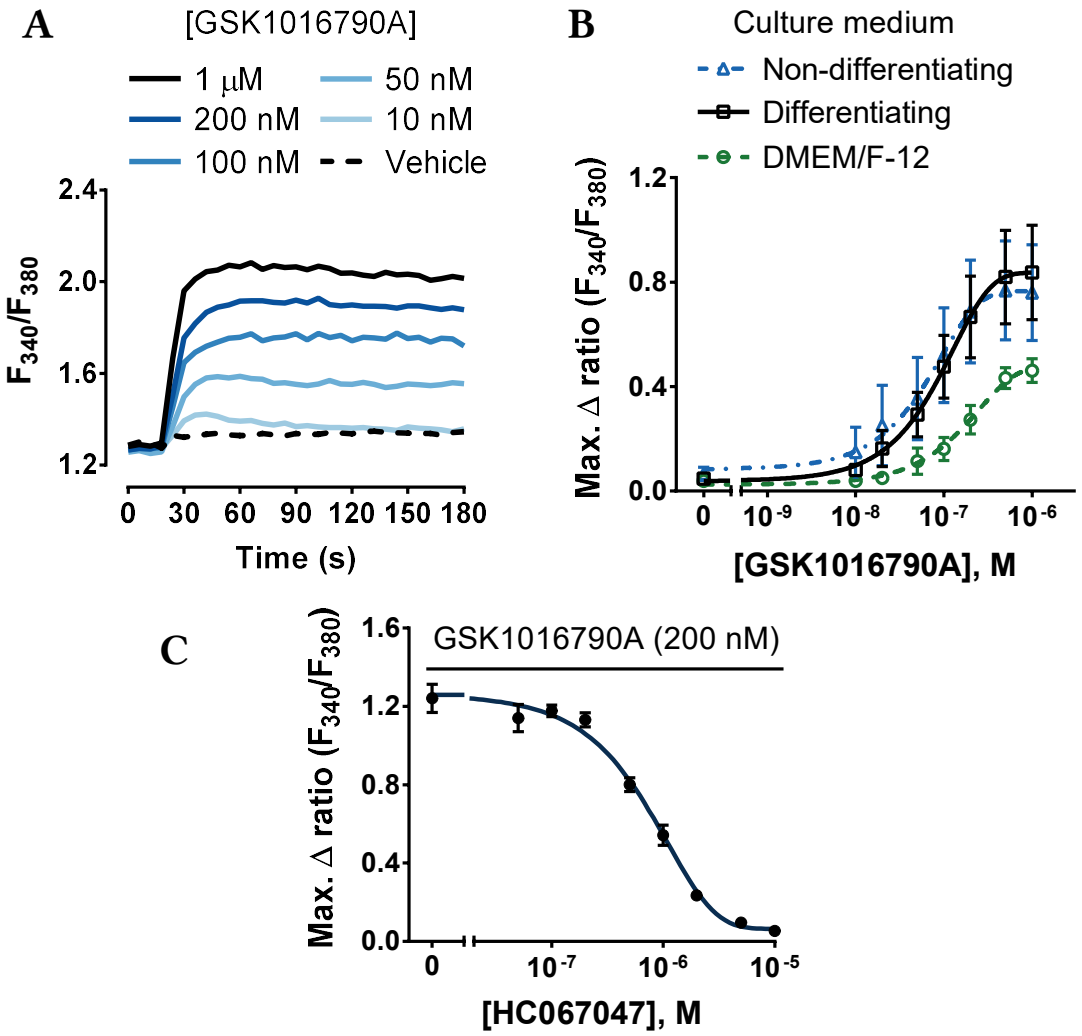

Figure 3.10 TRPV4 activation on OB cells causes a concentration-dependent increase in $[Ca^{2+}]_i$

A) Average traces of differentiated (odontoblast-like) cell responses to the TRPV4 agonist GSK1016790A (10 nM-1 μM) or 0.1% (v/v) DMSO used as a vehicle control. Fura-2AM fluorescence ratios (340 nm/380 nm) were recorded for 3 minutes, with GSK1016790A or vehicle addition at 20 seconds. Error bars and traces of cells exposed to 20 nM and 500 nM GSK1016790A have been omitted for clarity. *B)* GSK1016790A caused a concentration-dependent increase in intracellular Ca^{2+} concentration, irrespective of the differentiation status of 17IA4 cells. The amplitude of responses was lowest in undifferentiated 17IA4 cells grown in DMEM/F-12-based culture medium. Data are presented as mean maximal Fura-2AM ratio changes from baseline ± SEM (n = 4 triplicate measurements from 4 independent experiments). *C)* Concentration-response relationship of the TRPV4 antagonist HC067047 pre-treatment on the intracellular Ca^{2+} increase caused by GSK1016790A (200 nM) application (mean ± SEM; n = 4-8 triplicate measurements from 3 independent experiments). Cells were pre-treated with HC067047 (50 nM-10 μM) or its vehicle (0.2% (v/v) DMSO; '0' point on the x axis) for 15 minutes before the start of fluorescence recordings. Antagonist remained in contact with the cells throughout experimental runs.

3.3.3 Investigating the potential modulation of TRPV4 activity by bacterial wall components and host inflammatory mediators

Previous studies have demonstrated the expression of Toll-like receptors 2 and 4 (TLR2 and TLR4) in odontoblasts (Durand *et al.*, 2006; Veerayutthwilai *et al.*, 2007). OB cells were also found to express the genes for both TLR4 and TLR2 (see Figure 3.11).

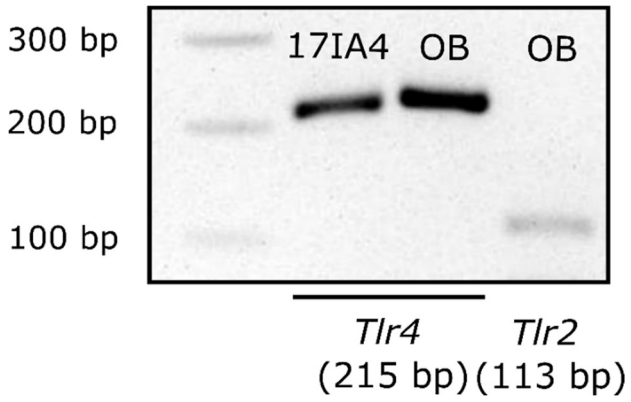

Figure 3.11 OB cells express Toll-like receptors 2 and 4

Gel electrophoresis of RT-PCR products from odontoblast-like (OB) cell samples produced bands for both *Tlr4* and *Tlr2*. A *Tlr4* band was also produced from pre-odontoblastic 17IA4 cell sample. Inverted colour image of the gel is presented in the figure. First lane contains Quick-Load® 100 bp DNA ladder (New England Biolabs).

Bacterial wall components that are known to activate these receptors, namely lipopolysaccharide (LPS; Gram-negative bacteria) and lipoteichoic acid (LTA; Gram-positive bacteria), were then tested for their ability to sensitise TRPV4 activity in OB cells. However, as seen in Figure 3.12A-B, a 1- or 24-hour cell pre-treatment with either LPS or LTA did not affect the increase in Fura-2AM emission ratio that was induced by a submaximal concentration of GSK1016790A (50 nM).

In addition, a short-term pre-treatment with an inflammatory mediator tumour necrosis factor alpha (TNFα) has been reported to sensitise TRPV4 channels on human odontoblast-like cells (El Karim *et al.*, 2015). However, pre-exposure of mouse OB cells to murine TNFα for 10 minutes or 1 hour failed to potentiate the TRPV4-dependent increase in $[Ca^{2+}]_i$ (Figure 3.12C).

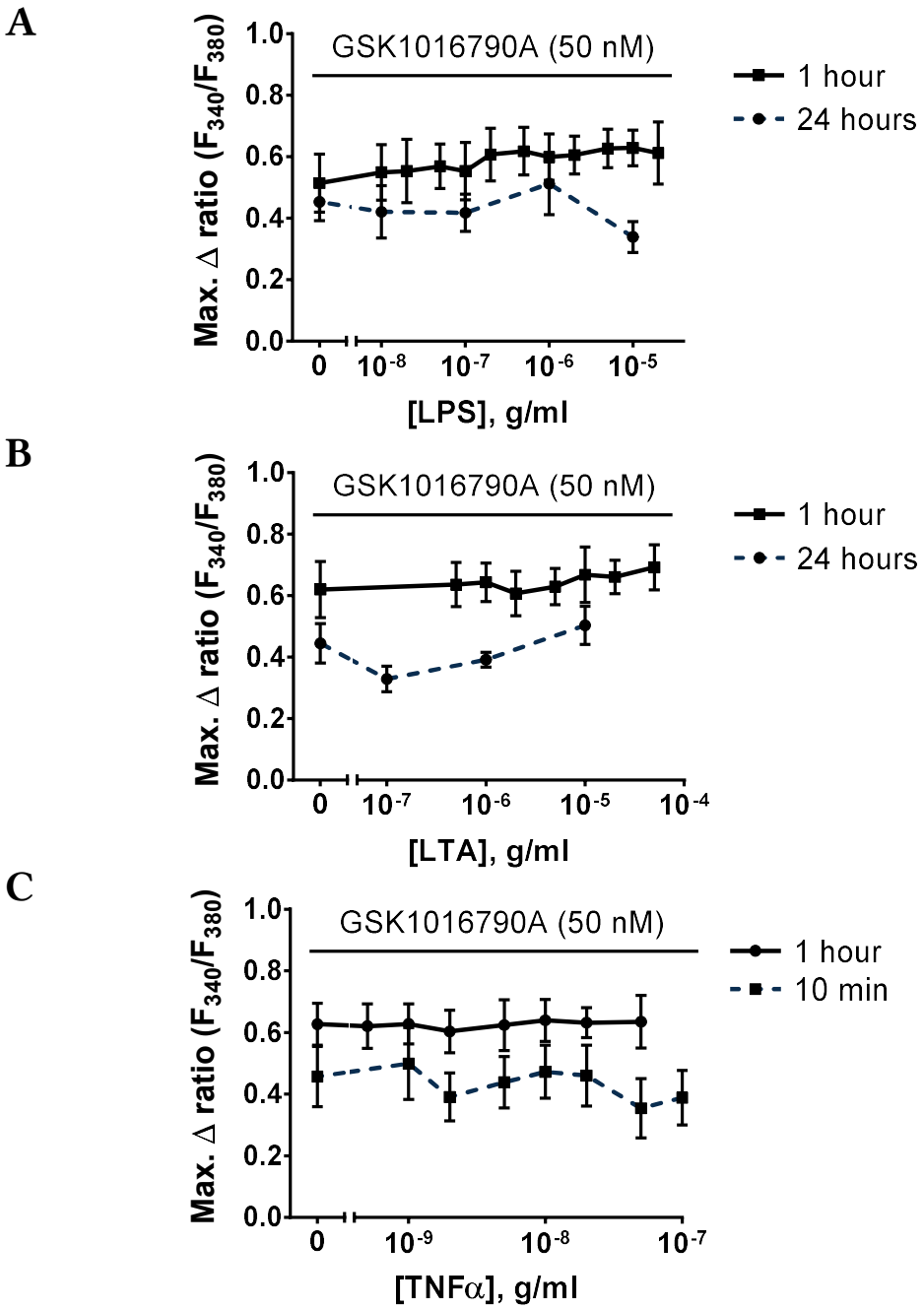

Figure 3.12 Bacterial wall components and inflammatory mediator TNFα fail to sensitise TRPV4 channels on OB cells

Concentration-response relationships for the modulating effects of OB cell pre-treatment with *A)* lipopolysaccharides (LPS) or *B)* lipoteichoic acid (LTA) for 1 hour or 24 hours, or *C)* 10-minute/1-hour pre-treatment with tumour necrosis factor alpha (TNFα) on 50 nM GSK1016790A-induced calcium flux. Point '0' on the *x* axis represents identical pre-treatment with a corresponding vehicle. Lowest concentrations of LPS (0.1 and 1 ng/ml) and LTA (0.1, 1, and 10 ng/ml) tested in the 24-hour pre-treatment experiments have been omitted for clarity. Data are mean maximal Fura-2AM ratio changes from baseline ± SEM (n = 3-5 triplicate measurements from 2-4 independent experiments).

These results suggest that TRPV4 channels in OB cells are not sensitised by bacterial wall components and inflammatory host mediators, at least in the case of molecules and conditions tested. Other aspects of the potential contribution of TRPV4 channels to the sensory role of odontoblasts were explored next.

3.3.4 OB CELLS RELEASE ATP IN RESPONSE TO TRPV4 CHANNEL ACTIVATION

To examine if mouse OB cells, similarly to human odontoblast-like cells (Egbuniwe *et al.*, 2014), release ATP in response to TRPV4 activation, extracellular ATP concentrations ($[ATP]_o$) were measured in the culture medium of OB cells exposed to the TRPV4 agonist GSK1016790A (100 nM and 1 μM). These concentrations approximately correspond to the EC_{50} and EC_{90} values previously identified in the calcium flux experiments (section 3.3.2, Figure 3.10). GSK1016790A caused a significant concentration-dependent increase in $[ATP]_o$ by 19.37 ± 4.97 nM (100 nM GSK1016790A) and 29.53 ± 5.39 nM (1 μM GSK1016790A) above respective vehicle control levels (p = 0.004 and $p < 0.001$, respectively; Figure 3.13A).

In a separate experiment, to confirm the involvement of TRPV4 in GSK1016790A-induced ATP release, OB cells were pre-treated with the selective TRPV4 antagonist HC067047 (10 μM), and the increase in $[ATP]_o$ induced by 100 nM GSK1016790A was measured (see Figure 3.13B). Mean $[ATP]_o$ from the cells pre-treated with HC067047 (9.33 ± 0.65 nM) was significantly lower than from vehicle-pre-treated cells (56.62 ± 10.83 nM; p = 0.002) and was comparable to the baseline levels observed in Figure 3.13A.

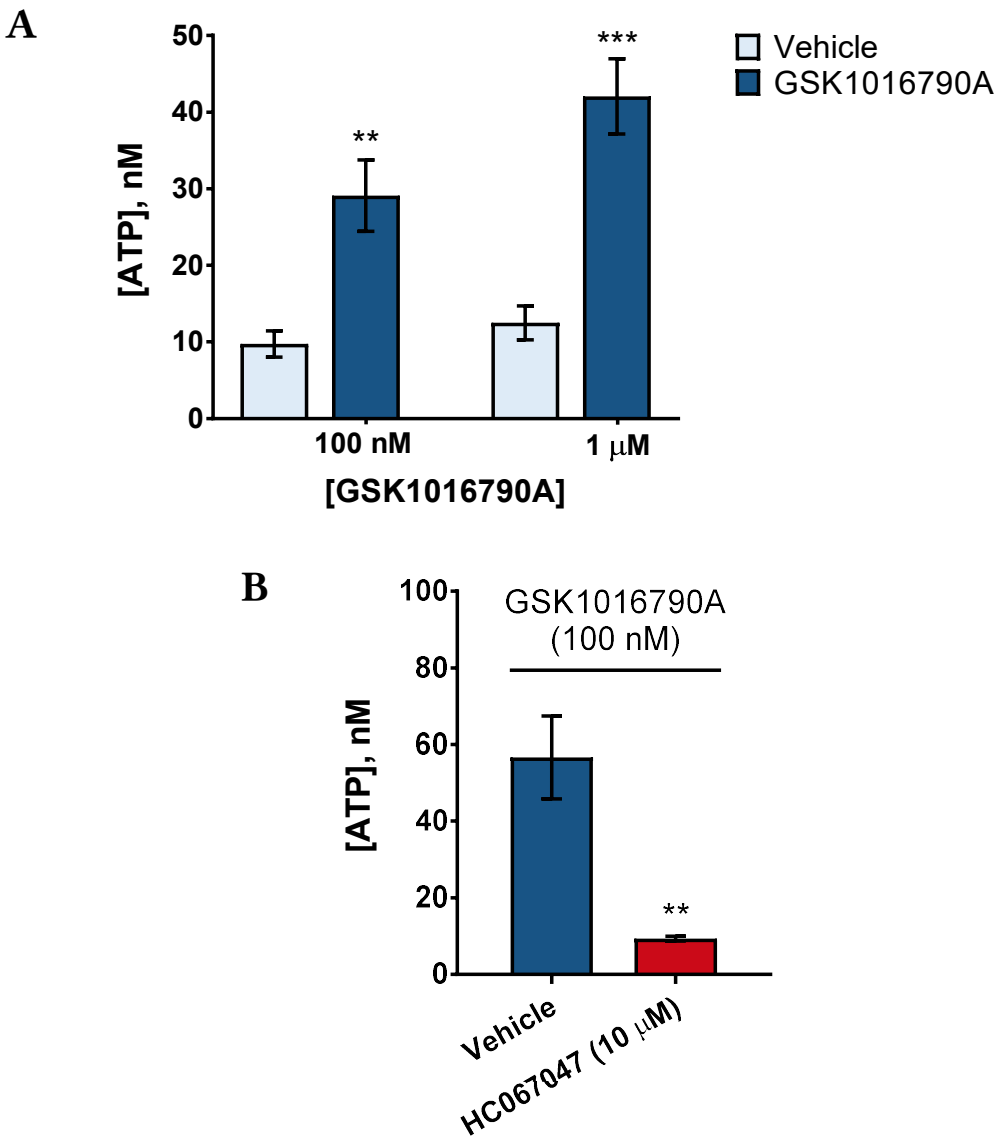

Figure 3.13 Selective TRPV4 activation stimulates ATP release from OB cells

A) OB cell treatment with the TRPV4 agonist GSK1016790A (0.1 and 1 μM) for 15 minutes caused a significant increase in extracellular ATP concentration, when compared with the respective DMSO vehicle (0.1% (v/v)). Data are presented as mean extracellular ATP concentration ± SEM. $^{**}p < 0.01$; $^{***}p < 0.005$ (two-way ANOVA with Bonferroni's *post hoc* test; $n = 5$ groups of paired duplicate measurements from 5 independent experiments). *B)* Pre-treatment of OB cells with the TRPV4 antagonist HC067047 (10 μM) for 15 minutes significantly inhibited the increase in extracellular ATP concentration induced by 100 nM GSK1016790A (mean ± SEM). $^{**}p < 0.01$ (unpaired *t*-test; $n = 5$ groups of paired duplicate measurements from 3 independent experiments). Both experiments were performed in complete OB culture medium.

In contrast, the TRPA1 agonist AITC failed to affect $[ATP]_o$ (see Figure 3.14A) when used at the same concentration that increased $[Ca^{2+}]_i$ in OB cells (Figure 3.7C) and that has been previously demonstrated to induce ATP release from human odontoblast-like cells (500 μM; Egbuniwe *et al.* (2014)). However, the lack of response is consistent with the absence of TRPA1 gene expression in OB cells (Figure 3.6).

Given the evidence of excitability of odontoblasts in the literature (Allard *et al.*, 2006; Byers & Westenbroek, 2011; Kojima *et al.*, 2015; Kojima *et al.*, 2017) the effect of a depolarising agent potassium chloride (KCl) on ATP release from OB cells was also examined (see Figure 3.14B). Detected $[ATP]_o$ was not significantly different between the cells exposed to high extracellular KCl (30 mM) and vehicle control (7.94 ± 1.43 nM and 10.17 ± 1.60 nM, respectively).

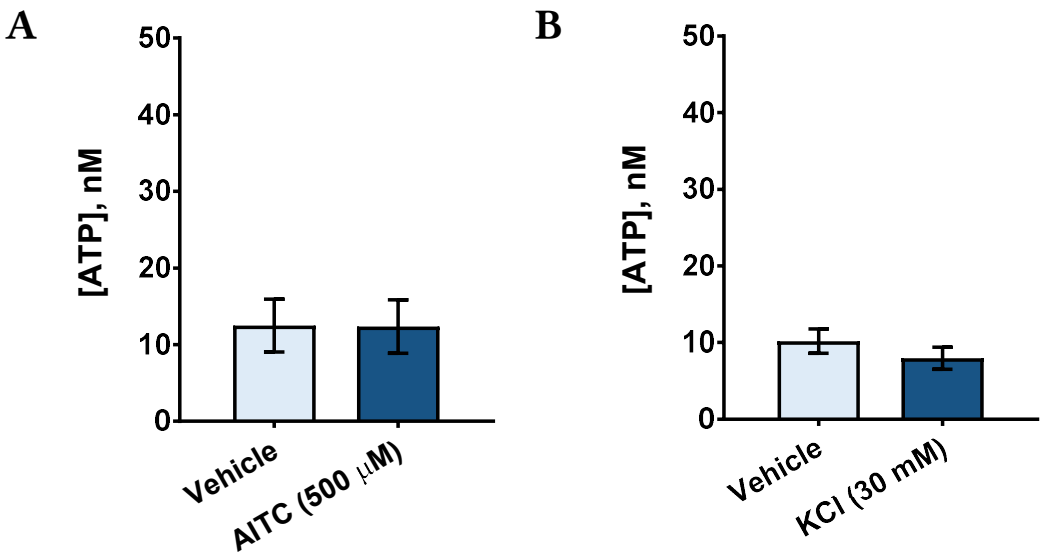

Figure 3.14 TRPA1 agonist AITC and depolarising agent potassium chloride fail to induce ATP release from OB cells

OB cell treatment with a high concentration of *A)* TRPA1 agonist AITC (500 μM) or *B)* potassium chloride (KCl; 30 mM) for 15 minutes did not increase extracellular ATP concentrations compared to vehicle-treated cells. Both experiments were performed in complete OB culture medium. Data are presented as mean ± SEM (n = 5 (AITC) or 8 (KCl) groups of paired duplicate measurements from 5 independent experiments).

In the next set of experiments, the measurement of ATP release in response to the TRPV4 agonist GSK1016790A (100 nM) was repeated in a standard extracellular solution (ECS) that enables easier control over the composition of OB cell extracellular environment, as well as in the complete OB culture medium used in the previous experiments. As can be seen in Figure 3.15A, ATP release in OB medium was consistent with the previous data (Figure 3.13A). On the other hand, baseline $[ATP]_o$ in ECS was low (2.26 ± 0.62 nM) and not significantly increased in GSK1016790A-treated cells (5.32 ± 1.15 nM). When the composition of ECS was altered to minimise extracellular Ca^{2+} concentration (described in section 2.1), $[ATP]_o$ after OB treatment with GSK1016790A (100 nM) was found to be slightly but statistically significantly higher (7.95 ± 1.45 nM) than in Ca^{2+}-containing ECS (3.77 ± 0.83 nM; $p = 0.031$; see Figure 3.15B).

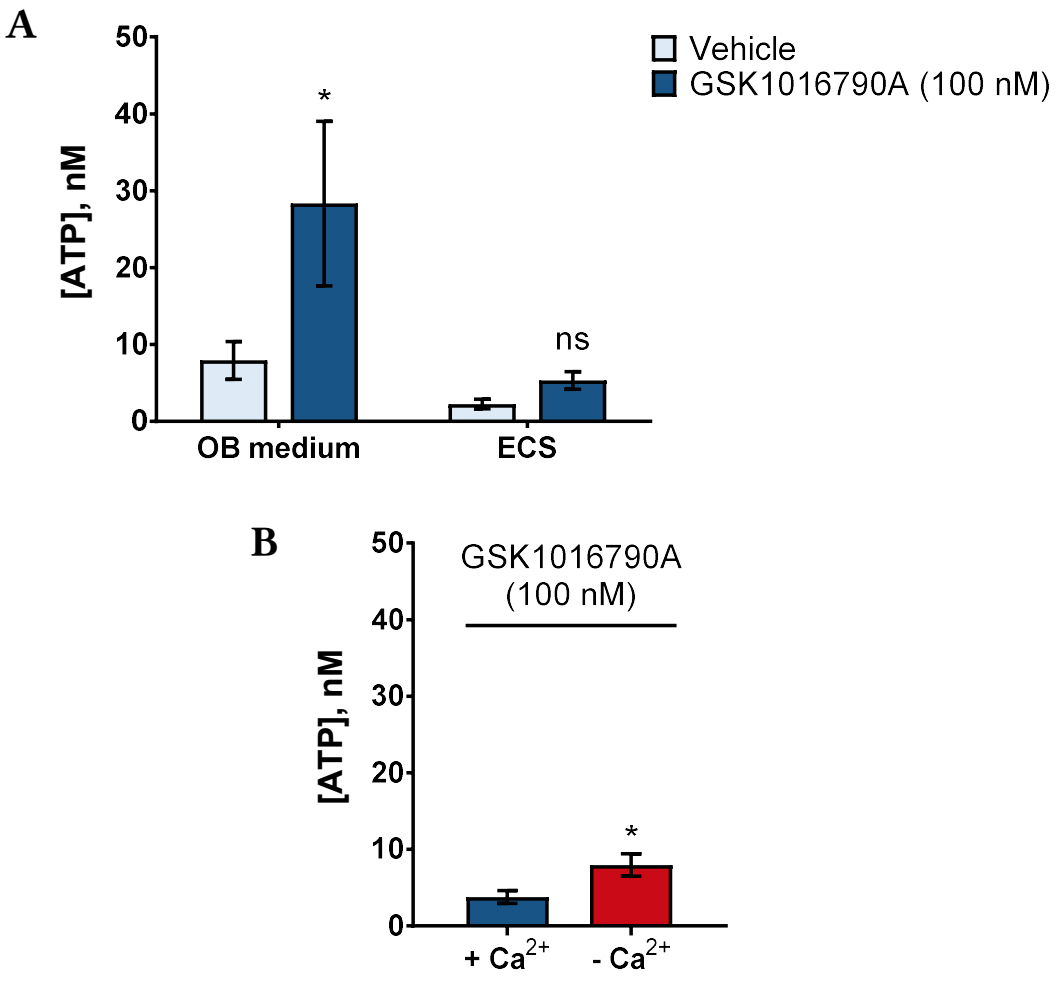

Figure 3.15 TRPV4-dependent ATP release from OB cells is impaired in standard extracellular solution

A) A significant increase in extracellular ATP concentration in response to a 15-minute treatment with GSK1016790A (100 nM) was observed when experiments were performed in complete OB culture medium, but not when in standard extracellular solution (ECS). Data are presented as mean ± SEM. $^{*}p < 0.05$; ns = not statistically significant, $p > 0.05$ *vs.* respective vehicle (two-way ANOVA with Bonferroni's *post hoc* test; $n = 3$ (OB) or 5 (ECS) groups of paired duplicate measurements from 2-3 independent experiments). *B)* Cells exposed to GSK1016790A (100 nM) in ECS lacking Ca^{2+} display higher extracellular ATP concentrations compared with the same treatment in standard ECS that contains Ca^{2+} (mean ± SEM). $^{*}p < 0.05$ (unpaired *t*-test; $n = 6$ groups of paired duplicate measurements from 4 independent experiments).

In order to determine whether TRPV4-dependent fluctuations in $[Ca^{2+}]_i$ are necessary for the GSK1016790A-induced ATP release from OB cells, attempts were made to create low Ca^{2+} conditions using the complete OB culture medium. A combination of EGTA and BAPTA-AM was used to chelate free Ca^{2+} both extracellularly and intracellularly to minimise any $[Ca^{2+}]_i$ fluctuations in response to GSK1016790A. In the microplate-based calcium flux assay, BAPTA-AM (200 μM), when used together with EGTA (1 mM), decreased the mean maximum change in Fura-2AM fluorescence intensity ratio by 91% (see Figure 3.16A). For subsequent ATP release experiments, a combination of 100 μM BAPTA-AM and 1 mM EGTA was chosen, as it was expected to sufficiently prevent the changes in $[Ca^{2+}]_i$ induced by a lower concentration of GSK1016790A (100 nM rather than 200 nM in the calcium flux experiment), while maintaining a lower solvent (DMSO) concentration. However, as seen in Figure 3.16B, pre-treatment of OB cells with this combination prior to the application of GSK1016790A did not significantly affect $[ATP]_o$ compared to the cells pre-treated with a vehicle (40.15 ± 6.39 nM and 32.54 ± 4.90 nM, respectively).

Given the previous observation that low extracellular Ca^{2+} can increase ATP release from OB cells in ECS (Figure 3.15B), the effect of BAPTA-AM and EGTA on $[ATP]_o$ was examined in the OB culture medium, without any stimulation with GSK1016790A. To eliminate the possibility that ATP concentration in the media samples is increased by the presence of detached cells, an additional filtration step was also included (described in section 3.2.6). As shown in Figure 3.16B, $[ATP]_o$ increased after the treatment with BAPTA-AM and EGTA (34.47 ± 1.35 nM), compared with the vehicle control levels (15.16 ± 0.81 nM; $p < 0.001$) and was in a similar range to the cells exposed to GSK1016790A, suggesting that ATP release induced by Ca^{2+} chelators themselves could have been masking any negative effect on the TRPV4-dependent ATP release.

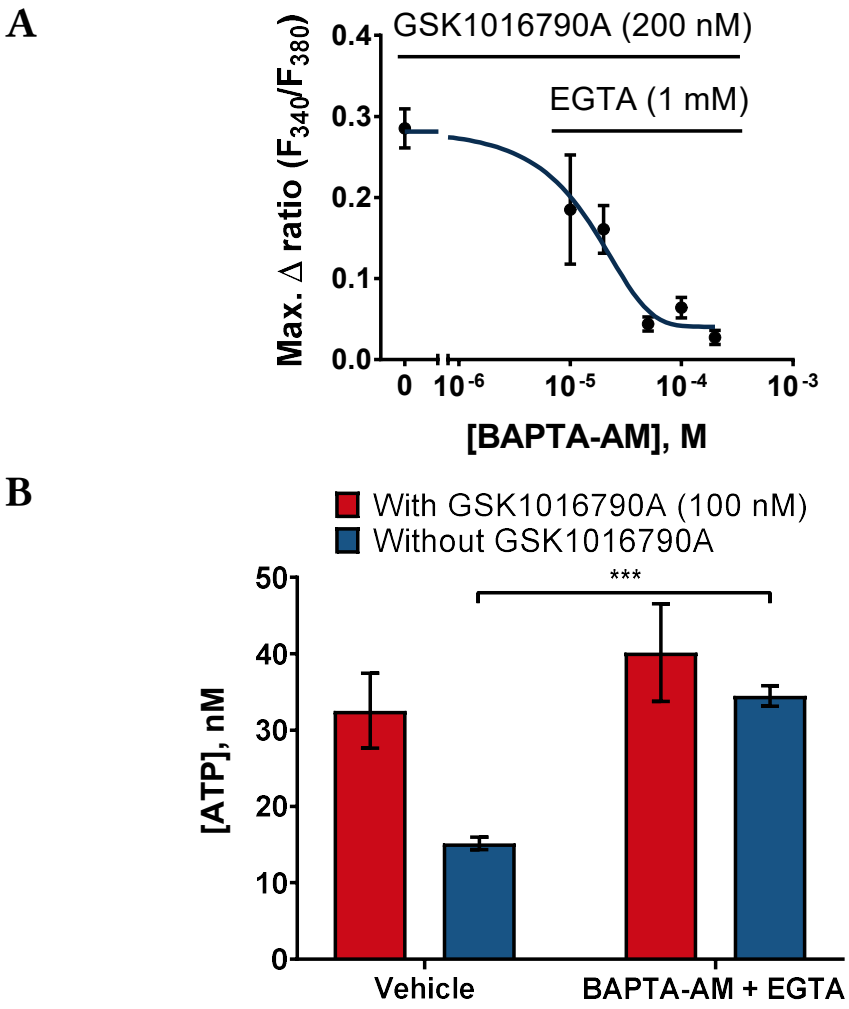

Figure 3.16 Ca^{2+} chelators prevent the TRPV4-dependent increase in $[Ca^{2+}]_i$, but not ATP release from OB cells

A) Pre-treatment of OB cells with a combination of BAPTA-AM (10-200 μM) and EGTA (1 mM, pH 7.4) inhibited the increase in intracellular Ca^{2+} concentration caused by GSK1016790A (200 nM). Point '0' on the *x* axis represents the pre-treatment with a DMSO vehicle (0.67% (v/v)). Ca^{2+} chelators remained in contact with the cells throughout experimental runs. Data are reported as mean ± SEM (n = 4 triplicate measurements from 2 independent experiments). *B)* Identical pre-treatment of OB cells with BAPTA-AM (100 μM) and EGTA (1 mM, pH 7.4) did not affect the increase in extracellular ATP concentration induced by 100 nM GSK1016790A, compared to 0.33% (v/v) DMSO vehicle (mean ± SEM; n = 4 groups of paired duplicate measurements from 3 independent experiments; *red columns*), but increased extracellular ATP concentration above control levels, without the application of GSK1016790A ($^{***}p < 0.005$ (unpaired *t*-test n = 6 groups of paired duplicate measurements from 3 independent experiments; *blue columns*).

Overall, these results provided evidence for the release of ATP from OB cells in response to the selective TRPV4 channel activation. However, a direct link between TRPV4-dependent changes in $[Ca^{2+}]_i$ and ATP release could not be conclusively established.

3.3.5 Investigating the mechanisms of TRPV4-dependent ATP release from OB cells

Connexin hemichannels and pannexin pore-forming channels have been considered as a means for ATP release from thermally and mechanically stimulated odontoblasts (Liu *et al.*, 2015; Shibukawa *et al.*, 2015). RT-PCR reactions with primers selective for the genes that encode connexin 43, also known as gap junction protein, alpha 1 (*Gja1*), and pannexins 1 and 3 (*Panx1* and *Panx3*) produced bands from OB cell cDNA (Figure 3.17).

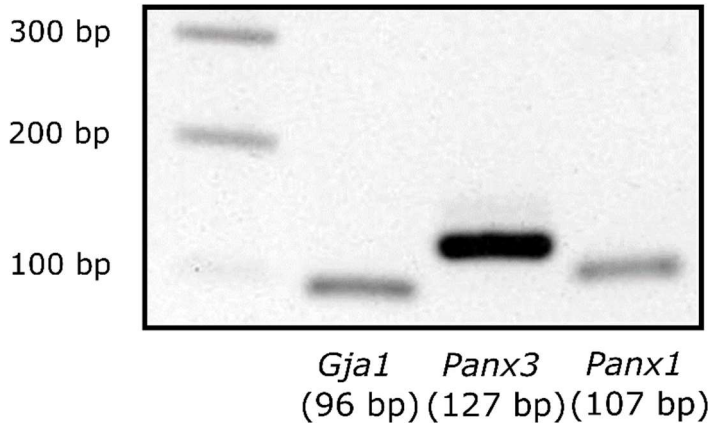

Figure 3.17 OB cells express connexin-43 and pannexins 1 and 3

Gel electrophoresis of RT-PCR products from OB samples produced bands for *Gja1*, *Panx1*, and *Panx3*. Inverted colour image of the gel is presented in the figure. First lane contains a 100 bp DNA ladder (Promega).

The involvement of these channels in the release of ATP induced by the activation of TRPV4 in OB cells was then investigated. Three non-selective inhibitors were tested, namely carbenoxolone, flufenamic acid, and probenecid. The concentration of probenecid used (500 μM) was 1.4-3.3 times higher than the reported IC_{50} values for blocking pannexin 1, whereas connexin hemichannels should not be affected by probenecid (Silverman *et al.*, 2008; Ma *et al.*, 2009). By comparison, flufenamic acid is widely used to block multiple connexin hemichannels and gap junction channels (Harks *et al.*, 2001; Eskandari *et al.*, 2002; Srinivas & Spray, 2003), but only moderately affects the pannexin 1 activity at the concentration used (100 μM; Bruzzone *et al.* (2005)). Carbenoxolone, while being the most potent out of the three compounds at blocking pannexin 1 channels (reported IC_{50} = 4-5 μM) was also expected to effectively inhibit connexin hemichannels at 100 μM (Bruzzone *et al.*, 2005; Ma *et al.*, 2009). However, pre-treatment of OB cells with any of these compounds did not significantly affect the changes in $[ATP]_o$ induced by 100 nM GSK1016790A, compared to the corresponding vehicle control levels (see Figure 3.18).

Odontoblasts also express $P2X_7$ receptors (Lee *et al.*, 2017; Shiozaki *et al.*, 2017), which have been demonstrated to mediate ATP release from other types of cells, such as osteoclasts and osteoblasts (Brandao-Burch *et al.*, 2012). The involvement of $P2X_7$ was then tested as an alternative mechanism for ATP release from OB cells. However, the $P2X_7$ antagonist brilliant blue G also did not significantly affect the GSK1016790A-induced ATP release.

Since ATP release from odontoblasts by the process of vesicular exocytosis has also been proposed (Ikeda *et al.*, 2016), three vesicular exocytosis inhibitors, each acting through a different mechanism, were also tested on OB cells in the ATP release assay. Clodronate, an inhibitor of vesicular nucleotide transporter (VNUT), and bafilomycin A1, which inhibits vacuolar H^+ ATPase (V-ATPase), both failed to significantly prevent the changes in $[ATP]_o$ in response to the cell treatment with GSK1016790A. In contrast, *N*-ethylmaleimide, known to inhibit vesicular fusion (Diaz *et al.*, 1989), significantly reduced $[ATP]_o$ resulting from 100 nM GSK1016790A application, compared with vehicle control (52.39 ± 12.59 nM and 5.34 ± 1.84 nM, respectively; $p < 0.001$, two-way ANOVA with Bonferroni's multiple comparisons test).

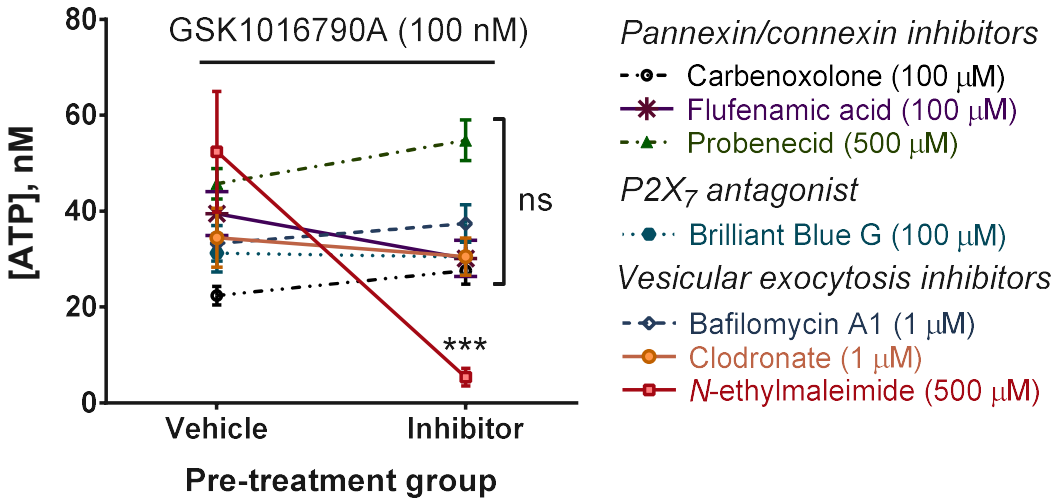

Figure 3.18 Pharmacological investigation of the TRPV4-dependent ATP release mechanism from OB cells

Pre-treatment of OB cells with the inhibitors of vesicular transport, pannexin and connexin channels, or $P2X_7$ receptors did not affect the increase in extracellular ATP concentration induced by GSK1016790A (100 nM). The only exception was *N*-ethylmaleimide, which significantly reduced ATP release, compared with the respective vehicle. Data are expressed as mean ± SEM. $^{***}p < 0.005$; ns = not statistically significant, $p > 0.05$ (two-way ANOVA with Bonferroni's *post hoc* test; n = 4-7 groups of paired duplicate measurements from 2-3 independent experiments).

3.3.6 PRELIMINARY EVIDENCE FOR TRPV4-DEPENDENT GLUTAMATE RELEASE FROM OB CELLS

In addition to ATP, glutamate has been proposed as an alternative mediator of intercellular signalling between odontoblasts and neurons (Cho *et al.*, 2016; Nishiyama *et al.*, 2016). In a preliminary experiment, glutamate release from OB cells in response to TRPV4 activation was tested. A significant increase in extracellular glutamate concentration from 0.28 ± 0.10 μM in vehicle-treated cells to 3.39 ± 1.28 μM in 1 μM GSK1016790A-treated cells was detected (p = 0.036). In the first two experiments, a comparable increase in extracellular glutamate was also detected using a different glutamate detection assay (Abcam, ab83389). However, in a subsequent experiment this assay failed to detect glutamate even in positive control solutions. Therefore, only the results obtained using Glutamate-Glo™ (Promega) assay are shown below.

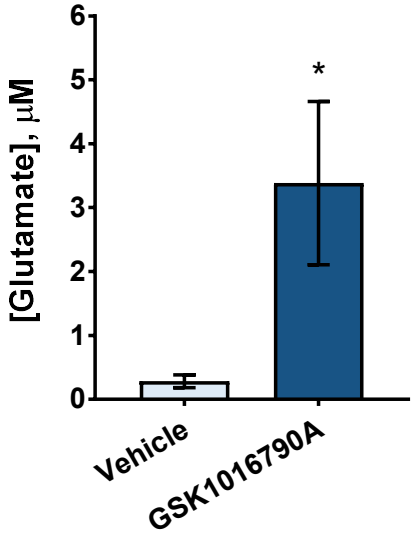

Figure 3.19 TRPV4 activation induces glutamate release from OB cells

OB cell treatment with the TRPV4 agonist GSK1016790A (1 μM) for 15 minutes caused a significant increase in extracellular glutamate concentration, when compared with the corresponding DMSO vehicle (0.1% (v/v)). Data are reported as mean ± SEM. *p < 0.05 (unpaired t-test; n = 6 from 3 independent experiments).

3.4 Discussion

3.4.1 Odontoblast-like phenotype of differentiated 17IA4 cells

Odontoblasts are specialised cells, responsible for dentine formation (Ruch *et al.*, 1995). Therefore, expression of the genes that encode dentine matrix proteins, enzymes, and transcription factors involved in mineralisation is commonly used to confirm odontoblastic phenotype. The dissociation of tooth germs at the mouse embryonic stage when no mature odontoblasts are present (ED18) enabled Priam and colleagues (2005) to isolate odontoblast precursor cells, which were named 17IA4. Although the originators have already confirmed the pre-odontoblastic phenotype of 17IA4 cells, initial checks were performed in our study to ensure the phenotype is as expected, and that odontoblastic differentiation could be induced. Gene expression of LHX6 and 8, key transcription factors in odontogenesis (Grigoriou *et al.*, 1998; Zhou *et al.*, 2015) supports the identity of 17IA4 cells. Moreover, the majority of odontoblastic marker genes, including those encoding ALP, the enzyme involved in dentine mineralisation, and COL1α1, the major component of dentine (Goldberg *et al.*, 2011), were expressed in cultured 17IA4 cells even before their differentiation into odontoblast-like cells. This demonstrates the commitment of 17IA4 cells to the odontogenic differentiation route. An alternative explanation is the induction of odontoblastic differentiation even by non-differentiating media. This could be related to the presence of ascorbic acid in αMEM basal medium that was used for preparing both non-differentiating and differentiating complete culture media. Ascorbic acid is one of the three main factors commonly used for stimulating odontoblastic differentiation (Wei *et al.*, 2007). Nonetheless, differentiation-related increase in several odontogenic marker gene expression, including ALP and COL1α1, dentine matrix proteins BGP and BSP2, and another transcription factor relevant to dentine formation, DLX3, were also detected by either semi-quantitative or quantitative analysis. Lower DMP1 gene expression levels in the cells exposed to the differentiating medium is also consistent with previous reports that DMP1 expression decreases in differentiated odontoblasts (Hao *et al.*, 2004; Balic & Mina, 2011). However, relatively low levels of DSPP gene expression, which tends to increase with odontoblast differentiation (Magne *et al.*, 2004; Balic & Mina, 2011), suggest that after 7 days in the differentiating medium, 17IA4 cells have not yet reached

a stage equivalent to mature odontoblasts. This is further supported by unchanged levels of RUNX2 transcription factor gene expression, which is downregulated in fully differentiated odontoblasts (D'Souza *et al.*, 1999; Komori, 2010). However, ALP enzymatic activity was also already significantly increased in 17IA4 cells at that timepoint, suggesting a differentiation-related increase in the mineralising function. One limitation of the experimental method used for measuring ALP activity is that it does not account for any potential effects of differentiating medium on cell proliferation, in addition to the effects on the odontoblastic differentiation. Nonetheless, the mineralising activity of differentiated 17IA4 cells was additionally demonstrated using a separate method, where increased alizarin red S staining indicated enhanced hydroxyapatite and calcium pyrophosphate dihydrate crystal deposition.

Collectively, this shows that despite the *in vitro* morphology that does not fully resemble *in vivo* mature columnar odontoblasts with a prominent cellular extension, differentiated 17IA4 cells express odontoblastic markers and function like odontoblasts. It is possible that for the typical odontoblastic morphology to appear, these cells need to be exposed to a different cell culture environment. In fact, some research groups demonstrated that culturing dental pulp cells in 3D cultures promotes their odontoblastic differentiation (Yamamoto *et al.*, 2014; Neunzehn *et al.*, 2017), whereas culturing them on dentin discs with open dentinal tubules additionally stimulates the development of monopolar cellular processes extending into dentinal tubules (Huang *et al.*, 2006; Shao *et al.*, 2011). While this is promising from the perspective of dental tissue engineering for tooth regeneration, it would have restricted our ability to study the sensory odontoblast function *in vitro*. Therefore, conventionally cultured mouse odontoblast-like (OB) cells provide a suitable model for our further experiments.

3.4.2 Differential TRP channel functional expression in odontoblasts

This study demonstrated the lack of TRPA1 and TRPM8 gene expression in mouse OB cells. This agrees with the published work from primary mouse odontoblasts (Son *et al.*, 2009), further supporting the relevance of our cellular model for studying odontoblast sensory function. In line with the lack of functional TRPM8 ion channels, the TRPM8 agonist icilin did not affect intracellular calcium concentrations ($[Ca^{2+}]_i$) in OB cells, even at 10 μM, a concentration 50-80 times higher than the reported EC_{50} values for

heterologously expressed mouse TRPM8 channels (Andersson *et al.* (2004); Behrendt *et al.* (2004)). Again, this agrees with the findings of Son and colleagues (2009). On the other hand, the expression of TRPM8 in odontoblasts from other species remains controversial. Even when considering only calcium flux data, to avoid comparisons between different experimental methods, evidence both for (El Karim *et al.*, 2011; Tsumura *et al.*, 2013) and against (Yeon *et al.*, 2009; Egbuniwe *et al.*, 2014) TRPM8 functional expression in rat and human odontoblasts or odontoblast-like cells has been reported, with no obvious species-dependence. This suggests that inconsistencies could be related to the use of different cellular models and culture conditions by different research groups. However, *in vitro* differentiated odontoblast-like cells and primary odontoblasts from the same species and, in the case of experimental animals, specific strains, have not yet been directly compared, especially in terms of functional TRP channel expression, to clarify these discrepancies.

Although most previous studies support TRPA1 expression in human and rat odontoblasts (Byers & Westenbroek, 2011; El Karim *et al.*, 2011; Tsumura *et al.*, 2013; Egbuniwe *et al.*, 2014), some controversy also exists. For example, recently Tazawa and colleagues (2017) reported TRPM8, but not TRPA1, gene and protein expression in acutely isolated human odontoblasts. On the other hand, while not as abundant, data from mouse odontoblasts consistently supports the lack of TRPA1 ion channels (Son *et al.*, 2009; Sato *et al.*, 2013), suggesting potential species differences. Although some increase in intracellular calcium concentrations could be detected in mouse OB cells in response to TRPA1 agonists allyl isothiocyanate and cinnamaldehyde, this only occurred at respective concentrations 9-83 or 3-14 times higher than the reported EC_{50} values for heterologously expressed mouse TRPA1 channels (Bandell *et al.*, 2004) or for native TRPA1 channels in human odontoblast-like cells (Egbuniwe *et al.*, 2014). Non-selective effects of high cinnamaldehyde concentrations on TRPV3 ion channels have also been reported (Macpherson *et al.*, 2006), and there is evidence for the presence of these channels in mouse odontoblasts (Son *et al.*, 2009). Together with the lack of TRPA1 gene expression in OB cells, this suggests that the observed increases in intracellular calcium were not specific to TRPA1 activation, and that any experiments using high concentrations (≥200 μM) of allyl isothiocyanate or cinnamaldehyde to activate TRPA1 should be interpreted carefully. Since both allyl isothiocyanate and cinnamaldehyde are

known reactive electrophilic substances, a non-electrophilic TRPA1 activator, such as carvacrol, could preferably have been included for comparison (Hasan *et al.*, 2017).

This study was the first to test the odontoblastic gene expression of TRPC5, another TRP channel implicated in cold and osmotic/mechanosensation (Zimmermann *et al.*, 2011; Shen *et al.*, 2015). However, similarly to TRPM8 and TRPA1, no TRPC5 gene expression could be detected in mouse OB cells. The fact that TRPA1, TRPC5, and TRPM8, the main TRP channels implicated in cold sensing (Lolignier *et al.*, 2016), are all absent in mouse odontoblast-like cells contradicts the ability of mouse odontoblasts to directly detect cold stimuli, suggested by the odontoblast transducer theory of dentine hypersensitivity.

The studies of heat-sensitive TRPV1 expression and function in odontoblasts from mice, rats, and humans are numerous but, again, with inconsistent findings. In this study, TRPV1 transcripts could be detected in mouse OB cells. However, functional calcium flux data revealed increased $[Ca^{2+}]_i$ only at the highest capsaicin concentrations tested (5 and 10 μM), whereas the published EC_{50} value for capsaicin-dependent activation of heterologously expressed mouse TRPV1 channels is 9 nM (Correll *et al.*, 2004). Most previous reports of capsaicin-induced effects on odontoblasts only included a single capsaicin concentration of 10 μM, but demonstrated an inhibition using a TRPV1 antagonist capsazepine (Okumura *et al.*, 2005; Son *et al.*, 2009; El Karim *et al.*, 2011; Tsumura *et al.*, 2012). One group reported an increase in intracellular calcium in mouse odontoblast-like cells in response to a lower (1 μM) capsaicin concentration (Sato, 2013). However, others who also tested capsaicin at 1 μM in rat odontoblasts were unable to detect any response (Yeon *et al.*, 2009), consistent with our data. A possible explanation might be related to the non-selective actions of both capsazepine (Docherty *et al.*, 1997; Behrendt *et al.*, 2004) and high capsaicin concentrations (Eun *et al.*, 2001; Lundbaek *et al.*, 2005; Yang *et al.*, 2014). The presence of TRPV1 transcripts combined with the lack of TRPV1-dependent increase in intracellular calcium seen in this study were also previously observed in this laboratory in human odontoblast-like cells (Egbuniwe *et al.*, 2014) and by other research groups in other cell types, e.g. human urothelial cells (Shabir *et al.*, 2013). This could potentially be explained by translation of TRPV1 mRNA or trafficking of TRPV1 proteins to the plasma membrane that occur only under certain

physiological or pathological conditions. However, this still needs to be investigated in odontoblasts, for example, by using immunocytochemistry to visualise protein expression.

Unlike the controversial TRP channels discussed above, evidence in the literature consistently supports the expression (Sole-Magdalena *et al.*, 2011; Kwon *et al.*, 2014; Tokuda *et al.*, 2015a) and function (Son *et al.*, 2009; Sato *et al.*, 2013; Egbuniwe *et al.*, 2014; El Karim *et al.*, 2015; Shibukawa *et al.*, 2015) of TRPV4 in odontoblasts from mice, rats, and humans. In this study, mouse OB cells were also found to express the gene encoding TRPV4. Based on the concentration-dependent increase in $[Ca^{2+}]_i$ in response to the TRPV4 agonist GSK1016790A application, TRPV4 channels were also confirmed to be functional in OB cells, although the estimated EC_{50} value for the cells grown in the differentiating medium (107 nM) was higher than previously observed in human odontoblast-like cells (32 nM; Egbuniwe *et al.* (2014)). The selective TRPV4 antagonist HC067047 inhibited this response in a concentration-dependent manner, demonstrating the specificity of GSK1016790A-dependent increase in $[Ca^{2+}]_i$ to the TRPV4 activation. The presence of functional TRPV4 ion channels supports odontoblast mechanosensitivity that is required for the detection of dentinal fluid movement. This encouraged us to further investigate the role of TRPV4 in OB cells in subsequent experiments.

In addition, the gene encoding TRPM7, a bi-functional protein containing both an ion channel and protein kinase activity, was also found to be expressed in mouse OB cells, which agrees with the published mouse odontoblast data (Nakano *et al.*, 2016; Ogata *et al.*, 2017). Both of these research groups employed genetic strategies to investigate the involvement of TRPM7 in mineralisation, linked to its well-established role in magnesium homeostasis (Schmitz *et al.*, 2003; Ryazanova *et al.*, 2010). Given the lack of selective pharmacological tools, we have not focused on TRPM7 in our subsequent experiments. However, recently Won and co-workers (2018) repurposed an opioid receptor antagonist naltriben as a TRPM7 agonist (as previously established by Hofmann *et al.* (2014)), as well as Mg^{2+} and sphingosine 1-phosphate (S1P) receptor agonist FTY720 (based on work by Qin *et al.* (2013)) as TRPM7 antagonists to demonstrate the involvement of TRPM7 in detecting hypotonicity-induced membrane

stretch by rat odontoblasts. They have also detected TRPM7 gene expression and immunoreactivity in the odontoblastic process, supporting the potential mechanosensory role of TRPM7 in detecting dentinal fluid movement by odontoblasts. While this is a promising finding, it does not exclude the potential contribution of other ion channels, such as TRPV4, to the sensory role of odontoblasts.

Overall, this study investigated the presence of TRP channel mRNA transcripts in odontoblasts by RT-PCR. For the most relevant TRP channels, this has been combined with calcium flux data to determine TRP channel function. A limitation of this study is the lack of protein expression data, which could be produced by using specific antibodies in immunocytochemistry or Western blotting experiments. There are, however, some concerns about the specificity of the commercially-available TRP channel antibodies. Without the knock-out tissue to confirm the specificity, any data gained would still be open to question.

3.4.3 Regulation of TRP channel activity in odontoblasts

Due to the *in vivo* location of the odontoblasts at the dentine-pulp junction, they can be exposed to both bacterial products and host inflammatory mediators. In agreement with published findings from odontoblasts (Durand *et al.*, 2006; Veerayutthwilai *et al.*, 2007), OB cells were found to express the genes encoding Toll-like receptors (TLRs) 2 and 4, pattern recognition receptors required for the detection of oral pathogens. Lipopolysaccharide (LPS), a wall component of Gram-negative bacteria, has previously been demonstrated to sensitise neuronal TRPV1 ion channels via activation of TLR4 (Diogenes *et al.*, 2011) and directly activate TRPV4 in airway epithelial cells (Alpizar *et al.*, 2017). Although direct activation was not measured in this study, pre-treatment of OB cells with a range of concentrations of either LPS or lipoteichoic acid (LTA), a wall component of Gram-positive bacteria, for 1 or 24 hours did not enhance TRPV4-dependent changes in OB cell $[Ca^{2+}]_i$, suggesting the absence of TRPV4 sensitisation under these conditions. However, stimulation of other processes in odontoblasts by LPS and LTA cannot be excluded. Indeed, LPS has previously been shown to stimulate the expression of vascular endothelial growth factor (VEGF) in odontoblasts (Botero *et al.*, 2006), whereas exposure to LTA increased the production of a pro-inflammatory chemokine CXCL8, also known as IL-8, from odontoblast-like cells (Keller *et al.*, 2010),

both relevant to pulpal inflammation and pain. It should be noted that LPS used in the present study was from *Escherichia coli*. Based on the reports that *E. coli* LPS upregulates TRPV1 expression (Chung *et al.*, 2011) and is the most effective at activating TRPA1 channels compared with several other species (Meseguer *et al.*, 2014), this bacterial species has been chosen to maximise the possibility of detecting any LPS-dependent regulation of TRP channels in the preliminary experiments. Although there is some evidence in the literature that *E. coli* is present in the oral cavity of, for example, patients with chronic periodontitis (Souto *et al.*, 2006), *E. coli* is not the most relevant species for studying the mechanisms of pulpitis pain. To address this, LPS from Gram-negative bacterial species, such as those belonging to the *Prevotella* or *Porphyromonas* genera, which have been identified as particularly prevalent in symptomatic endodontic infections (Jacinto *et al.*, 2006; Sakamoto *et al.*, 2006), could instead be used in future studies.

In this study, a classical inflammatory mediator TNFα also failed to sensitise TRPV4 on OB cells, even at treatment times and conditions that were previously reported to increase both TRPV4- and TRPA1-dependent changes in $[Ca^{2+}]_i$ in human odontoblast-like cells (El Karim *et al.*, 2015). To help clarify the discrepancy, in the future experiments, it would be crucial to first determine the expression of TNFα receptors TNFR1 and TNFR2 in odontoblasts, which, to the best of my knowledge, has not yet been demonstrated.

Overall, the preliminary results from the present study do not support the hypothesis that odontoblastic TRPV4 activity is modulated by the bacterial wall components LPS and LTA, or the inflammatory mediator TNFα.

3.4.4 ATP RELEASE FROM STIMULATED ODONTOBLASTS

In addition to the TRPV4-dependent increase in $[Ca^{2+}]_i$, the TRPV4 agonist GSK1016790A caused an increase in ATP concentration in mouse OB cell culture medium, which was inhibited by the TRPV4 antagonist HC067047. This suggests that selective activation of TRPV4 triggers a release of ATP from OB cells, consistent with previous findings from human odontoblast-like cells (Egbuniwe *et al.*, 2014). Extracellular ATP concentrations in the nanomolar range, as measured in bulk solutions

from vehicle- and GSK1016790A-treated OB cells, were also similar to the resting and stimulated bulk ATP concentrations from other types of cells (Praetorius & Leipziger, 2009). On the other hand, as predicted by the species difference in TRP channel expression, mouse OB cells, unlike human odontoblast-like cells, did not release ATP in response to the TRPA1 agonist allyl isothiocyanate (AITC) application. Given that the same concentration of AITC increased $[Ca^{2+}]_i$ in OB cells, this calls into question a direct link between the increase in $[Ca^{2+}]_i$ and ATP release. Attempts to study the importance of TRPV4-dependent Ca^{2+} influx to the TRPV4-induced ATP release by repeating the experiments in Ca^{2+}-containing and Ca^{2+}-lacking standard extracellular solution (ECS) revealed some unexpected findings. First, average baseline extracellular ATP concentrations were lower in ECS and no significant increase was induced by the TRPV4 activation, suggesting that the processes required for the TRPV4-induced ATP release are impaired under those conditions. Since appropriate measures were taken to ensure this is not an artefact arising from different solution effects on the ATP detection reaction or luminescence reading (see section 2.6.1), a possible explanation for this could be related to the presence of multiple additional ingredients in complete culture medium that are absent in ECS. So far, it was only possible to narrow it down to the factors present in the supplements, most likely serum, rather than in basal αMEM. Further experiments are needed to determine whether these factors are necessary for the ATP release process from OB cells in general, or whether they specifically affect TRPV4-dependent ATP release. The additional finding that removal of Ca^{2+} from ECS increased extracellular ATP concentrations following the GSK1016790A treatment, compared with the Ca^{2+}-containing ECS, suggests that low extracellular Ca^{2+} potentially stimulates an ATP release mechanism, separate from the TRPV4-induced ATP release. This was later supported by experiments using intracellular (BAPTA-AM) and extracellular (EGTA) Ca^{2+} chelators, which increased ATP release from OB cells even in the absence of TRPV4 stimulation. However, this also prevented assessment of the requirement of TRPV4-dependent Ca^{2+} influx for the TRPV4-induced ATP release. Given the mineralising function of odontoblasts, it seems plausible that they would contain intrinsic mechanisms to detect and signal changes in extracellular Ca^{2+}. A recent review by An (2018) summarised the mechanisms involved in the maintenance of calcium homeostasis by odontoblasts and dental pulp cells. However, the sensor proteins involved and the link with ATP release from odontoblasts need further

investigation. Some of the potential players include a G protein-coupled calcium-sensing receptor (CaSR), previously demonstrated to be involved in odontoblastic differentiation (Mizumachi *et al.*, 2017), an ATP-permeable calcium homeostasis modulator 1 (CALHM1), activated by low extracellular Ca^{2+} (Ma *et al.*, 2012), although not yet identified in odontoblasts, and connexin 43 hemichannels that can open under extremely low extracellular Ca^{2+} conditions to enable ATP release (Contreras *et al.*, 2003).

In this study, the genes encoding connexin 43, as well as pore-forming pannexin channels 1 and 3 were found to be expressed in mouse OB cells. These channels were further studied as potential mechanisms for TRPV4-induced ATP release. However, multiple connexin and pannexin inhibitors failed to inhibit ATP release from OB cells, evoked by the TRPV4 agonist. This result is inconsistent with findings by some other research groups that blocked pannexin 1 channels and reported inhibition of ATP release in human teeth in response to cold or mechanical stimulation of the dentine (Liu *et al.*, 2015) or reduction in responses dependent on ATP released from mechanically stimulated rat odontoblasts (Shibukawa *et al.*, 2015). However, it is possible that different methods of cell stimulation might activate distinct signalling pathways and employ different ATP release mechanisms. The non-selectivity of pharmacological tools that are commonly used to block these channels should also be taken into consideration. For example, probenecid, used for blocking pannexin channels, is also an activator of TRPV2 ion channels (Bang *et al.*, 2007), which are expressed in odontoblasts (Son *et al.*, 2009; Wen *et al.*, 2017). To avoid the issue of compound non-selectivity, genetic knock-down strategies might need to be utilised in future experiments to clarify pannexin and connexin involvement in ATP release from stimulated odontoblasts. Inhibition of other potential ATP release mechanisms from odontoblasts, including $P2X_7$ receptors (Pellegatti *et al.*, 2005) and vesicular exocytosis (Ikeda *et al.*, 2016), similarly did not significantly affect ATP release from TRPV4-induced OB cells. The only exception was *N*-ethylmaleimide, known for its ability to inhibit vesicular fusion (Diaz *et al.*, 1989). While this result points to the vesicle-mediated mechanism of ATP release, it should be noted that *N*-ethylmaleimide also acts as a broad-activity agent that can react with sulfhydryl groups present on multiple protein targets, including pannexin 1 (Bunse *et al.*, 2011). Moreover, *N*-ethylmaleimide has previously been reported to interfere with

ATP synthesis (Horn & Haugaard, 1966; Mukohata & Yoshida, 1987), which could reduce the pool of ATP available for release. Therefore, rather than revealing the exact mechanism of TRPV4-induced ATP release, *N*-ethylmaleimide could be used as a tool compound to prevent such release.

The depolarisation-dependent ATP release from OB cells was also briefly investigated. This process has previously been demonstrated in non-neuronal but excitable taste cells (Romanov *et al.*, 2007). Based on the expression and *in vitro* function of various voltage-gated ion channels, odontoblast excitability has also been suggested in the literature (Allard *et al.*, 2006; Byers & Westenbroek, 2011; Kojima *et al.*, 2015; Kojima *et al.*, 2017). However, potassium chloride (KCl), tested at a concentration that would cause depolarisation of neurons (30 mM), failed to increase OB extracellular ATP concentrations. While it cannot be excluded that the magnitude of depolarisation was insufficient to stimulate ATP release from odontoblasts, their excitability remains controversial.

Although the exact mechanisms could not be conclusively determined in the present study, the demonstration that mouse OB cells consistently release ATP in response to the selective activation of TRPV4 supports the ability of stimulated odontoblasts to convey a signal to adjacent neurons – a prerequisite for their hypothesised sensory role in dentine hypersensitivity. While modulation of trigeminal neuron activity by ATP released from OB cells will be further investigated in Chapters 5 and 6, the finding by Lee and colleagues (2017) that odontoblasts themselves express both ionotropic and metabotropic ATP receptors also suggests an additional function of released ATP in intercellular communication among odontoblasts. Whether this can additionally contribute to pain signalling, for instance, by initiating a positive feedback loop, also remains to be elucidated.

3.4.5 Glutamate as an alternative mediator released by odontoblasts

Preliminary experiments have also demonstrated glutamate release from OB cells in response to the TRPV4 agonist GSK1016790A. However, the direct link between TRPV4 activation and glutamate release still needs to be determined by pre-treating the cells with the TRPV4 antagonist before the agonist application in future experiments. The

only other study that directly measured glutamate release from cultured odontoblasts detected an increase in response to a Ca^{2+} ionophore ionomycin that is used to raise $[Ca^{2+}]_i$ (Cho *et al.*, 2016), suggesting that TRPV4-evoked glutamate release in our study could also arise directly from TRPV4-dependent increase in $[Ca^{2+}]_i$. Although extracellular glutamate concentrations detected from both vehicle- and GSK1016790A-treated OB cells (0.3 and 3.4 μM, respectively) were almost 10 times lower than the resting and stimulated values reported by Cho and colleagues (2016), this is most likely due to a different cell number/density, as our experiments were performed when the cells reached confluence, whereas they studied the cells after 21 days in culture.

It should be noted that the bioluminescence-based glutamate detection assay used in the present study utilises the enzymatic activity of an ATP-dependent luciferase. Therefore, the TRPV4-induced ATP release from OB cells could potentially affect the luminescence values. However, unlike ATP release, the increase in extracellular glutamate concentrations in response to the TRPV4 agonist stimulation occurred in ECS, without the need for factors present in complete culture medium. By performing glutamate release experiments in ECS, any interference from simultaneously stimulated ATP release should have been avoided. Moreover, this difference suggests a distinct mechanism for glutamate release from OB cells compared to the one employed in ATP release. Work by Nishiyama and colleagues (2016) supports the involvement of anion channels, including volume-sensitive outwardly rectifying (VSOR) anion channels, in glutamate release from mechanically stimulated odontoblasts. However, inhibition of these channels did not completely prevent glutamate-induced responses in their experiments. Indeed, multiple other mechanisms for glutamate release from non-neuronal cells, such as astrocytes, have been described in the literature (reviewed by Malarkey and Parpura (2008)). Interestingly, bone-producing osteoblasts have also been reported to release glutamate in response to shear stress via vesicular exocytosis (Tsuchiya *et al.*, 2015). Based on the proposed role of glutamate signalling in bone health (Cowan *et al.*, 2012) it might be speculated that odontoblasts similarly depend on glutamate for the maintenance of dentine. Since both adjacent pulpal nerve fibres and odontoblasts themselves express mGluRs (Kim *et al.*, 2009; Cho *et al.*, 2016; Nishiyama *et al.*, 2016), released glutamate, like ATP, might act in an autocrine manner or mediate odontoblast-odontoblast signalling in a paracrine manner, in addition to the potential

involvement in odontoblast-neuron communication. However, the exact mechanisms and potential relevance of such signalling to both the mineralisation processes, such as tertiary dentine formation, as well as dental pain, remain to be determined. In relation to pain signalling, the ability of glutamate to directly activate trigeminal ganglion neurons will be explored in Chapter 5.

Chapter 4

Acid sensing by odontoblast-like cells

4.1 Introduction

4.1.1 Acids and pH changes in the oral cavity

The oral environment is subject to extreme fluctuations in extracellular proton concentrations, or pH. In addition to frequent exposure to various acidic foods and drinks, the teeth come in contact with acids released as metabolic end-products by acidogenic oral bacteria, such as *Streptococcus mutans* and *Lactobacillus* spp. (Takahashi & Nyvad, 2011). Weak organic acids, namely lactic, acetic, and propionic acids, have been identified as the main acids in human dental plaque (Geddes, 1975), with reported mean plaque fluid pH values ranging from 5.30 to 7.08, depending on the time after meal and the presence of caries (Margolis & Moreno, 1994; Gao *et al.*, 2001). However, the average pH value of carious dentine can be as low as 4.9 in active lesions (Hojo *et al.* (1994), as cited in Takahashi and Nyvad (2011)).

Damage to tooth layers and exposure of dentinal tubules to acids of bacterial or dietary origin might subsequently lead to acidification of dentinal fluid that reaches odontoblast processes. In addition, the pH of the odontoblast microenvironment could theoretically also be affected by tissue acidosis from the pulpal side, in the case of inflammation (Punnia-Moorthy, 1987). Experiments described in this chapter tested the hypothesis

that odontoblasts are able to directly detect extracellular acidification caused by biologically relevant acids, and that this leads to the release of ATP – a proposed mediator of odontoblast signalling to dental pulp afferent neurons, with potential relevance to odontogenic pain.

4.1.2 Current knowledge of odontoblast ability to detect pH changes

One line of evidence in support of the proposed odontoblast ability to detect extracellular acidification is their reported expression of several ion channels that are known to be acid sensitive. These include the members of the family of acid-sensing ion channels (ASICs), which are mainly Na^+-permeable channels activated by protons at a wide range of pH values (pH 6.8-4), depending on the subtype (Wemmie *et al.*, 2013). Moreover, lactic acid was shown to additionally enhance the activity of ASICs (Immke & McCleskey, 2001). However, to date ASIC expression in odontoblasts has only been demonstrated in one study, where ASIC1-3 immunostaining was detected in human odontoblasts (Sole-Magdalena *et al.*, 2011).

Some TRP channels previously shown to be expressed in odontoblasts also demonstrate sensitivity to acid. TRPV1 activity is known to be modulated by extracellular protons, so that mildly acidic pH sensitises TRPV1 to other stimuli (Caterina *et al.*, 1997), whereas pH ≤ 5.9 activates TRPV1 at room temperature (Tominaga *et al.*, 1998). However, functional TRPV1 expression in odontoblasts remains controversial. Additionally, in contrast to ASICs, lactic acid was shown to inhibit TRPV1 in neurons (de la Roche *et al.*, 2016), suggesting that odontoblast TRPV1 expression is unlikely to allow them to detect plaque acids. TRPV4 is similarly gated by a drop in pH below 6, with a maximum current around pH 4, and mice lacking TRPV4 display impaired acidic nociception, induced by acetic acid injection into the abdomen (Suzuki *et al.*, 2003). Interestingly, Suzuki and colleagues (2003) also detected some TRPV4 activation by propionic acid, but not acetic or lactic acids, at neutral pH. TRPA1, generally found to be expressed in human and rat, but not mouse odontoblasts, has previously been implicated in the detection of weak organic acids, but not strong acids (Wang *et al.*, 2011). Further studies found that while both rodent and human TRPA1 is sensitive to intracellular acidification, only human TRPA1 is activated by extracellular protons (de la Roche *et al.*, 2013). In addition, two studies demonstrated the expression of TRPP2, also known as polycystic kidney disease

2-like 1 protein (PKD2L1), in odontoblasts (Thivichon-Prince *et al.*, 2009; Jerman *et al.*, 2014). TRPP2 has been proposed to function as a component of a sour taste receptor, activated by acid application to taste cells, with a threshold of around pH 5 (Kawaguchi *et al.*, 2010). Moreover, odontoblasts have been reported to express the K_{2P} channel TREK-1 (Magloire *et al.*, 2003). However, these channels are known to be gated by intracellular rather than extracellular increases in proton concentration (Maingret *et al.*, 1999). The effect of lactic acid on TREK-1 is also complex, as it either potentiates or reduces TREK-1 activity, depending on pH (Ghatak & Sikdar, 2016).

Few functional studies have specifically studied odontoblast responses to altered pH. Kimura and colleagues (2016) studied the effects of an alkaline environment, which can be created by pulp capping and root canal filling materials, on odontoblasts. They demonstrated a TRPA1-dependent increase in odontoblast intracellular Ca^{2+} concentrations in response to high-pH solutions (Kimura *et al.*, 2016). Another two reports of application of low-pH solutions to either mouse odontoblast-like cells (Utreras *et al.*, 2013) or rat odontoblasts (Tsumura *et al.*, 2012) could be identified in the literature. However, the authors used acidic solutions (pH 5.6, prepared using MES buffering agent, or pH 4 Krebs solution created with an unspecified acid, respectively) with the aim of specifically stimulating TRPV1-dependent Ca^{2+} influx. Only Tsumura and colleagues (2012) have demonstrated that the induced response can be inhibited by the TRPV1 inhibitor capsazepine. Nonetheless, the inhibition was only partial, suggesting an additional TRPV1-independent acid-sensitive component in rat odontoblasts.

No functional studies investigating the effects of biologically relevant acids on odontoblasts could be identified in the literature. Therefore, the three main acids that odontoblasts might get exposed to *in vivo* (see Table 4.1) were tested in the present *in vitro* study.

Table 4.1 Weak organic acids tested in this study

Name	Alternative name	Dissociation constant (K_a)*	pK_a (-log K_a)*	Structure
Acetic acid	Ethanoic acid	1.74×10^{-5}	4.76	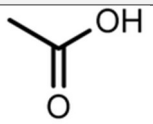
Lactic acid	2-Hydroxypropanoic acid	1.38×10^{-4}	3.86	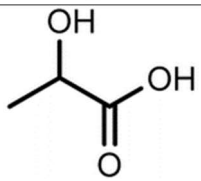
Propionic acid	Propanoic acid	1.35×10^{-5}	4.87	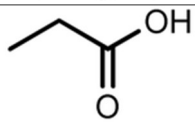

*At 25°C, values from (Lide, 2009).

4.1.3 OBJECTIVES OF THE PRESENT STUDY

To assess the acid-sensing ability of odontoblasts, the following specific objectives were formulated:

- To determine whether mouse odontoblast-like (OB) cells respond to extracellular acidification and biologically relevant acids using a microplate-based calcium flux assay.
- To test the ability of OB cells to release ATP in response to acid stimulation by measuring changes in ATP concentrations in OB cell culture medium.
- To investigate the potential mechanisms of acid sensing and acid-induced ATP release using pharmacological tools and calcium flux as well as ATP release assays.

4.2 Materials and methods

4.2.1 Reagents

Acetic acid, DL-lactic acid, and amiloride hydrochloride were obtained from Sigma, UK. Propionic acid was purchased from Fisher Chemicals. See Chapter 2 (section 2.2) for information on other reagents that were used in multiple chapters.

Amiloride was dissolved in dimethyl sulfoxide (DMSO; Sigma) and further diluted on the day of the experiment in complete culture medium. Stock acid solutions were diluted in extracellular solution (ECS) or complete culture medium to achieve appropriate pH (indicated in the text and figures).

4.2.2 Detection of changes in intracellular calcium concentration

The effect of different acids on OB cell intracellular Ca^{2+} concentration ($[Ca^{2+}]_i$) was investigated using a microplate-based calcium flux assay (described in section 2.5.1). These experiments involved a final 3:4 dilution of acidic or control solutions, performed by automated addition at 30 seconds of 120 µl of test solution to 40 µl of ECS already present in the cell-containing wells of a 96-well plate. The pH of acid solutions required to achieve the appropriate final pH was determined separately by direct measurement using a pH meter. TRPV4 antagonist experiments involved pre-treatment of the cells with HC067047 (0.1-10 µM) or DMSO vehicle for 15 minutes. Antagonist remained in contact with the cells throughout experimental runs. Independent experiments were performed using cells from different passages.

4.2.3 Measurement of ATP release

ATP release from OB cells was detected using the method for measuring extracellular ATP concentrations ($[ATP]_o$) described in section 2.6. To ensure that OB cells are exposed to the appropriate extracellular pH, treatments with acidic or control solutions were performed by directly replacing the culture medium in the wells with 500 µl/well of pre-warmed fresh complete culture medium that was pre-adjusted to the appropriate final pH using acetic, lactic, or propionic acid stock solutions or HCl, as specified in the

result figures and their captions. The medium was sampled 15 minutes later, and the same subsequent procedures were followed. In the inhibitor experiments, HC067047, amiloride, or DMSO vehicle were added to the culture medium for 15 minutes (or 30 minutes in the case of *N*-ethylmaleimide and dH_2O vehicle) before changing to the acidic or control media that also contained the same final concentrations of antagonists or respective vehicles. Comparisons were made with corresponding control wells from the same 4-well plate.

4.2.4 PrestoBlue cell viability assay

OB cells were seeded in clear 96-well plates at equal density per well and grown to confluence. On the day of the experiment, old culture medium was replaced with pre-warmed medium (100 µl/well) adjusted to the appropriate final pH using weak organic acids or HCl, as indicated. Acidic or control media were removed and washed out immediately (for 0-minute wells) or 5-30 minutes later, before adding fresh medium (100 µl/well) and 10x PrestoBlue® reagent (11 µl/well; Invitrogen). The wash step was included based on previous experiments (not shown), where acidic solutions by themselves were found to affect the fluorescence of PrestoBlue. The plates were incubated at 37°C for 20 minutes before measuring the fluorescence from the bottom of each well using FLUOstar Omega microplate reader (BMG Labtech; excitation filter at 544 nm and emission filter at 620-10 nm). An average of 3 wells was considered an n = 1.

4.2.5 Detection of acid-sensing ion channel gene expression in OB cells

RT-PCR and agarose gel electrophoresis were performed using the methods described in section 2.4. Samples loaded onto the gel were from odontoblast-like cells obtained by growing 17IA4 cells in the differentiating medium for 7 days.

4.2.6 Statistics

Differences in mean $[ATP]_o$ between OB cells exposed to acidic media at different pH and OB cells exposed to control (pH 7.4) medium were analysed using two-way ANOVA with Dunnett's multiple comparisons test. Two-way ANOVA with Bonferroni's

multiple comparisons test was used to compare the effects of inhibitors (HC067047, amiloride, and *N*-ethylmaleimide) to their respective vehicles on the responses induced by acidic media. A half maximal effective extracellular pH for HCl was estimated using GraphPad Prism 7 software after fitting a four-parameter (variable slope) sigmoidal pH-response curve.

4.3 Results

4.3.1 OB CELLS SENSE EXTRACELLULAR ACIDIFICATION AND RESPOND BY RELEASING ATP

A microplate-based calcium flux assay was first used to determine if lowering extracellular pH (pH_o) by adding hydrochloric acid (HCl) to the extracellular solution affects intracellular Ca^{2+} concentration in OB cells. While an initial drop in Fura-2AM emission intensity ratio (F_{340}/F_{380}) was detected at 30 seconds, as seen in Figure 4.1A, it is an artefact from the addition of a comparatively large volume of solution, visible in both acid-treated and control wells. Lowering pH_o from 7.4 to 6 increased F_{340}/F_{380} above baseline, with pH_o of 5 producing the largest increase (0.69 ± 0.05). However, in all cases, the increase was short-lasting, and F_{340}/F_{380} returned to baseline by the end of the experimental runs. The estimated half maximal effective pH_o for HCl was 6.14 ± 0.27 (see Figure 4.1B).

To better replicate the *in vivo* situation (Geddes, 1975; Hojo *et al.*, 1994) weak organic acids, namely acetic, lactic, and propionic acid, were then tested for their effects on OB cell intracellular Ca^{2+} concentration. As seen in Figure 4.2A-C, similarly to HCl, all three weak organic acids induced increases in $[Ca^{2+}]_i$ above baseline at pH_o below 6.5. However, unlike with HCl, most responses did not return to baseline by the end of experimental runs. Moreover, although not directly comparable with HCl, the amplitude of responses was lower, with the greatest mean maximum F_{340}/F_{380} changes of 0.32 ± 0.02, 0.38 ± 0.04, and 0.33 ± 0.05, observed at pH_o 5.5 for acetic, lactic, and propionic acid, respectively. There was also a detectable decrease in the amplitude of responses when pH_o was lowered below 5.5 (see Figure 4.2D).

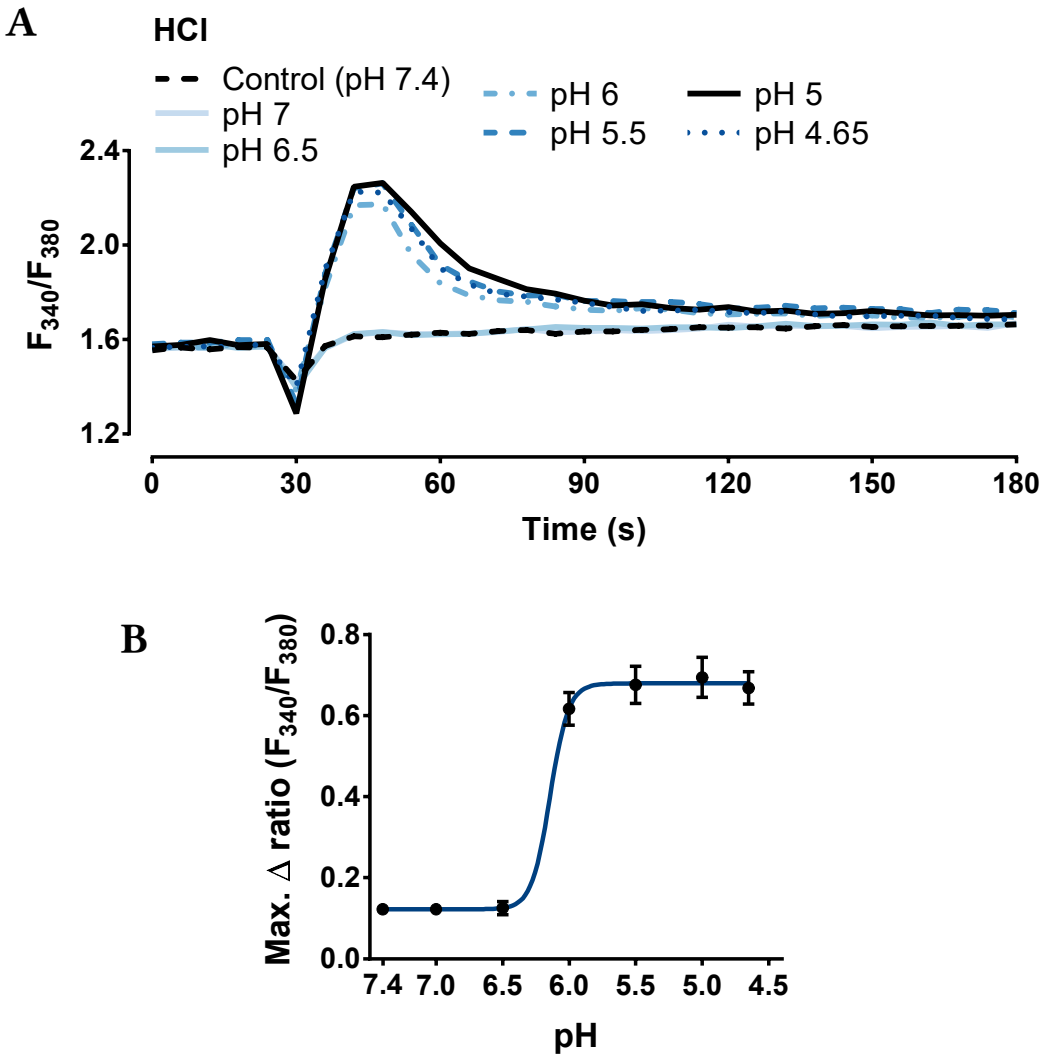

Figure 4.1 Extracellular acidification below pH 6.5 increases $[Ca^{2+}]_i$ in OB cells

A) Average traces of OB cell responses to increasingly acidic extracellular solutions prepared using hydrochloric acid (HCl; final pH 7.4-4.65). Fura-2AM fluorescence ratios (340 nm/380 nm) were recorded for 3 minutes, with automated addition of control or acidic solutions at 30 seconds. Error bars have been omitted for clarity. *B)* Extracellular acidification caused a pH-dependent increase in intracellular Ca^{2+} concentration. Data are mean maximal Fura-2AM ratio changes from baseline ± SEM (n = 9 triplicate measurements from 3 independent experiments).

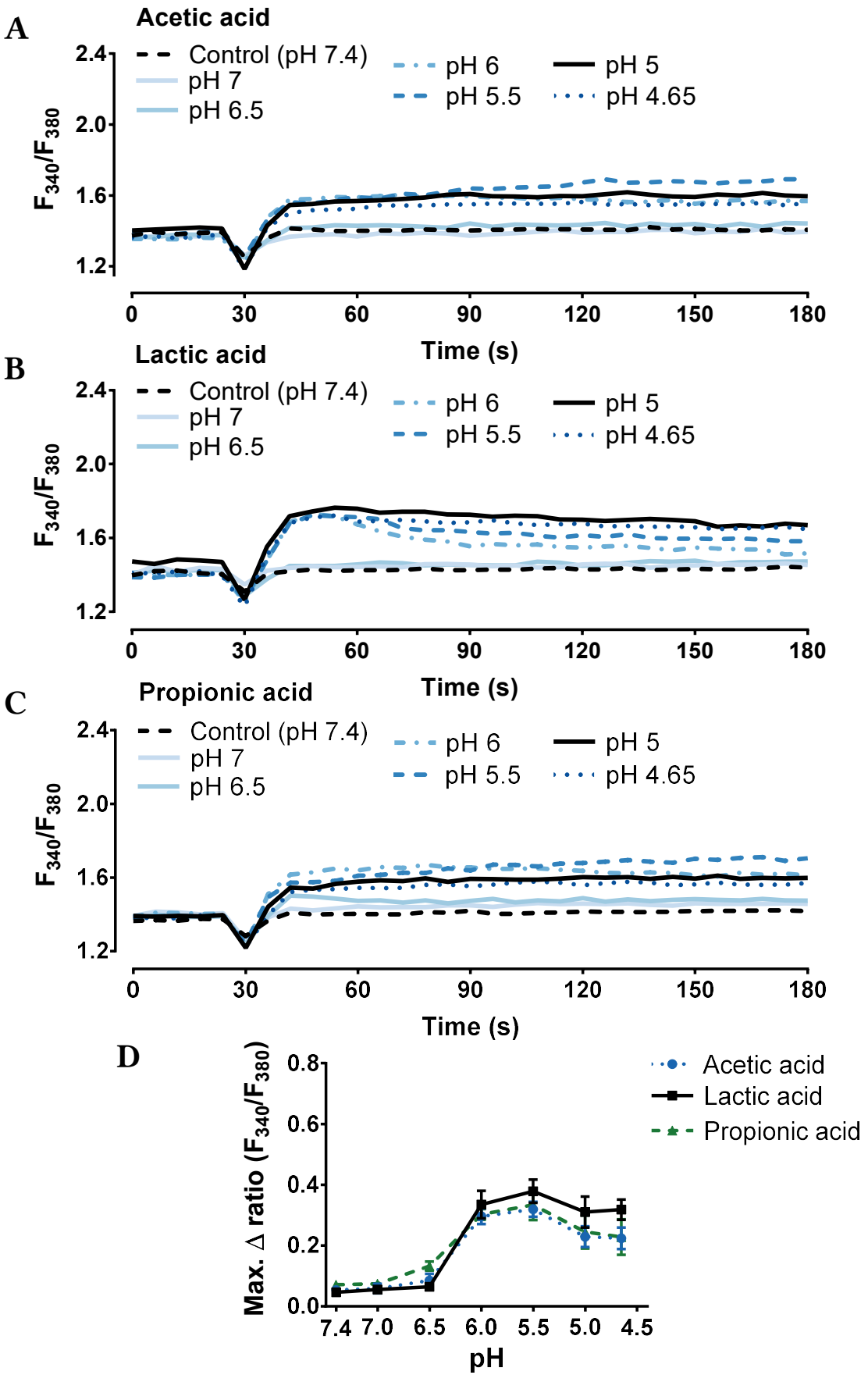
A
Acetic acid
Control (pH 7.4)
pH 7
pH 6.5
pH 6
pH 5.5
pH 5
pH 4.65
F340/F380
2.4
2.0
1.6
1.2
0
30
60
90
120
150
180
Time (s)
B
Lactic acid
Control (pH 7.4)
pH 7
pH 6.5
pH 6
pH 5.5
pH 5
pH 4.65
F340/F380
Time (s)
C
Propionic acid
Control (pH 7.4)
pH 7
pH 6.5
pH 6
pH 5.5
pH 5
pH 4.65
F340/F380
Time (s)
D
Max. Δ ratio (F340/F380)
0.8
0.6
0.4
0.2
0.0
7.4 7.0 6.5 6.0 5.5 5.0 4.5
pH
Acetic acid
Lactic acid
Propionic acid

Figure 4.2 Weak organic acids increase $[Ca^{2+}]_i$ in OB cells at pH below 6.5

A-C) Average traces of OB cell responses to acetic *(A)*, lactic *(B)*, and propionic *(C)* acid solutions at pH 7-4.65 or control extracellular solution (pH 7.4). Fura-2AM fluorescence ratios (340 nm/380 nm) were recorded for 3 minutes, with automated addition of control or acidic solutions at 30 seconds. Error bars have been omitted for clarity. *D)* Extracellular pH-response relationships for acetic, lactic, and propionic acid-induced changes in OB cell intracellular Ca^{2+} concentration. Data are presented as mean maximal Fura-2AM ratio changes from baseline ± SEM (n = 4-5 triplicate measurements from 4-5 independent experiments).

In addition to increased $[Ca^{2+}]_i$, all three weak organic acids and HCl significantly enhanced extracellular ATP concentration ($[ATP]_o$) in OB cell culture medium (Figure 4.3A). However, two different patterns of responses could be seen among the four acids in terms of the pH value that produced the highest increase in $[ATP]_o$. Acetic and propionic acids, the two weakest acids with the lowest acid dissociation constant (K_a) values (see Table 4.1), increased $[ATP]_o$ by 29.09 ± 3.56 nM ($p < 0.001$) and 11.55 ± 3.68 nM ($p = 0.02$) above pH 7.4 levels, respectively, with no significant increase at pH 5 or 7. In contrast, both lactic acid and HCl produced the highest increases in $[ATP]_o$ of 15.75 ± 3.55 nM ($p < 0.001$) and 19.43 ± 3.64 nM ($p < 0.001$) above pH 7.4 levels at pH 5. HCl, but not lactic acid, also caused an increase in $[ATP]_o$ at pH 6 ($p = 0.007$).

A cell viability assay was then performed to confirm that increased $[ATP]_o$ was not simply due to direct damage of OB cells, leading to cell lysis and ATP release. At all incubation times, including the one that directly matches ATP release experiments (15 minutes), and pH values that produced the highest increase in $[ATP]_o$, acidic solutions did not decrease cell viability below control (pH 7.4) levels (Figure 4.3B).

Collectively, these findings supported the ability of OB cells to detect extracellular acidification, including pH_o changes produced by biologically relevant weak organic acids. Moreover, OB cells respond to acidic stimulation by releasing ATP. Potential mechanisms responsible for acid sensing by OB cells were investigated next.

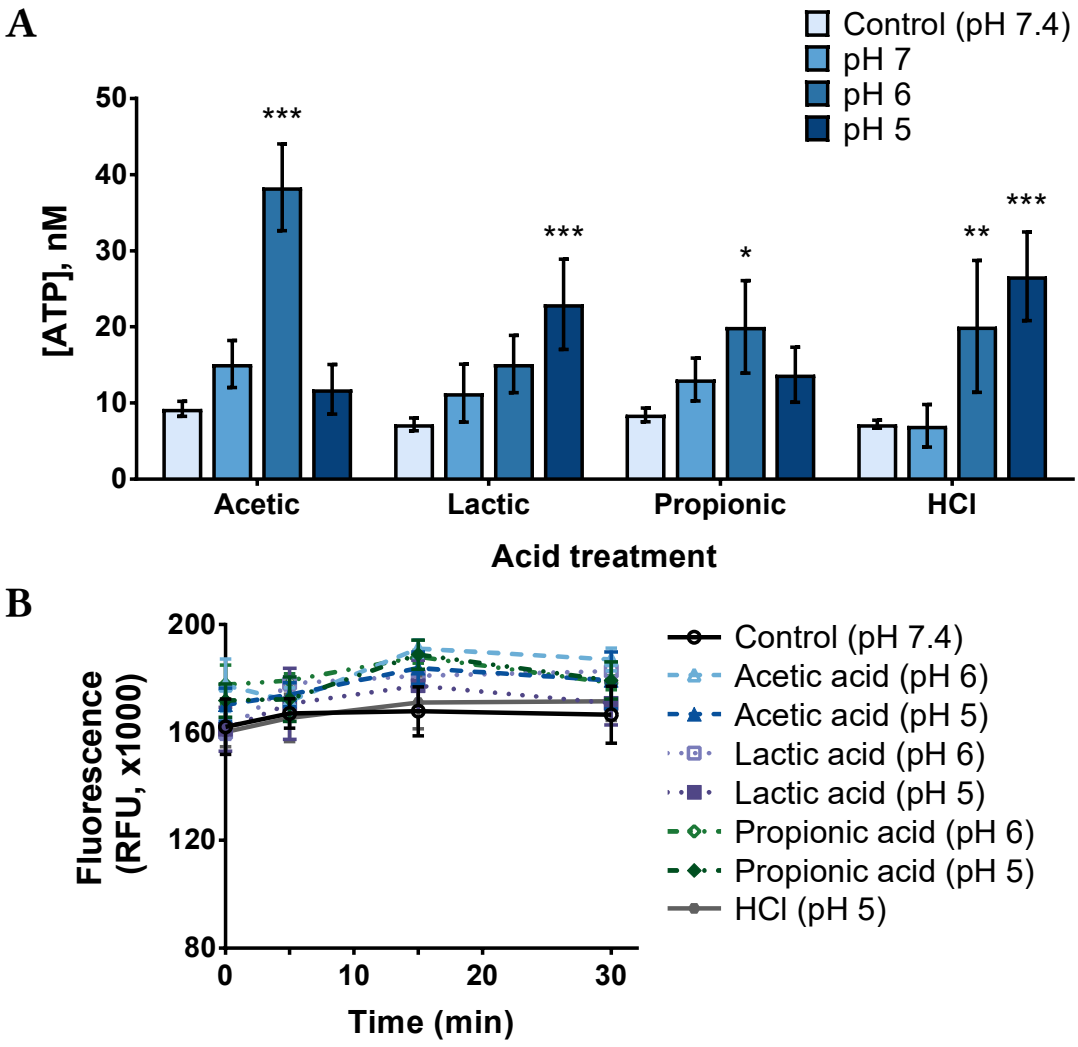

Figure 4.3 Weak organic acids and HCl at pH 6 and/or 5 induce ATP release from OB cells without affecting their viability

A) OB cell treatment with acetic or propionic acids (pH 6), lactic acid (pH 5) or HCl (pH 6-5) for 15 minutes caused a significant increase in extracellular ATP concentration, when compared with a control medium (pH 7.4). Data are presented as mean extracellular ATP concentration ± SEM. $^{*}p < 0.05$; $^{**}p < 0.01$; $^{***}p < 0.005$ (two-way ANOVA with Dunnett's *post hoc* test; n = 4-6 groups of paired duplicate measurements from 2-5 independent experiments). *B)* Identical treatment of OB cells with weak organic acid (pH 6-5) and HCl (pH 5) solutions did not decrease cell viability below control (pH 7.4) levels, as measured using PrestoBlue® reagent. Data are mean relative fluorescence units (RFU; excitation at 544 nm, emission at 620-10 nm) ± SEM (n = 3-5).

4.3.2 Investigating the mechanisms of acid detection by OB cells

Based on the previous finding that OB cells express functional TRPV4 ion channels and the reported TRPV4 acid sensitivity (Suzuki *et al.*, 2003), the effects of the selective TRPV4 antagonist HC067047 were first tested on acid-induced OB responses in both calcium flux and ATP release assays. Only those acidic solution pH values that were previously identified to produce the greatest increase in $[ATP]_o$ were used in ATP release assays. Nonetheless, HC067047 failed to affect the changes in $[Ca^{2+}]_i$ or $[ATP]_o$ induced by any of the acids (Figure 4.4).

The gene expression of acid-sensing ion channels (ASICs) was also tested in OB cells by RT-PCR. Faint bands of predicted sizes were produced by primers selective for the genes that encode ASICs 1 and 3, but not ASICs 2 and 4, despite the latter two being detected in TG tissues that were used as a positive control (Figure 4.5A). The effects of a non-selective ASIC blocker amiloride were then tested on changes in $[Ca^{2+}]_i$ and $[ATP]_o$ in OB cells produced by acid application. Since amiloride was found to directly increase baseline fluorescence during the calcium flux assay, its effects on acid-induced changes in $[Ca^{2+}]_i$ could not be conclusively determined (data not shown). However, pre-treatment of OB cells with amiloride at a concentration (100 μM) higher than the reported IC_{50} values (10-63 μM; Lingueglia and Lazdunski (2013)) did not significantly affect acid-induced ATP release (Figure 4.5B).

An intracellular pH indicator (pHrodo™ Red AM; Thermo Fisher Scientific) was later used to investigate intracellular pH (pH_i) changes in response to extracellular acid application. However, preliminary experiments revealed acid-induced changes in pHrodo Red fluorescence even in cell-free wells (data not shown), and the method for pH_i measurement could not be optimised due to time constraints.

Finally, the effects of *N*-ethylmaleimide pre-treatment were tested to provide more information about the mechanism of acid-induced ATP release from OB cells. *N*-ethylmaleimide significantly reduced $[ATP]_o$ below the levels produced by the application of weak organic acids or HCl ($p \leq 0.006$; see Figure 4.6).

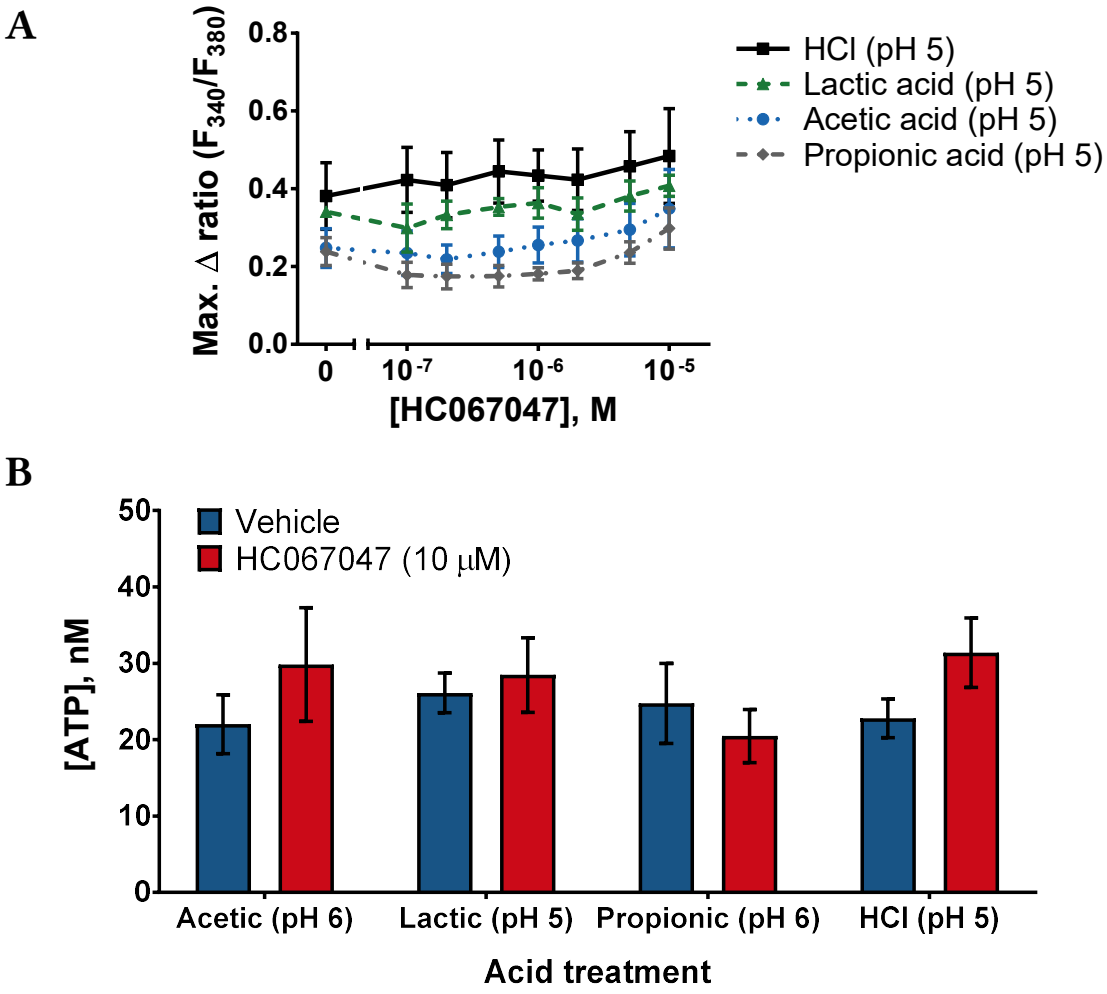

Figure 4.4 Inhibition of TRPV4 channels does not affect acid-induced calcium flux and ATP release from OB cells

A) Concentration-response relationship for the TRPV4 inhibitor HC067047 on acid-induced calcium flux in OB cells. Cells were pre-treated with HC067047 (0.1-10μM) or DMSO vehicle (0.2% (v/v); '0' point on the *x* axis) for 15 minutes before the start of fluorescence recordings. Antagonist remained in contact with the cells throughout experimental runs. Data are presented as mean maximal Fura-2AM ratio changes from baseline ± SEM (*n* = 2-3 triplicate measurements from 2-3 independent experiments). *B)* Pre-treatment of OB cells with HC067047 (10 μM) for 15 minutes did not significantly affect the increase in extracellular ATP concentration induced by weak organic acids or HCl (mean ± SEM; *n* = 4 groups of paired duplicate measurements from 4 independent experiments).

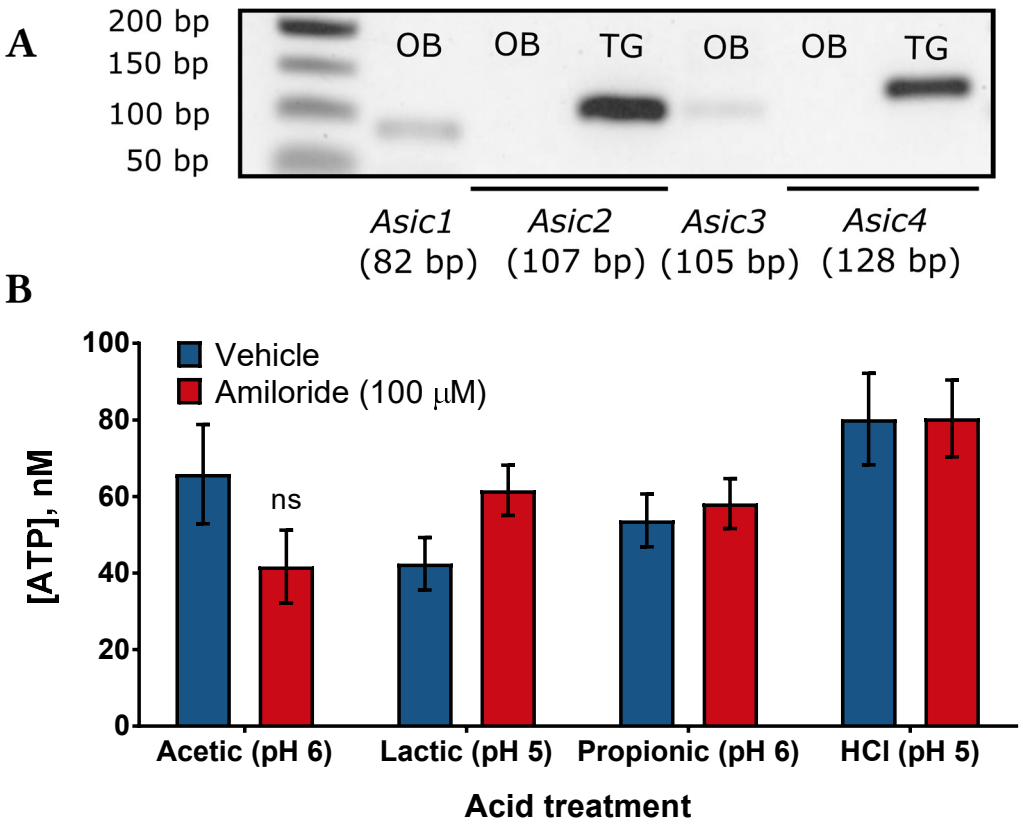

Figure 4.5 Blocking acid-sensing ion channels (ASICs) on OB cells does not prevent acid-induced ATP release

A) Gel electrophoresis of RT-PCR products from odontoblast-like (OB) cell samples produced bands for *Asic1* and *Asic3*, but not for *Asic2* or *Asic4*. The same primers for *Asic2* and *Asic4* produced intense bands from mouse trigeminal ganglion (TG) tissue sample, used as a positive control. Inverted colour images are presented in the figure. First lane contains Quick-Load® Purple 50 bp DNA Ladder (New England Biolabs). *B)* Pre-treatment of OB cells with a non-selective ASIC inhibitor amiloride (100 μM) for 15 minutes did not significantly affect the increase in extracellular ATP concentration induced by weak organic acids or HCl. Data are presented as mean ± SEM. ns = not statistically significant, $p > 0.05$ (two-way ANOVA; $n = 5$ groups of paired duplicate measurements from 3 independent experiments).

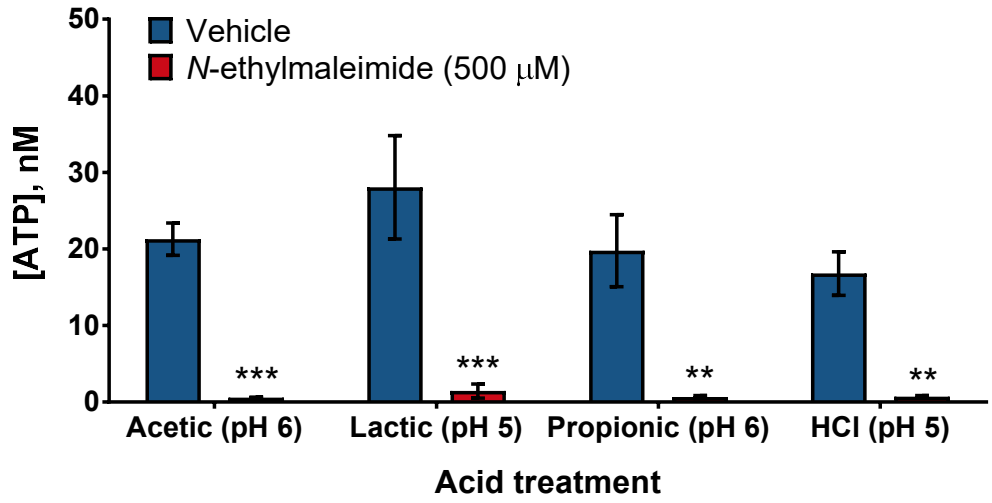

Figure 4.6 *N*-ethylmaleimide prevents acid-induced ATP release from OB cells

Pre-treatment of OB cells with *N*-ethylmaleimide (500 μM) for 30 minutes significantly reduced ATP release induced by weak organic acids or HCl, when compared with the respective vehicle. Data are expressed as mean ± SEM. $^{**}p < 0.01$; $^{***}p < 0.005$ (two-way ANOVA with Bonferroni's *post hoc* test; $n = 4$ groups of paired duplicate measurements from 3-4 independent experiments).

4.4 Discussion

4.4.1 Detection of biologically relevant acidification by odontoblasts

The present study is the first to investigate odontoblast responses to extracellular acidification that is biologically relevant in terms of the range of pH values and the acid types. The effect of increasing extracellular proton concentrations on mouse odontoblast-like (OB) cells was first tested by adjusting extracellular pH (pH_o) using a strong acid (HCl). Lowering pH_o below 6.5 caused a pH-dependent increase in OB intracellular Ca^{2+} concentrations ($[Ca^{2+}]_i$), with a half maximal effective pH of 6.14. Given that typical extracellular pH that odontoblast processes are exposed to in the pre-dentine layer is 7 (Lundgren *et al.*, 1992), this suggests odontoblast sensitivity to a relatively modest extracellular acidification. The responses persisted at lower pH values, but the amplitude plateaued at pH 5.5-5, similar to the range of pH found in active carious lesions in human teeth, as measured *in vivo* (Kuribayashi *et al.*, 2012). The proton-induced increase in $[Ca^{2+}]_i$ was transient at all pH values tested. One limitation

of the microplate-based calcium flux assay used in this experiment is the inability to wash off the test solutions. Therefore, repeated applications of acidic solutions could not be performed to determine the desensitisation profile of proton-induced responses. Although this could be achieved using a microscope-based calcium imaging system, acidification using a strong acid represents neither physiological nor pathological conditions. Therefore, weak organic acids were used instead of HCl to adjust pH_o in the next set of experiments.

As predicted by the fact that the same extracellular proton concentrations were tested, the threshold for acid-induced $[Ca^{2+}]_i$ increase (around pH 6.5) for all three weak acids (acetic, lactic, and propionic) resembled the one observed previously with HCl. However, the maximum weak acid-induced increase in $[Ca^{2+}]_i$ was produced at a higher pH (5.5 compared with 5.0 for HCl), with lower pH values producing smaller response amplitudes. As a result, sigmoidal curves could not be fitted. However, the most striking difference between weak acids and HCl was the duration of the acid-induced increase in $[Ca^{2+}]_i$. In particular, acetic and propionic acids, the weakest acids in terms of the lowest acid dissociation constant (K_a), generally appeared to produce the longest-lasting increase that did not return to baseline during the experimental runs, whereas lactic acid, consistent with its higher K_a value, displayed an intermediate profile between the other two weak acids and HCl. This highlights a possible relationship between the response profile and the distinct chemical characteristic of weak acids – their existence in solutions as both dissociated and undissociated forms. First of all, the weaker the acid, the higher its pK_a (negative logarithm of K_a) value (Table 4.1). The pK_a value is equal to the pH at which a certain weak acid exists as 50% dissociated form (anion and H^+) and 50% undissociated acid molecule (Featherstone & Lussi, 2006). Therefore, for example, at pH 5, a greater proportion of lactic acid than acetic or propionic acids is in the dissociated form (see Figure 4.7 for illustration), whereas HCl is completely dissociated at all pH values. As a result, all protons from HCl can act on OB cells at the same time, producing a transient response. However, as protons from dissociated weak acids interact with OB cells, the equilibrium might shift, leading to more protons being released from previously undissociated weak acids. In the case of lactic acid, the fact that it is primarily dissociated at some of the higher effective pH values (e.g. pH 6) suggests a limited supply of additional protons from the undissociated form, potentially

explaining why the responses are similar in duration to the ones produced by HCl, whereas at lower pH values, responses to lactic acid resemble prolonged increases in $[Ca^{2+}]_i$ observed with acetic and propionic acids, indicating continued release of protons from the undissociated acid molecules throughout the duration of experimental runs. However, since the concentration of available extracellular protons that the cells are initially exposed to is known and increases with decreasing pH, this does not explain the smaller amplitude of OB cell responses to weak acids seen at the lowest pH values tested (pH 5 and 4.65). One possible explanation might be related to the availability of anions that increase concurrently with protons when pH_o is adjusted using weak acids. Following weak acid dissociation, anions are able to interact with cations, such as Ca^{2+} and Mg^{2+}. The stability constant indicates the strength of this interaction for each anion-cation complex. While acetate and propionate complexes with both Ca^{2+} and Mg^{2+} have a low stability constant, the binding of lactate to these divalent cations is slightly stronger (Furia, 1972). This phenomenon is particularly relevant to the dental demineralisation processes *in vivo*, as in addition to hydroxyapatite crystal attack by protons, lactate anions contribute to tooth erosion by chelating calcium (Featherstone & Lussi, 2006). In relation to our data, it might be speculated that lowered extracellular Ca^{2+} concentrations could have negatively affected the amplitude of acid-induced OB cell responses at low pH values. However, this might not be biologically significant in terms of odontoblast responsiveness to acids from the oral cavity, as higher Ca^{2+} concentrations were found to be present in dentinal fluid in carious teeth (Larmas, 2001). Nonetheless, it suggests a potential involvement of Ca^{2+}-permeable ion channels in acid detection by OB cells and encouraged us to investigate the mechanism further.

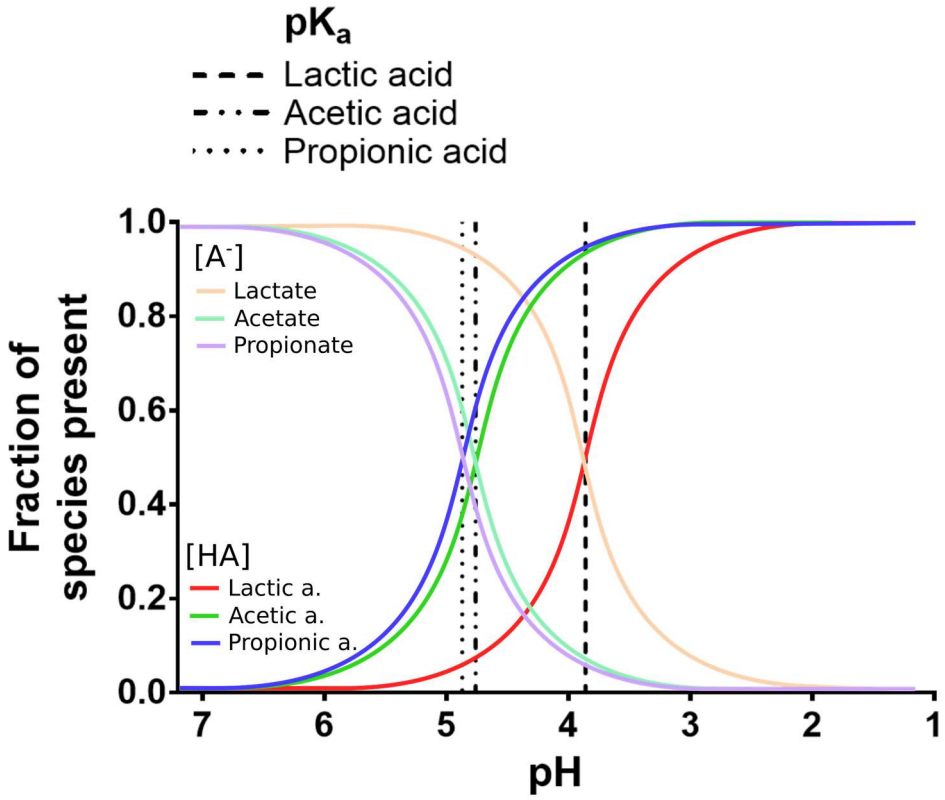

Figure 4.7 Illustration of weak organic acid dissociation at different pH values

The fraction of acetic, lactic, and propionic acids that exist in solution as a protonated/undissociated acid ([HA]) or deprotonated anion species ([A^-]), as predicted from their pK_a values.

Although functional expression of TRPV4 in mouse OB cells has already been confirmed (as discussed in Chapter 3), pre-treatment of OB cells with the selective TRPV4 antagonist HC067047 failed to reduce the acid-evoked increase in intracellular Ca^{2+} concentration. This, combined with the mismatch between the reported pH values that activate TRPV4 (pH < 6; Suzuki *et al.* (2003)) and threshold pH values identified in the present study (approximately pH 6.5), suggested that TRPV4 is not involved in acid-sensing by OB cells.

Due to the intrinsic fluorescence of the non-selective ASIC inhibitor amiloride, the involvement of ASICs in acid-sensing by OB cells could not be reliably determined using the same calcium flux assay. Weak gene expression for ASICs 1 and 3, but not 2 and 4, was detected in OB cells by RT-PCR. Since ASIC protein expression has not been investigated in this study, it is currently unclear whether ASIC proteins are present.

Moreover, the data from this study only partially agrees with human odontoblast data (Sole-Magdalena *et al.*, 2011), where immunostaining for ASIC2 was found to be more intense than for ASICs 1 and 3, which might represent another difference between odontoblasts from the two species. Some combinations of ASIC subunits (e.g. ASIC1b homomer or ASIC1b and 3 heteromer) have been demonstrated by others (Hesselager *et al.*, 2004) to have similar threshold pH and half maximal effective pH values to the ones detected in this study. However, ASICs are generally Na^+-permeable and would require an additional mechanism to mediate acid-induced increase in $[Ca^{2+}]_i$ in OB cells. The only exception is homomeric ASIC1a that demonstrates some permeability to Ca^{2+} (Bassler *et al.*, 2001). Nonetheless, the extent of Ca^{2+} entry via ASIC1a was later demonstrated to be negligible (Samways *et al.*, 2009). Therefore, ASICs seem unlikely to provide a direct mechanism for the acid-induced increase in $[Ca^{2+}]_i$ in OB cells observed in this study. Future experiments could be performed in extracellular solutions lacking either Ca^{2+} or Na^+ ions to help clarify the source of increased intracellular Ca^{2+} and the involvement of ASICs. On the other hand, while intracellular Ca^{2+} concentrations were measured in this study, elevation in Na^+, rather than Ca^{2+}, might be important for potential onward signalling from stimulated odontoblasts to neurons, proposed to be relevant in dental pain. Ideally, immunocytochemistry or Western blotting would be used to investigate ASIC protein expression in odontoblasts, whereas electrophysiological techniques would help to demonstrate ASIC activity, as ASIC desensitisation could explain the observed transient response profile resulting from HCl application to odontoblasts.

4.4.2 Acid-induced ATP release from odontoblasts

In this study, HCl and weak organic acids were also demonstrated to stimulate ATP release from OB cells. In the case of HCl, changes in extracellular ATP concentrations correlated well with pH and $[Ca^{2+}]_i$, with ATP release only observed at pH values of 5 and 6, but not 7. On the other hand, the finding that lactic acid only stimulated ATP release at pH 5, whereas the weakest acids (acetic and propionic) induced ATP release at pH 6, but not 5, cannot solely be explained by differences in $[Ca^{2+}]_i$. An additional characteristic of weak acids that has not been considered in the previous section is their ability to cross the cell membranes in the undissociated/protonated form, but not as

deprotonated anions, which can eventually result in intracellular acidification (Malhotra & Casey, 2015). A similar lack of correlation between the stimulus pH and response has been observed in the detection of weak acids by taste receptor cells, where intracellular acidification was eventually identified as one of the key events (Lyall *et al.*, 2001). Therefore, the measurement of OB cell intracellular pH changes induced by extracellular weak acid application might provide more information about the processes involved. However, it was also important to determine that increased extracellular ATP concentrations were not simply a consequence of acid-induced OB cell death. Low pH_o has previously been reported to induce human dental pulp cell death within days (Hirose *et al.*, 2016). Although a detrimental effect in response to a long-term exposure to acids cannot be excluded, treatment duration applicable to our experiments did not affect OB cell viability, suggesting that ATP was released as a response to a stimulus and could potentially act as a means of acid-induced signal transduction to adjacent cells.

In relation to the possible mechanisms for the acid detection and subsequent ATP release by OB cells, TRPV4 was further demonstrated not to be involved, as the same concentration of the selective TRPV4 antagonist that previously successfully blocked TRPV4-induced ATP release from OB cells did not affect acid-evoked ATP release from OB cells in the present study. While the non-selective ASIC inhibitor amiloride similarly failed to significantly affect acid-induced ATP release, suggesting that alternative acid-sensitive ion channels might be involved, *N*-ethylmaleimide did significantly inhibit acid-induced ATP release from OB cells, demonstrating that this process can be prevented. As discussed in the previous chapter, the latter observation does not necessarily demonstrate the involvement of vesicular exocytosis in acid-induced ATP release. However, the fact that both TRPV4-dependent (Chapter 3) and TRPV4-independent (acid-induced) enhancement of OB cell extracellular ATP concentration is sensitive to the inhibition by *N*-ethylmaleimide suggests the activity of this compound on a shared mechanism in the pathways leading to ATP release or a non-specific blockade of upstream processes, such as ATP generation.

Overall, acid-sensing by OB cells and subsequent acid-induced ATP release from OB cells further support the sensory role of odontoblasts, with potential relevance to either

dentine hypersensitivity (in response to highly acidic foods and drinks) or to inflammation-associated dental pain (by detecting caries-related acid production).

Chapter 5

Investigation of mouse trigeminal ganglion neuron activation and sensitisation *in vitro*

5.1 Introduction

5.1.1 Mechanisms of inflammation-related peripheral sensitisation

Tissue damage and inflammation is associated with the production of multiple inflammatory mediators by resident and infiltrating immune cells, as well as other disrupted local cells. As this "inflammatory soup" floods the microenvironment of peripheral sensory nerve afferents, its components can interact with specific receptors present on afferent terminals and activate a range of intracellular signalling pathways that ultimately lead to an increase in neuronal excitability (peripheral sensitisation; Hucho and Levine (2007)). Examples of some of the mechanisms involved in peripheral sensitisation are illustrated in Figure 5.1.

In relation to odontogenic pain, ATP is of interest as one of the components of the inflammatory soup, with a potential role in pain associated with dental pulp inflammation, as well as its proposed role in intercellular odontoblasts-neuron communication. ATP is known to influence neuronal activity via its actions on two

distinct families of receptors. It can directly cause neuronal membrane depolarisation by activating cation channels that belong to the ionotropic P2X receptor family or indirectly modulate neuronal activity via metabotropic (G protein-coupled) P2Y receptors (Tsuda *et al.*, 2010). P2Y receptors $P2Y_1$, $P2Y_2$, $P2Y_4$, $P2Y_6$, and $P2Y_{11}$, which primarily couple to the $G_{q/11}$ subfamily of G-proteins (Erb & Weisman, 2012), stimulate phospholipase C (PLC), which in turn cleaves the membrane phospholipid phosphatidylinositol-4,5-bisphosphate (PIP_2) into inositol triphosphate (IP_3) and diacylglycerol (DAG). IP_3 activity on its receptor IP_3R can elevate intracellular Ca^{2+} concentrations in neurons via Ca^{2+} release from the intracellular stores, whereas one of the actions of DAG is to stimulate protein kinase C (PKC). The binding of other inflammatory mediators, such as bradykinin and prostaglandin E_2 (PGE_2), to their specific GPCRs can also activate stimulatory G_s, leading to adenylyl cyclase-dependent synthesis of cyclic adenosine monophosphate (cAMP) and subsequent activation of protein kinase A (PKA). PKC and PKA can modulate the activity of neuronal ion channels, including transient receptor potential (TRP) channels, via their phosphorylation (Lechner & Boehm, 2004; Kadkova *et al.*, 2017). In particular, TRPA1 and TRPV1 have been extensively linked to orofacial pain states (Henry & Hargreaves, 2007; Mickle *et al.*, 2016). Therefore, they were the focus of the investigations into the trigeminal ganglion (TG) neuron sensitisation discussed in this chapter. Another TRP channel, TRPV4, was also studied. TRPV4 expression in sensory neurons is controversial, although it was recently detected on the nerve fibres in human dental pulps and found to be upregulated during inflammation (Bakri *et al.*, 2018).

The prototypical pro-inflammatory cytokines tumour necrosis factor alpha (TNFα) and interleukin 1 beta (IL-1β) might also be relevant to odontogenic pain, as they have been detected in dentinal fluid (Geraldeli *et al.*, 2012) and are upregulated in inflamed dental pulps (Kokkas *et al.*, 2007; Silva *et al.*, 2009). TNFα and IL-1β act on specific cytokine receptors and can affect neuronal excitability through multiple pathways (reviewed by Üçeyler *et al.* (2009)), including transcriptional changes via the activation of nuclear factor-κB (NF-κB) and mitogen-activated protein kinases (MAPK), namely extracellular signal-regulated kinases (ERK), p38 MAPK, and cJun NH_2-terminal kinases (JNK) (Zhang & An, 2007; Sabio & Davis, 2014).

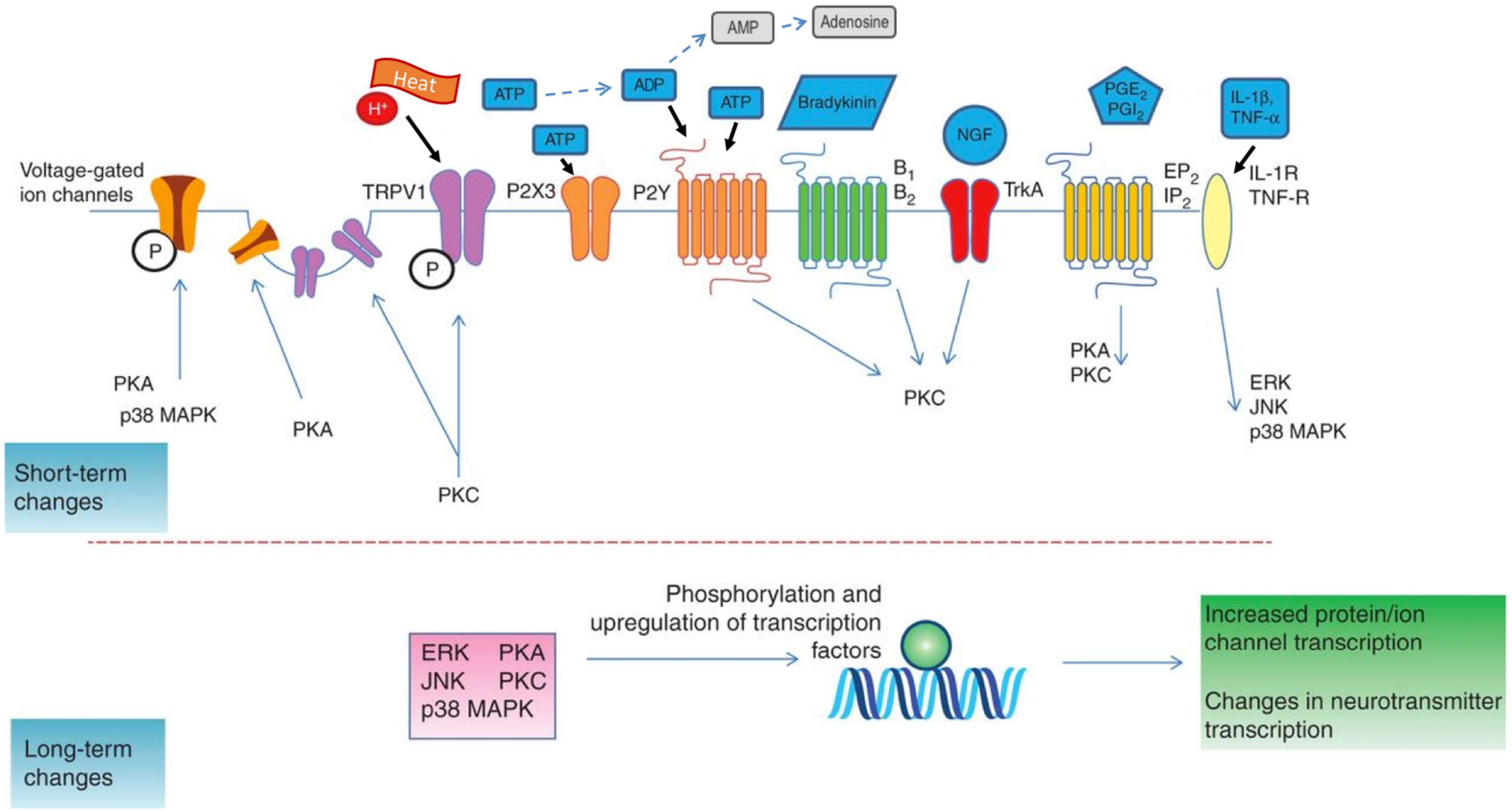
Heat
H+
ATP
AMP
Adenosine
ADP
ATP
ATP
Bradykinin
NGF
PGE2
PGI2
IL-1β,
TNF-α
Voltage-gated
ion channels
TRPV1
P2X3
P2Y
B1
B2
TrkA
EP2
IP2
IL-1R
TNF-R
P
P
PKA
p38 MAPK
PKA
PKC
PKC
PKA
PKC
ERK
JNK
p38 MAPK
Short-term
changes
Phosphorylation and
upregulation of transcription
factors
ERK PKA
JNK PKC
p38 MAPK
Increased protein/ion
channel transcription
Changes in neurotransmitter
transcription
Long-term
changes

Figure 5.1 Schematic representation of the mechanisms involved in peripheral sensitisation

Components of the "inflammatory soup" can cause peripheral sensitisation by acting on specific receptors on peripheral sensory nerve endings. Neurotrophic factor NGF acts via its receptor tyrosine kinase TrkA. ATP can directly stimulate P2X ligand-gated ion channels. Both ATP and its degradation product, ADP, can activate P2Y G protein-coupled receptors (GPCRs). Bradykinin and prostaglandins E_2 and I_2 activate B_1/B_2, EP_2 and IP_2 GPCRs, respectively. Activation of these receptors can initiate downstream signalling pathways that typically culminate in the stimulation of protein kinases PKA and PKC. Short-term changes induced by inflammatory mediators include PKA/PKC-dependent post-translational modifications of ion channels important to neuronal excitability, including transduction channels and voltage-gated ion channels. For example, PKC activity induces trafficking of TRPV1 to the plasma membrane and its phosphorylation, leading to a decrease in TRPV1 activation threshold. Long-term transcriptional changes can also be initiated by inflammatory mediators, such as a pro-inflammatory cytokine TNFα, which acts on TNFR receptors, resulting in the stimulation of mitogen-activated protein kinases. Black arrows indicate the mechanisms relevant to the experiments described in this chapter. Adapted from (Ellis & Bennett, 2013) with permission from Elsevier.

5.1.2 Objectives of the present study

To establish a functional TG neuron sensitisation assay, the following objectives were formulated:

- To identify the concentrations of TRPA1, TRPV1, and TRPV4 agonists, as well as ATP, that produce a submaximal increase in the proportion of sensitive cultured mouse TG neurons and/or intracellular Ca^{2+} concentrations, using calcium imaging.

- To test the effects of short-term (1-hour) and long-term (24-hour) TG neuron pre-treatments with classical inflammatory mediators TNFα and IL-1β on the sensitivity of TG neurons, using the established calcium imaging-based system.

Moreover, calcium imaging experiments described in this chapter aimed to further investigate the ability of cultured mouse TG neurons to detect the molecules identified in Chapter 3 as being released from stimulated odontoblasts, namely ATP and glutamate. Objectives of these experiments are as follows:

- To investigate which purinergic P2 receptors are functional on TG neurons, using selective agonists of the most relevant P2X and P2Y receptors.
- To examine the ability of glutamate to increase intracellular Ca^{2+} concentrations in TG neurons.

5.2 Materials and methods

5.2.1 Reagents

L-glutamic acid (L-glutamate) and alpha,beta-methylene ATP (α,β-meATP) were obtained from Sigma. MRS2365 and 2-ThioUTP were purchased from Tocris, whereas recombinant mouse interleukin 1 beta (IL-1β) was obtained from R&D Systems. For information on other reagents used in multiple chapters see Chapter 2 (section 2.2). MRS2365, 2-ThioUTP, L-glutamate, and α,β-meATP were all initially dissolved in dH_2O. IL-1β was initially reconstituted in DPBS containing 0.2% BSA. All compounds were further diluted in ECS on the day of the experiment to the appropriate concentrations indicated in subsequent sections.

5.2.2 Calcium imaging of mouse trigeminal ganglion (TG) neurons

Primary mouse TG neurons were prepared as described in Chapter 2 (section 2.3.2), and calcium imaging experiments were performed as described in section 2.5.2. Typical experimental runs testing the concentration-response relationships of different agonists involved an initial baseline recording, during which TG neurons were perfused with a standard extracellular solution (ECS), followed by one-minute applications with increasing concentrations of the appropriate compound, with one-minute ECS washes in between each concentration, with the exception of some L-glutamate experiments, where perfusion with each concentration of L-glutamate lasted for 3 minutes. Other L-glutamate experiments, and some ATP experiments, as indicated, involved the application of a single agonist concentration or a corresponding vehicle. Experimental runs testing different selective P2 receptor agonists involved longer washes with ECS between each agonist application. Moreover, the order of P2 agonists was changed in each experimental run.

In the short-term sensitisation experiments, TG neurons were exposed to TNFα (30 ng/ml), IL-1β (10 ng/ml), or a respective vehicle for 1 hour during the incubation with Fura-2AM. Long-term (24-hour) sensitisation experiments involved the addition of TNFα/IL-1β/vehicle into the neuronal culture medium approximately 23 hours before the loading of TG neurons with Fura-2AM. The neurons were then exposed to TNFα, IL-1β, or a respective vehicle for another hour during the incubation with Fura-2AM. After the application of the compound of interest, experimental runs involved the application of 1 μM capsaicin before the final application of 50 mM KCl, except for the initial sensitisation experiments testing the effects of 1-hour TNFα pre-treatment, which only included the final depolarising challenge with 50 mM KCl.

Two main parameters have been chosen as the endpoints of the calcium imaging assay: the overall percentage of TG neurons that demonstrate an increase in $[Ca^{2+}]_i$ in response to a particular stimulus, detected as increased Fura-2AM emission intensity ratio (F_{340}/F_{380}) above the 20% threshold of the corresponding maximum increase in response to KCl (50 mM; or capsaicin (1 μM), where applicable) and the mean amplitude of the response displayed by the responding neurons.

Neurons from at least 3 mice were imaged to complete each set of experiments. The exact number of experimental runs and the total number of neurons are indicated in result figures and/or their captions.

5.2.3 Statistics

Differences in the percentage of responding TG neurons were analysed using Fisher's exact test. Unpaired *t*-test was used to compare the amplitudes of responding TG neuron responses to the agonist application, except for the responses to different glutamate concentrations, which were compared using one-way ANOVA. To compare the cumulative distributions of individual TG neuron responses, Kolmogorov-Smirnov test was performed using an online tool, provided by Saint John's University, USA (http://www.physics.csbsju.edu/stats/KS-test.html). Results from this test are indicated in the text in the results section.

5.3 Results

5.3.1 Functional characterisation of mouse TG neurons and development of TG neuron sensitisation assay

In order to establish a calcium imaging-based TG neuron sensitisation assay, the concentrations of the agonists for the ion channels and receptors of interest (allyl isothiocyanate (AITC) for TRPA1, capsaicin for TRPV1, GSK1016790A for TRPV4, and ATP for purinergic P2 receptors) that provide a sufficient window for potentiation of TG neuron responses had to be identified. Therefore, the lower range of their effective concentrations that increase intracellular Ca^{2+} concentrations ($[Ca^{2+}]_i$), have been tested.

AITC produced a concentration-dependent increase in the percentage of responding TG neurons from 5.3% (25/468 neurons) at 2 μM to 22.9% (107/468 neurons) at 10 μM AITC. However, no change in the mean amplitude of TG neuron responses could be detected with increasing AITC concentrations (Figure 5.2). In contrast, capsaicin caused a concentration-dependent increase in both the percentage of responding neurons (from 13.0% (57/438 neurons) at 10 nM to 40.4% (177/438 neurons) at 50 nM capsaicin) and the size of the response (from 42.7 ± 5.1% to 62.4 ± 3.8% of KCl response at 10 nM and 50 nM, respectively; see Figure 5.3).

Based on the same criteria used to identify the responders to AITC and capsaicin (>20% of the corresponding maximum response, as discussed in section 5.2.2), less than 3% of TG neurons from wild-type mice (up to 7 out of 250) were found to be responsive to any of the GSK1016790A concentrations tested (10, 20, and 50 nM; Figure 5.4), with no obvious concentration-dependent effect on the magnitude of the responses (data not shown). Moreover, no significant difference could be detected between the TG neurons from the wild-type and TRPV4 knock-out mice.

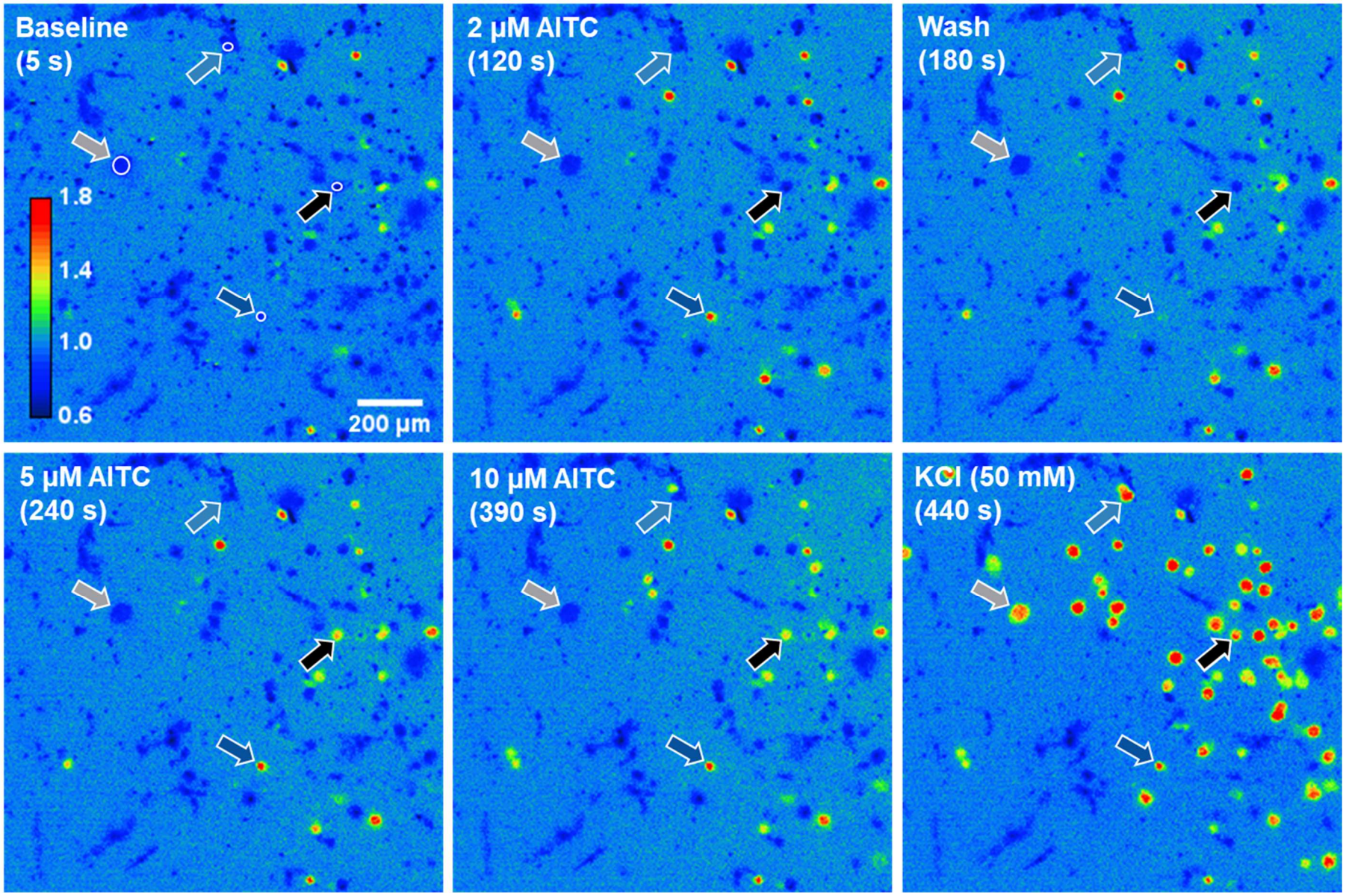
A
Baseline
(5 s)
1.8
1.4
1.0
0.6
200 μm
2 μM AITC
(120 s)
Wash
(180 s)
5 μM AITC
(240 s)
10 μM AITC
(390 s)
KCl (50 mM)
(440 s)

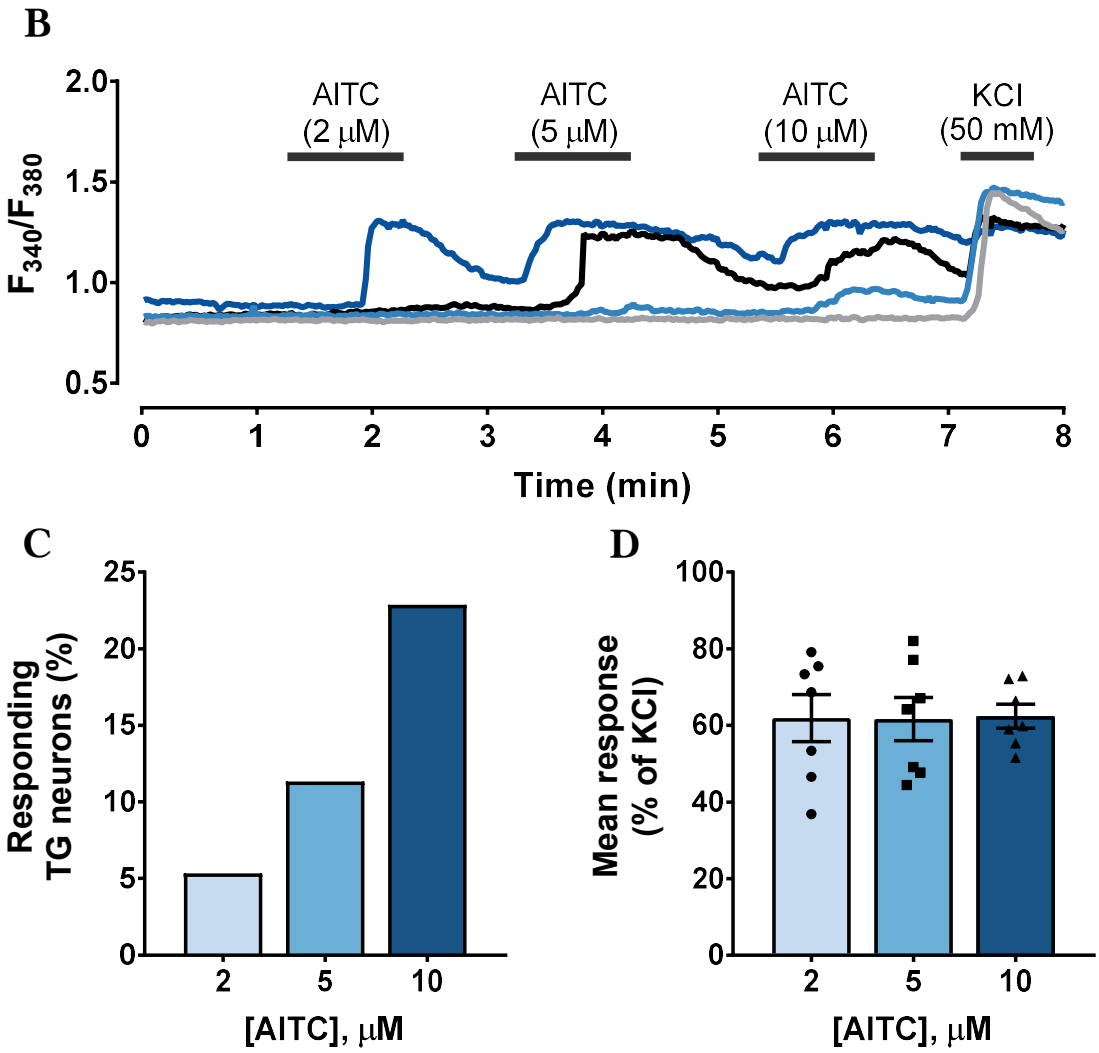

Figure 5.2 Activation of TRPA1 ion channels on TG neurons by allyl isothiocyanate

Example pseudocolour images *(A)* and traces *(B)* of TG neuron responses to consecutive application of increasing concentrations of the TRPA1 agonist allyl isothiocyanate (AITC). The arrows in *A* indicate the same TG neurons as the colour-coded traces in *B*. The calcium image colour range represents Fura-2AM fluorescence ratio. *C)* AITC produces a concentration-dependent increase in the proportion of TG neurons that respond with an increase in intracellular Ca^{2+} concentration. *D)* The amplitude of TG neuron responses to increasing concentrations of AITC as a percentage of corresponding responses to 50 mM KCl. Data are presented as mean ± SEM (n = 7; 468 neurons).

A

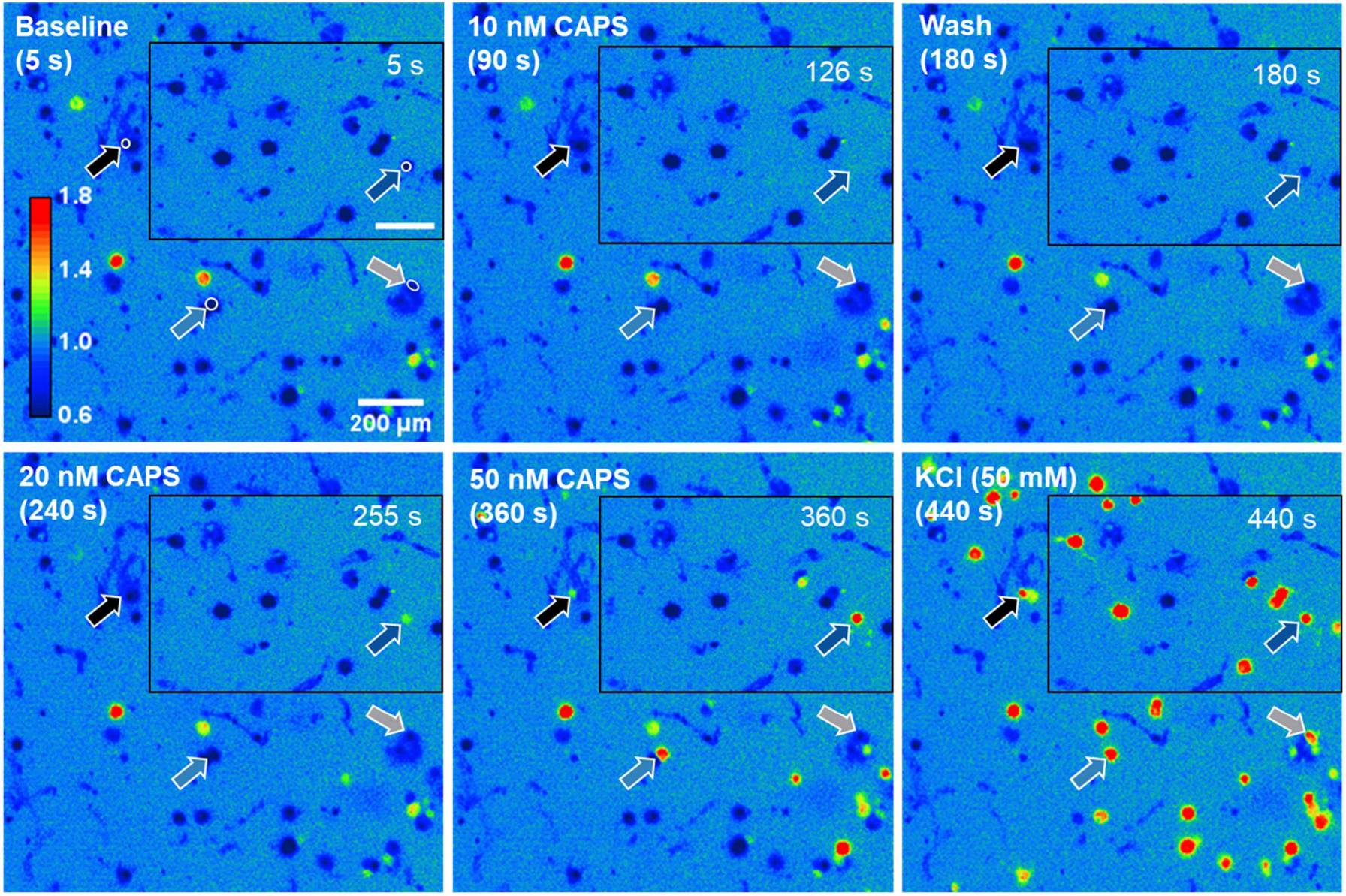
Baseline
(5 s)
5 s
1.8
1.4
1.0
0.6
200 µm
10 nM CAPS
(90 s)
126 s
Wash
(180 s)
180 s
20 nM CAPS
(240 s)
255 s
50 nM CAPS
(360 s)
360 s
KCl (50 mM)
(440 s)
440 s

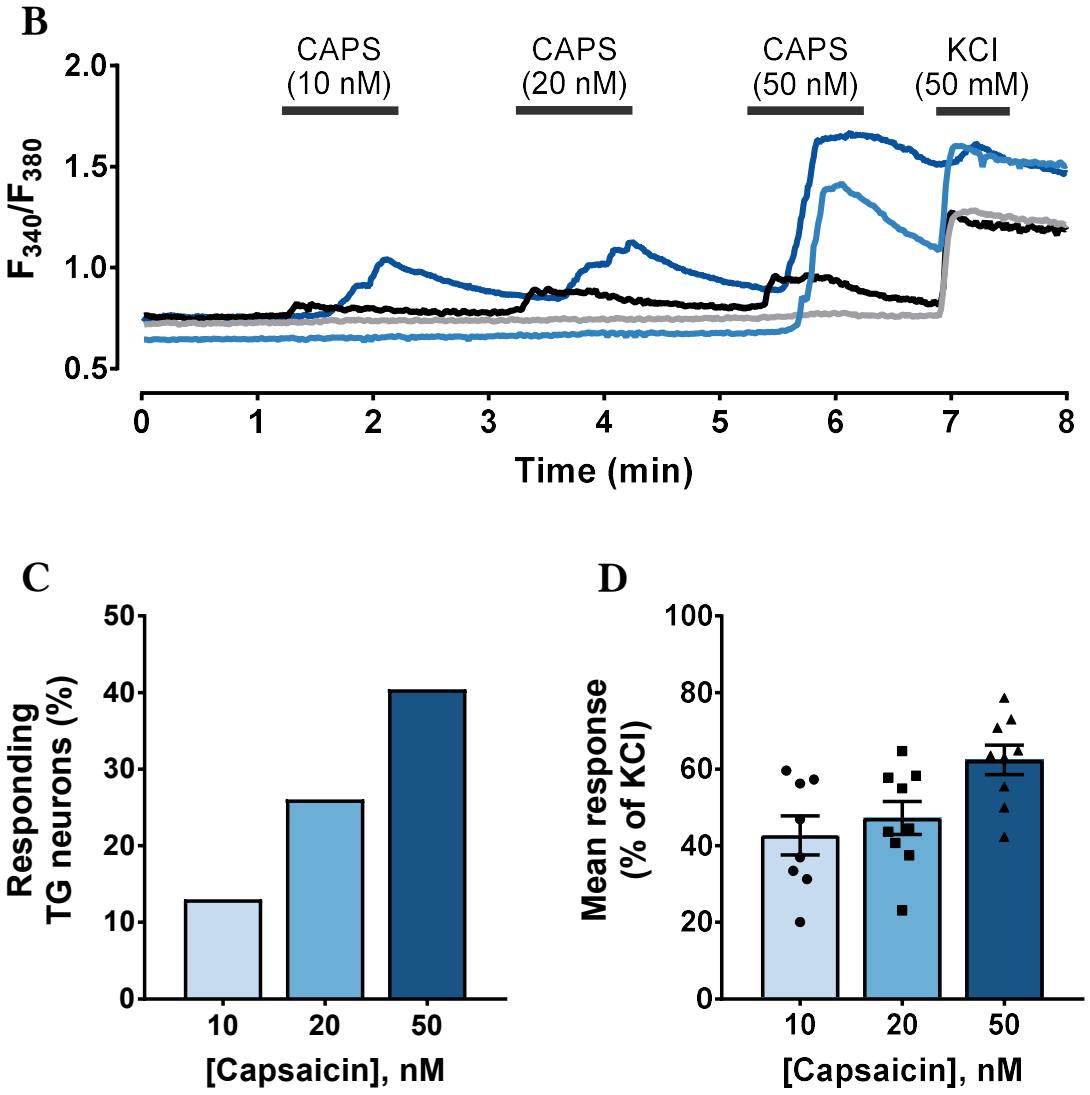

Figure 5.3 Activation of TRPV1 ion channels on TG neurons by capsaicin

Example pseudocolour images *(A)* and traces *(B)* of TG neuron responses to consecutive application of increasing concentrations of the TRPV1 agonist capsaicin (CAPS). The arrows in *A* indicate the same TG neurons as the colour-coded traces in *B*. The calcium image colour range represents Fura-2AM fluorescence ratio. The inset represents a separate experimental run. Scale bar = 200 μM. *C)* Capsaicin produces a concentration-dependent increase in the proportion of TG neurons that respond with an increase in intracellular Ca^{2+} concentration. *D)* The amplitude of TG neuron responses to increasing concentrations of capsaicin as a percentage of corresponding responses to 50 mM KCl. Data are presented as mean ± SEM (n = 9; 438 neurons).

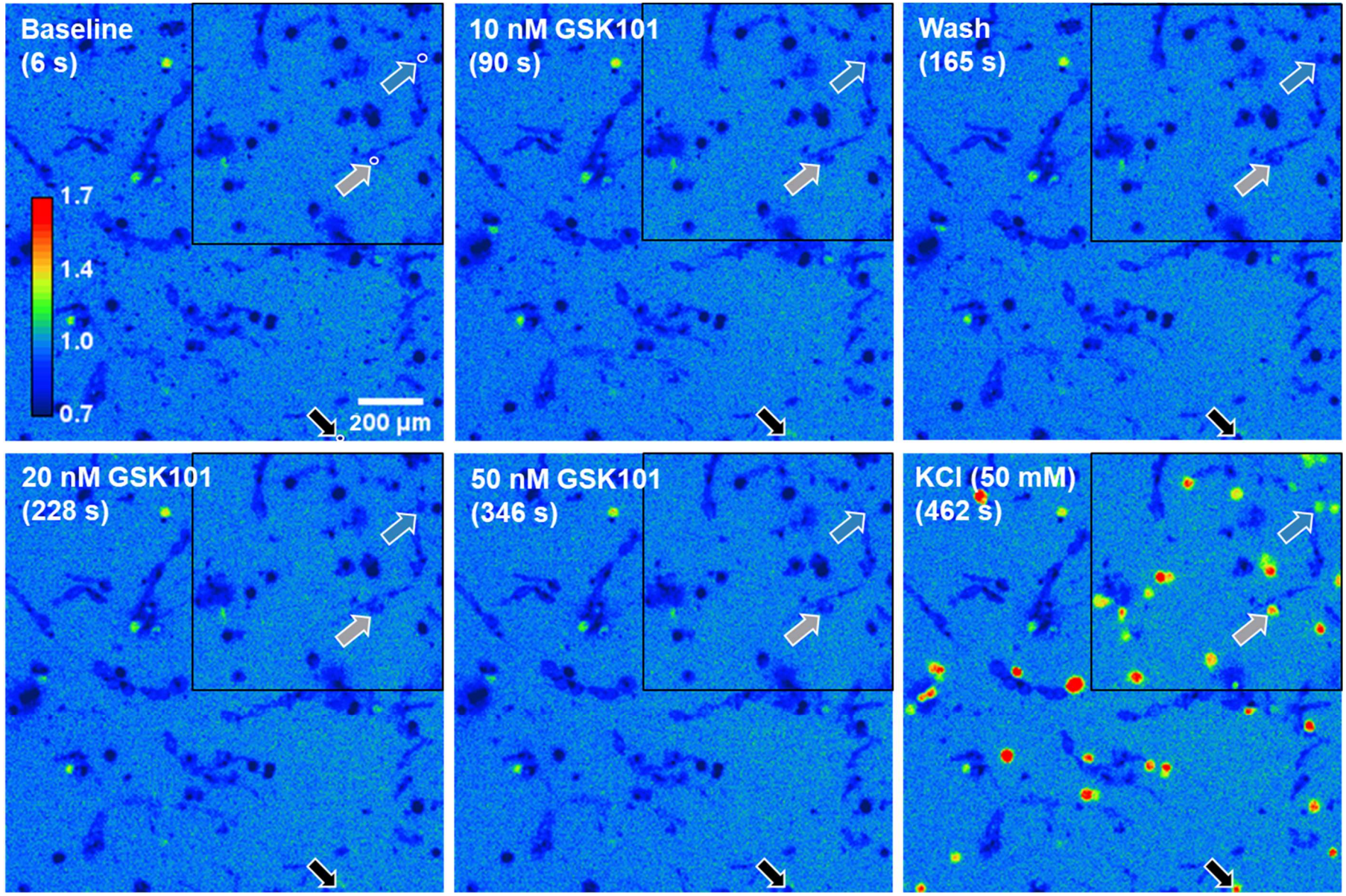
A
Baseline
(6 s)
1.7
1.4
1.0
0.7
200 µm
10 nM GSK101
(90 s)
Wash
(165 s)
20 nM GSK101
(228 s)
50 nM GSK101
(346 s)
KCl (50 mM)
(462 s)

B

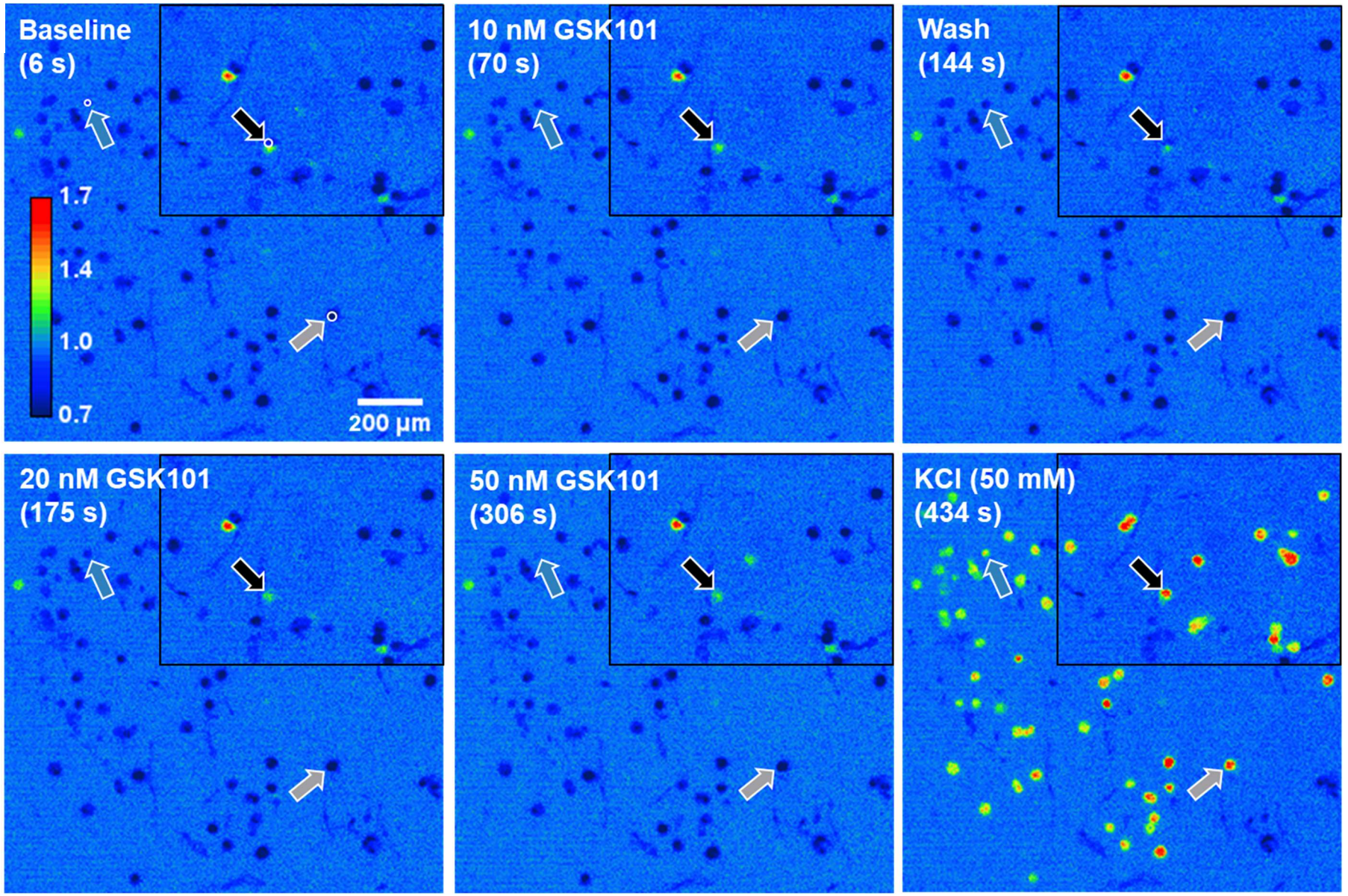
Baseline
(6 s)
1.7
1.4
1.0
0.7
200 µm
10 nM GSK101
(70 s)
Wash
(144 s)
20 nM GSK101
(175 s)
50 nM GSK101
(306 s)
KCl (50 mM)
(434 s)

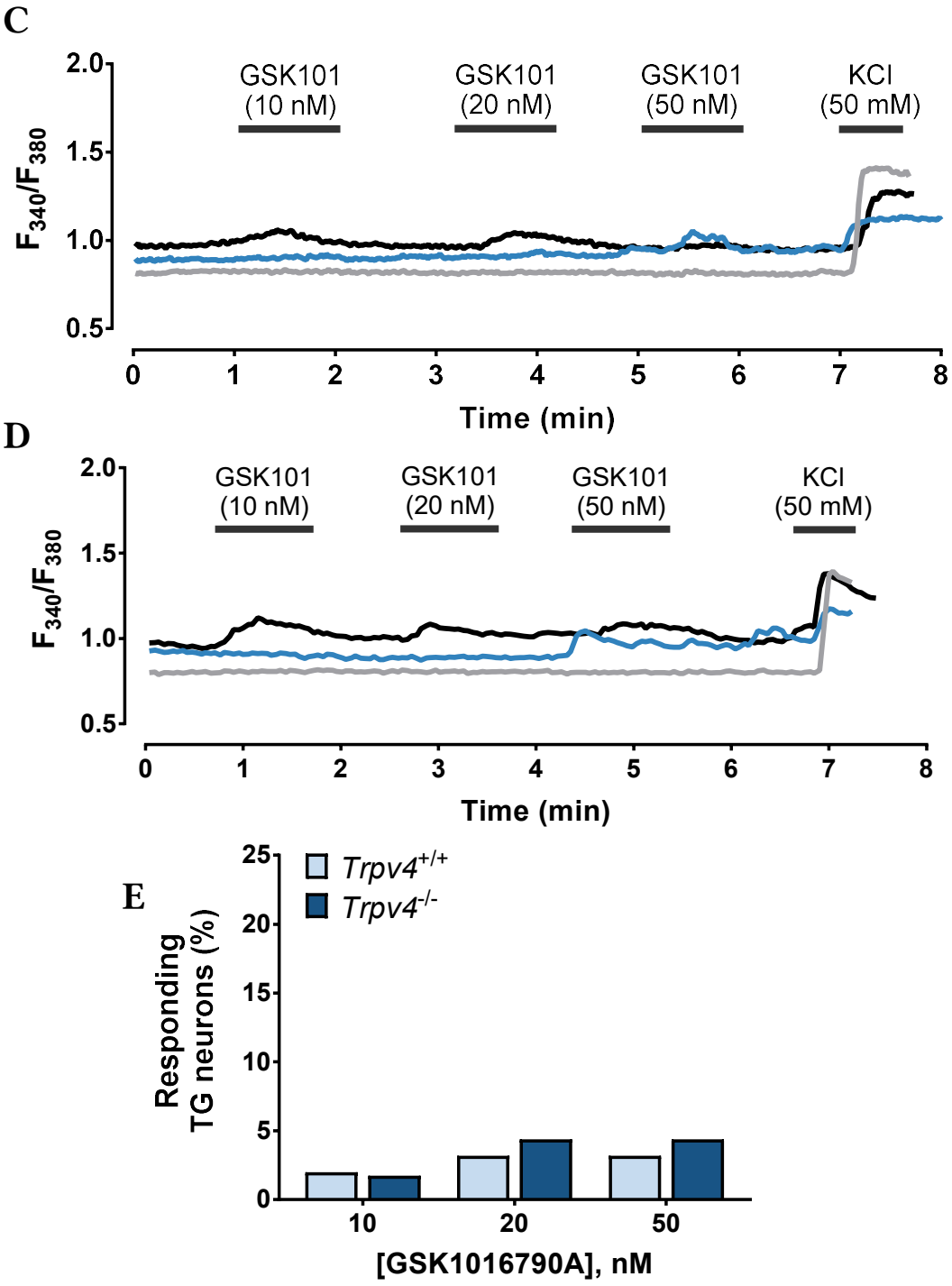

Figure 5.4 The absence of TRPV4 functionality in TG neurons

Example pseudocolour images and traces of wild-type (*A* and *C*) and TRPV4-lacking (*B* and *D*) TG neuron responses to consecutive application of increasing concentrations of the TRPV4 agonist GSK1016790A (GSK101). The arrows in *A* and *B* indicate the same TG neurons as the colour-coded traces in *C* and *D*. The calcium image colour range represents Fura-2AM fluorescence ratio. The insets represent separate experimental runs. *E)* Overall percentage of TG neurons from wild-type (*Trpv4*$^{+/+}$) and TRPV4 knock-out (*Trpv4*$^{-/-}$) mice that respond to the application of GSK1016790A with an increase in intracellular Ca^{2+} concentration. *Trpv4*$^{+/+}$: n = 7 (250 neurons); *Trpv4*$^{-/-}$: n = 10 (228 neurons).

When the same protocol was used to test the effects of ATP, the initial exposure of TG neurons to ATP was often found to inhibit any subsequent responses (Figure 5.5A-B). Therefore, it was decided to perform separate experimental runs for each concentration of ATP tested (2, 5, and 10 μM). An increase in the percentage of responding TG neurons from 11.4% (29/255 neurons) in response to 2 μM to 17.9% (50/279 neurons) in response to 10 μM ATP was detected (Figure 5.5C), whereas the mean magnitude of the detected increases in F_{340}/F_{380} was relatively consistent (Figure 5.5D). An additional experiment was then performed to study the desensitisation profiles of TG neuron responses to repeated applications of 5 μM ATP. Four distinct groups of TG neurons could be identified, with neurons that demonstrate sudden desensitisation after the first response, with no subsequent recovery of responses, being the most common (see Figure 5.6).

In the next series of experiments, to further examine what P2 receptors are functional on TG neurons, a few agonists, including α,β-meATP, which acts on $P2X_1$, $P2X_{2/3}$, and $P2X_3$ receptors, the selective $P2Y_1$ agonist MRS2365, the $P2Y_2$ agonist 2-ThioUTP, and ATP were tested (see Figure 5.7). In this case, concentrations of each agonist previously identified as producing a near-maximal response were used. ATP (50 μM) stimulated the largest proportion of TG neurons, followed by 2-ThioUTP (5 μM), α,β-meATP (50 μM), and MRS2365 (5 nM). Some ATP-sensitive TG neurons responded to multiple selective P2 receptor agonists (Figure 5.8). It should also be noted that a proportion of TG neurons that responded to the selective P2 agonists did not display a subsequent response to ATP, but the majority also responded to capsaicin (see Table 5.1).

Finally, TG neuron responses to glutamate were investigated. Some individual TG neurons displayed an increase in $[Ca^{2+}]_i$ above vehicle levels in response to glutamate (10, 50, or 100 μM) application (Figure 5.9A, C, and F). However, the difference between mean response sizes was not statistically significant (p = 0.107; one-way ANOVA). Moreover, this increase in $[Ca^{2+}]_i$ above threshold levels occurred only in 1.8-4.8% of TG neurons, compared to 2.9% sensitive to the application of a corresponding vehicle (Figure 5.9E). The difference was not statistically significant with any of the pairwise comparisons ($p > 0.05$; Fisher's exact test).

A

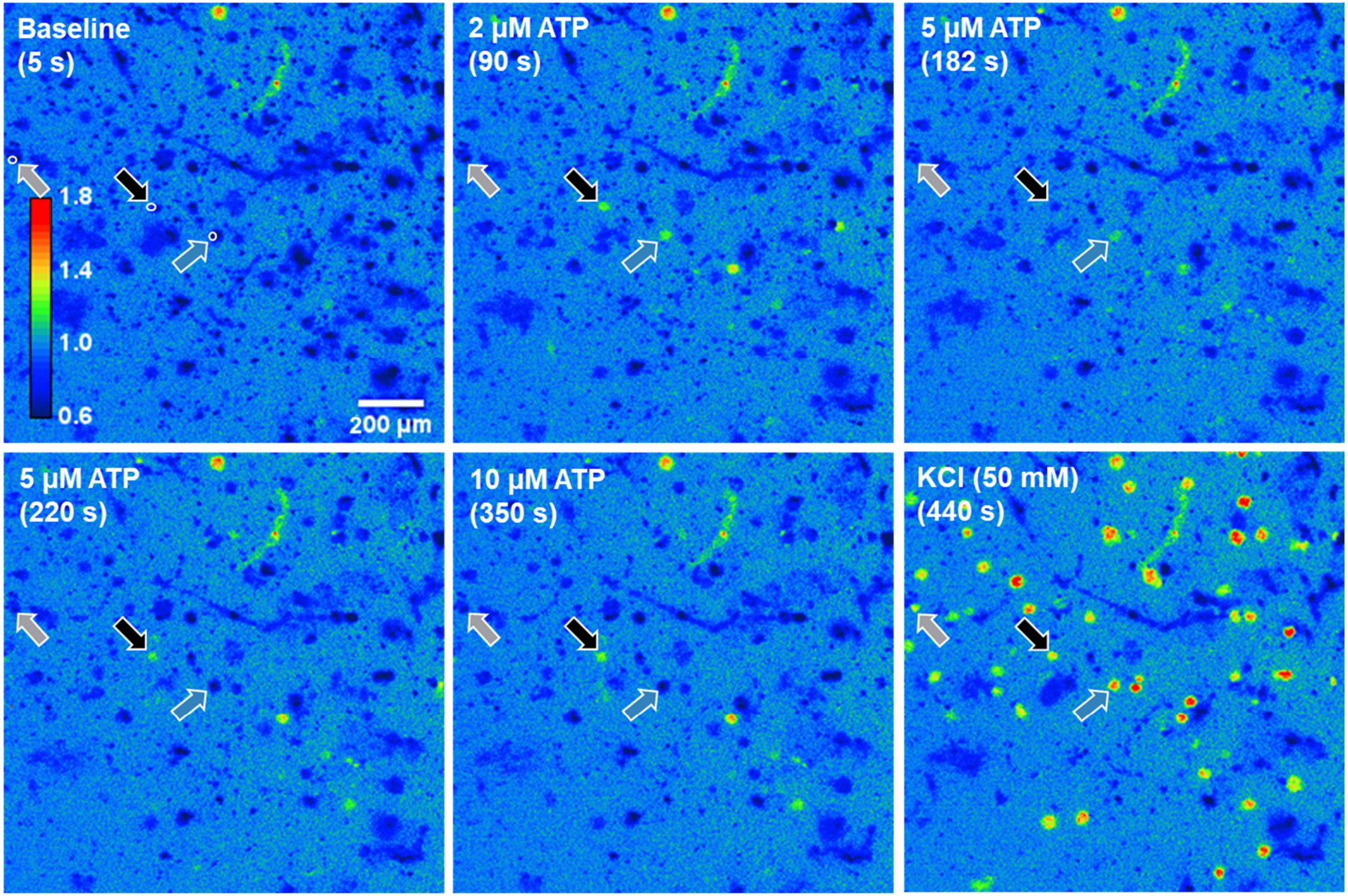
Baseline
(5 s)
1.8
1.4
1.0
0.6
200 µm
2 µM ATP
(90 s)
5 µM ATP
(182 s)
5 µM ATP
(220 s)
10 µM ATP
(350 s)
KCl (50 mM)
(440 s)

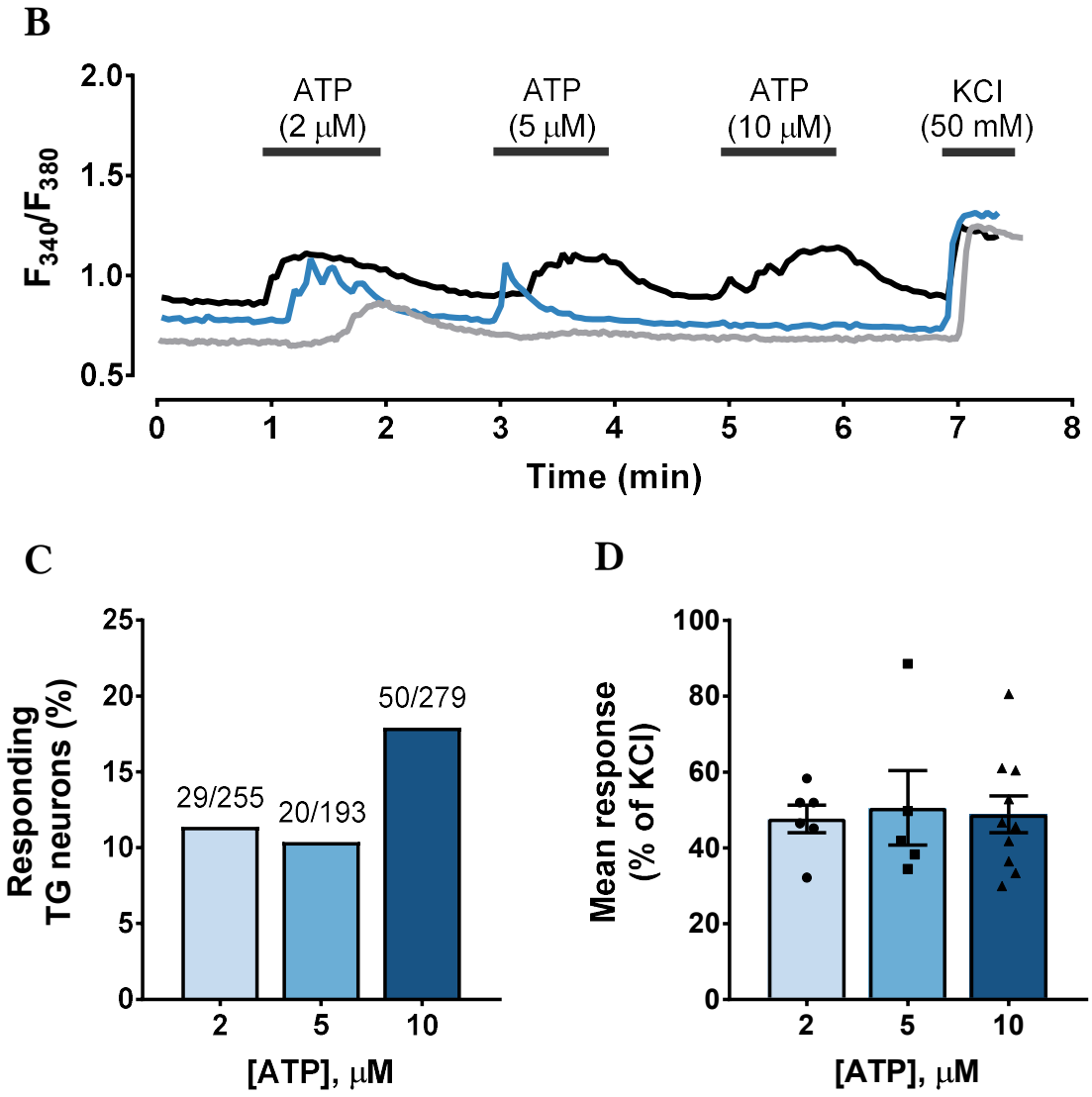

Figure 5.5 Activation of purinergic P2 receptors on TG neurons by ATP

Example pseudocolour images *(A)* and traces *(B)* of TG neuron responses to consecutive application of increasing concentrations of ATP. The arrows in *A* indicate the same TG neurons as the colour-coded traces in *B*. The calcium image colour range represents Fura-2AM fluorescence ratio. Desensitisation of some TG neuron responses to ATP was observed when increasing concentrations of ATP were applied in the same experimental run. *C)* Overall percentage of TG neurons responding to different ATP concentrations, applied in separate experimental runs, with an increase in intracellular Ca^{2+} concentration. The number of responding neurons and the total number of neurons tested is indicated in the graph, above the bars. *D)* The amplitude of TG neuron responses to ATP, with different ATP concentrations applied in separate experimental runs, expressed as a percentage of corresponding responses to 50 mM KCl. Data are presented as mean ± SEM (n = 5-8).

A

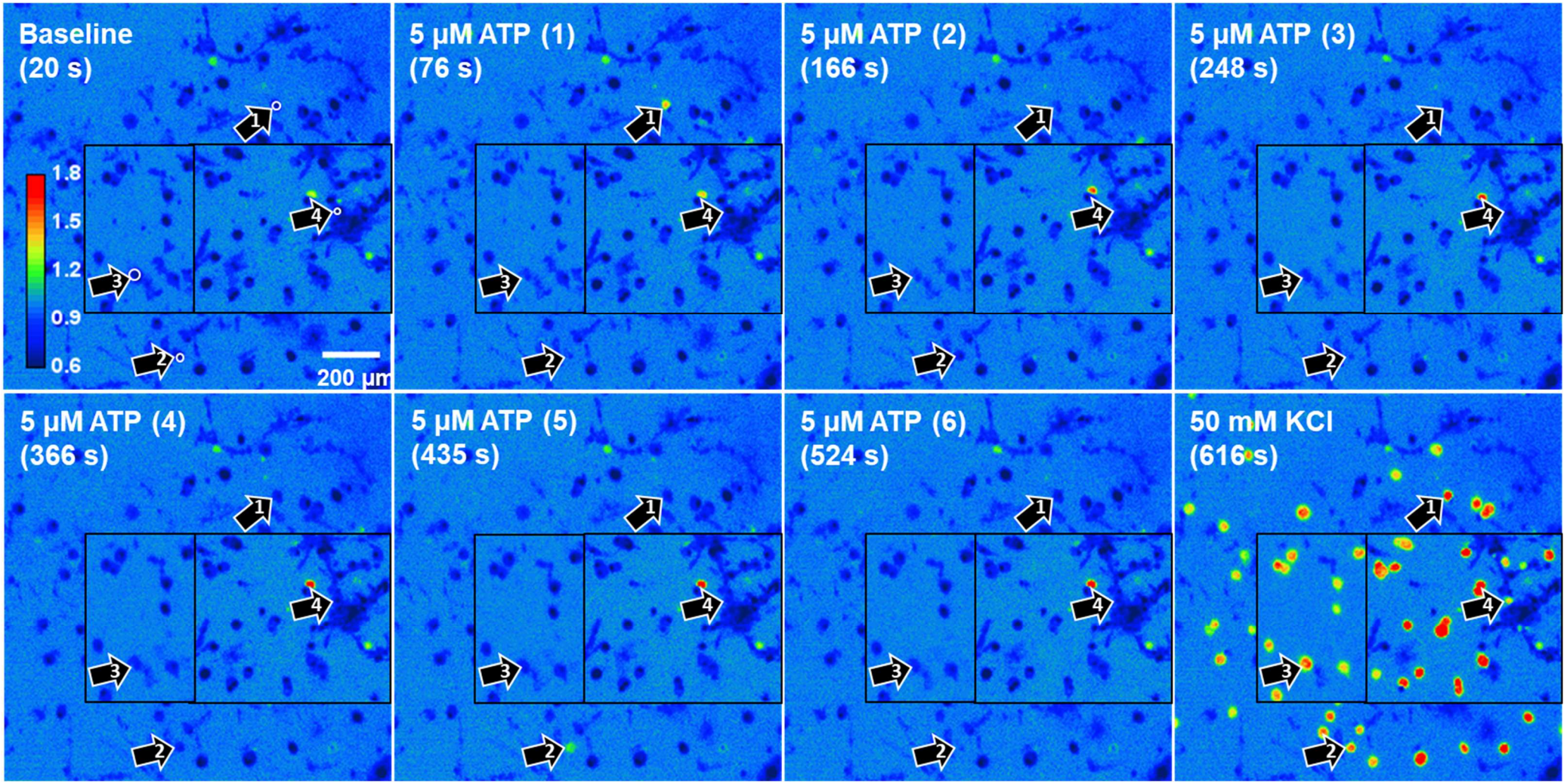
Baseline
(20 s)
1.8
1.5
1.2
0.9
0.6
200 µm
5 µM ATP (1)
(76 s)
5 µM ATP (2)
(166 s)
5 µM ATP (3)
(248 s)
5 µM ATP (4)
(366 s)
5 µM ATP (5)
(435 s)
5 µM ATP (6)
(524 s)
50 mM KCl
(616 s)

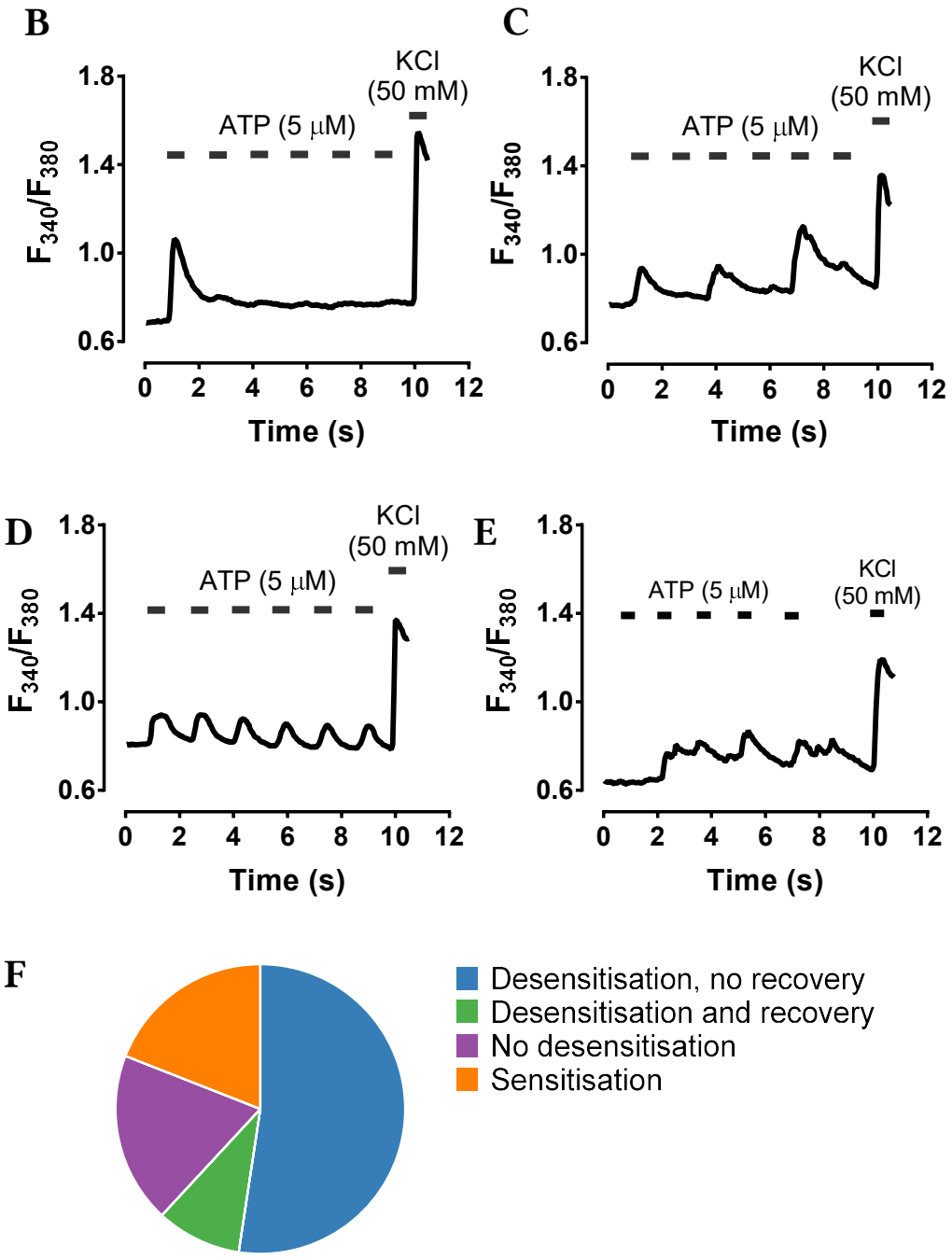

Figure 5.6 Desensitisation profiles of TG neuron responses to ATP

Example pseudocolour images *(A)* and traces *(B-E)* of TG neuron responses to six consecutive applications of ATP (5 μM), including TG neurons displaying: *B)* desensitisation without recovery, *C)* desensitisation with recovery (although the example shown also displays some potential sensitisation), *D)* no desensitisation, and *E)* sensitisation, seen as the absence of initial response(s), followed by responses to subsequent ATP applications. The arrows in *A* (numbered 1-4) indicate the same TG neurons as traces in *B-E* (in the same order). The calcium image colour range represents Fura-2AM fluorescence ratio. The insets represent a separate experimental run. *F)* Proportion of TG neurons displaying each desensitisation pattern. n = 4 (164 neurons).

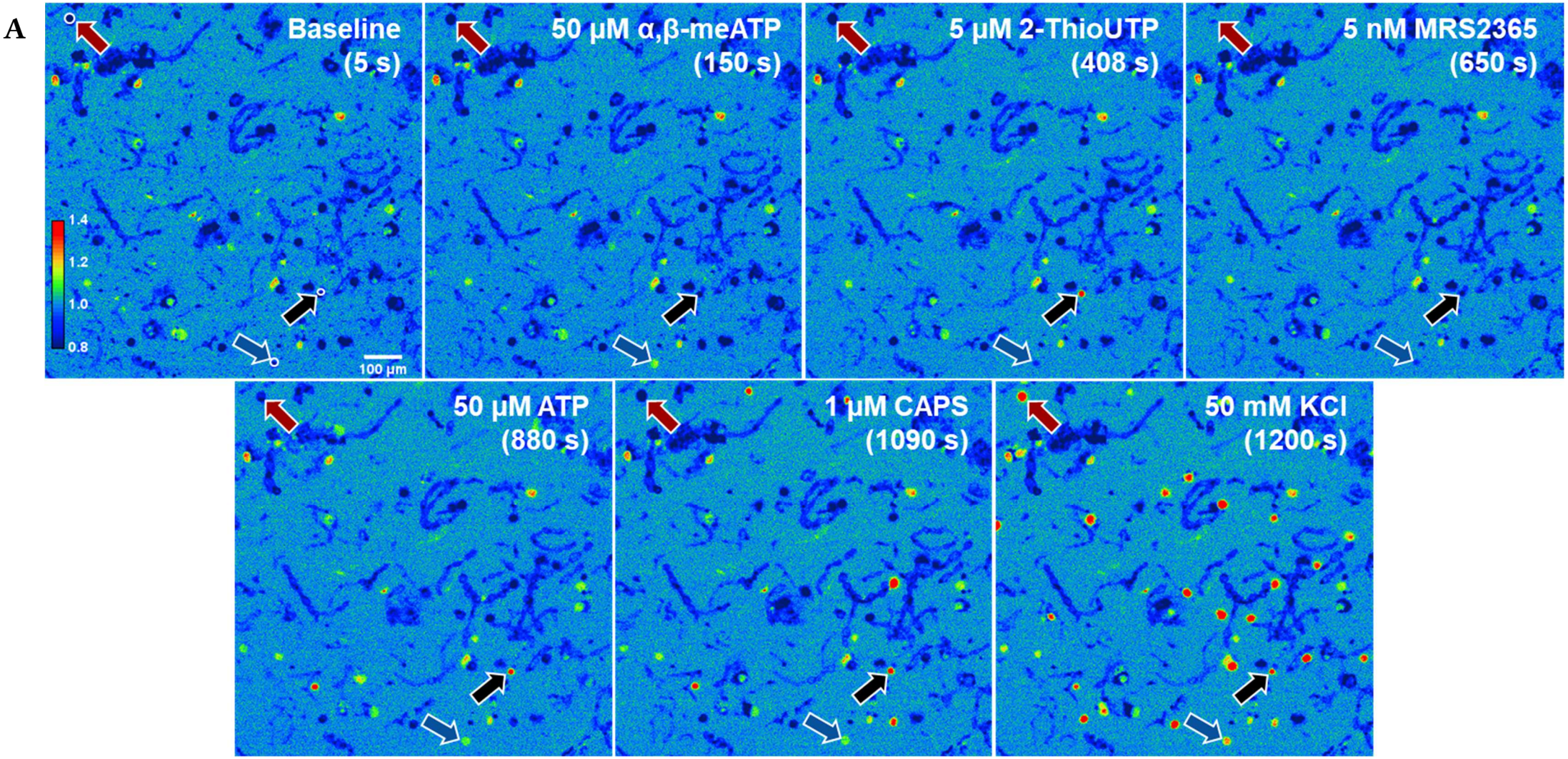
A
Baseline
(5 s)
50 µM α,β-meATP
(150 s)
5 µM 2-ThioUTP
(408 s)
5 nM MRS2365
(650 s)
1.4
1.2
1.0
0.8
100 µm
50 µM ATP
(880 s)
1 µM CAPS
(1090 s)
50 mM KCl
(1200 s)

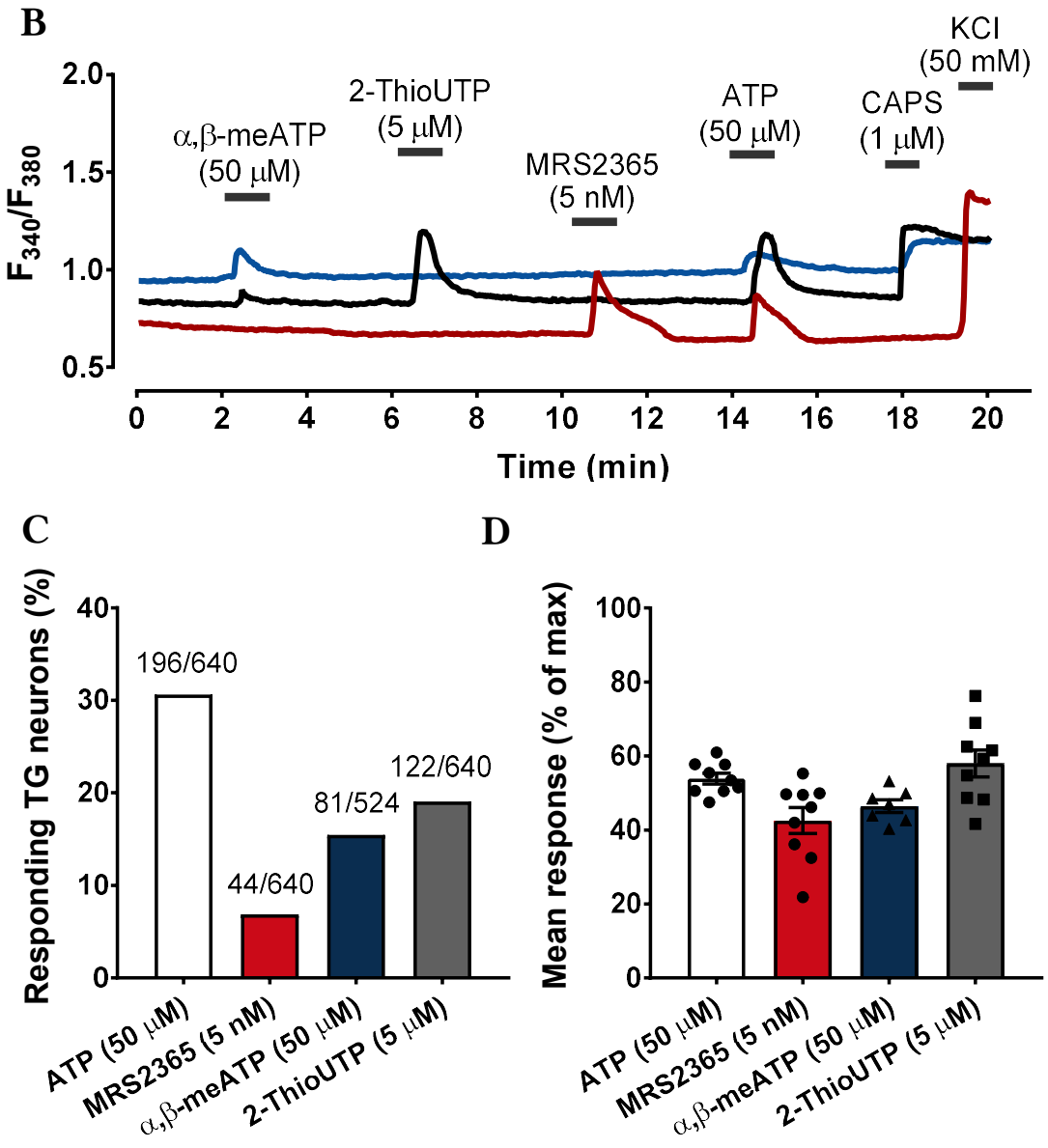

Figure 5.7 TG neurons detect ATP via multiple P2 receptors

Example pseudocolour images *(A)* and traces *(B)* of changes in TG neuron intracellular Ca^{2+} concentration in response to the $P2X_1/P2X_{2/3}/P2X_3$ agonist α,β-meATP, $P2Y_1$ agonist MRS2365, $P2Y_2$ agonist 2-ThioUTP, and ATP. The arrows in *A* indicate the same TG neurons as the colour-coded traces in *B*. The calcium image colour range represents Fura-2AM fluorescence ratio. *C)* Overall percentage of TG neurons responding to each P2 receptor agonist. The number of responding neurons and the total number of neurons tested for each concentration is indicated in the graph, above the bars. *D)* The amplitude of TG neuron responses to each P2 receptor agonist, expressed as a percentage of the corresponding maximum response to either 50 mM KCl or 1 μM capsaicin (CAPS). Data presented are mean ± SEM (n = 6-9).

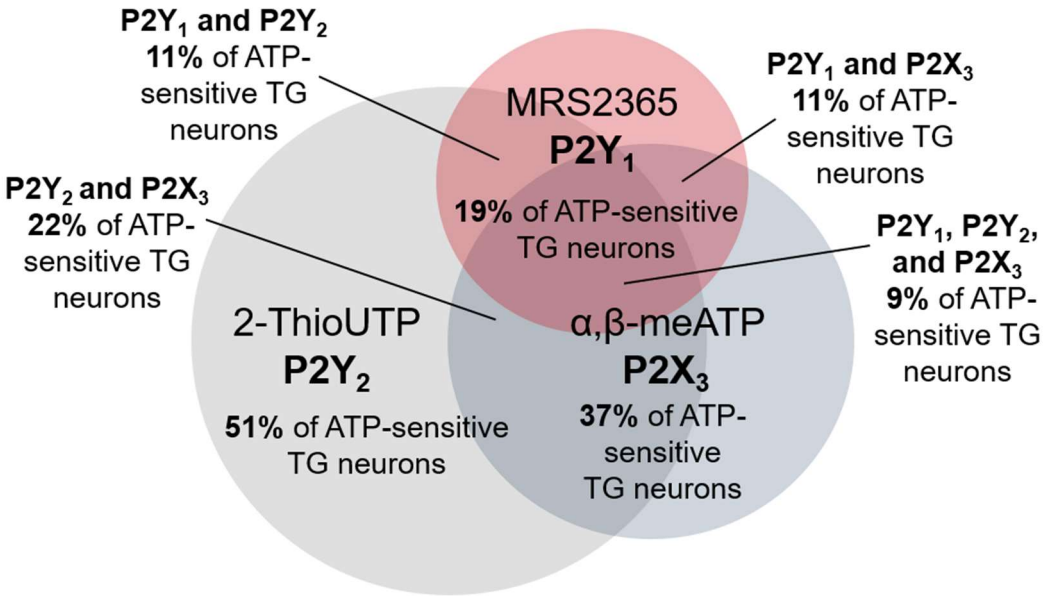

Figure 5.8 TG neurons demonstrate overlapping P2 receptor function

Quantitative Venn diagram representing the overlap among ATP-sensitive TG neurons responding to other P2 receptor agonists.

Table 5.1 Percentage of TG neurons sensitive to P2 receptor agonists that also respond to ATP and capsaicin

TG neuron group	% sensitive to ATP (50 μM)	% sensitive to capsaicin (1 μM)	% sensitive to ATP and capsaicin
All neurons	30.6	49.0	27.1
Responders to MRS2365 (5 nM)	84.1	84.0	76.0
Responders to 2-ThioUTP (5 μM)	82.0	96.2	88.7
Responders to α,β-meATP (50 μM)	75.3	95.8	87.5

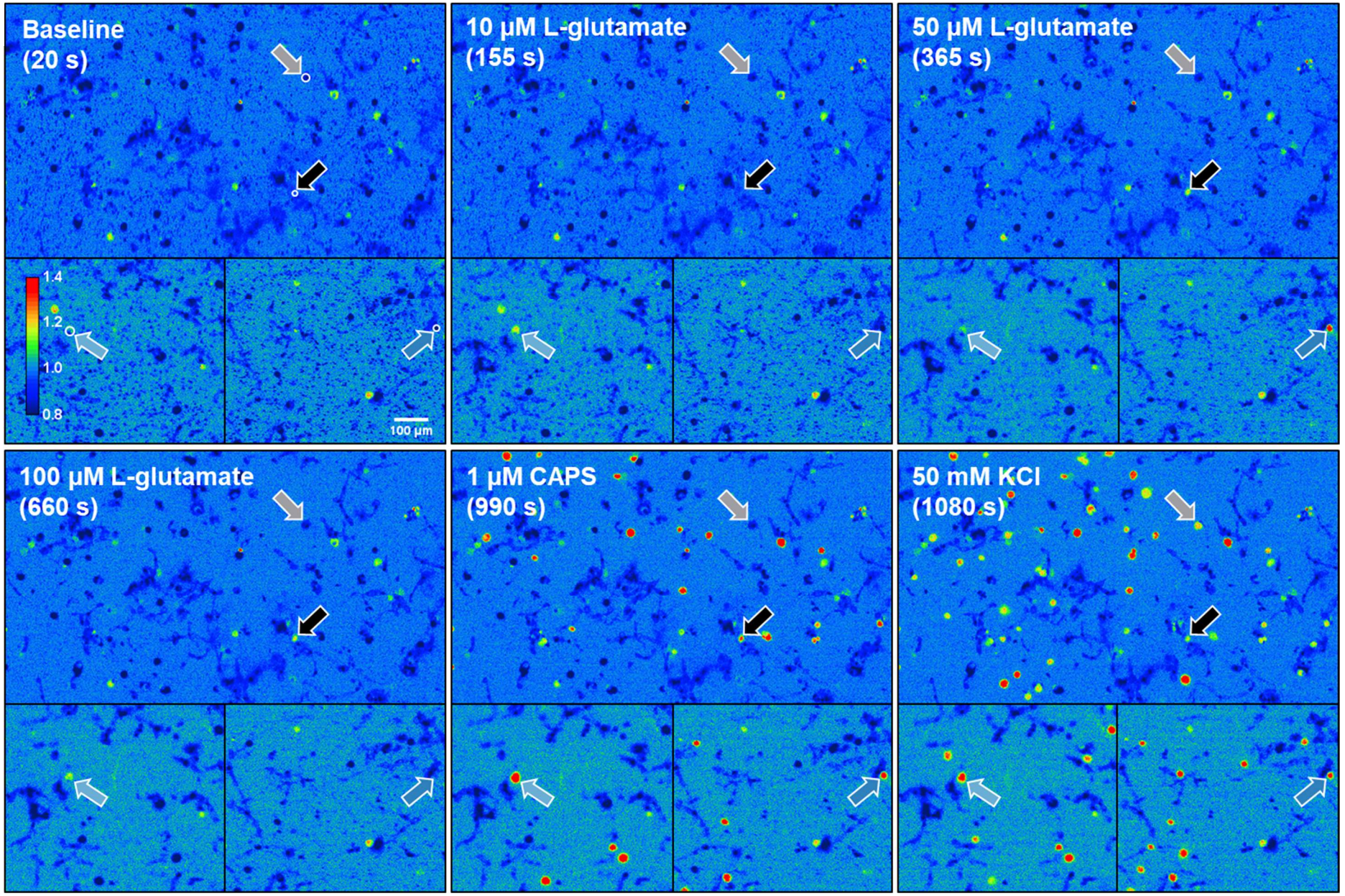
A
Baseline
(20 s)
10 μM L-glutamate
(155 s)
50 μM L-glutamate
(365 s)
1.4
1.2
1.0
0.8
100 μm
100 μM L-glutamate
(660 s)
1 μM CAPS
(990 s)
50 mM KCl
(1080 s)

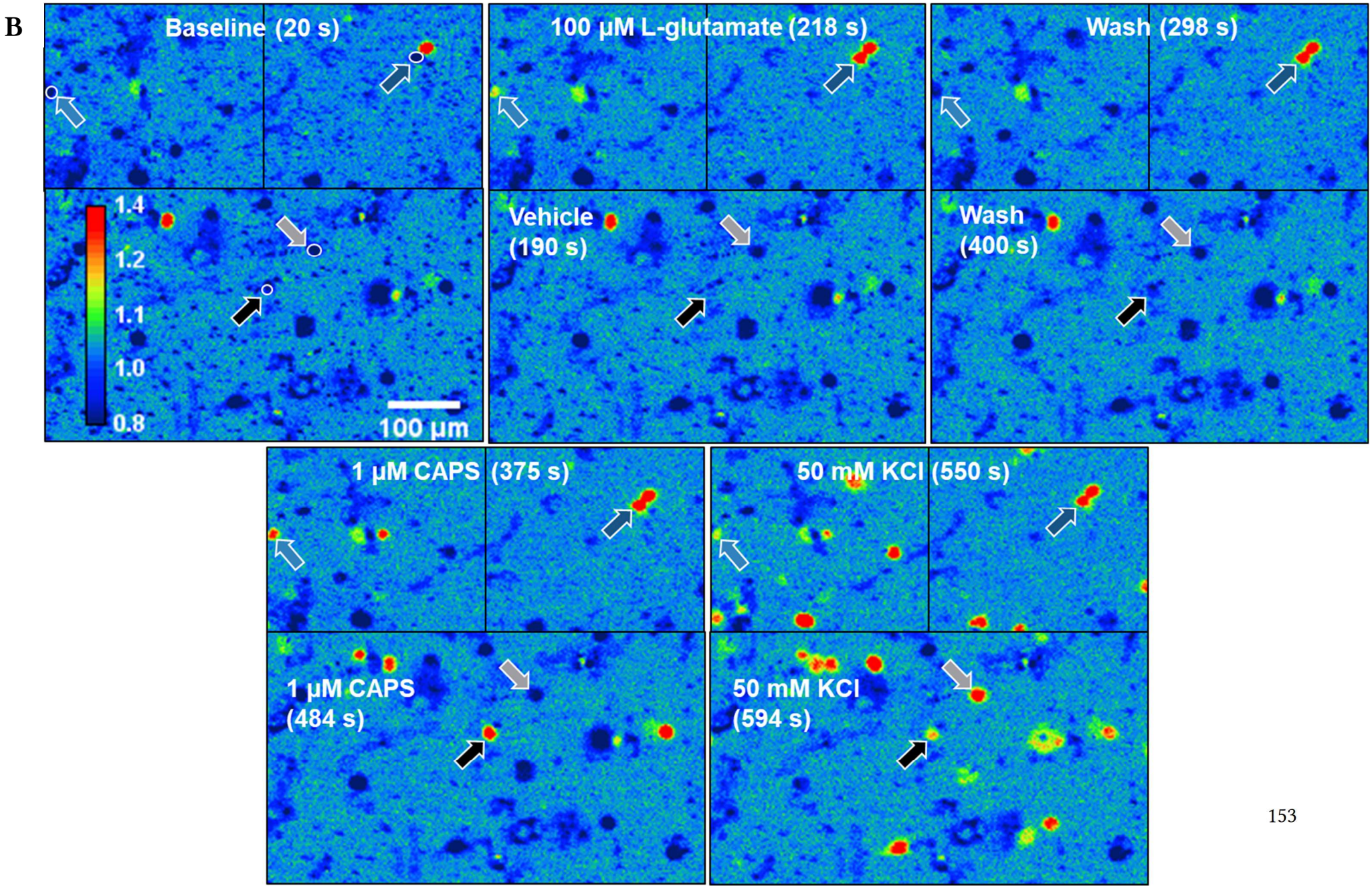
B
Baseline (20 s)
100 µM L-glutamate (218 s)
Wash (298 s)
1.4
1.2
1.1
1.0
0.8
100 µm
Vehicle
(190 s)
Wash
(400 s)
1 µM CAPS (375 s)
50 mM KCl (550 s)
1 µM CAPS
(484 s)
50 mM KCl
(594 s)

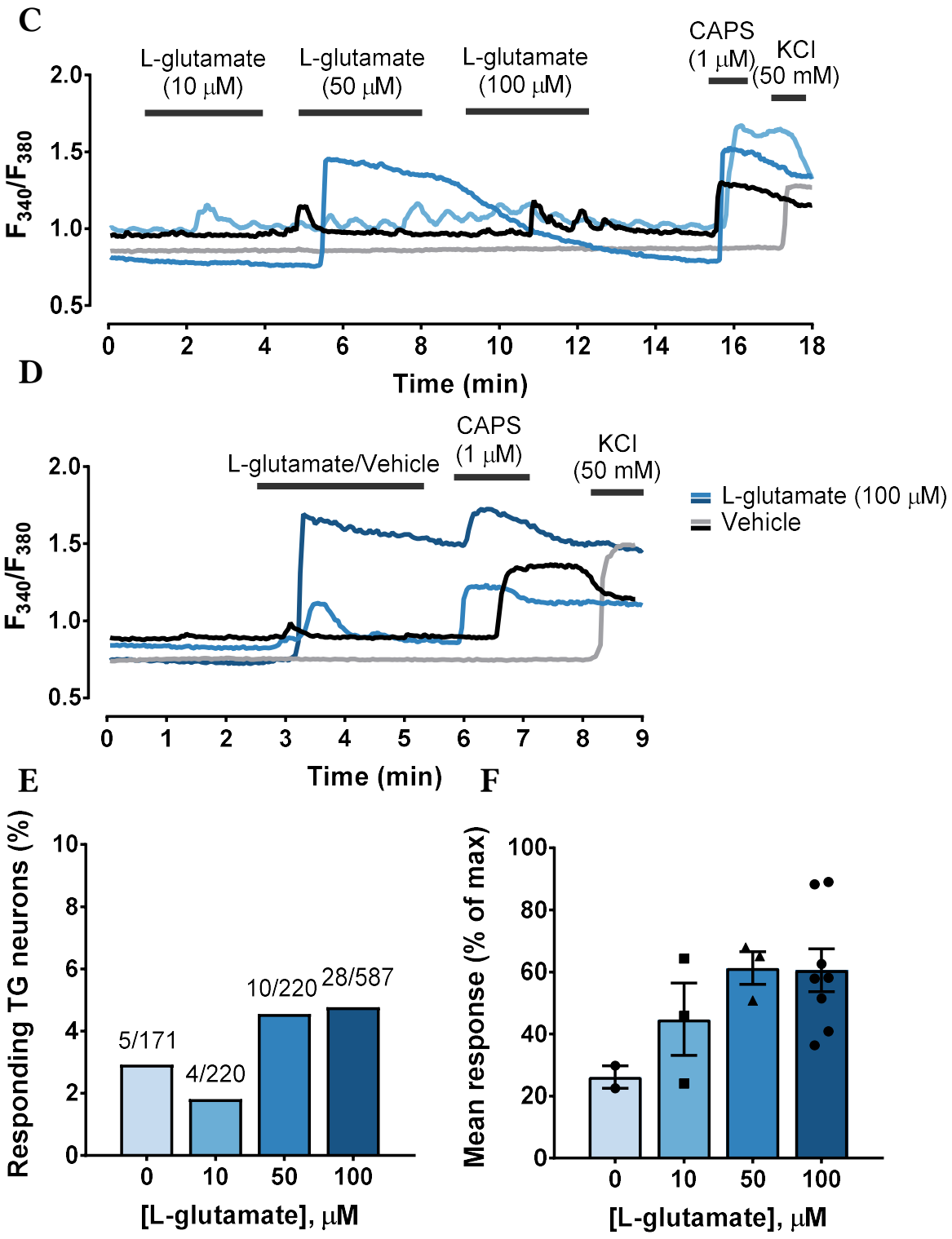

Figure 5.9 Glutamate activates a negligible proportion of TG neurons

Example pseudocolour images *(A-B)* and traces *(C-D)* of TG neuron responses to consecutive application of increasing concentrations of L-glutamate (*A* and *C*) or L-glutamate (100 μM) and a corresponding vehicle (*B* and *D*). The arrows in indicate the same TG neurons as the corresponding colour-coded traces. The calcium image colour range represents Fura-2AM fluorescence ratio. The insets represent a separate experimental run. *E)* Overall percentage

of TG neurons responding to L-glutamate and vehicle. The number of responding neurons and the total number of neurons tested in each case is indicated in the graph, above the bars. *F)* The amplitude of TG neuron responses to L-glutamate or the corresponding vehicle, expressed as a percentage of the maximum response to 50 mM KCl or 1 μM capsaicin (CAPS). Data are mean ± SEM (n = 3-5).

5.3.2 Investigating the sensitisation of TG neuron activity by inflammatory mediators

Since a significant increase in at least one of the parameters was detectable with the ranges of concentrations of AITC, capsaicin, and ATP tested previously, it was initially decided to use the lowest concentrations of these agonists for the sensitisation experiments. However, the results of preliminary sensitisation experiments (not shown) suggested that the use of 20 nM capsaicin and 5 μM ATP improved reproducibility of the responses. Moreover, a sustained elevation in $[Ca^{2+}]_i$ was occasionally observed in response to any agonist that was applied first, which would affect the subsequent responses to other compounds. In order to ensure that agonists are not masking the responses to one another, and that there are no other unpredicted interactions, it was decided to test the ability of inflammatory mediators to sensitise TG neuron responses to AITC, capsaicin, and ATP in separate experimental runs.

5.3.2.1 Short-term pre-treatment of TG neurons with TNFα or IL-1β

TG neuron pre-treatment with tumour necrosis factor-α (TNFα) for 1 hour did not affect the percentage of TG neurons sensitive to 2 μM AITC, compared to the pre-treatment with the corresponding vehicle (Figure 5.10A). However, a statistically significant increase from 37.3 ± 4.3% to 63.3 ± 7.0% (of KCl response) was detected in the magnitude of TG neuron responses to 2 μM AITC ($p = 0.008$; Figure 5.10B). When comparing all TG neuron responses, both the activation by AITC in vehicle pre-treated neurons and TNFα-dependent sensitisation of TG neuron responses to AITC were prevented in the TRPA1 knock-out mice ($D = 0.421$ and 0.228, respectively, $p < 0.001$, Kolmogorov-Smirnov test; Figure 5.10C).

The proportion of TG neurons sensitive to 20 nM capsaicin increased from 18.0% to 28.4% ($p = 0.004$) following the 1-hour TNFα pre-treatment (Figure 5.11A). Although

an increase in the amplitude of TG neuron responses to 20 nM capsaicin, from 60.1 ± 5.0% to 70.4 ± 1.1% (of KCl response) was also detected with TNFα pre-treatment, this effect did not reach statistical significance (p = 0.052, Figure 5.11B). Comparison of all TG neuron responses revealed that both the activation by capsaicin in vehicle pre-treated neurons and TNFα-dependent sensitisation of TG neuron responses to capsaicin were prevented in the TRPV1 knock-out mice (D = 0.410 and 0.334, respectively, p < 0.001, Kolmogorov-Smirnov test; Figure 5.11C).

A short-term (1-hour) pre-treatment with TNFα appeared to cause a reduction in the percentage of TG neurons responsive to 5 μM ATP (p = 0.020; see Figure 5.12A). However, it should be noted that the percentage of ATP-sensitive TG neurons detected after the pre-treatment with vehicle in this set of experiments is approximately 3-fold higher than the corresponding result in the initial set of experiments (Figure 5.5B). In terms of the amplitude of TG neuron responses to 5 μM ATP, no change was detected between the treatment groups (Figure 5.12B). The difference between the cumulative distributions of all TG neuron responses was also statistically significant (D = 0.124, p = 0.035; see Figure 5.12C).

When the same experiment was repeated using α,β-meATP (10 μM) instead of ATP, no significant effect of TNFα pre-treatment could be detected on the proportion of responding TG neurons or the size of their response (Figure 5.13 A and B). However, the difference between the cumulative distributions of all TG neuron responses was statistically significant (D = 0.123, p = 0.016; Figure 5.13C).

In contrast to TNFα, 1-hour pre-treatment with interleukin 1 beta (IL-1β; 10 ng/ml) did not significantly affect TG neuron responses to AITC (Figure 5.14), capsaicin (Figure 5.15), or ATP (Figure 5.16).

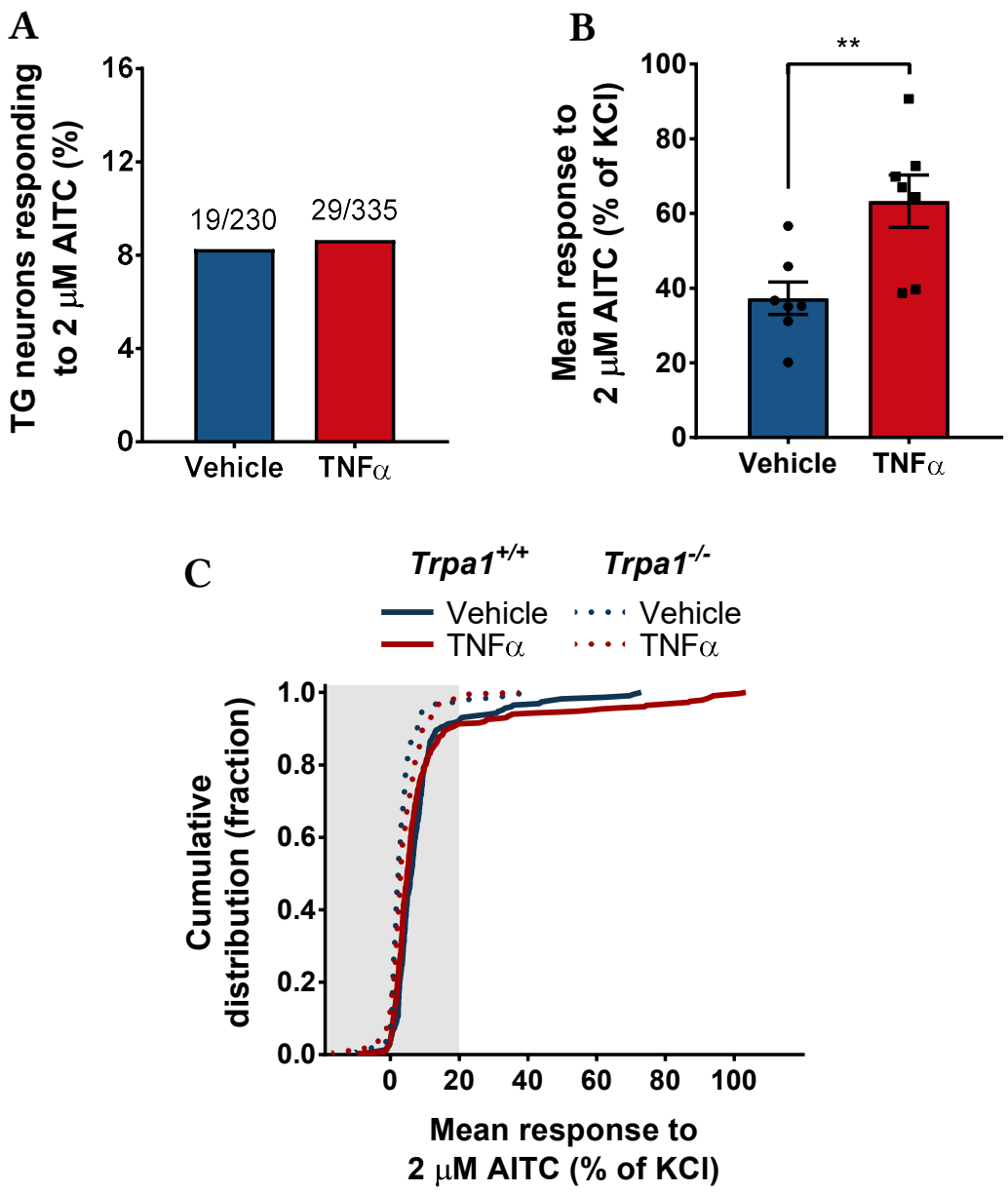

Figure 5.10 Short-term pre-treatment with TNFα increases the amplitude of TG neuron responses to TRPA1 activation

A) The percentage of TG neurons responding to the TRPA1 agonist AITC (2 μM), following a 1-hour pre-treatment with either TNFα (30 ng/ml) or a corresponding vehicle. The number of responding neurons and the total number of neurons tested in each case is indicated in the graph, above the bars. *B)* TNFα significantly increased the amplitude of TG neuron responses to 2 μM AITC above vehicle levels. Data are presented as mean ± SEM. $^{**}p < 0.01$ (unpaired *t*-test). *C)* Cumulative distribution plot showing the responses of all TG neurons, either from wild-type (*Trpa1*$^{+/+}$, as above) or from TRPA1 knock-out (*Trpa1*$^{-/-}$) mice to 2 μM AITC, following the pre-treatment with TNFα (30 ng/ml) or vehicle. The shaded area represents neuronal responses below the threshold value (20% of the response to 50 mM KCl) used for distinguishing the responding TG neurons from non-responders. *Trpa1*$^{+/+}$: n = 7 (for both vehicle and TNFα); *Trpa1*$^{-/-}$: n = 4-5 (154 neurons for vehicle and 228 neurons for TNFα).

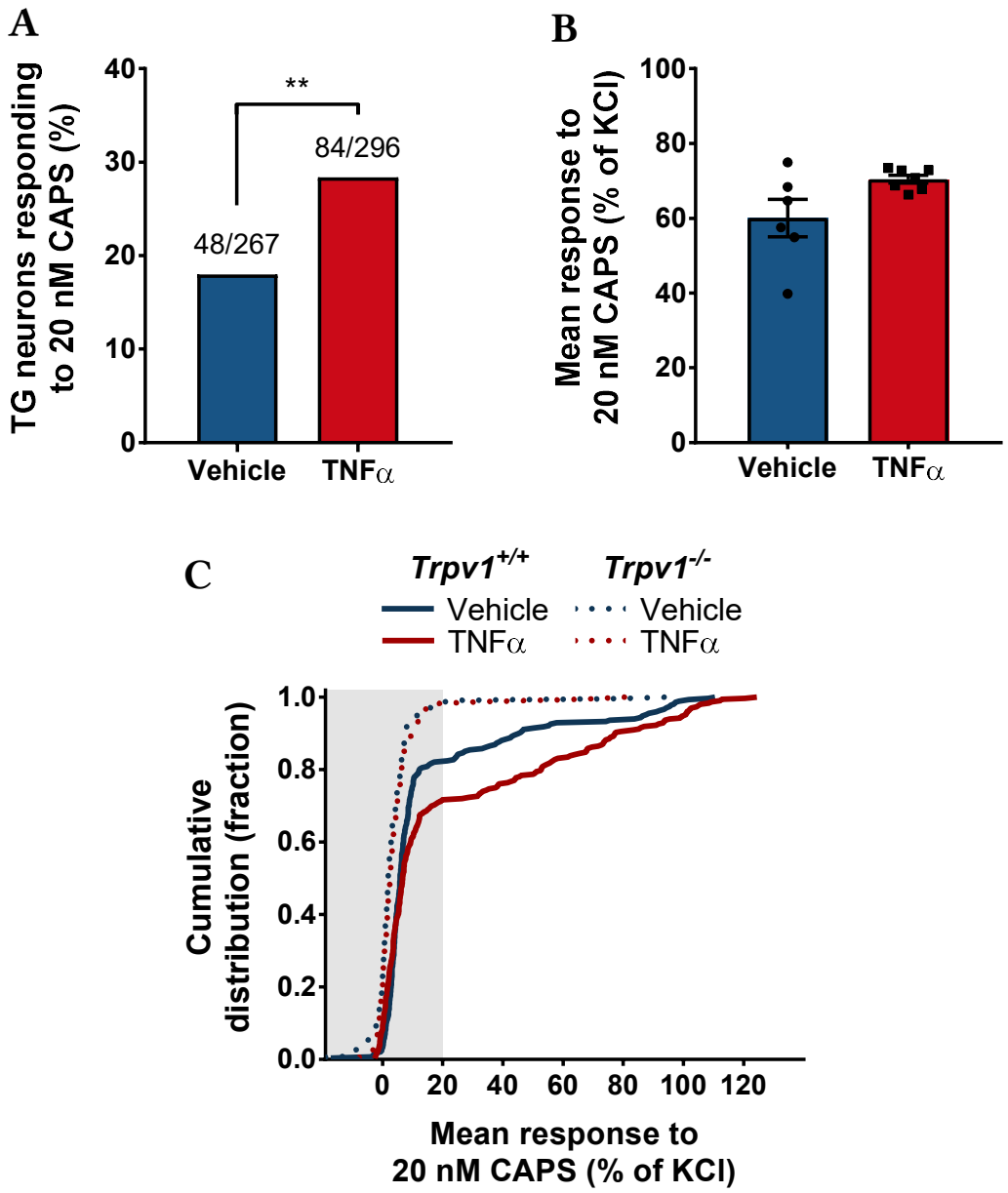

Figure 5.11 Short-term pre-treatment with TNFα increases the proportion of TG neurons responding to TRPV1 activation

A) One-hour pre-treatment with TNFα (30 ng/ml) significantly increased the percentage of TG neurons responding to the TRPV1 agonist capsaicin (CAPS, 20 nM), compared with pre-treatment with a corresponding vehicle. The number of responding neurons and the total number of neurons tested in each case is indicated in the graph, above the bars. *B)* The amplitude of TG neuron responses to 20 nM CAPS was not significantly increased following the pre-treatment with TNFα, compared with vehicle. Data are mean ± SEM. *C)* Cumulative distribution plot showing the responses of individual TG neurons, either from wild-type (*Trpv1*$^{+/+}$, as above) or from TRPV1 knock-out (*Trpv1*$^{-/-}$) mice to 20 nM CAPS, following the pre-treatment with TNFα (30 ng/ml) or vehicle. The shaded area represents neuronal responses below the threshold value (20% of the response to 50 mM KCl) used for distinguishing the responding TG neurons from non-responders. *Trpv1*$^{+/+}$: n = 6-7; *Trpa1*$^{-/-}$: n = 9-10 (217 neurons for vehicle and 160 neurons for TNFα).

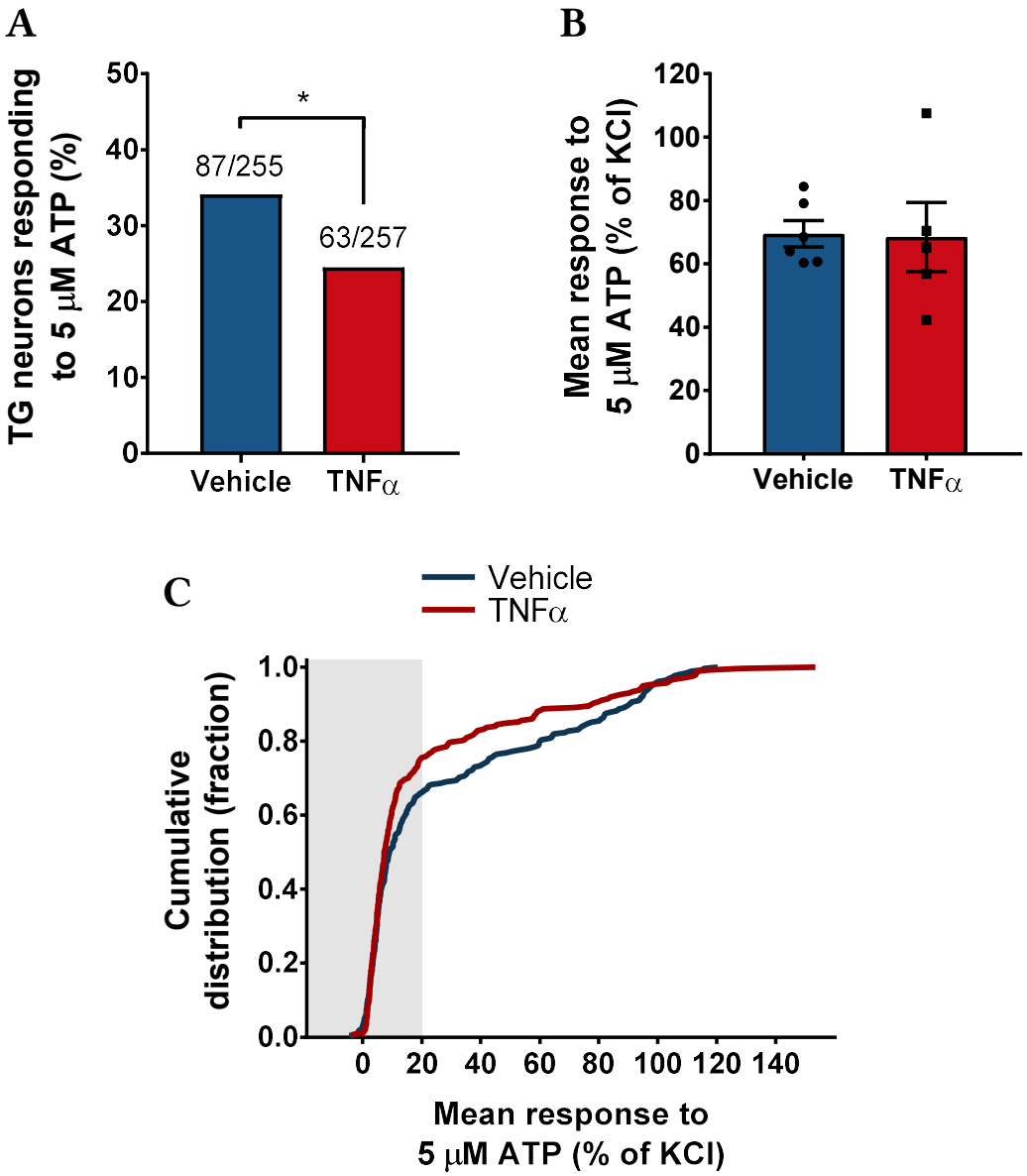

Figure 5.12 Short-term pre-treatment with TNFα decreased the proportion of ATP-sensitive TG neurons

A) One-hour pre-treatment with TNFα (30 ng/ml) significantly decreased the percentage of TG neurons responding to ATP (5 μM), compared with pre-treatment with a corresponding vehicle. The number of responding neurons and the total number of neurons tested in each case is indicated in the graph, above the bars. *B)* The amplitude of TG neuron responses to 5 μM ATP was not affected by the pre-treatment with TNFα, compared with vehicle. Data are mean ± SEM (n = 5-6). *C)* Cumulative distribution plot showing the responses of individual TG neurons to 5 μM ATP, following the pre-treatment with TNFα (30 ng/ml) or vehicle. The shaded area represents neuronal responses below the threshold value (20% of the response to 50 mM KCl) used for distinguishing the responding TG neurons from non-responders.

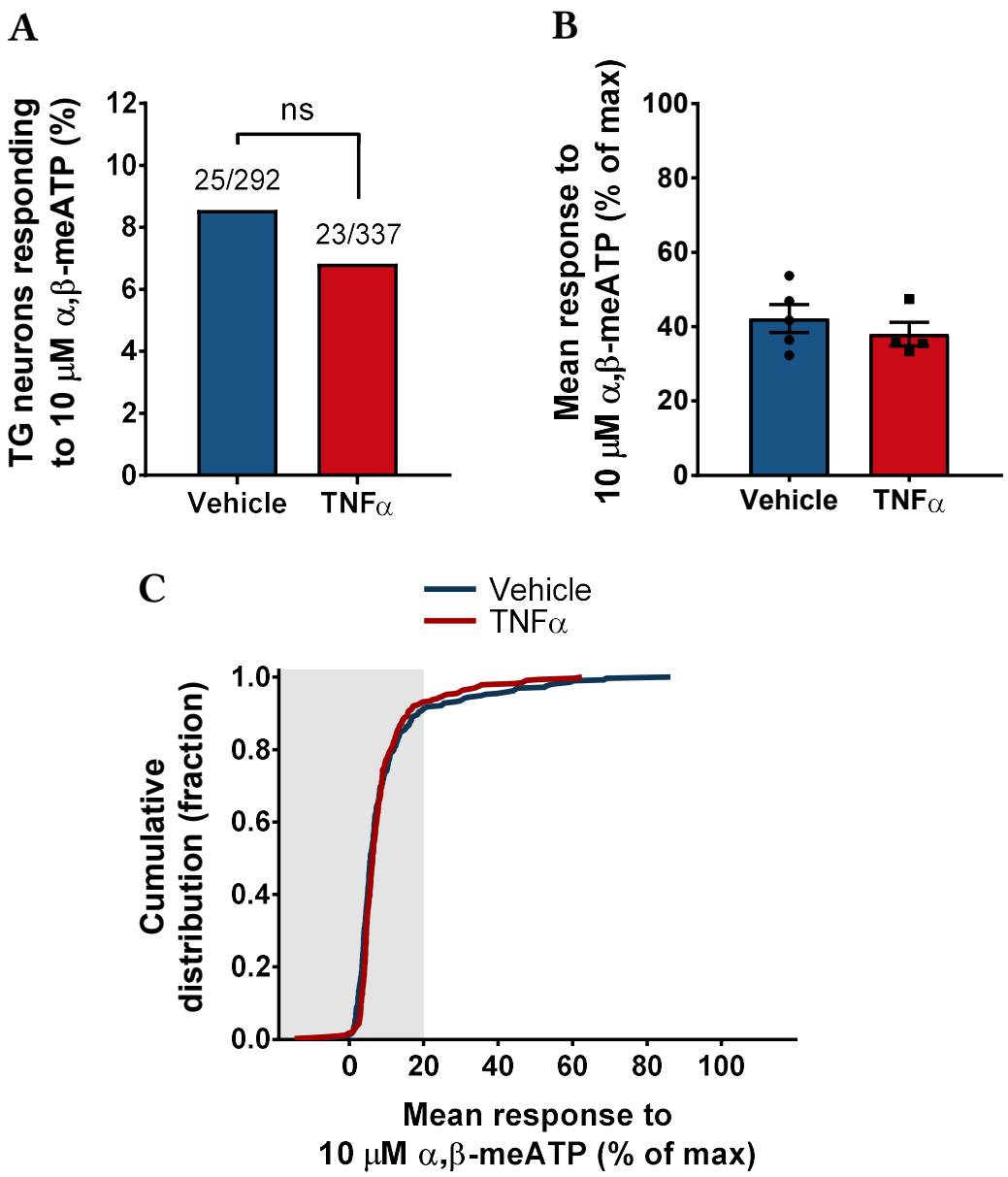

Figure 5.13 Short-term pre-treatment with TNFα does not significantly affect TG neuron responses to α,β-meATP

A) The percentage of TG neurons responding to the $P2X_3$ agonist α,β-meATP (10 μM) was not significantly affected by a 1-hour pre-treatment with TNFα (30 ng/ml), compared with a corresponding vehicle. ns = not statistically significant, $p > 0.05$ (Fisher's exact test). The number of responding neurons and the total number of neurons tested in each case is indicated in the graph, above the bars. *B)* The amplitude of TG neuron responses to 10 μM α,β-meATP, following the pre-treatment with TNFα or vehicle. Data are mean ± SEM (n = 4-5). *C)* Cumulative distribution plot showing the responses of individual TG neurons to 10 μM α,β-meATP, following the pre-treatment with TNFα (30 ng/ml) or vehicle. The shaded area represents neuronal responses below the threshold value (20% of the maximum response to either 50 mM KCl or 1 μM capsaicin) used for distinguishing the responding TG neurons from non-responders.

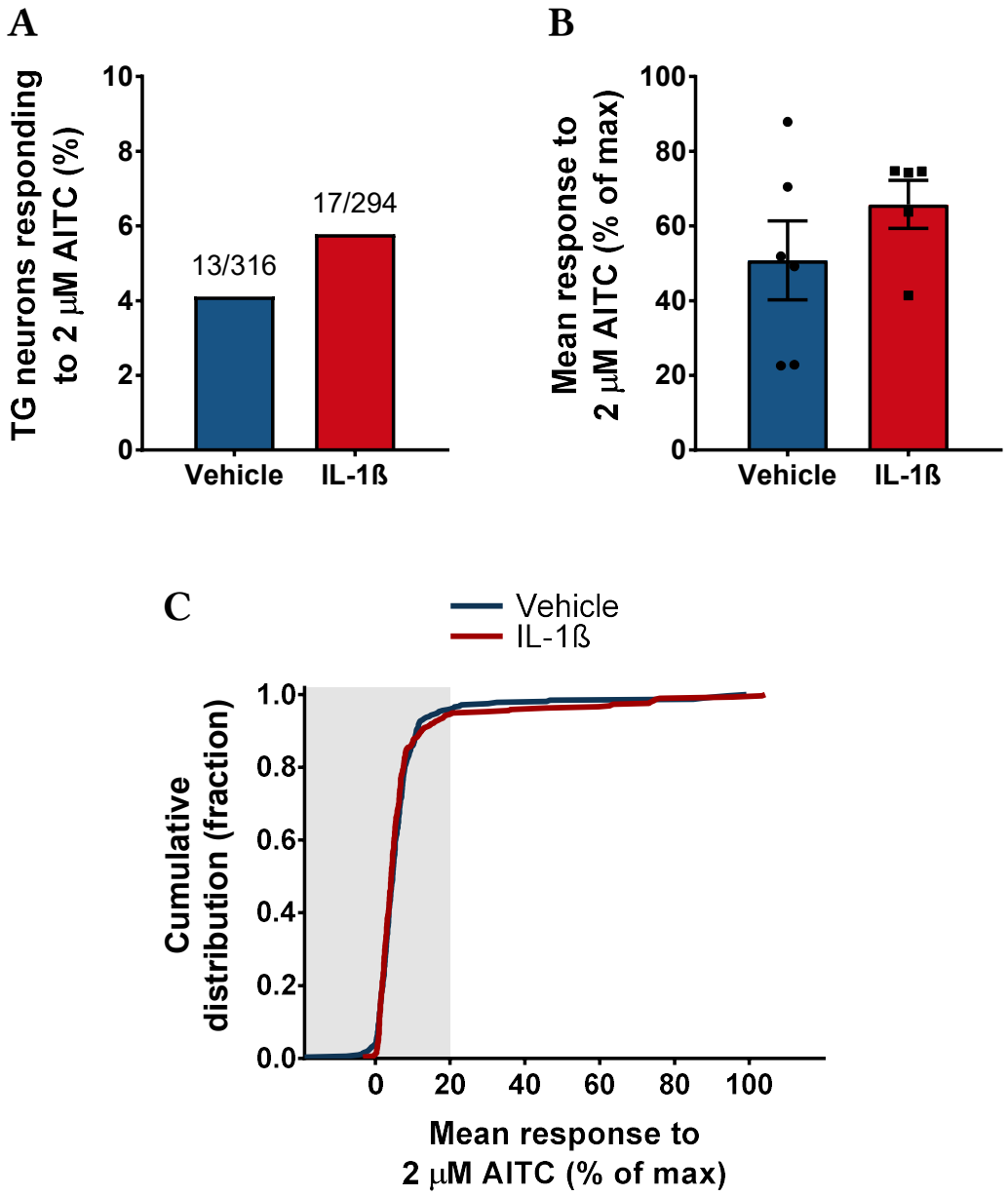

Figure 5.14 Short-term pre-treatment with IL-1β does not significantly affect TG neuron responses to TRPA1 activation

A) The percentage of TG neurons responding to the TRPA1 agonist AITC (2 μM), following a 1-hour pre-treatment with either IL-1β (10 ng/ml) or a corresponding vehicle. The number of responding neurons and the total number of neurons tested in each case is indicated in the graph, above the bars. *B)* The amplitude of TG neuron responses to 2 μM AITC, following the pre-treatment with IL-1β or vehicle. Data are mean ± SEM (n = 9). *C)* Cumulative distribution plot showing the responses of individual TG neurons to 2 μM AITC, following the pre-treatment with IL-1β (10 ng/ml) or vehicle. The shaded area represents neuronal responses below the threshold value (20% of the maximum response to 50 mM KCl or 1 μM capsaicin) used for distinguishing the responding TG neurons from non-responders.

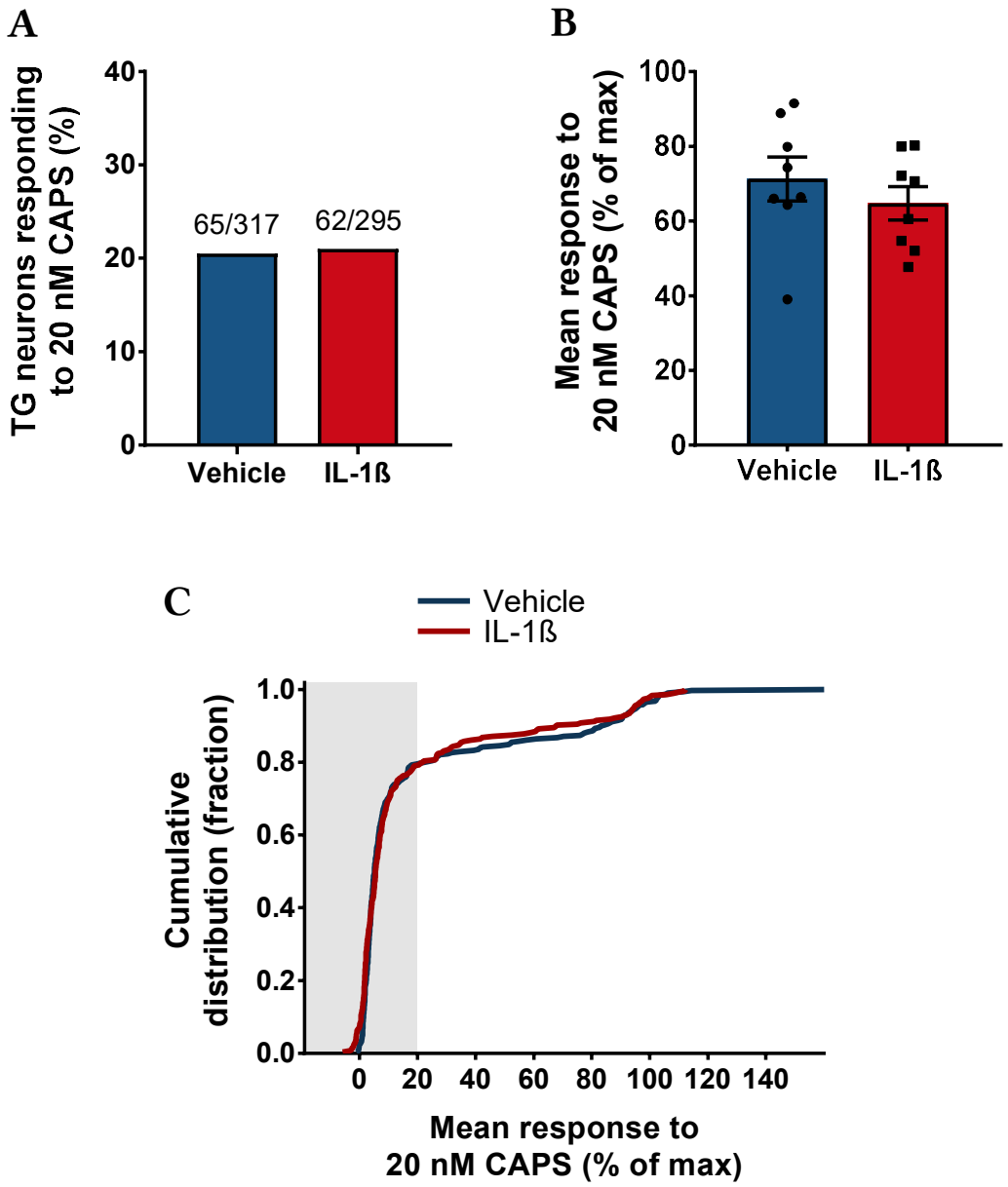

Figure 5.15 Short-term pre-treatment with IL-1β does not significantly affect TG neuron responses to TRPV1 activation

A) The percentage of TG neurons responding to the TRPV1 agonist capsaicin (CAPS; 20 nM), following a 1-hour pre-treatment with either IL-1β (10 ng/ml) or a corresponding vehicle. The number of responding neurons and the total number of neurons tested in each case is indicated in the graph, above the bars. *B)* The amplitude of TG neuron responses to 20 nM CAPS, following the pre-treatment with IL-1β or vehicle. Data are presented as mean ± SEM (n = 8). *C)* Cumulative distribution plot showing the responses of individual TG neurons to 20 nM CAPS, following the pre-treatment with IL-1β (10 ng/ml) or vehicle. The shaded area represents neuronal responses below the threshold value (20% of the maximum response to either 50 mM KCl or 1 μM CAPS) used for distinguishing the responding TG neurons from non-responders.

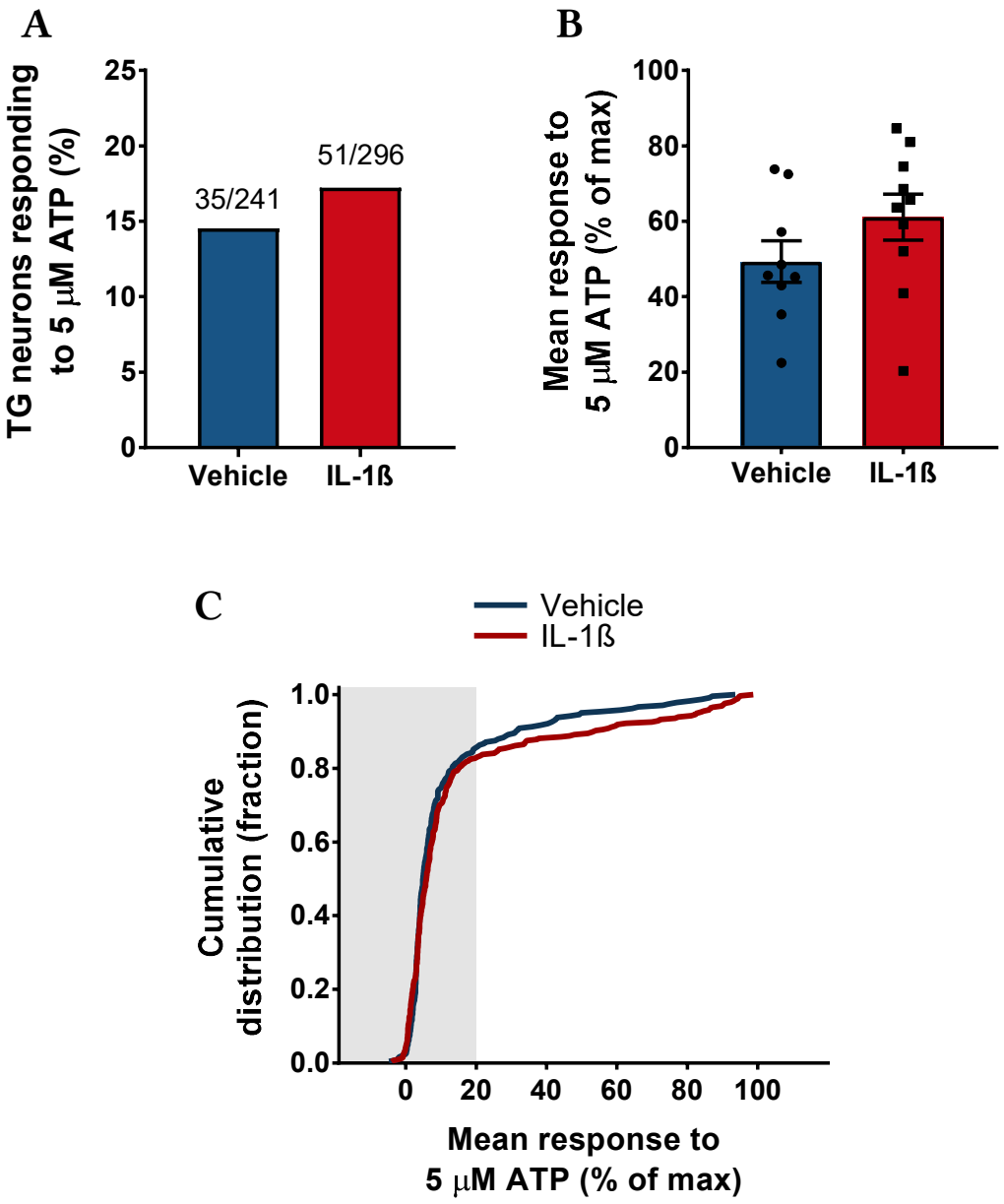

Figure 5.16 Short-term pre-treatment with IL-1β does not significantly affect TG neuron responses to ATP

A) The percentage of TG neurons responding to ATP (5 μM), following a 1-hour pre-treatment with either IL-1β (10 ng/ml) or a corresponding vehicle. The number of responding neurons and the total number of neurons tested in each case is indicated in the graph, above the bars. *B)* The amplitude of TG neuron responses to 5 μM ATP, following the pre-treatment with IL-1β or vehicle. Data are mean ± SEM (n = 9-10). *C)* Cumulative distribution plot showing the responses of individual TG neurons to 5 μM ATP, following the pre-treatment with IL-1β (10 ng/ml) or vehicle. The shaded area represents neuronal responses below the threshold value (20% of the maximum response to either 50 mM KCl or 1 μM capsaicin) used for distinguishing the responding TG neurons from non-responders.

5.3.2.2 Long-term pre-treatment of TG neurons with TNFα or IL-1β

Long-term (24-hour) TG neuron pre-treatment with the same concentration of TNFα (30 ng/ml) did not significantly affect the percentage of TG neurons sensitive to 2 μM AITC or the amplitude of their responses, compared to the analogous pre-treatment with the corresponding vehicle (Figure 5.17). Cumulative distribution of all TG neuron responses was also not significantly different between the two treatment groups. Similarly, no significant effect of the 24-hour pre-treatment with TNFα could be detected on the proportion of responding TG neurons, the size of their response, or the cumulative distribution of all TG neuron responses to 20 nM capsaicin (Figure 5.18).

Long-term pre-treatment with IL-1β (10 ng/ml) also did not significantly affect the proportion of responding TG neurons or the size of their response to 2 μM AITC (Figure 5.19 A and B). However, IL-1β caused a decrease in TG neuron sensitivity to AITC, based on the statistically significant shift in the cumulative distribution of all TG neuron responses ($D = 0.119$, $p = 0.019$, Kolmogorov-Smirnov test; Figure 5.19C). On the other hand, pre-treatment with IL-1β for 24 hours failed to cause any significant effects on TG neuron responses to 20 nM capsaicin (Figure 5.20).

The data from the above experiments have been additionally analysed to determine if the long-term pre-treatment with TNFα or IL-1β affected the percentage of TG neurons sensitive to a high concentration of capsaicin (1 μM) applied at the end of each experimental run (see Table 5.2 and further discussion in section 5.4.4).

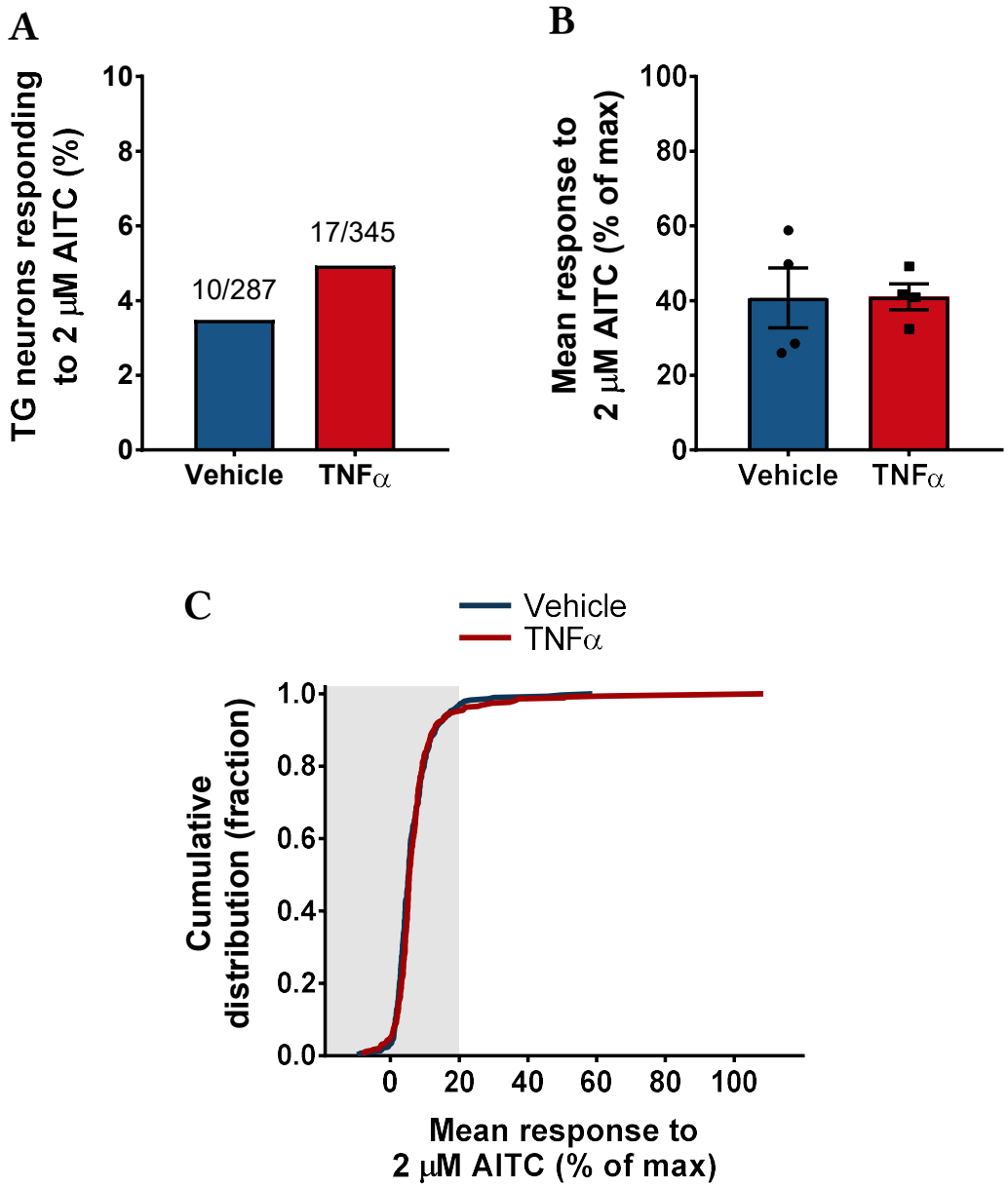

Figure 5.17 Long-term pre-treatment with TNFα does not significantly affect TG neuron responses to TRPA1 activation

A) The percentage of TG neurons responding to the TRPA1 agonist AITC (2 μM), following a 24-hour pre-treatment with either TNFα (30 ng/ml) or a corresponding vehicle. The number of responding neurons and the total number of neurons tested in each case is indicated in the graph, above the bars. *B)* The amplitude of TG neuron responses to 2 μM AITC, following the pre-treatment with TNFα or vehicle. Data are mean ± SEM (n = 5). *C)* Cumulative distribution plot showing the responses of individual TG neurons to 2 μM AITC, following the pre-treatment with TNFα (30 ng/ml) or vehicle. The shaded area represents neuronal responses below the threshold value (20% of the maximum response to 50 mM KCl) used for distinguishing the responding TG neurons from non-responders.

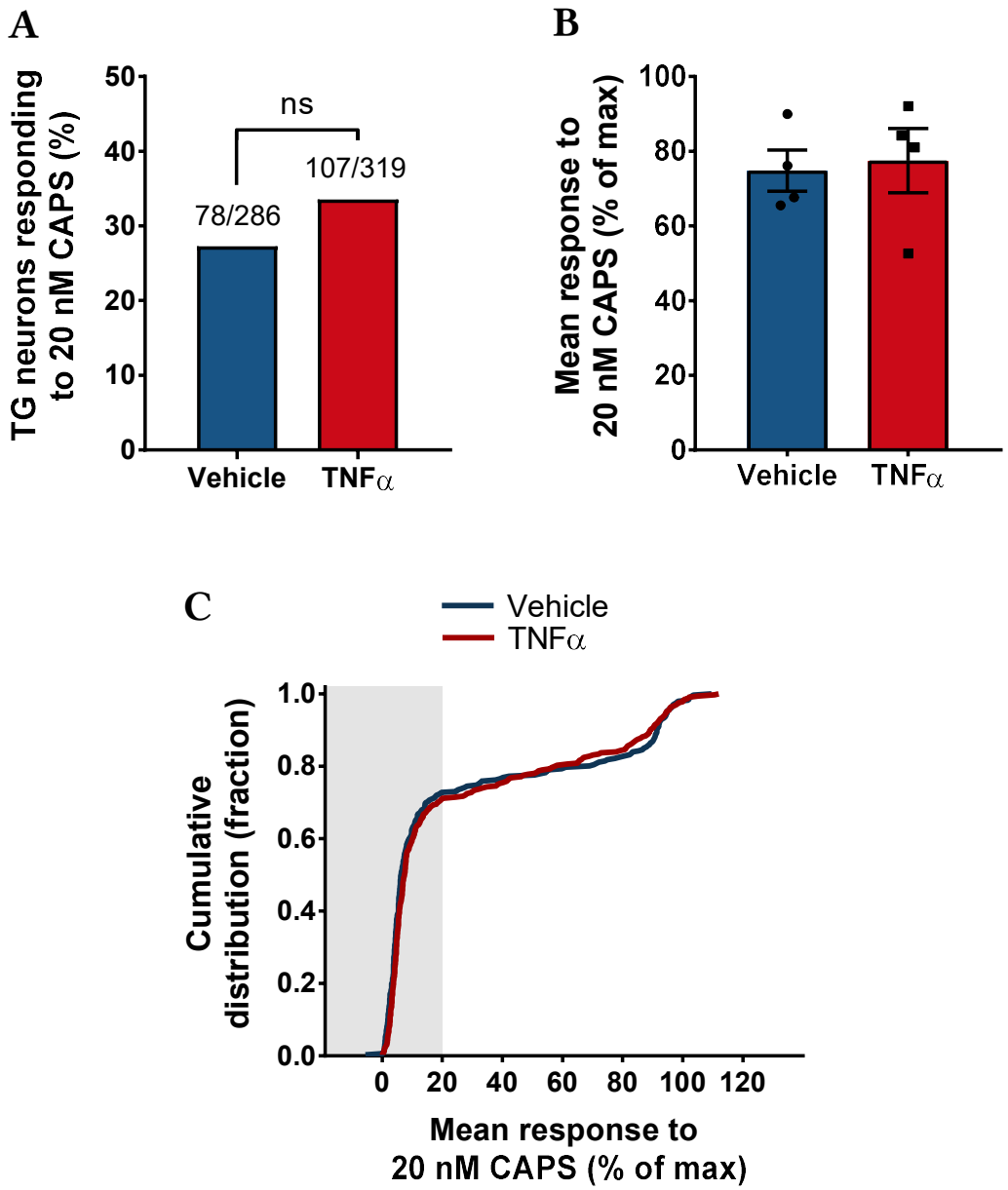

Figure 5.18 Long-term pre-treatment with TNFα does not significantly affect TG neuron responses to TRPV1 activation

A) The percentage of TG neurons responding to the TRPV1 agonist capsaicin (CAPS; 20 nM) was not significantly increased by a 1-hour pre-treatment with TNFα (30 ng/ml), compared with a corresponding vehicle. ns = not statistically significant, $p > 0.05$ (Fisher's exact test). The number of responding neurons and the total number of neurons tested in each case is indicated in the graph, above the bars. *B)* The amplitude of TG neuron responses to 20 nM CAPS, following the pre-treatment with TNFα or vehicle. Data are mean ± SEM (n = 4). *C)* Cumulative distribution plot showing the responses of individual TG neurons to 20 nM CAPS, following the pre-treatment with TNFα (30 ng/ml) or vehicle. The shaded area represents neuronal responses below the threshold value (20% of the maximum response to either 50 mM KCl or 1 μM CAPS) used for distinguishing the responding TG neurons from non-responders.

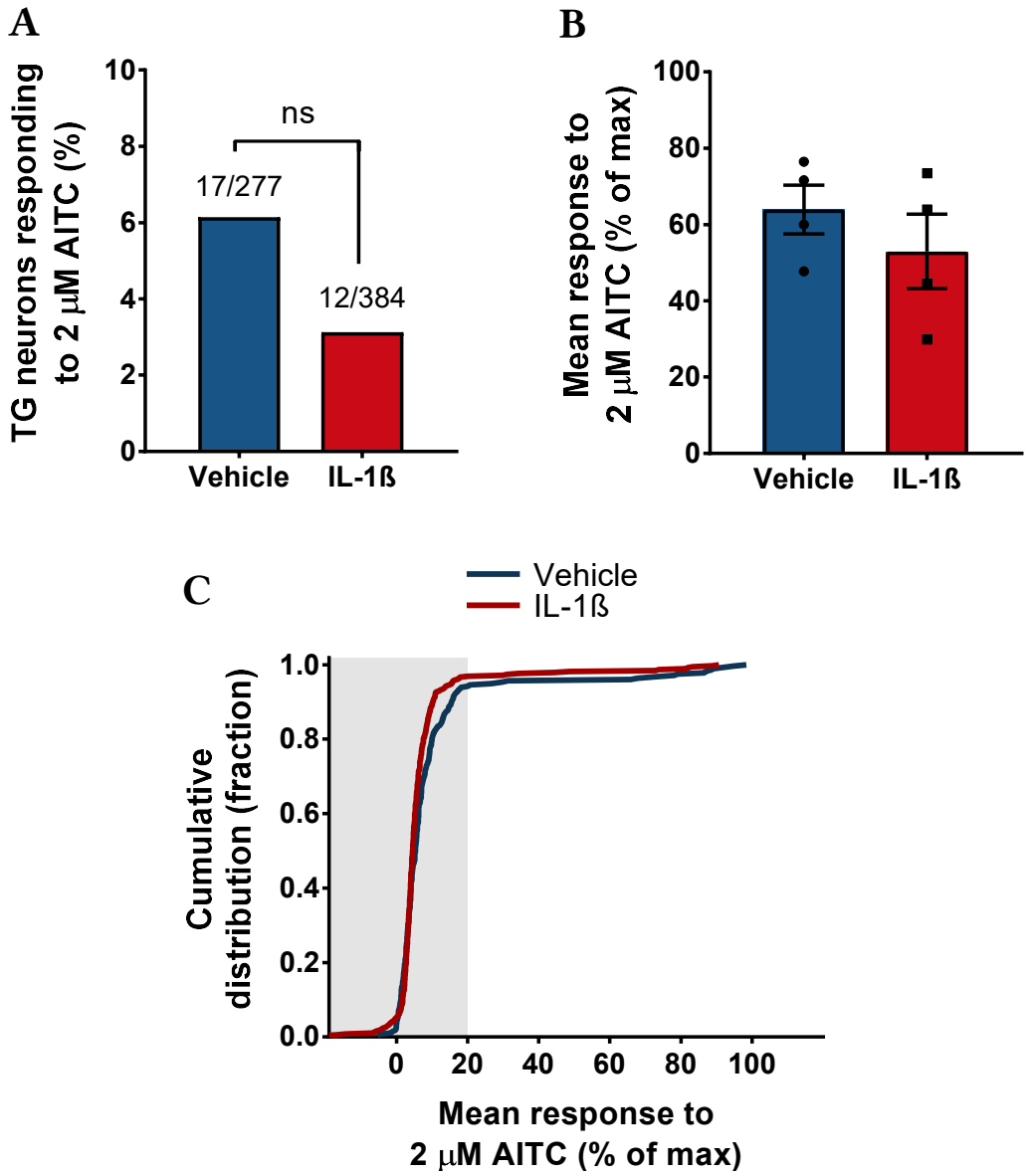

Figure 5.19 Long-term pre-treatment with IL-1β does not significantly affect TG neuron responses to TRPA1 activation

A) The percentage of TG neurons responding to the TRPA1 agonist AITC (2 μM) was not significantly affected by a 1-hour pre-treatment with IL-1β (10 ng/ml), compared with a corresponding vehicle. ns = not statistically significant, $p > 0.05$ (Fisher's exact test). The number of responding neurons and the total number of neurons tested in each case is indicated in the graph, above the bars. *B)* The amplitude of TG neuron responses to 2 μM AITC, following the pre-treatment with IL-1β or vehicle. Data are mean ± SEM (n = 4). *C)* Cumulative distribution plot showing the responses of individual TG neurons to 2 μM AITC, following the pre-treatment with IL-1β (10 ng/ml) or vehicle. The shaded area represents neuronal responses below the threshold value (20% of the maximum response to either 50 mM KCl or 1 μM capsaicin) used for distinguishing the responding TG neurons from non-responders.

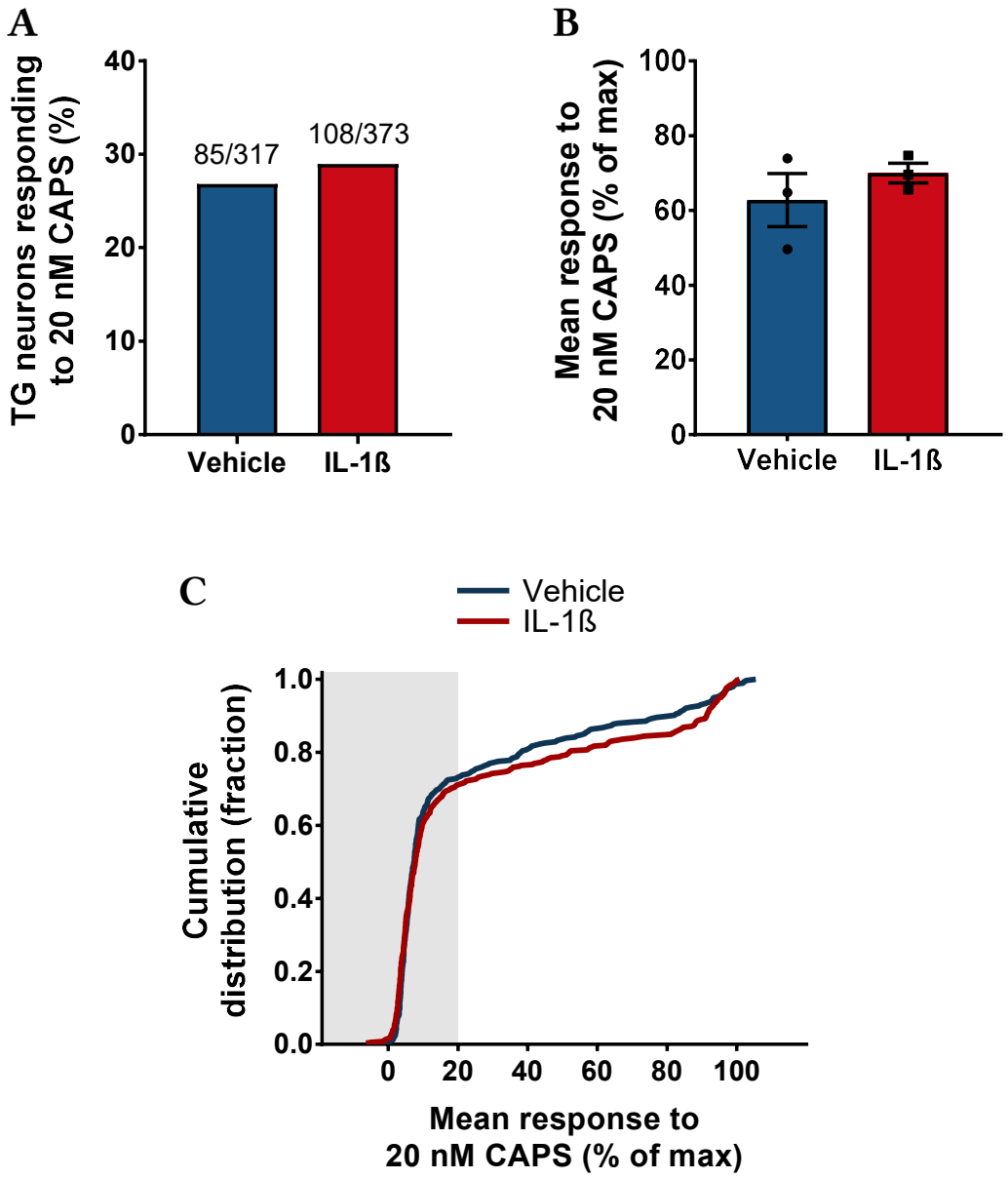

Figure 5.20 Long-term pre-treatment with IL-1β does not significantly affect TG neuron responses to TRPV1 activation

A) The percentage of TG neurons responding to the TRPV1 agonist capsaicin (CAPS; 20 nM), following a 24-hour pre-treatment with either IL-1β (10 ng/ml) or a corresponding vehicle. The number of responding neurons and the total number of neurons tested in each case is indicated in the graph, above the bars. *B)* The amplitude of TG neuron responses to 20 nM CAPS, following the pre-treatment with IL-1β or vehicle. Data are presented as mean ± SEM (n = 3). *C)* Cumulative distribution plot showing the responses of individual TG neurons to 20 nM CAPS, following the pre-treatment with IL-1β (10 ng/ml) or vehicle. The shaded area represents neuronal responses below the threshold value (20% of the maximum response to either 50 mM KCl or 1 µM CAPS) used for distinguishing the responding TG neurons from non-responders.

Table 5.2 Sensitisation of cultured mouse TG neuron responses to a high concentration of capsaicin

Long-term pre-treatment of TG neurons with TNFα or IL-1β significantly increased the percentage of TG neurons sensitive to capsaicin (1 μM). The data was collected during the same experiments described in section 5.3.2.

Pre-treatment group	Overall proportion of TG neurons responding to 1 μM capsaicin (%)	*p*-value
TNFα (30 ng/ml; 24 hours)		
Vehicle	45.8	0.009
TNFα	53.3	
IL-1β (10 ng/ml; 1 hour)		
Vehicle	41.1	0.772
IL-1β	41.8	
IL-1β (10 ng/ml; 24 hours)		
Vehicle	48.7	0.003
IL-1β	56.9	

5.4 Discussion

5.4.1 Mouse TG neurons express functional TRPA1 and TRPV1, but not TRPV4 ion channels

Initial findings described in this chapter support the functional expression of TRPA1 and TRPV1, selected for their well-established link to various pain states in humans (Mickle *et al.*, 2016), on cultured mouse TG neurons. Allyl isothiocyanate (AITC) induced an increase in intracellular Ca^{2+} concentration ($[Ca^{2+}]_i$) in a proportion of primary mouse TG neurons, even at concentrations approximately 2-10 times lower than the reported EC_{50} value for heterologously expressed mouse TRPA1 channels (Bandell *et al.*, 2004), suggesting the presence of functional TRPA1 ion channels. As expected from the fact that TRPA1 is expressed in a subset of TRPV1-expressing sensory neurons (Story *et al.*, 2003), the TRPV1 ion channel agonist capsaicin also successfully stimulated TG neurons in this study. The proportion of TG neurons responding to the highest concentrations of either agonist is in the same range as published rat TG neuron data (Jordt *et al.*, 2004; Bautista *et al.*, 2005). It should be noted that a final application of a high concentration of the agonists has not been

included in these experimental runs. As a result, the overall population of neurons sensitive to each agonist cannot be conclusively determined from these particular experiments.

While both agonists produced a concentration-dependent increase in the percentage of responding TG neurons, only capsaicin also caused a concentration-dependent increase in the magnitude of the response. It is possible that the difference in TG neuron responses to AITC might have been detected using a wider range of AITC concentrations. The difference between the agonists might also be related to the nature of interaction with their respective target ion channel. AITC is known to activate TRPA1 via a covalent modification (Hinman *et al.*, 2006), whereas a combination of van der Waals interactions and hydrogen bonds is important in capsaicin-TRPV1 interaction (Yang *et al.*, 2015). Moreover, AITC has also been reported to activate TRPV1 (Gees *et al.*, 2013). Other possible explanations for the consistently large amplitude of AITC-induced increase in TG neuron $[Ca^{2+}]_i$ include TRPA1-driven Ca^{2+} release from the intracellular stores (Shang *et al.*, 2016) or additional Ca^{2+}-dependent regulation of TRPA1 activity (Hasan & Zhang, 2018).

Unlike AITC and capsaicin, the selective TRPV4 agonist GSK1016790A did not produce any concentration-dependent effects on $[Ca^{2+}]_i$ in mouse TG neurons. As shown in Chapter 3, the same GSK1016790A concentrations successfully increased $[Ca^{2+}]_i$ in mouse odontoblast-like cells in a concentration-dependent manner. A limited percentage of TG neurons displayed small but detectable increases in $[Ca^{2+}]_i$, coinciding with the agonist application. It cannot be excluded that higher concentrations of GSK1016790A could have activated a greater proportion of TG neurons, as reported elsewhere for DRG neurons (Kim *et al.*, 2016). However, in our experiments, a similar percentage of responders was detected in TG neurons from both wild-type and TRPV4 knock-out mice, suggesting that the observed fluctuations in $[Ca^{2+}]_i$ were not specific to the TRPV4 activation. Therefore, subsequent experiments testing the potential sensitisation of TG neurons (discussed in section 5.4.4) did not include TRPV4 as a target of interest.

Although some researchers argue the presence of TRPV4 on mouse TG neurons (Chen *et al.*, 2013), the lack of TRPV4-specific response to GSK1016790A in TG

neurons in this study agrees with mouse TG neuron-specific RNA sequencing (RNA-seq) data (Lopes *et al.*, 2017), as well as the absence of TRPV4 gene expression in retrogradely-traced rat dental primary afferents (Hermanstyne *et al.*, 2008). This suggests that TRPV4 is unlikely to be involved in dental pain as a neuronal mechanoreceptor, responsible for the direct detection of dentinal fluid movement by neurons, as proposed by the hydrodynamic theory of dentine hypersensitivity. The above observations also contradict the findings of Bakri and colleagues (2018), who detected TRPV4 on human dental pulp afferents using immunostaining techniques. While there is a possibility that this represents a species difference, another possible explanation is the non-specificity of anti-TRPV4 antibodies used in that study.

5.4.2 Detection of ATP by TG neurons

The presence of functional purinergic P2 receptors on TG neurons is crucial for the proposed mechanism of dentine hypersensitivity that involves stimulation of dental primary afferents by ATP released from odontoblasts. Given the close contact between the neurons innervating the teeth and odontoblasts *in vivo* (Shiromoto, 1984; Ibuki *et al.*, 1996), higher concentrations of ATP were tested in calcium imaging experiments described in this chapter (2-10 μM) than previously detected in the culture medium of stimulated mouse odontoblast-like cells (~30-40 nM; Chapter 3). This replicates the reported difference between evoked bulk phase and near-membrane ATP concentrations in other types of non-neuronal cells (Praetorius & Leipziger, 2009). In the present study, ATP, at all concentrations tested, increased $[Ca^{2+}]_i$ in a proportion of TG neurons, supporting the presence of functional ATP receptors. As a result, it was decided to include ATP as one of the agonists tested in the TG neuron sensitisation assay (discussed in section 5.4.4). The percentage of TG neurons responding to the highest ATP concentration is also consistent with published mouse TG neuron calcium imaging data (Hanstein *et al.*, 2016).

Multiple consecutive ATP application in another set of experiments revealed distinct desensitisation profiles of TG neuron responses to ATP, suggesting the heterogeneity of purinergic P2 receptors present on different TG neurons. Indeed, subsequent observation of increased $[Ca^{2+}]_i$ in TG neurons in response to selective pharmacological agents supported the presence of functional ionotropic P2X and

metabotropic P2Y receptors. Although α,β-meATP is known to activate $P2X_1$, $P2X_{2/3}$, and $P2X_3$ receptors (North, 2002), $P2X_3$ is the most highly expressed P2X receptor subunit in mouse TG neurons, with low $P2X_2$ and no $P2X_1$ expression detected by RNA-seq (Lopes *et al.*, 2017). Therefore, α,β-meATP-induced increase in $[Ca^{2+}]_i$ most likely represents the activation of homomeric $P2X_3$ and potentially heteromeric $P2X_{2/3}$ receptors on TG neurons. More than half of TG neurons desensitised rapidly in the experiments involving repeated ATP applications in this study, which potentially reflects fast desensitisation of $P2X_3$ (Lewis *et al.*, 1995). The observation that some TG neurons that were sensitive to α,β-meATP did not subsequently respond to ATP could also be explained by the desensitisation of $P2X_3$. Therefore, the proportion of ATP-sensitive TG neurons expressing functional $P2X_3$ was likely underestimated in this study. The functional expression of other P2X receptor subunits, such as $P2X_4$ and $P2X_6$, on TG neurons was not investigated in this study due to the lack of selective agonists. Selective antagonists could be used in the future experiments to determine the exact contribution of different purinergic P2 receptors to the detection of ATP by TG neurons.

In addition to the P2X receptors, mouse TG neurons express the genes encoding $P2Y_1$ and $P2Y_2$ (Lopes *et al.*, 2017). In the present study, a selective $P2Y_1$ agonist MRS2365 successfully increased $[Ca^{2+}]_i$ in a small proportion of TG neurons, supporting the presence of functional $P2Y_1$. It should be noted that ATP acts as a partial agonist at $P2Y_1$ receptors but is spontaneously hydrolysed by ectonucleotidases to ADP, a full agonist of $P2Y_1$ receptors (Hechler *et al.*, 1998). This suggests that ADP signalling via $P2Y_1$ should also be considered when investigating ATP-dependent effects on TG neurons. However, this was out of scope of this study. Interestingly, out of the three selective agonists tested, the $P2Y_2$ agonist 2-ThioUTP activated the greatest proportion of ATP-sensitive TG neurons. In theory, the concentration of 2-ThioUTP tested could also have activated $P2Y_4$ and $P2Y_6$ receptors (El-Tayeb *et al.*, 2006). However, these receptors are not expressed in mouse TG neurons (Lopes *et al.*, 2017). The relatively high percentage of TG neurons that demonstrate functional $P2Y_2$ expression, combined with the fact that ATP acts as a full agonist at $P2Y_2$ receptors (Lazarowski *et al.*, 1995), suggests a potentially important role for $P2Y_2$ in ATP-dependent modulation of TG neuron activity.

Responsiveness of some ATP-sensitive TG neurons to more than one selective P2 receptor agonist suggests the presence of multiple functional P2 receptors on the same TG neuron, with a potential regulation of P2X activity by P2Y receptors. Although both $P2Y_1$ and $P2Y_2$ receptors are primarily $G_{q/11}$-coupled GPCRs (Erb & Weisman, 2012), $P2Y_1$ has previously been demonstrated to inhibit $P2X_3$ (Gerevich *et al.*, 2007), whereas reports of both inhibition and facilitation of $P2X_3$-dependent currents by $P2Y_2$ exist in the literature (Chen *et al.*, 2010; Mo *et al.*, 2013). Moreover, the observation that most ATP-sensitive TG neurons also respond to the TRPV1 agonist capsaicin indicates an extensive overlap between purinergic P2 receptor and TRPV1 ion channel expression, again, with a potential interaction between the two types of proteins. Indeed, potentiation of TRPV1 activity by $P2Y_1$, $P2Y_2$, and $P2X_3$ has already been demonstrated and proposed to be important in pain (Tominaga *et al.*, 2001; Lakshmi & Joshi, 2005; Yousuf *et al.*, 2011; Saloman *et al.*, 2013).

Since the experiments described in this chapter were performed using all mouse TG neurons, rather than just those innervating the teeth, the above findings could potentially be applicable to various orofacial pain states. However, functional expression of $P2X_3$, $P2Y_1$, and $P2Y_2$ has recently been confirmed by calcium imaging of retrogradely-labelled mouse dental primary afferent neurons (Katharina Zimmermann, personal communication), which indicates the relevance of the findings from the present study to the neurons innervating the teeth. Overall, TG neuron ability to detect ATP supports the potential ATP-dependent modulation of adjacent nerve fibre activity by odontoblasts.

5.4.3 Potential activation of TG neurons by glutamate

In addition to ATP, stimulated odontoblasts have also been demonstrated to release glutamate (Cho *et al.* (2016) and Chapter 3 of this thesis), which was proposed as an alternative mediator of intercellular signalling between odontoblasts and neurons, relevant in dentinal pain (Nishiyama *et al.*, 2016). In the present study, to determine if glutamate can directly activate TG neurons, it was tested at concentrations up to 30 times higher than those previously detected in the solution from stimulated mouse odontoblast-like cells. Although glutamate caused large increases in $[Ca^{2+}]_i$ in some TG neurons, suggesting potential TG neuron activation, the resulting overall

percentage of glutamate-sensitive TG neurons was low and not significantly different from the proportion of TG neurons sensitive to the corresponding vehicle. It is possible that even higher concentrations of glutamate are required to activate a considerable proportion of TG neurons. For instance, at 200 μM, compared with 10-100 μM tested in the present study, glutamate has been reported to successfully stimulate a large proportion of cultured dorsal root ganglion (DRG) neurons (Kung *et al.*, 2013). Any sensitisation of TG neurons exposed to glutamate, potentially dependent on mGluR activation, also cannot be excluded at this stage. Nonetheless, based on these preliminary results, it seemed unlikely that glutamate would play a major role as a mediator of odontoblast-TG neuron communication. Therefore, further experiments, described in Chapter 6, focused on ATP rather than glutamate signalling.

5.4.4 TG NEURON SENSITISATION ASSAY

The observation that increasing concentrations of AITC, capsaicin, and ATP successfully increased the proportion of responding cultured mouse TG neurons, or the amplitude of their responses, demonstrated a window for potentiation of TRPA1 and TRPV1 ion channel, as well as purinergic P2 receptor, activity on TG neurons. Two well-established inflammatory mediators, namely tumour necrosis factor alpha (TNFα) and interleukin 1 beta (IL-1β), were chosen for the initial TG neuron sensitisation experiments, in order to validate the assay and provide more information about their potential sensitising effects on the above targets.

The chosen concentration of TNFα (30 ng/ml) was based on a previous study by Khan and colleagues (2008), who demonstrated the TNFα-dependent sensitisation of rat TG neuron responses to capsaicin (25 nM). A similar concentration of capsaicin (20 nM) was used in the present study. The chosen concentration of IL-1β (10 ng/ml) was also previously demonstrated to cause an increase in the excitability of DRG neurons (Binshtok *et al.*, 2008). The sensitising effects in both studies were observed following the neuron pre-treatment for up to 30 minutes. Therefore, the pre-treatment duration of 1 hour was expected to produce a detectable sensitisation of TG neurons in the short-term sensitisation experiments.

The findings from the short-term sensitisation experiments again highlighted the difference between TRPV1 and TRPA1. The proportion of neurons responsive to capsaicin was the main parameter increased after the pre-treatment of TG neurons with TNFα, whereas an identical pre-treatment caused a significant increase only in the magnitude of the responses to AITC among the AITC-sensitive neurons. The specificity of these neuronal responses to the activation of TRPV1 and TRPA1 was also supported by their absence in TG neurons from the TRPV1 and TRPA1 knock-out mice, respectively. It is currently unclear whether these changes represent a decrease in the channel activation threshold or increase of the channel expression in the neuronal cell membranes, or both, as the identification of the mechanisms responsible for the sensitisation observed in each case was not possible from these preliminary experiments. However, Meng and co-workers (2016) demonstrated TNFα-induced vesicular co-trafficking of TRPV1 and TRPA1 ion channels to the trigeminal neuron plasma membrane, which is likely to be one of the mechanisms underlying the observations from the present study.

Unexpectedly, a decrease in the percentage of TG neurons responding to ATP was detected following the short-term pre-treatment with TNFα. While this finding was statistically significant, its biological significance is unclear, as the overall percentage of ATP-sensitive neurons in the vehicle group was considerably higher than in the previous concentration-response experiments. However, a significantly different cumulative distribution of individual TG neuron responses to the P2X agonist α,β-meATP, following the short-term pre-treatment with TNFα, combined with a trend towards a reduction in the percentage of neurons responding to α,β-meATP, support the presence of a TNFα-mediated negative effect on purinergic P2 receptor activity. Since ATP has previously been reported to trigger TNFα release (Hide *et al.*, 2000), this could potentially represent a negative feedback mechanism in TNFα signalling.

In contrast to TNFα, no sensitisation of TG neurons could be detected after either the short-term (1-hour) or the long-term (24-hour) pre-treatments with IL-1β. Again, the recently available mouse TG neuron RNA-seq data (Lopes *et al.*, 2017) provided a likely explanation, as the gene encoding TNFα receptor TNFR1, but not interleukin 1 receptor IL-1R1, was found to be expressed on TG neurons. This suggests that any

IL-1β-dependent sensitising effects on TG neurons are indirect, via IL-1R1 receptors on non-neuronal cells. In that case, the inability to detect any direct IL-1β-mediated sensitisation of TG neuron activity would support the accuracy of the assay. On the other hand, TNFα-mediated sensitisation could also not be detected following the long-term (24-hour) pre-treatment. This might represent a methodological issue. One modification of the experimental runs that was made after the short-term sensitisation experiments testing the effects of TNFα was the inclusion of a challenge with a high concentration of capsaicin (1 μM) just before the final application of potassium chloride in the subsequent short-term and long-term sensitisation experiments. This was done to identify the TRPV1-expressing TG neuron population among all viable neurons. However, it was noticed that those neurons that responded to 1 μM capsaicin displayed reduced response amplitude to subsequent KCl application. As the maximum Fura-2AM ratio change in response to KCl was used for the calculations of each TG neuron response size to the test compound, this reduction was predicted to artificially alter the calculated response amplitudes. Therefore, the response to either 50 mM KCl or 1 μM capsaicin, whichever was greater, was used as a maximum response in the analysis of short-term IL-1β and long-term TNFα and IL-1β experiments. It was not anticipated that TNFα or IL-1β would sensitise TG neuron responses to such a high concentration of capsaicin. However, a recent study demonstrated a significant enhancement of rat TG neuron responses to 1 μM capsaicin, following a 24-hour pre-treatment with TNFα (Meng *et al.*, 2016). Indeed, the comparison of the proportion of TG neurons sensitive to 1 μM capsaicin, as identified in the present study, also revealed a statistically significant increase in response to the long-term pre-treatment with TNFα and IL-1β, but not the short-term pre-treatment with IL-1β. This not only supports the sensitisation of TRPV1 by these inflammatory mediators, but also provides a potential explanation for the lack of potentiation of TG neuron responses to the low concentrations of AITC and capsaicin, observed in the long-term sensitisation experiments. Since both TRPA1 and TRPV1 are expressed in the population of TRPV1-positive neurons that are sensitive to the high concentration of capsaicin, any inflammatory mediator-dependent increase in the proportion of TG neurons sensitive to 1 μM capsaicin would affect the calculated TG neuron response sizes to either 2 μM AITC or 20 nM capsaicin. Therefore, the initial experimental protocol, which included the final KCl

application, without the preceding application of 1 μM capsaicin, is the preferred strategy for studying the potential sensitisation of TG neuron responses to these agonists in the future.

The finding that 24-hour pre-treatment with IL-1β potentiated TG neuron responses to 1 μM capsaicin again poses a question about the underlying mechanism. If IL-1R1 is not present on TG neurons, this effect would indicate the presence of non-neuronal cells, most likely satellite glia, in TG neuron cultures. This would not be completely unexpected, as no additional purification steps, such as the filtering of TG neuron cell suspension through a bovine serum albumin (BSA) gradient or the use of any anti-mitotic chemical agents, were included in the present protocol to ensure the depletion of non-neuronal cells. At the same time, this better replicates the *in vivo* situation, where any interactions between neuronal and non-neuronal cells are intact.

To sum up, the optimised calcium imaging-based *in vitro* assay is sufficiently sensitive to detect the sensitisation of TRPA1 and TRPV1 ion channels on cultured TG neurons and could be used to test other inflammatory mediators or bacterial products that are relevant to the inflammatory odontogenic pain for their ability to sensitise TG neurons. A different strategy was adopted for studying the potential role of TG neuron interaction with odontoblasts in dentine hypersensitivity, which will be discussed in the next chapter.

Chapter 6

Signalling between odontoblast-like cells and trigeminal ganglion neurons in co-cultures

6.1 Introduction

6.1.1 Studying intercellular interactions in the teeth using co-cultures

Chapters 3-5 of this thesis discussed characterisation of the two main cell types proposed to be involved in dental pain initiation using monocultures of either mouse odontoblast-like (OB) cells or mouse trigeminal ganglion (TG) neurons. However, the interaction between different types of cells can also be directly investigated in co-cultures *in vitro* (reviewed by Goers *et al.* (2014)). Several studies using co-cultures to investigate intercellular interactions in the teeth have been identified in the literature. For instance, Lillesaar and colleagues (1999; 2001) demonstrated that both dental pulp tissue explants and cultured pulpal cells, but not 3T3 fibroblastic cells, promote neurite outgrowth from co-cultured TG tissue explants via the secretion of neurotrophic factors. Neurite outgrowth also occurs towards odontoblasts in odontoblast-TG neuron co-cultures (Maurin *et al.*, 2004). Dental tissues were later found to either attract or repel neurites, depending on the developmental stage, as

observed in both conventional co-cultures with TG neurons (Lillesaar & Fried, 2004) and compartmentalised microfluidic co-culture systems (Pagella *et al.*, 2014). While these studies primarily focused on the developmental processes of tooth innervation, the findings support the ability of signals from non-neuronal cells in the teeth, including odontoblasts, to affect TG neurons.

With regard to pain-relevant odontoblast communication with TG neurons, Allard and co-workers (2006) demonstrated clustering of voltage-gated sodium channel subunits at locations of interaction between odontoblasts and TG neurons in co-cultures and proposed ephaptic transmission, which involves current flow through the extracellular space, as a means of action potential propagation from odontoblasts to TG neurons. On the other hand, co-culture studies performed by another research group later provided evidence for a less controversial mechanism of signal transmission that involves ATP- or glutamate-dependent paracrine signalling from mechanically stimulated odontoblasts to TG neurons (Shibukawa *et al.*, 2015; Nishiyama *et al.*, 2016), as discussed in Chapters 3 and 5. The ability of OB cells to communicate with TG neurons in co-cultures via paracrine signalling, involving ATP as a mediator, was evaluated in this study.

6.1.2 Objectives of the present study

Specific objectives of the experiments described in this chapter are as follows:

- To establish an OB cell and TG neuron co-culture that would enable simultaneous calcium imaging of both cell types, allowing direct detection of any intercellular communication.
- To investigate using calcium imaging of OB-TG neuron co-cultures whether stimulation of TRPV4 ion channels on OB cells is sufficient to activate and/or sensitise the adjacent TG neurons.
- To examine the role of ATP as a mediator of any OB-dependent effects on TG neuron activity by using inhibitors of ATP signalling.

6.2 Materials and methods

6.2.1 Reagents

Apyrase (from potatoes, grade III) was obtained from Sigma, whereas PPADS tetrasodium salt was obtained from Tocris. For information on other reagents used in multiple chapters see Chapter 2 (section 2.2). Apyrase and PPADS were initially dissolved in dH_2O and further diluted on the day of the experiment to the appropriate concentration in culture medium, as indicated in subsequent sections.

6.2.2 Mixed odontoblast-like cell and TG neuron co-cultures

Mouse odontoblast-like (OB) cells were seeded directly onto sterile round glass coverslips and grown in the differentiating medium (formulation in Chapter 2, section 2.3.1) in 4-well plates until confluence. Primary mouse TG neurons were dissociated as described in Chapter 2 (section 2.3.2), resuspended in pre-warmed supplemented F12-based TG neuron culture medium, and plated onto the OB cell monolayer (see Figure 6.1A for illustration) in a sufficient volume to cover the coverslip (approximately 30-40 µl). After allowing the TG neurons to attach for 20-30 minutes at 37°C, the wells were flooded with a 1:1 mix of the differentiating OB culture medium and supplemented F12-based TG neuron culture medium (to 500 µl). Co-cultures were maintained in a humidified incubator at 37°C and 5% CO_2.

6.2.3 Calcium imaging of OB-TG neuron co-cultures

OB-TG neuron co-cultures were used for calcium imaging experiments 24-48 hours after the plating of TG neurons. The co-cultures were loaded with Fura-2AM (4 µM) for 1 hour at 37°C in either the standard extracellular solution (ECS; in the case of experiments where ECS was also used for perfusing the cells during the experimental runs) or fresh co-culture medium (in the case of experiments where calcium imaging was performed in the complete OB culture medium). The co-cultures were imaged through the glass coverslip using an inverted microscope-based system, as described in Chapter 2, section 2.5.2 (see Figure 6.1B for example baseline fluorescence images).

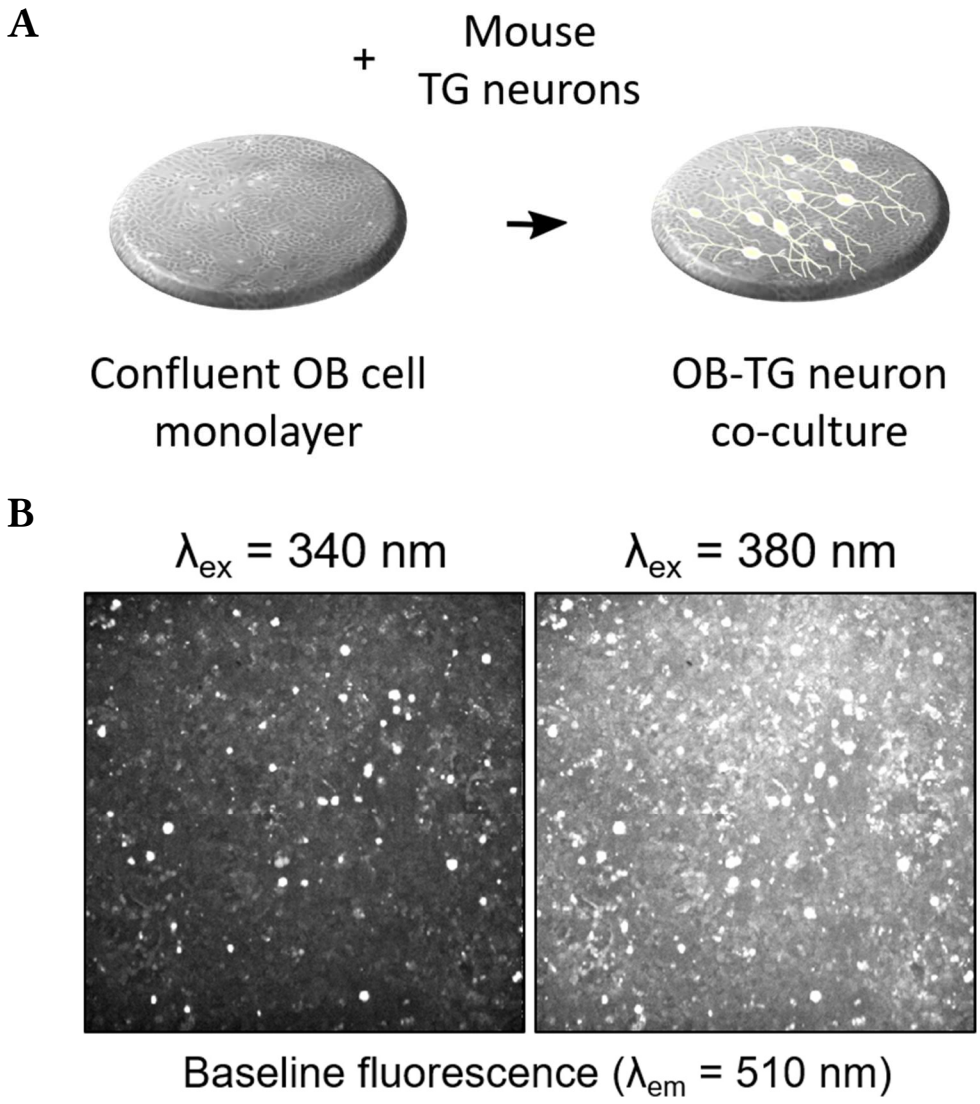

Figure 6.1 Illustration of OB-TG neuron co-culture calcium imaging experiments

A) Mixed odontoblast-like cell (OB) and trigeminal ganglion (TG) neuron co-cultures were established by plating dissociated mouse TG neuron cell suspension onto a confluent monolayer of mouse OB cells. *B)* Example images of OB-TG neuron co-culture baseline Fura-2AM fluorescence measured at 510 nm in response to excitation at two different wavelengths (340 nm and 380 nm). While bright round TG neuron cell bodies are clearly visible, OB cell fluorescence forms the background and is less well-defined.

Initial co-culture calcium imaging experiments involved a baseline recording of Fura-2AM fluorescence ratio (F_{340}/F_{380}) during the perfusion of either ECS or complete OB culture medium onto the cells, as indicated. The cells were then perfused with either the TRPV4 agonist GSK1016790A (100 nM) or a corresponding DMSO vehicle (0.01% (v/v)) for 1 minute, followed by the incubation with these compounds for another 5

minutes after stopping the flow of the solutions. The cells were then washed with either ECS or the complete OB medium, as appropriate, and subsequently exposed to ATP, capsaicin (CAPS), and KCl. TG neurons could be distinguished from OB cells based on the greatest increase in F_{340}/F_{380} in response to KCl or CAPS, whereas OB cells displayed the greatest increase in F_{340}/F_{380} in response to GSK1016790A or ATP. It should be noted that while care was taken to select and include all viable TG neurons present in the field of view in the analysis, only several traces of OB cell responses are shown due to the difficulty selecting individual fluorescent OB cells.

Further calcium imaging experiments involved pre-exposure of OB-TG neuron co-cultures to either a purinergic P2 receptor blocker PPADS (100 μM) or a corresponding dH_2O vehicle for 1 hour at 37°C, during the incubation of the cells with Fura-2AM. Moreover, co-cultures were perfused with a combination of PPADS and apyrase enzyme or respective vehicles for 1 minute, followed by another 5 minutes of incubation after stopping the solution flow. The application of GSK1016790A was performed in the presence of both apyrase and PPADS, whereas ATP was applied after washing off apyrase, only in the presence of PPADS. To minimise the possibility of detecting false positive responses, the pattern of switching between the solutions was also replicated in vehicle experimental runs. The initial baseline was used for the analysis of all TG neurons, as previously, whereas analysis that excluded the neurons responding to the first vehicle/inhibitor application used the initial baseline for calculating response sizes to vehicles/inhibitors and KCl, but a separate baseline (an average of 30 seconds before GSK1016790A application) was used for calculating TG neuron response sizes to GSK1016790A, ATP, and capsaicin. This was done to ensure that any shift in the baseline caused by the initial vehicle/inhibitor application did not artificially increase the amplitudes of subsequent TG neuron responses (see Figure 6.2 for illustration). TG neurons included in the latter analysis displayed an increase in F_{340}/F_{380} in response to the first vehicle/inhibitor application of less than 20% of the maximum response (either to 50 mM KCl or 1 μM capsaicin, whichever is larger for that particular neuron).

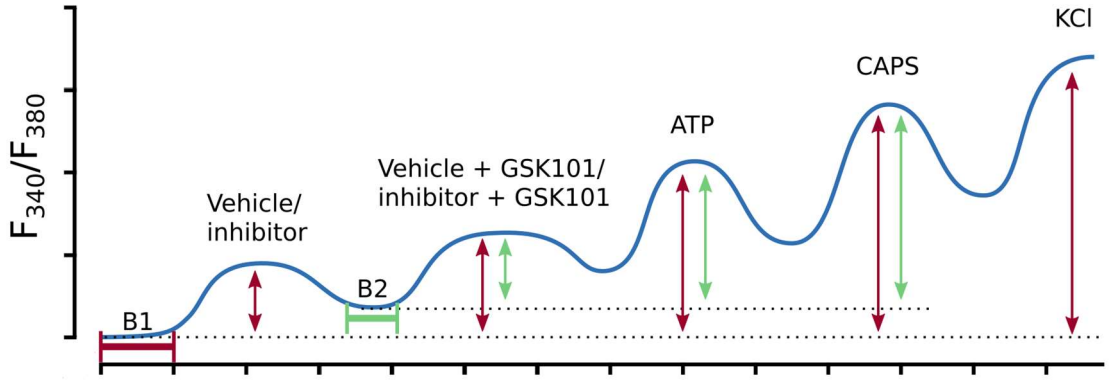

Figure 6.2 Illustration of baselines used for the analysis of co-culture calcium imaging experiments

Initial baseline (B1; average Fura-2AM fluorescence ratio from the first 60 seconds) was typically used for the analysis of both monoculture and co-culture calcium imaging experiments, except for the co-culture experiments that involved pre-exposure of TG neurons to the inhibitors of ATP signalling (PPADS and apyrase) or their vehicles. In that case, B1 baseline was used for calculating all TG neuron responses to all compounds tested (red arrows), whereas the analysis that excluded the responders to the initial vehicle or inhibitor application used B1 baseline for calculating the size of the first vehicle/inhibitor response and the last/maximum response to KCl, but B2 baseline (average of 30 seconds before the second compound application) was used for calculating the size of subsequent responses (green arrows) to 1) vehicles/inhibitors combined with GSK1016790A (GSK101), 2) ATP and 3) capsaicin (CAPS).

6.2.4 Statistics

Differences in the percentage of responding TG neurons were analysed using Fisher's exact test. Two-way ANOVA with Bonferroni's multiple comparisons test was used to compare the amplitudes of TG neuron responses.

6.3 Results

6.3.1 Activation of TRPV4 on OB cells modulates TG neuron activity in OB-TG neuron co-cultures

Based on the evidence for TRPV4 ion channel functional expression in OB cells (as discussed in Chapter 3), but not in mouse TG neurons (Chapter 5), pharmacological activation of TRPV4 ion channels was chosen as an OB-specific stimulus to study the

effects of OB activation on TG neuron activity in OB-TG neuron co-cultures. Calcium imaging experiments performed in the standard extracellular solution (ECS) detected increased intracellular Ca^{2+} concentrations ($[Ca^{2+}]_i$) above vehicle levels in OB cells, but not in TG neurons, in response to the TRPV4 agonist GSK1016790A (100 nM) application (Figure 6.3). However, as demonstrated in Chapter 3, ECS provides suboptimal conditions for ATP release from stimulated OB cells. Therefore, subsequent calcium imaging experiments were performed in complete OB culture medium, which did not seem to interfere with the Fura-2AM fluorescence detection. In these experiments, increased $[Ca^{2+}]_i$ in response to GSK1016790A, but not to the corresponding DMSO vehicle, was detected in both OB cells and some TG neurons (see Figure 6.4). However, response profiles were different between the two cell types. While the increase in $[Ca^{2+}]_i$ in OB cells was generally sudden and persisted throughout the duration of experimental runs, TG neurons demonstrated either a short-lasting or a delayed gradual increase in $[Ca^{2+}]_i$ (Figure 6.4C).

Quantification of TG neuron responses from the above experiments revealed a significantly greater proportion of TG neurons activated by the exposure of OB-TG neuron co-cultures to GSK1016790A (23.4%), compared with vehicle (7.9%), in OB culture medium ($p < 0.001$), whereas only a small percentage of TG neurons responded to either vehicle or GSK1016790A treatments (1.4% and 1.7%, respectively) in ECS (see Figure 6.5A). Although the amplitude of TG neuron responses following the treatment of co-cultures with GSK1016790A was also slightly increased in OB medium, compared with the corresponding vehicle (Figure 6.5B), this increase was not statistically significant ($p = 0.51$).

The proportion of TG neurons sensitive to the subsequent application of ATP (50 μM) was relatively consistent in the vehicle and GSK1016790A experimental runs performed in ECS, as well as vehicle runs in OB medium (31.9-38.0%). However, a significantly greater proportion of TG neurons (54.9%; $p < 0.001$, compared with the corresponding vehicle) responded to ATP following the GSK1016790A treatment of OB-TG neuron co-cultures in OB medium. The amplitude of TG neuron responses to ATP was consistent among the different conditions.

A similar pattern was observed with subsequent TG neuron responses to the TRPV1 agonist capsaicin (1 μM), where the treatment of OB-TG neuron co-cultures with GSK1016790A in OB medium significantly increased the proportion of TG neurons sensitive to capsaicin, compared with the vehicle for GSK1016790A (53.5% and 41.5%, respectively; $p = 0.008$), with no such increase detected in the experiments performed in ECS. However, the amplitude of TG neuron responses to capsaicin was significantly smaller following the treatment of co-cultures with GSK1016790A in OB medium, compared with the corresponding vehicle ($p = 0.002$).

Overall, this provided sufficient evidence that stimulated OB cells can modulate TG neuron activity in OB-TG neuron co-cultures, but only when experiments are performed in complete OB culture medium. Therefore, further calcium imaging experiments were only performed in OB medium.

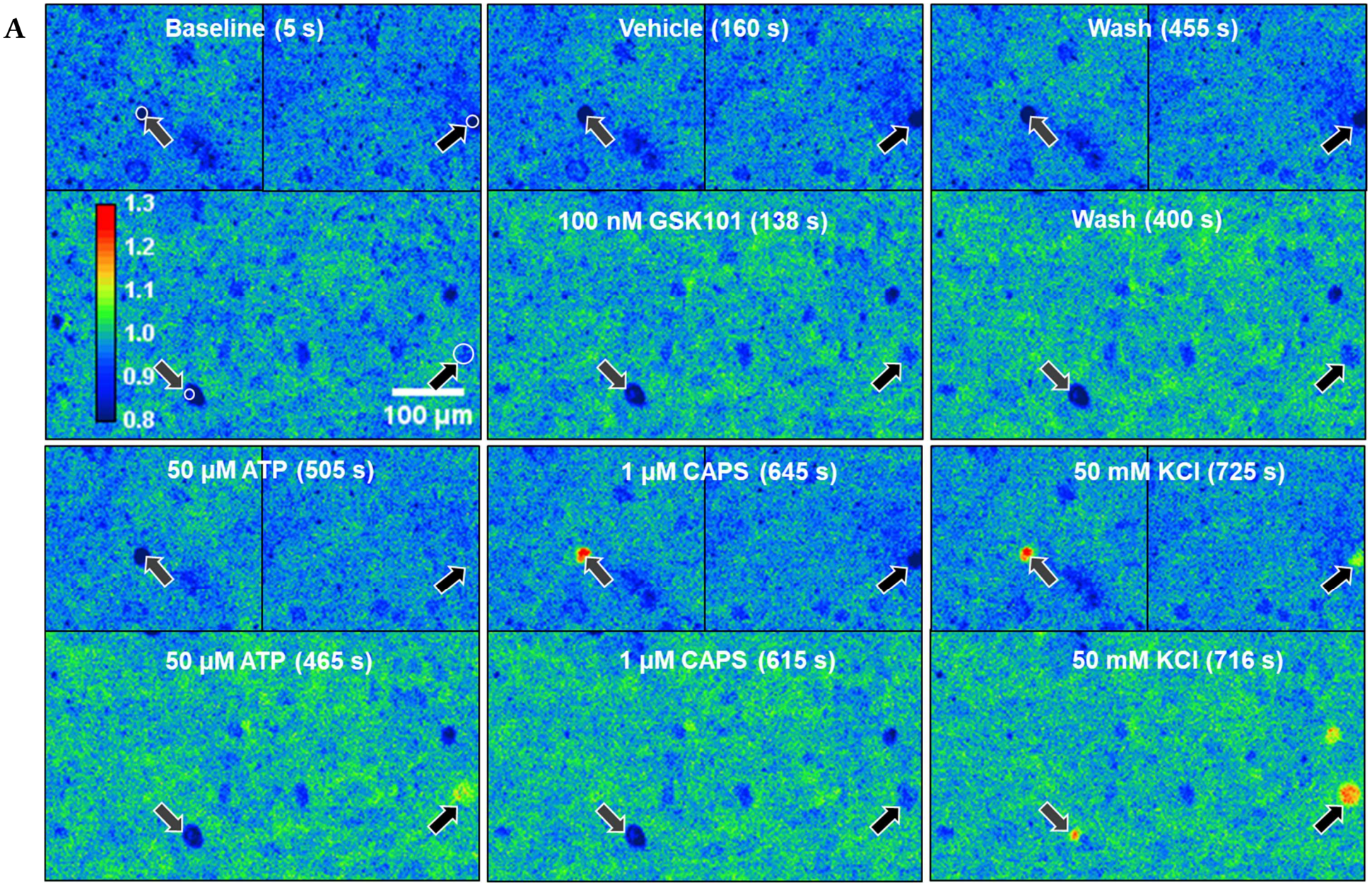
A
Baseline (5 s)
Vehicle (160 s)
Wash (455 s)
1.3
1.2
1.1
1.0
0.9
0.8
100 µm
100 nM GSK101 (138 s)
Wash (400 s)
50 µM ATP (505 s)
1 µM CAPS (645 s)
50 mM KCl (725 s)
50 µM ATP (465 s)
1 µM CAPS (615 s)
50 mM KCl (716 s)

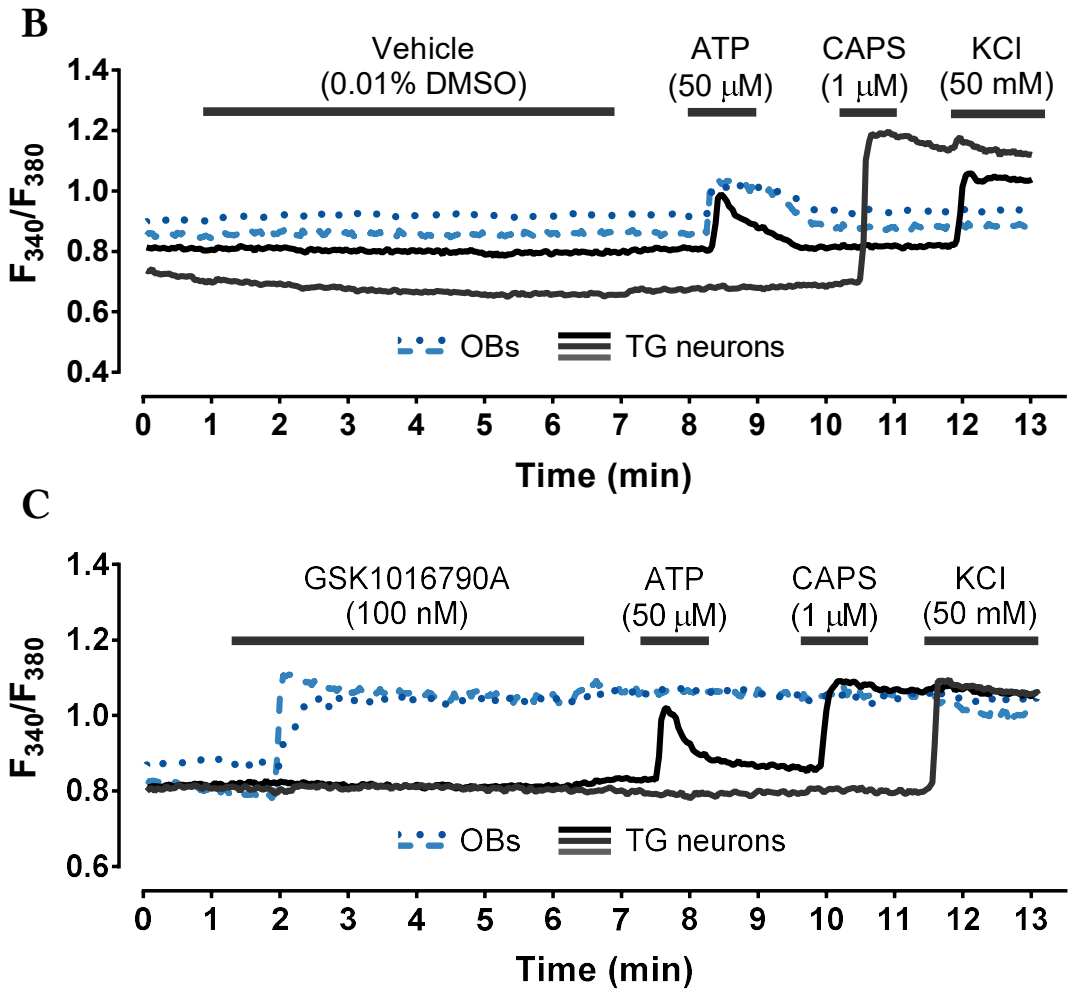

Figure 6.3 Calcium imaging of OB-TG neuron co-cultures in the standard extracellular solution (ECS)

A) Example pseudocolour images of TG neuron responses to the treatment of OB-TG neuron co-cultures with the TRPV4 agonist GSK1016790A (GSK101 (100 nM); *bottom panel*) or a corresponding vehicle (0.01% DMSO; *top panel*), followed by ATP (50 μM), capsaicin (CAPS; 1 μM), and potassium chloride (KCl; 50 mM). The arrows in *A* indicate the same TG neurons as the corresponding colour-coded traces in *B* and *C*. The calcium image colour range represents Fura-2AM fluorescence ratio. *B)* Representative traces demonstrating the lack of OB cell and TG neuron responses to the DMSO vehicle application in experimental runs performed in ECS. *C)* Representative traces of OB cell responses to the TRPV4 agonist GSK1016790A (blue truncated lines). No increase in TG neuron (black and grey solid lines) Fura-2AM fluorescence ratio could be detected in experimental runs performed in ECS.

A

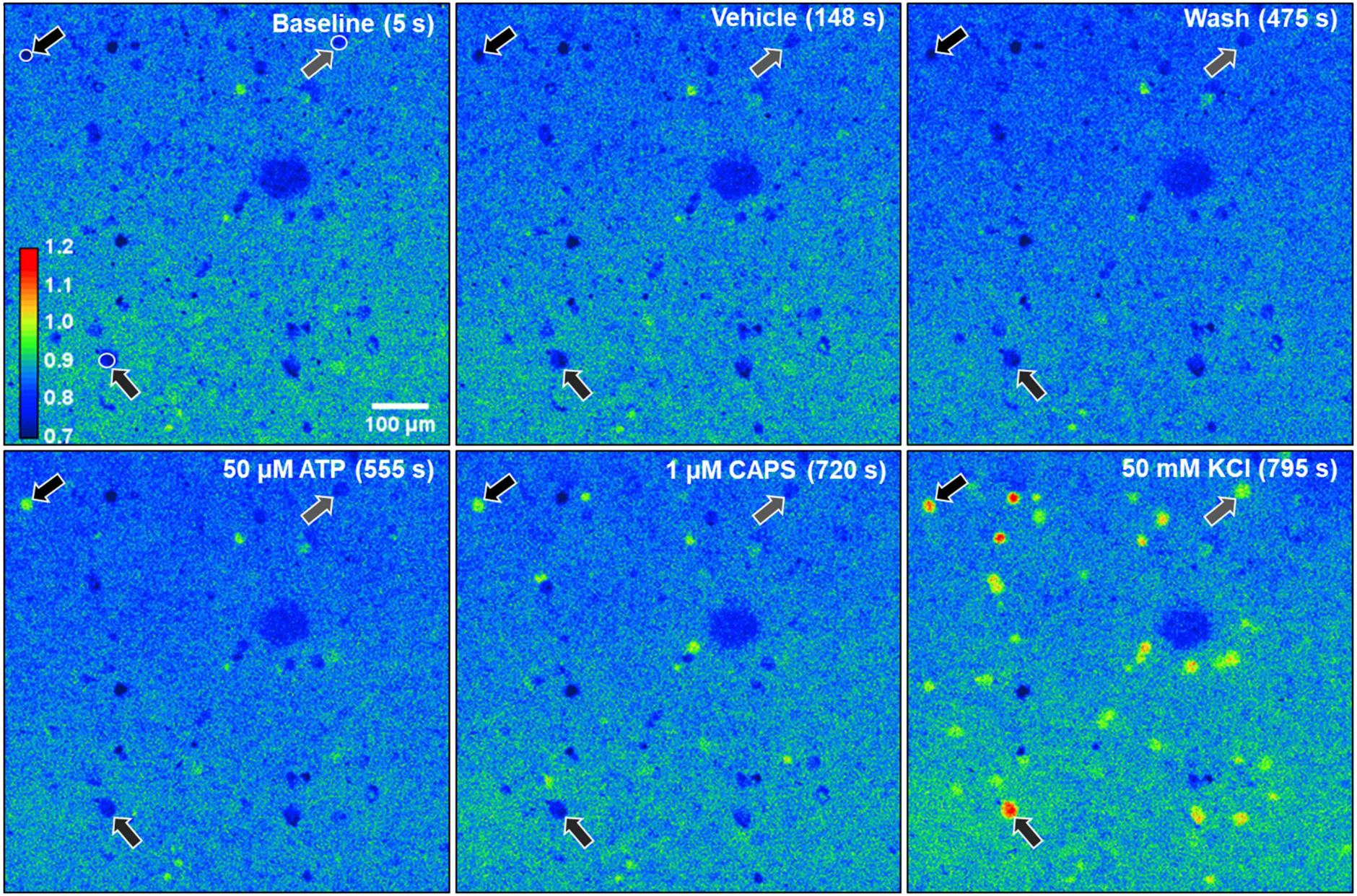
Baseline (5 s)
Vehicle (148 s)
Wash (475 s)
1.2
1.1
1.0
0.9
0.8
0.7
100 µm
50 µM ATP (555 s)
1 µM CAPS (720 s)
50 mM KCl (795 s)

B

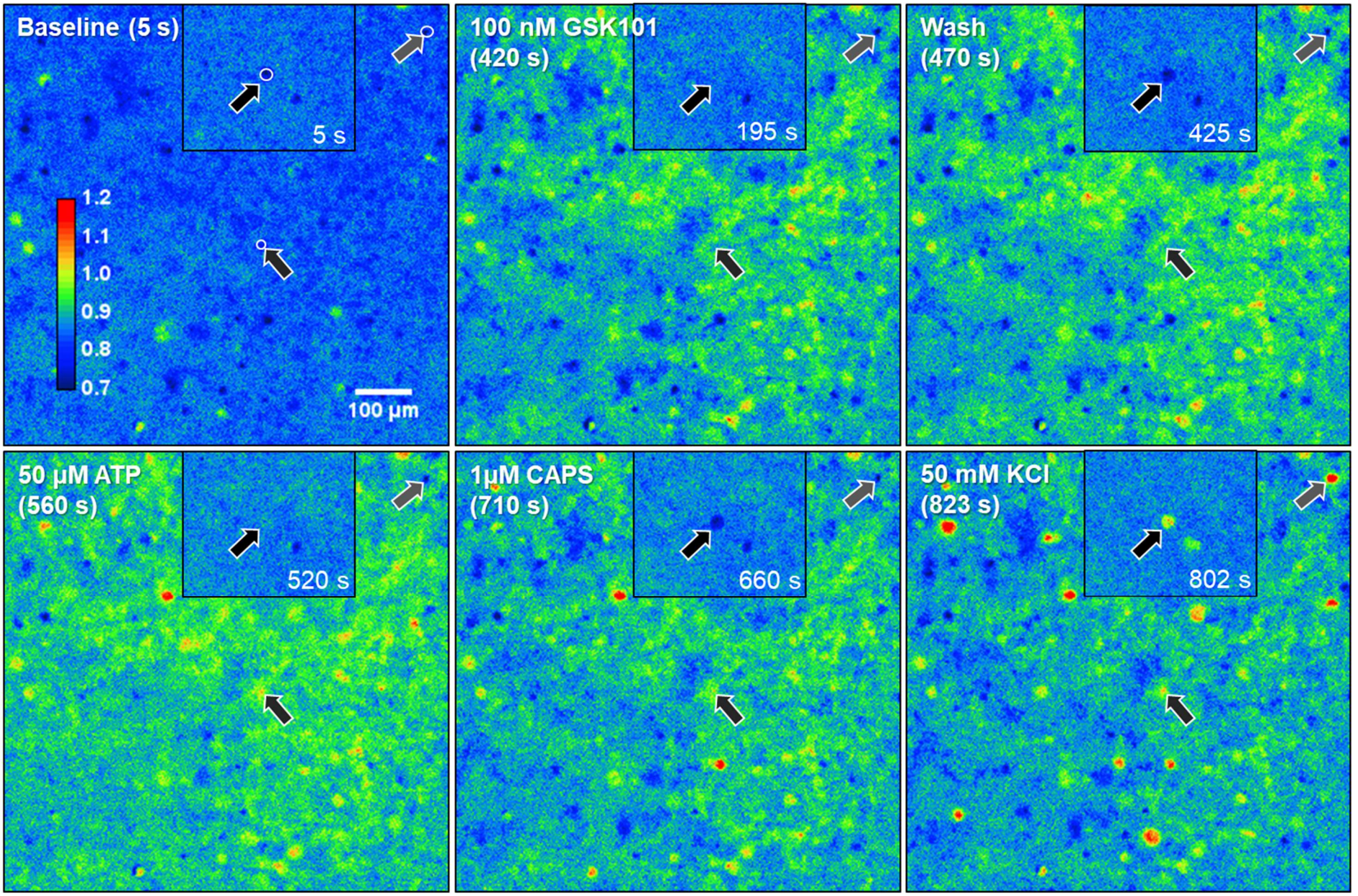
Baseline (5 s)
5 s
1.2
1.1
1.0
0.9
0.8
0.7
100 µm
100 nM GSK101
(420 s)
195 s
Wash
(470 s)
425 s
50 µM ATP
(560 s)
520 s
1µM CAPS
(710 s)
660 s
50 mM KCl
(823 s)
802 s

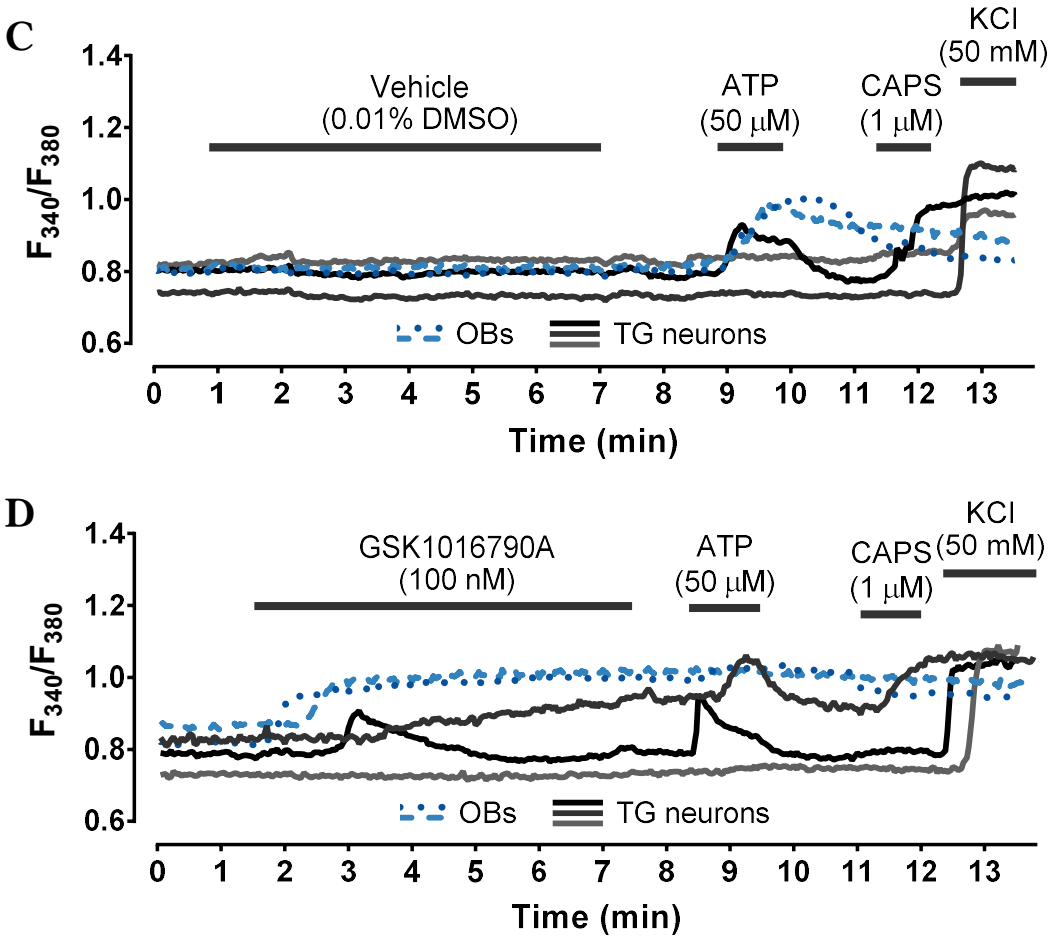

Figure 6.4 Calcium imaging of OB-TG neuron co-cultures in OB culture medium

Example pseudocolour images of TG neuron responses to the treatment of OB-TG neuron co-cultures with the TRPV4 agonist GSK1016790A (GSK101 (100 nM); *A*) or a corresponding vehicle (0.01% DMSO; *B*), followed by ATP (50 μM), capsaicin (CAPS; 1 μM), and potassium chloride (KCl; 50 mM). The arrows in *A* and *B* indicate the same TG neurons as the corresponding colour-coded traces in *C* and *D*. The calcium image colour range represents Fura-2AM fluorescence ratio. *C)* Representative traces from experimental runs testing the effects of DMSO vehicle application on OB-TG neuron co-cultures, which caused no significant increase in Fura-2AM fluorescence ratio in either cell type. *D)* Representative traces of OB (blue truncated lines) responses to the TRPV4 agonist GSK1016790A and resulting TG neuron (black and grey solid lines) responses.

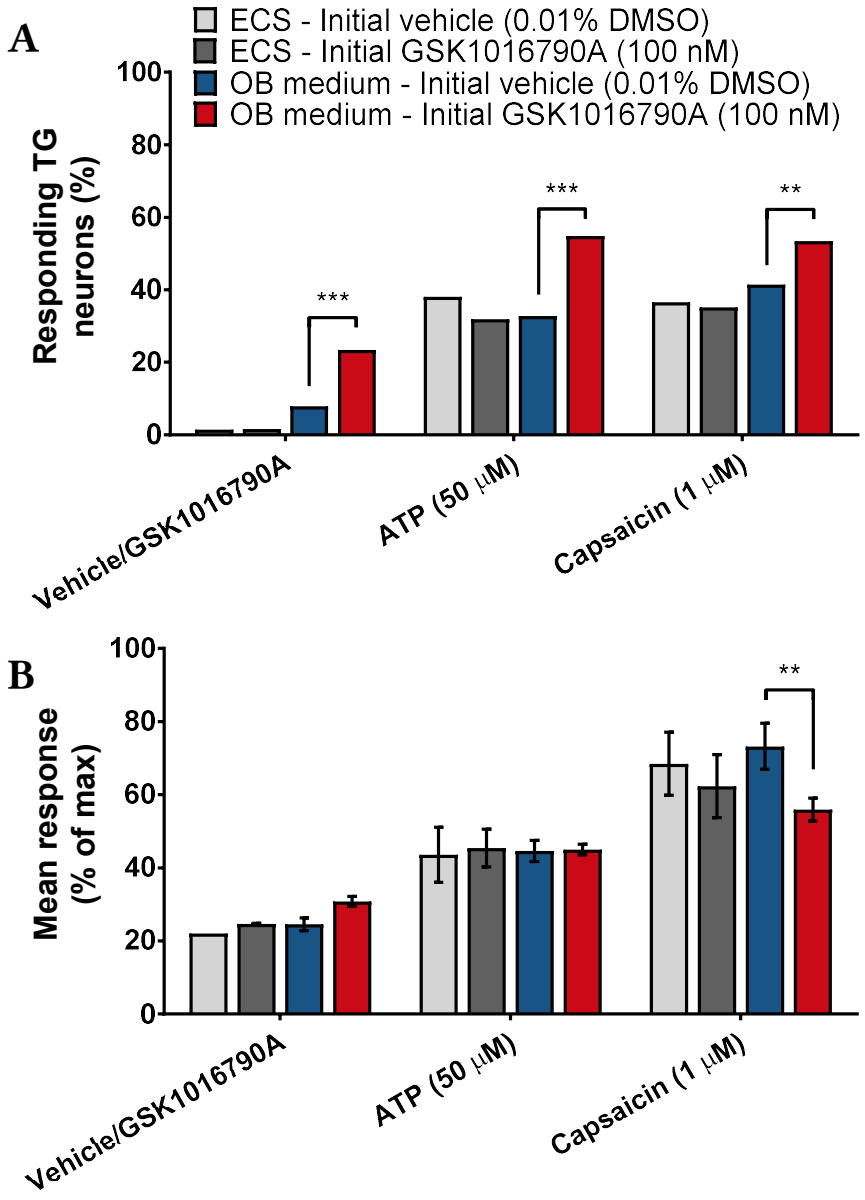

Figure 6.5 Activation of TRPV4 on OB cells modulates TG neuron activity in co-culture calcium imaging experiments performed in OB medium, but not in ECS.

A) In OB culture medium, but not in ECS, stimulation of OB cells with the TRPV4 agonist GSK1016790A (100 nM) indirectly activated a proportion of TG neurons in OB-TG neuron co-cultures and increased the percentage of TG neurons responding to subsequent applications of ATP (50 μM) and the TRPV1 agonist capsaicin (1 μM). $^{**}p < 0.01$; $^{***}p < 0.005$ *vs.* respective vehicle (Fisher's exact test). *B)* The amplitude of TG neuron responses was generally unaffected by OB stimulation with GSK1016790A, with the exception of decreased capsaicin response size in the experiments performed in OB medium. Data are presented as mean response sizes expressed as a percentage of maximum response for that experimental run (either to 50 mM KCl or 1 μM capsaicin) ± SEM. $^{**}p < 0.01$ *vs.* respective vehicle (two-way ANOVA with Bonferroni's *post hoc* test). ECS: n = 6 (71-182 neurons from 3 mice); OB medium: *n* = 4-5 (229-286 neurons from 3-4 mice).

6.3.2 OB-DRIVEN MODULATION OF TG NEURON ACTIVITY INVOLVES ATP SIGNALLING

To investigate the potential involvement of ATP in the OB-driven modulation of TG neuron activity, a combination of a non-selective P2 purinergic receptor antagonist PPADS and an ATP hydrolysing enzyme apyrase was used to inhibit ATP signalling. Following the application of GSK1016790A to the OB-TG neuron co-cultures, TG neuron, but not OB cell, responses were affected by the inhibition of ATP signalling (see Figure 6.6). Some TG neurons demonstrated increased F_{340}/F_{380} ratio in response to both consecutive vehicle/inhibitor applications, irrespective of the presence of GSK1016790A in the treatment solution. The proportion of such responders to the first compound application was greater among the neurons exposed to the inhibitors, compared with those exposed to the respective vehicles ($p = 0.019$; Figure 6.7A). On the other hand, a greater proportion of TG neurons displayed increased $[Ca^{2+}]_i$ in response to the treatment of OB-TG neuron co-cultures with GSK1016790A in vehicle than in inhibitor experimental runs, although this difference was not statistically significant ($p = 0.064$). However, exposure of co-cultures to the inhibitors of ATP signalling significantly decreased the proportion of TG neurons sensitive to subsequent applications of ATP and capsaicin ($p < 0.001$ and $p = 0.025$, respectively). The amplitude of TG neuron responses was not significantly affected by the inhibitors of ATP signalling (Figure 6.7B).

Based on the observation that more TG neurons respond to the first treatment (PPADS and apyrase) than to the identical vehicle application, it was speculated that these responses could potentially be masking any effect of ATP signalling inhibition on TG neuron responses during the second treatment (a combination of PPADS, apyrase, and GSK1016790A). The analysis was then repeated only on those TG neurons that did not respond to the initial vehicle or inhibitor application. This did not affect the proportion of TG neurons responding to ATP or capsaicin, or the amplitude of TG neuron responses to any of the agonists (Figure 6.8). However, the proportion of TG neurons sensitive to the exposure of OB-TG neuron co-cultures to GSK1016790A was found to be statistically significantly lower in the inhibitor experimental runs (10.0%) compared with the corresponding vehicle runs (17.4%; $p = 0.021$).

A

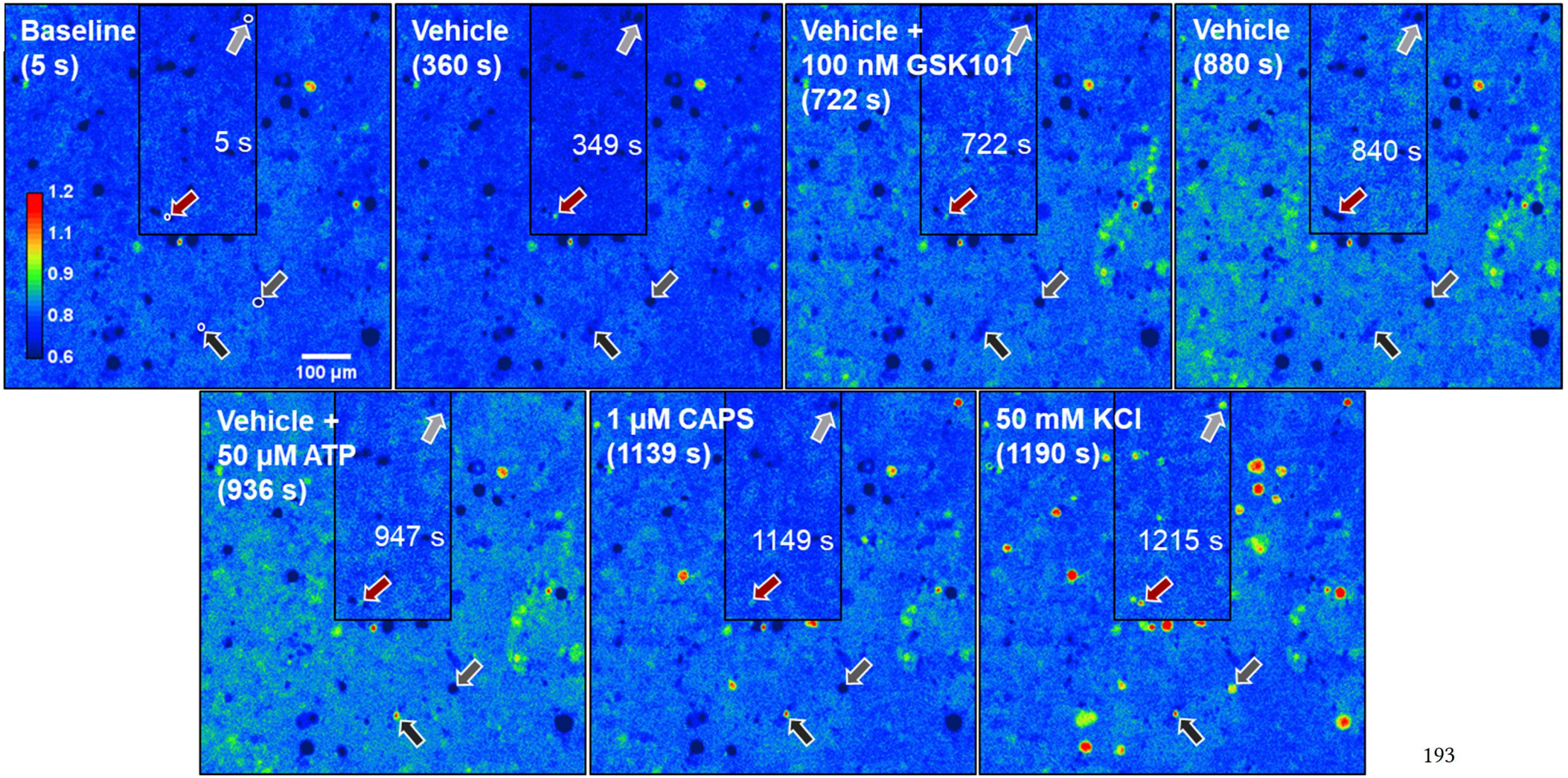
Baseline
(5 s)
5 s
1.2
1.1
0.9
0.8
0.6
100 µm
Vehicle
(360 s)
349 s
Vehicle +
100 nM GSK101
(722 s)
722 s
Vehicle
(880 s)
840 s
Vehicle +
50 µM ATP
(936 s)
947 s
1 µM CAPS
(1139 s)
1149 s
50 mM KCl
(1190 s)
1215 s

B

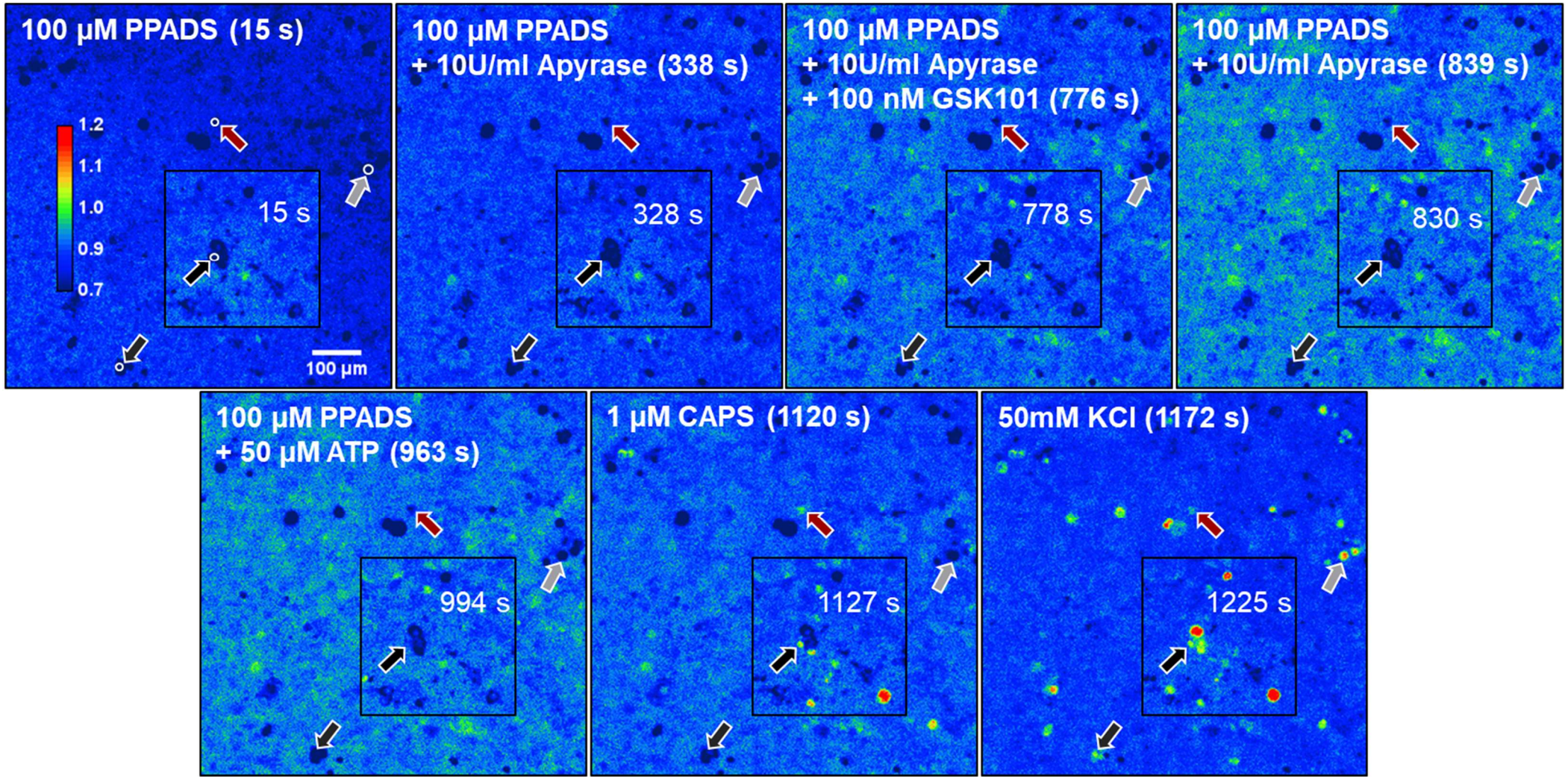
100 µM PPADS (15 s)
1.2
1.1
1.0
0.9
0.7
15 s
100 µm
100 µM PPADS
+ 10U/ml Apyrase (338 s)
328 s
100 µM PPADS
+ 10U/ml Apyrase
+ 100 nM GSK101 (776 s)
778 s
100 µM PPADS
+ 10U/ml Apyrase (839 s)
830 s
100 µM PPADS
+ 50 µM ATP (963 s)
994 s
1 µM CAPS (1120 s)
1127 s
50mM KCl (1172 s)
1225 s

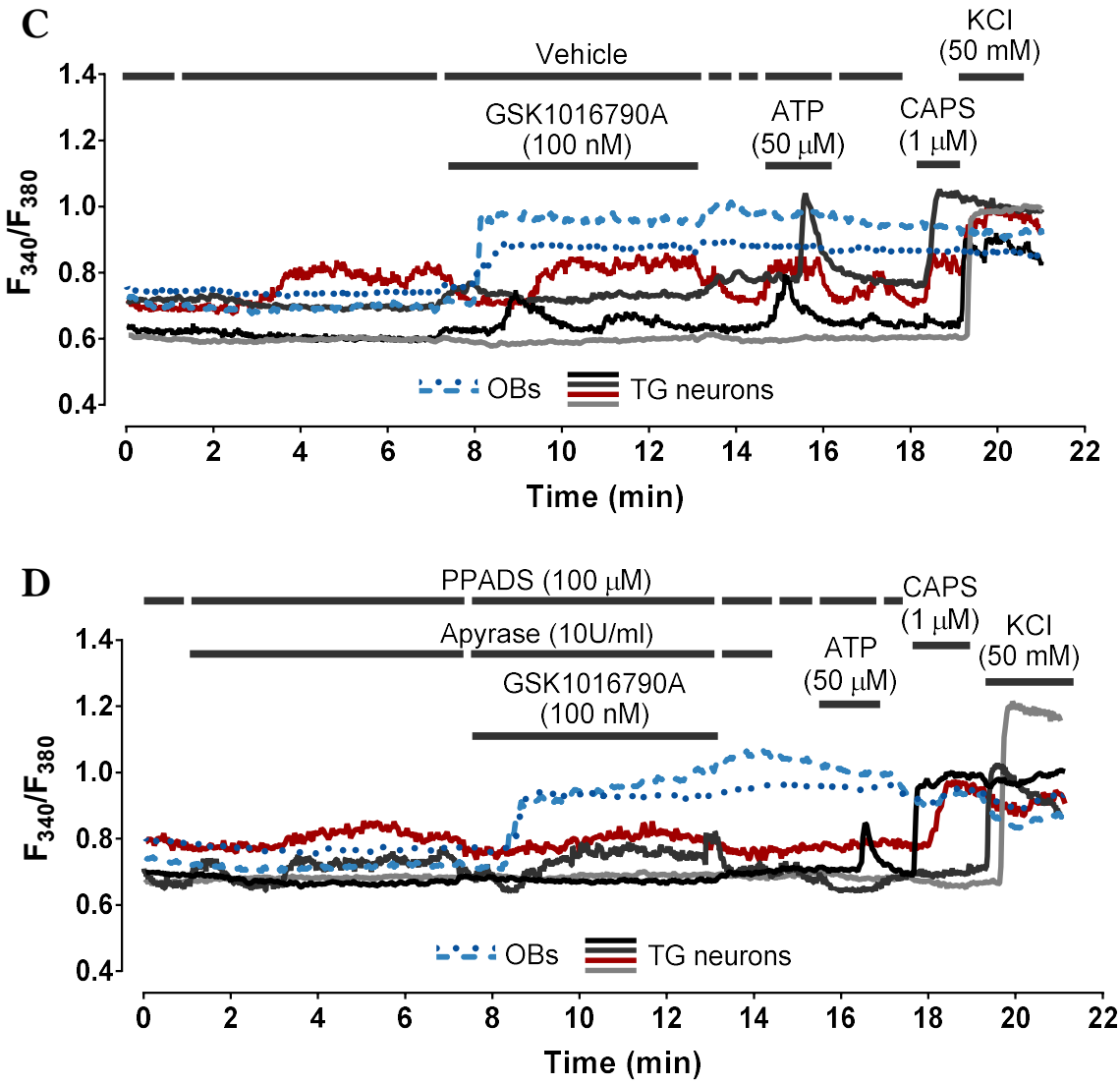

Figure 6.6 Calcium imaging of OB-TG neuron co-cultures in the presence of inhibitors of ATP signalling

Example pseudocolour images of TG neuron responses to the exposure of OB-TG neuron co-cultures to the TRPV4 agonist GSK1016790A (GSK101 (100 nM)), followed by ATP (50 μM), capsaicin (CAPS; 1 μM), and potassium chloride (KCl; 50 mM), in the presence of *A)* vehicle or *B)* P2 purinergic receptor inhibitor PPADS (100 μM) and apyrase enzyme (10U/ml), as indicated. The arrows in *A* and *B* indicate the same TG neurons as the corresponding colour-coded traces in *C* and *D*. The calcium image colour range represents Fura-2AM fluorescence ratio. Some TG neurons in both inhibitor and vehicle experimental runs displayed intracellular Ca^{2+} concentrations that were increased in response to both vehicle/inhibitor and GSK1016790A application.

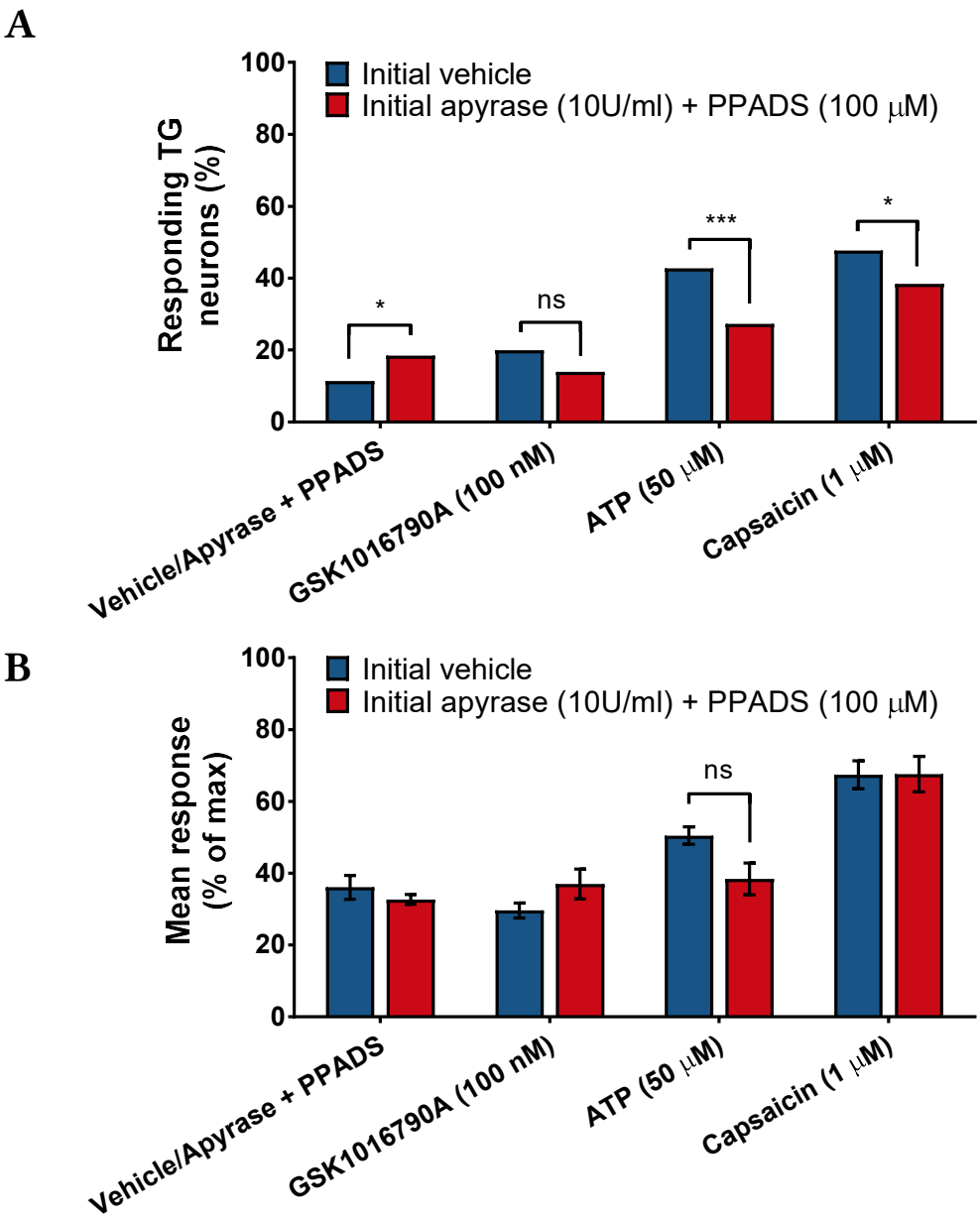

Figure 6.7 OB-driven modulation of TG neuron activity in OB-TG neuron co-cultures involves ATP signalling

A) Inhibition of ATP signalling by the purinergic P2 receptor antagonist PPADS and apyrase enzyme significantly reduced the proportion of TG neurons responding to ATP (50 μM) and the TRPV1 agonist capsaicin (1 μM), following the application of the TRPV4 agonist GSK1016790A (100 nM). However, inhibitors of ATP signalling themselves activated a proportion of TG neurons above respective vehicle levels, potentially masking any effect on TG neuron responses to the TRPV4 activation on OB cells. ns = not statistically significant, $p > 0.05$; $^{*}p < 0.05$; $^{***}p < 0.005$ *vs.* respective vehicle (Fisher's exact test). *B)* Inhibition of ATP signalling did not affect the amplitude of TG neuron responses. Data are mean response sizes expressed as a percentage of maximum response for that experimental run (either to 50 mM KCl or 1 μM capsaicin) ± SEM. ns = not statistically significant, $p > 0.05$ (two-way ANOVA). $n = 5$ (322 neurons (PPADS and apyrase runs) and 331 neurons (vehicle runs) from 5 mice).

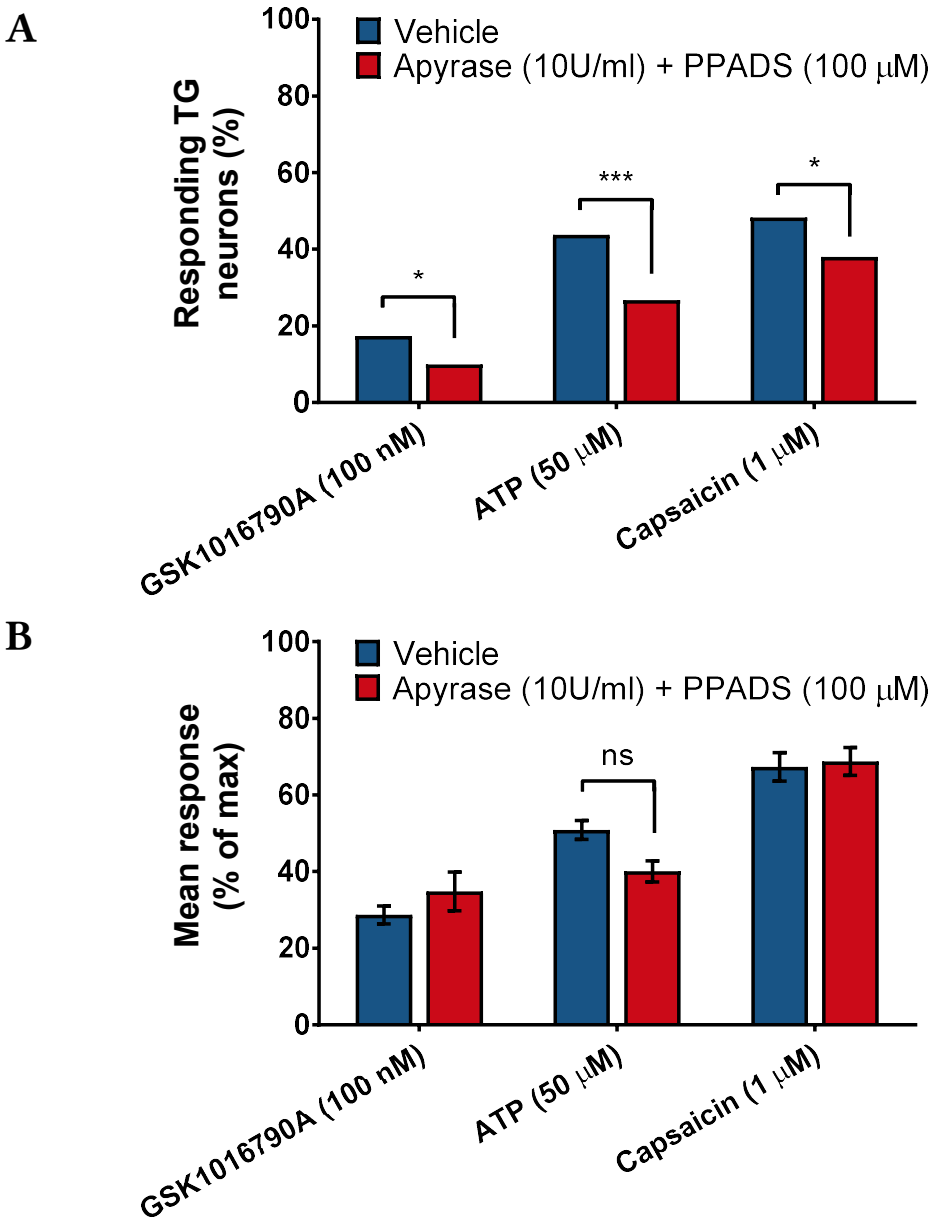

Figure 6.8 TRPV4 activation on OB cells causes ATP-dependent stimulation of TG neurons in OB-TG neuron co-cultures

A) When only those TG neurons that do not respond to the first vehicle/inhibitor application are included in the analysis, a significant reduction in the proportion of TG neurons sensitive to the activation of TRPV4 on OB cells could be detected following the treatment of OB-TG neuron co-cultures with the purinergic P2 receptor antagonist PPADS and apyrase enzyme. $^{*}p < 0.05$; $^{***}p < 0.005$ (Fisher's exact test). *B)* Analysis of TG neurons that did not respond to the initial vehicle/inhibitor application did not reveal any effect on the amplitude of TG neuron responses following the inhibition of ATP signalling. Data are mean response sizes expressed as a percentage of maximum response for that experimental run (either to 50 mM KCl or 1 μM capsaicin) ± SEM. ns = not statistically significant, $p > 0.05$ (two-way ANOVA). $n = 5$ (271 neurons (PPADS and apyrase runs) and 325 neurons (vehicle runs) from 5 mice).

6.4 Discussion

6.4.1 Odontoblast-dependent activation of TG neurons and methodological considerations for co-culture studies

The ability to modulate the activity of adjacent neurons in the teeth is essential for the proposed role of odontoblasts as sensory cells. In the present study, an OB cell-TG neuron co-culture was successfully established, and a calcium imaging-based method was optimised for the detection of an indirect, OB-dependent activation of TG neurons in OB-TG neuron co-cultures.

The initial observation that, despite the successful activation of TRPV4 channels on OB cells, co-cultured TG neurons displayed no increase in intracellular Ca^{2+} concentrations ($[Ca^{2+}]_i$) when calcium imaging experiments were performed in the standard extracellular solution (ECS), is consistent with the findings in Chapter 3. There, despite the detection of a TRPV4-dependent increase in $[Ca^{2+}]_i$ in OB cells that occurs in ECS, a significant increase in ATP release from OB cells, stimulated with the same selective TRPV4 agonist, occurred only in complete OB cell culture medium, but not in ECS. When co-culture calcium imaging experiments were repeated in OB medium, a significantly greater proportion of TG neurons displayed increased $[Ca^{2+}]_i$ in response to the TRPV4 activation on OB cells. This suggests that the amounts of mediators, such as ATP, released from stimulated OB cells are sufficient to activate adjacent TG neurons under those conditions. It might be speculated that different response profiles among the TG neurons in co-cultures correspond to their activation either by different mediators released from OB cells or via different receptors detecting the same mediator, such as ionotropic P2X and metabotropic P2Y receptors for ATP. A potential issue with the co-culture method used in this study, where TG neurons are added onto the layer of OB cells, is related to the imaging of TG neurons through OB cells, which might result in OB cell responses being mistaken as TG neuron responses. However, distinct response profiles to the TRPV4 agonist observed between the two types of cells in co-cultures suggest that increased Fura-2AM fluorescence ratio in TG neurons is not simply an artefact from fluorescence changes in stimulated underlying OB cells. In the future, OB cells could be co-cultured with

TG neurons in the compartmentalised microfluidic co-culture systems. This would not only allow the use of separate culture media optimised for that particular cell type and enable isolated treatment of only one type of cell at a time, but also represent a more biologically relevant situation, where neurites, rather than TG neuron cell bodies, are in close proximity with OB cells.

The fact that various cell-based *in vitro* assays are typically performed in solutions that are similar in composition to the ECS used in this study calls into question whether they sufficiently reflect the *in vivo* situation, particularly when studying intercellular interactions. On the other hand, it is also unclear how the presence of multiple additional factors in the serum-containing complete culture medium compares with the conditions present *in vivo*. The observation that TG neuron responses to ATP or the TRPV1 agonist capsaicin detected in co-culture calcium imaging experiments performed in OB medium were not different from the ones detected in either co-culture (this chapter) or monoculture (Chapter 5) experiments performed in ECS does not support the presence of any unintended sensitisation of TG neurons by the components of OB medium. At the same time, a slightly greater proportion of TG neurons responding to the DMSO vehicle was detected in co-culture calcium imaging experiments performed in OB medium, compared with the previous findings in ECS. Since direct comparisons were always made between vehicle and treatment experiments performed under the same conditions, this did not affect the identification of TG neuron responses arising specifically from the TRPV4 activation in OB cells.

However, in the subsequent experiments that involved the pre-treatment of OB-TG neuron co-cultures with the inhibitors of ATP signalling (PPADS and apyrase), these agents significantly increased $[Ca^{2+}]_i$ in TG neurons above the vehicle levels detected in OB medium, suggesting additional activation of TG neurons, either directly or via stimulation of OB cells in co-cultures. Alternatively, it can be speculated that these agents might have affected the Ca^{2+} binding affinity or dissociation constant properties of Fura-2AM. Analysis of only those TG neurons that did not display the initial increase in $[Ca^{2+}]_i$ caused by ATP signalling inhibitors or their respective vehicles revealed a statistically significant reduction in the proportion of TG neurons

sensitive to the stimulation of TRPV4 ion channels on co-cultured OB cells, supporting the involvement of ATP signalling in OB-dependent activation of TG neurons. This is consistent with the findings of Shibukawa and colleagues (2015), who detected ATP-dependent activation of TG neurons following mechanical stimulation of co-cultured odontoblasts.

While there is no obvious reason why exclusion of TG neurons that respond to the first application of ATP signalling inhibitors or their vehicles from the analysis would specifically affect the proportion of responders to the TRPV4 agonist, different strategies could be employed in the future experiments to help avoid this issue and provide more information about the involvement of ATP signalling in OB-dependent TG neuron activation. The use of selective P2 purinergic receptor inhibitors would help to further investigate the exact receptors involved in the proposed ATP-dependent activation of TG neurons that occurs following OB cell stimulation. So far, selective inhibition of each purinergic receptor $P2X_3$, $P2Y_1$, and $P2Y_{12}$ has been demonstrated to reduce, but not completely block, TG neuron activation in response to the mechanical stimulation of co-cultured odontoblasts (Shibukawa *et al.*, 2015). Moreover, to avoid any artefacts from pharmacological pre-treatments, supporting evidence could be provided by repeating co-culture calcium imaging experiments using TG neurons from mice lacking those P2 receptors that are identified as the most relevant using the pharmacological approach.

6.4.2 Odontoblast-dependent sensitisation of TG neuron activity via ATP signalling

In addition to the OB-dependent activation of TG neurons, co-culture experiments revealed an increased proportion of TG neurons sensitive to ATP and capsaicin, following the treatment of OB-TG neuron co-cultures with the TRPV4 agonist. Based on the evidence supporting the lack of TRPV4 ion channels on TG neurons discussed in Chapter 5, and the fact that the same responses are not observed in the co-culture calcium imaging experiments performed in ECS, it is unlikely that this sensitisation is induced directly by the TRPV4 agonist effects on TG neurons. In the future, OB

cells could be co-cultured with TRPV4-deficient TG neurons to clarify the mechanism of the observed sensitisation.

In theory, the increased percentage of TG neurons responding to the ATP treatment of OB-TG neuron co-cultures might represent an ATP-induced ATP release from OB cells, a phenomenon reported in other non-neuronal cells, such a astrocytes (Anderson *et al.*, 2004). However, the fact that a significant increase in the proportion of TG neurons responding to ATP only occurs after the treatment with the TRPV4 agonist in OB medium points to the OB-dependent sensitisation of purinergic P2 receptors. This might represent either an ATP-dependent sensitisation or the involvement of other mediators released from stimulated OB cells. While some contribution of the latter mechanism cannot be excluded at this stage, inhibition of ATP signalling in the subsequent co-culture calcium imaging experiments prevented the increase in ATP-sensitive TG neurons, demonstrating the involvement of ATP as the main mediator of such sensitisation.

Similarly, both ATP and other factors released from stimulated OB cells might contribute to the increase in the proportion of TG neurons responding to capsaicin, detected after the treatment of OB-TG neuron co-cultures with the TRPV4 agonist. However, again, inhibition of ATP signalling prevented this, pointing to the ATP-dependent sensitisation of TRPV1 ion channels as an underlying mechanism. Although such sensitisation of TG neurons has already been described in the literature (Saloman *et al.*, 2013), this is the first demonstration that stimulated odontoblasts can sensitise TRPV1 ion channels on adjacent TG neurons in co-cultures. While a statistically significant decrease in the amplitude of TG neuron responses to capsaicin was simultaneously observed following exposure of co-cultures to the TRPV4 agonist, this likely occurs due to a greater proportion of the same neurons having already responded to ATP during experimental runs (44.8% of GSK1016790A-treated TG neurons responded to both ATP and capsaicin, compared with 22.3% of vehicle-treated TG neurons).

Collectively, the findings described in this chapter suggest that ATP signalling is involved in the direct odontoblast-driven activation and/or sensitisation of purinergic receptors and TRPV1 channels in TG neurons. This interaction between

odontoblasts and TG neurons may play an important role in the initiation of dental pain *in vivo*.

Chapter 7

General discussion

The importance of studying the trigeminal nociceptive system, rather than relying on the findings from the spinal nociceptive system, is being increasingly recognised, as indicated by a steady rise in the number of relevant publications (Hargreaves, 2011). However, dentistry-related issues, including odontogenic pain, deal with the unique structures of the tooth and are, to some extent, overlooked from the basic science perspective. This might be related to the availability of non-pharmacological treatment strategies, such as dental treatments or tooth extractions, in the case of odontogenic pain associated with pulpal inflammation, or dentinal tubule occlusion, in the case of dentine hypersensitivity. This thesis aimed to expand the knowledge on the cellular and molecular mechanisms of odontogenic pain, with a focus on two types of cells, odontoblasts and neurons, and their interaction.

7.1 Summary of key findings

The key findings and contributions of the work described in this thesis are as follows (see Figure 7.1 for illustration):

- Differentiated mouse dental pulp 17IA4 cells display an odontoblast-like (OB) phenotype and provide a suitable cellular model for studying odontoblast function *in vitro (an extension of the previous characterisation of these cells).*

- OB cells express functional TRPV4 ion channels and mRNA for ASIC1, ASIC3, TRPM7, and TRPV1, but not TRPA1 or TRPC5 *(new findings from this particular cell line; extension of previous knowledge on odontoblasts and odontoblast-like cells in general; a new finding regarding TRPC5 expression in odontoblasts).*

- Pharmacological activation of TRPV4 stimulates ATP release from OB cells *(confirmation of previous observations in odontoblast-like cells from different species)*, with preliminary evidence suggesting simultaneous glutamate release *(a new finding).*

- Biologically relevant extracellular acidification stimulates ATP release from OB cells, without affecting their viability. TRPV4 is not involved in acid detection by OB cells *(both new findings).*

- Trigeminal ganglion (TG) neurons express functional ATP receptors, including $P2X_3$, $P2Y_1$, and $P2Y_2$. Glutamate activated a negligible proportion of TG neurons *(functional data provided extends previous knowledge).*

- A calcium imaging-based assay was optimised to detect the sensitisation of TRPA1 and TRPV1 ion channels on TG neurons *(a methodological contribution).* The assay was validated using prototypical inflammatory mediators IL-1β and TNFα. Short-term exposure to TNFα, but not to IL-1β, sensitised TRPA1 and TRPV1 on TG neurons.

- A mixed OB cell-TG neuron co-culture was successfully established *(a methodological contribution).*

- The amount of ATP released from OB cells in response to TRPV4 activation was sufficient to activate co-cultured TG neurons *(an extension of previous knowledge)* and sensitise their responses to subsequent purinergic receptor and TRPV1 activation *(a new finding).*

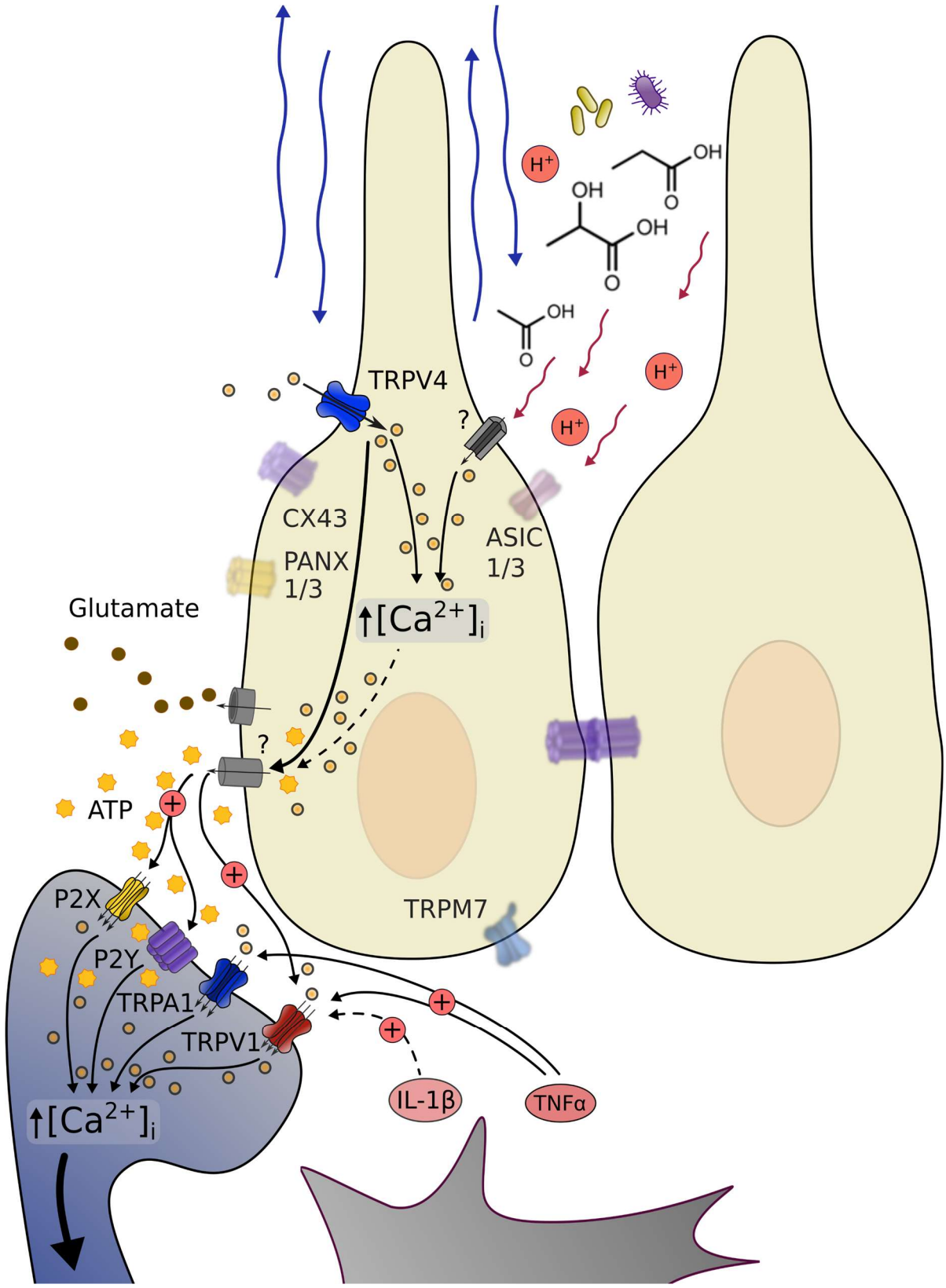

Figure 7.1 Illustration of the main findings and proposed mechanisms

Based on the presence of TRPV4 mRNA transcripts and calcium flux data, odontoblasts express functional TRPV4 ion channels. Dentinal fluid movement in response to stimulation of exposed dentine might activate TRPV4, resulting in an increase in odontoblast intracellular Ca^{2+} concentrations ($[Ca^{2+}]_i$) and ATP release via an unknown mechanism, likely not involving vesicular exocytosis or pannexin (e.g. Panx1 or Panx3) or connexin (e.g. Cx43) channels. Glutamate is also released in response to TRPV4 activation. Acids of bacterial or dietary origin act via an unknown mechanism that does not seem to involve TRPV4 or ASIC ion channels to induce an increase in $[Ca^{2+}]_i$ and ATP release from odontoblasts. Grey receptors/channels and question marks in the figure represent unknown mechanisms or proteins involved. Blurred, semi-transparent receptors/channels indicate that only the presence of mRNA, but not protein or its function, has been confirmed in this study.

ATP released from odontoblasts can act on purinergic P2X and P2Y receptors on adjacent sensory nerve terminals to modulate the neuronal activity, including the sensitisation of responses to TRPV1 ion channel activation and ATP, as determined in the present study using calcium imaging. Moreover, inflammatory mediators IL-1β and TNFα, produced by e.g. dendritic cells, can contribute to the sensitisation of TRPV1 (long-term, IL-1β) or both TRPV1 and TRPA1 (both short-term and long-term, TNFα).

7.2 Odontoblasts: highly specialised mineralising cells with a sensory role

Odontoblast cell layer is located at the dentine-pulp junction in the teeth (Pashley, 1996). This position closest to the dentine and the external environment provides a hint as to the potential roles of odontoblasts. Their secretory and mineralising functions are required for the production of dentine throughout the life of the tooth (Goldberg *et al.*, 2011). In the present study, multiple indicators of the secretory and mineralising abilities, both indirect (genetic markers) and direct (mineralisation *in vitro*), were used to confirm the successful differentiation of pre-odontoblastic precursor cells into the odontoblast-like cells. This was a useful strategy that enabled *in vitro* investigations into other odontoblast functions. A potential limitation of this strategy is the absence of direct comparisons with mature native human odontoblasts. However, a study by Pääkkönen and colleagues (2009) demonstrated a remarkable similarity between native human odontoblasts and cultured odontoblast-like cells, with only minor differences in the gene expression levels of some neuropeptides, such as galanin. Future work in the area could focus on the improvement of the newly developed methods for isolating mature human odontoblasts (Cuffaro *et al.*, 2016) to sufficiently preserve their integrity for functional studies. Alternatively, useful functional data could be provided by the

establishment of new methods for direct electrophysiological recordings of the odontoblasts in extracted teeth.

The main focus of this thesis was on the sensory role of odontoblasts, with potential relevance to dentine hypersensitivity. The presence of a functional polymodal sensory transducer channel TRPV4 on mouse odontoblast-like cells is consistent with other studies from both rodents and humans (listed in Chapter 3, section 3.1.2) and further supports the ability of odontoblasts to detect external (e.g. osmotic or mechanical) stimuli. In order to play a role in the transmission of tooth pain, odontoblasts must also have the ability to signal to adjacent dental afferent fibres. The finding that odontoblast-like cells release ATP and glutamate upon stimulation supports paracrine signalling as a means of odontoblast-dependent modulation of neuronal activity. This agrees with the finding of ATP release in human teeth in response to the stimulation of exposed dentine (Liu *et al.*, 2015). Future work could investigate the potential interaction between ATP and glutamate signalling on both odontoblast and neuronal function. Another finding from the present study was that ATP release resulting from the pharmacological stimulation of TRPV4 did not appear to employ some of the main mechanisms for ATP release, including pannexin channels, connexin hemichannels, $P2X_7$ receptors, and vesicular exocytosis (Praetorius & Leipziger, 2009). Although it would be interesting to determine the exact mechanism for ATP release in the future studies, the use of a physiological stimulus would provide more information on the odontoblast sensory role.

The present study is the first to demonstrate odontoblast sensitivity to biologically relevant acids, including increased intracellular free calcium concentrations and the release of ATP, further supporting the sensory function of these cells and the potential role of ATP as a mediator of paracrine signalling from odontoblasts. Moreover, the observed differences in the odontoblast-like cell responses to weak organic acids, compared with hydrochloric acid, applied at the same pH values, demonstrate the activity of biological acids distinct from the activity of just protons. This emphasises the importance of using the experimental conditions that match the ones present *in vivo* as closely as possible when conducting *in vitro* studies. In addition, since acid-evoked stimulation of odontoblasts was found to be independent

of TRPV4 activity, it suggests that TRPV4 is not the only functional transducer in odontoblasts. Although ASIC mRNA transcripts were detected in the odontoblast-like cells, preliminary findings do not support their involvement, at least in the pathways that stimulate ATP release. Therefore, the exact acid-sensing mechanism present in odontoblasts remains to be determined. This information might provide insights into the mechanisms of both dentine hypersensitivity to dietary acids and inflammatory odontogenic pain, where acids are produced by oral bacteria.

The position of odontoblasts as the first cells to encounter invading oral bacteria or bacterial toxins also point to their immune role. Although this was not the focus of the present study, the presence of TLR2 and TLR4 receptor mRNA transcripts in odontoblast-like cells supports the proposed role of odontoblasts in innate immunity (Yumoto *et al.*, 2018). Given that untreated caries affects as many as 2.4 billion people worldwide (Kassebaum *et al.*, 2015), the processes involved in maintaining dental pulp homeostasis in response to a bacterial challenge are important to study further, particularly in relation to the mechanisms of dental pain, given its impact on patients' lives (Joury *et al.*, 2018).

7.3 Intercellular odontoblast-neuron communication in odontogenic pain

One of the hypotheses tested in the present study was that odontogenic pain involves intercellular communication between odontoblasts and adjacent dental primary afferent neurons. In the co-culture experiments, activation of TRPV4 ion channels on odontoblast-like cells both activated adjacent trigeminal ganglion (TG) neurons, indicating initiation of neuronal firing, and sensitised their responses to ATP and the TRPV1 activation. Although further work is required to identify the mechanisms responsible for the odontoblast-dependent activation and sensitisation of adjacent neurons, these findings support TRPV4 ion channels as potential mechanosensors involved in the detection of fluid movement in the dentinal tubules by odontoblasts. In relation to the theories of dentine hypersensitivity discussed in the introduction, the findings from this thesis support the most recent theory proposed by Shibukawa and colleagues (2015) and called the "odontoblast hydrodynamic receptor theory".

This theory combines the components of both the hydrodynamic (external stimuli recognition via detection of fluid movement) and odontoblast-transducer (odontoblasts acting as sensory cells) theories. Alternatively, if the odontoblast-dependent increase in neuronal sensitivity to a mechanical stimulation could be demonstrated, our observation of the odontoblast-driven neuronal sensitisation could potentially also support the original hydrodynamic theory (Brannstrom *et al.*, 1967) of dentine hypersensitivity, suggesting that dentinal fluid movement can directly stimulate the nerve endings of sensitised TG neurons. A recent publication by Michot and co-workers (2018) provides new evidence that dental pulp sensitivity to cold does not depend on neuronal TRPA1 and TRPM8 ion channels. This either indicates the presence of an unknown cold-sensing mechanism on dental pulp afferents or contradicts the direct stimulation of the nerve endings suggested by the neural theory of dentine hypersensitivity, further supporting one of the indirect mechanisms mentioned above. However, further work is needed to determine the mechanisms underlying dentine hypersensitivity to different types of external stimuli.

The findings from the present study also highlight the role of ATP as an important mediator of odontoblast-TG neuron communication. This supports a less well-explored role of ATP as a sensory transmitter from non-neuronal cells, previously reported in other cells, such as keratinocytes and corneal epithelial cells (Oswald *et al.*, 2012; Moehring *et al.*, 2018). A similar role for glutamate in the odontoblast-TG neuron communication has previously been proposed in the literature (Nishiyama *et al.*, 2016). However, our findings from the co-culture and monoculture experiments, which involved the pharmacological activation of TRPV4 as a stimulus, do not support this role. On the other hand, it is possible that other types of stimuli that do not activate TRPV4 might induce glutamate signalling more extensively.

Overall, the findings from the present study demonstrate the utility of a co-culture strategy, rather than studying one cell type in isolation, particularly when the cells are known to be in close contact *in vivo* and share the same microenvironment, as in the case of odontoblasts and adjacent nerve fibres in the dentinal tubules. Although, ideally, these interactions would be studied *in vivo*, *in vitro* studies, such as the one

described in this thesis, enable precise manipulation of the conditions and allow detailed investigations into the specific cellular and molecular processes involved. As previously mentioned, a strategy of co-culturing the cells in the microfluidic co-culture systems could be utilised in the future to directly study the interactions between the neurites of TG neurons and odontoblasts. Moreover, patch clamp electrophysiological recordings could be used to supplement current calcium imaging data and provide more direct evidence for any odontoblast-dependent effects on the neuronal excitability. In fact, during the finalisation of this thesis, Sato and colleagues (2018) have published the findings supporting ATP-dependent action potential generation in TG neurons in response to mechanical stimulation of co-cultured odontoblasts. This is in direct agreement with our observations and strengthens the validity of the findings presented in this thesis.

An additional level of complexity arises from the potential involvement of bacteria, immune cells, and satellite glial cells in odontogenic pain. In the present study, the sensitisation of TG neurons by the pro-inflammatory mediators IL-1β and TNFα has been investigated. Dendritic cells are a potential source of IL-1β and TNFα in the teeth, as they have been demonstrated to release these mediators *in vitro* in response to the TLR2 receptor activation by a bacterial cell wall component lipoteichoic acid (Keller *et al.*, 2010). Moreover, odontoblasts themselves produce pro-inflammatory mediators, such as IL-6 and CXCL8 (Farges *et al.*, 2011). Both bacterial products and host-derived inflammatory mediators could be tested in the future, using the calcium imaging-based assay described in this thesis, to see if they can modulate the activity of TG neurons, with a potential contribution to increased sensitivity in pulpal pain. These sensitisation experiments focused on TRPA1 and TRPV1, which recently have been confirmed to be functionally interdependent in humans (Nielsen *et al.*, 2018). Multiple novel strategies have already been proposed for targeting both TRPA1 and TRPV1, with a potential therapeutic value in orofacial pain (Gualdani *et al.*, 2015; Meng *et al.*, 2016).

Although, at this stage, the findings from the present study do not directly offer any viable therapeutic strategies, this thesis contributed to the knowledge of the underlying cellular and molecular mechanisms of odontogenic pain.

References

About I (2014). Pulp Vascularization and Its Regulation by the Microenvironment. In The Dental Pulp: Biology, Pathology, and Regenerative Therapies. ed Goldberg M. Springer Berlin Heidelberg: Berlin, Heidelberg, pp 61-74. https://doi.org/10.1007/978-3-642-55160-4_5

About I, Laurent-Maquin D, Lendahl U, and Mitsiadis TA (2000). Nestin Expression in Embryonic and Adult Human Teeth under Normal and Pathological Conditions. *The American Journal of Pathology* **157**: 287-295.

About I, Proust JP, Raffo S, Mitsiadis TA, and Franquin JC (2002). In vivo and in vitro expression of connexin 43 in human teeth. *Connect Tissue Res* **43**: 232-237.

Absi EG, Addy M, and Adams D (1987). Dentine hypersensitivity. A study of the patency of dentinal tubules in sensitive and non-sensitive cervical dentine. *J Clin Periodontol* **14**: 280-284.

Adachi K, Shimizu K, Hu JW, Suzuki I, Sakagami H, Koshikawa N, Sessle BJ, Shinoda M, Miyamoto M, Honda K, and Iwata K (2010). Purinergic receptors are involved in tooth-pulp evoked nocifensive behavior and brainstem neuronal activity. *Molecular Pain* **6**: 59-59.

Addy M, Mostafa P, and Newcombe RG (1987). Dentine hypersensitivity: the distribution of recession, sensitivity and plaque. *J Dent* **15**: 242-248.

Ahlquist ML, Edwall LG, Franzen OG, and Haegerstam GA (1984). Perception of pulpal pain as a function of intradental nerve activity. *Pain* **19**: 353-366.

Ahuja D, Sáenz-Robles MT, and Pipas JM (2005). SV40 large T antigen targets multiple cellular pathways to elicit cellular transformation. *Oncogene* **24**: 7729.

Alavi AM, Dubyak GR, and Burnstock G (2001). Immunohistochemical evidence for ATP receptors in human dental pulp. *J Dent Res* **80**: 476-483.

Allard B, Couble ML, Magloire H, and Bleicher F (2000). Characterization and gene expression of high conductance calcium-activated potassium channels displaying mechanosensitivity in human odontoblasts. *J Biol Chem* **275**: 25556-25561.

Allard B, Magloire H, Couble ML, Maurin JC, and Bleicher F (2006). Voltage-gated sodium channels confer excitability to human odontoblasts: possible role in tooth pain transmission. *J Biol Chem* **281**: 29002-29010.

Alpizar YA, Boonen B, Sanchez A, Jung C, López-Requena A, Naert R, Steelant B, Luyts K, Plata C, De Vooght V, Vanoirbeek JAJ, Meseguer VM, Voets T, Alvarez JL, Hellings PW, Hoet PHM, Nemery B, Valverde MA, and Talavera K (2017). TRPV4 activation triggers protective responses to bacterial lipopolysaccharides in airway epithelial cells. *Nature Communications* **8**: 1059.

An S (2018). The emerging role of extracellular Ca(2+) in osteo/odontogenic differentiation and the involvement of intracellular Ca (2+) signaling: From osteoblastic cells to dental pulp cells and odontoblasts. *J Cell Physiol*.

Anderson CM, Bergher JP, and Swanson RA (2004). ATP-induced ATP release from astrocytes. *J Neurochem* **88**: 246-256.

Anderson DJ, and Matthews B (1967). Osmotic stimulation of human dentine and the distribution of dental pain thresholds. *Arch Oral Biol* **12**: 417-426.

Andersson DA, Chase HW, and Bevan S (2004). TRPM8 activation by menthol, icilin, and cold is differentially modulated by intracellular pH. *J Neurosci* **24**: 5364-5369.

Andrew D, and Matthews B (2000). Displacement of the contents of dentinal tubules and sensory transduction in intradental nerves of the cat. *J Physiol* **529**: 791-802.

Arana-Chavez VE, and Katchburian E (1997). Development of tight junctions between odontoblasts in early dentinogenesis as revealed by freeze-fracture. *Anat Rec* **248**: 332-338.

Artese L, Rubini C, Ferrero G, Fioroni M, Santinelli A, and Piattelli A (2002). Vascular endothelial growth factor (VEGF) expression in healthy and inflamed human dental pulps. *J Endod* **28**: 20-23.

Arvidsson J, and Gobel S (1981). An HRP study of the central projections of primary trigeminal neurons which innervate tooth pulps in the cat. *Brain Res* **210**: 1-16.

Awawdeh L, Hemaidat K, and Al-Omari W (2017). Higher Maximal Occlusal Bite Force in Endodontically Treated Teeth Versus Vital Contralateral Counterparts. *J Endod* **43**: 871-875.

Awawdeh L, Lundy FT, Shaw C, Lamey PJ, Linden GJ, and Kennedy JG (2002). Quantitative analysis of substance P, neurokinin A and calcitonin gene-related peptide in pulp tissue from painful and healthy human teeth. *Int Endod J* **35**: 30-36.

Bae JM, Clarke JC, Rashid H, Adhami MD, McCullough K, Scott JS, Chen H, Sinha KM, de Crombrugghe B, and Javed A (2018). Specificity Protein 7 Is Required for Proliferation and Differentiation of Ameloblasts and Odontoblasts. *J Bone Miner Res* **33**: 1126-1140.

Bakri MM, Yahya F, Munawar KMM, Kitagawa J, and Hossain MZ (2018). Transient receptor potential vanilloid 4 (TRPV4) expression on the nerve fibers of human dental pulp is upregulated under inflammatory condition. *Arch Oral Biol* **89**: 94-98.

Balic A, and Mina M (2011). Identification of secretory odontoblasts using DMP1-GFP transgenic mice. *Bone* **48**: 927-937.

Bandell M, Story GM, Hwang SW, Viswanath V, Eid SR, Petrus MJ, Earley TJ, and Patapoutian A (2004). Noxious Cold Ion Channel TRPA1 Is Activated by Pungent Compounds and Bradykinin. *Neuron* **41**: 849-857.

Bang S, Kim KY, Yoo S, Lee SH, and Hwang SW (2007). Transient receptor potential V2 expressed in sensory neurons is activated by probenecid. *Neurosci Lett* **425**: 120-125.

Barclay CW, Spence D, and Laird WR (2005). Intra-oral temperatures during function. *J Oral Rehabil* **32**: 886-894.

Basbaum AI, Bautista DM, Scherrer G, and Julius D (2009). Cellular and Molecular Mechanisms of Pain. *Cell* **139**: 267-284.

Bassler EL, Ngo-Anh TJ, Geisler HS, Ruppersberg JP, and Grunder S (2001). Molecular and functional characterization of acid-sensing ion channel (ASIC) 1b. *J Biol Chem* **276**: 33782-33787.

Bautista DM, Movahed P, Hinman A, Axelsson HE, Sterner O, Högestätt ED, Julius D, Jordt S-E, and Zygmunt PM (2005). Pungent products from garlic activate the sensory ion channel TRPA1. *Proc Natl Acad Sci U S A* **102**: 12248-12252.

Bautista DM, Siemens J, Glazer JM, Tsuruda PR, Basbaum AI, Stucky CL, Jordt SE, and Julius D (2007). The menthol receptor TRPM8 is the principal detector of environmental cold. *Nature* **448**: 204-208.

Behrendt HJ, Germann T, Gillen C, Hatt H, and Jostock R (2004). Characterization of the mouse cold-menthol receptor TRPM8 and vanilloid receptor type-1 VR1 using a fluorometric imaging plate reader (FLIPR) assay. *Br J Pharmacol* **141**: 737-745.

Bekes K, and Hirsch C (2013). What is known about the influence of dentine hypersensitivity on oral health-related quality of life? *Clin Oral Investig* **17 Suppl 1**: S45-51.

Bereiter DA, Hirata H, and Hu JW (2000). Trigeminal subnucleus caudalis: beyond homologies with the spinal dorsal horn. *Pain* **88**: 221-224.

Bergenholtz G (1977). Effect of bacterial products on inflammatory reactions in the dental pulp. *Scand J Dent Res* **85**: 122-129.

Bhave G, and Gereau RWt (2004). Posttranslational mechanisms of peripheral sensitization. *J Neurobiol* **61**: 88-106.

Binshtok AM, Wang H, Zimmermann K, Amaya F, Vardeh D, Shi L, Brenner GJ, Ji R-R, Bean BP, Woolf CJ, and Samad TA (2008). Nociceptors Are Interleukin-1β Sensors. *J Neurosci* **28**: 14062-14073.

Blausen B (2014). Medical gallery of Blausen Medical 2014: WikiJournal of Medicine 1 (2).

Bloom B, Simile CM, Adams PF, and Cohen RA (2012). Oral health status and access to oral health care for U.S. adults aged 18-64: National Health Interview Survey, 2008. *Vital Health Stat 10*: 1-22.

Boissonade FM, and Matthews B (1993). Responses of trigeminal brain stem neurons and the digastric muscle to tooth-pulp stimulation in awake cats. *J Neurophysiol* **69**: 174-186.

Botero TM, Shelburne CE, Holland GR, Hanks CT, and Nör JE (2006). TLR4 Mediates LPS-Induced VEGF Expression in Odontoblasts. *J Endod* **32**: 951-955.

Bowles WR, Withrow JC, Lepinski AM, and Hargreaves KM (2003). Tissue Levels of Immunoreactive Substance P are Increased in Patients with Irreversible Pulpitis. *J Endod* **29**: 265-267.

Brandao-Burch A, Key ML, Patel JJ, Arnett TR, and Orriss IR (2012). The P2X7 Receptor is an Important Regulator of Extracellular ATP Levels. *Front Endocrinol (Lausanne)* **3**: 41.

Brannstrom M, Linden LA, and Astrom A (1967). The hydrodynamics of the dental tubule and of pulp fluid. A discussion of its significance in relation to dentinal sensitivity. *Caries Res* **1**: 310-317.

Brown AC, Beeler WJ, Kloka AC, and Fields RW (1985). Spatial summation of pre-pain and pain in human teeth. *Pain* **21**: 1-16.

Bruzzone R, Barbe MT, Jakob NJ, and Monyer H (2005). Pharmacological properties of homomeric and heteromeric pannexin hemichannels expressed in Xenopus oocytes. *J Neurochem* **92**: 1033-1043.

Bunse S, Schmidt M, Hoffmann S, Engelhardt K, Zoidl G, and Dermietzel R (2011). Single cysteines in the extracellular and transmembrane regions modulate pannexin 1 channel function. *J Membr Biol* **244**: 21-33.

Burns LE, Ramsey AA, Emrick JJ, Janal MN, and Gibbs JL (2016). Variability in Capsaicin-Stimulated CGRP Release from Human Dental Pulp. *J Endod* **42**: 542-546.

Byers MR (1985). Terminal arborization of individual sensory axons in dentin and pulp of rat molars. *Brain Res* **345**: 181-185.

Byers MR, and Dong WK (1983). Autoradiographic location of sensory nerve endings in dentin of monkey teeth. *Anat Rec* **205**: 441-454.

Byers MR, and Narhi MV (1999). Dental injury models: experimental tools for understanding neuroinflammatory interactions and polymodal nociceptor functions. *Crit Rev Oral Biol Med* **10**: 4-39.

Byers MR, Narhi MV, and Dong WK (1987). Sensory innervation of pulp and dentin in adult dog teeth as demonstrated by autoradiography. *Anat Rec* **218**: 207-215.

Byers MR, Närhi MVO, and Mecifi KB (1988). Acute and chronic reactions of dental sensory nerve fibers to cavities and desiccation in rat molars. *Anat Rec* **221**: 872-883.

Byers MR, Neuhaus SJ, and Gehrig JD (1982). Dental sensory receptor structure in human teeth. *Pain* **13**: 221-235.

Byers MR, Suzuki H, and Maeda T (2003). Dental neuroplasticity, neuro-pulpal interactions, and nerve regeneration. *Microsc Res Tech* **60**: 503-515.

Byers MR, and Taylor PE (1993). Effect of sensory denervation on the response of rat molar pulp to exposure injury. *J Dent Res* **72**: 613-618.

Byers MR, and Westenbroek RE (2011). Odontoblasts in developing, mature and ageing rat teeth have multiple phenotypes that variably express all nine voltage-gated sodium channels. *Arch Oral Biol* **56**: 1199-1220.

Byers MR, Wheeler EF, and Bothwell M (1992). Altered expression of NGF and P75 NGF-receptor by fibroblasts of injured teeth precedes sensory nerve sprouting. *Growth Factors* **6**: 41-52.

Cadden SW, Lisney SJ, and Matthews B (1983). Thresholds to electrical stimulation of nerves in cat canine tooth-pulp with A beta-, A delta- and C-fibre conduction velocities. *Brain Res* **261**: 31-41.

Cadden SW, Mason AG, and Van Der Glas HW (2013). Selective stimulation of human tooth-pulp with a new stable method: responses and validation. *Muscle Nerve* **48**: 256-264.

Carda C, and Peydro A (2006). Ultrastructural patterns of human dentinal tubules, odontoblasts processes and nerve fibres. *Tissue Cell* **38**: 141-150.

Caterina MJ, Schumacher MA, Tominaga M, Rosen TA, Levine JD, and Julius D (1997). The capsaicin receptor: a heat-activated ion channel in the pain pathway. *Nature* **389**: 816-824.

Caviedes-Bucheli J, Gutierrez-Guerra JE, Salazar F, Pichardo D, Moreno GC, and Munoz HR (2007). Substance P receptor expression in healthy and inflamed human pulp tissue. *Int Endod J* **40**: 106-111.

Caviedes-Bucheli J, Lombana N, Azuero-Holguin MM, and Munoz HR (2006). Quantification of neuropeptides (calcitonin gene-related peptide, substance P, neurokinin A, neuropeptide Y and vasoactive intestinal polypeptide) expressed in healthy and inflamed human dental pulp. *Int Endod J* **39**: 394-400.

Caviedes-Bucheli J, Muñoz HR, Azuero-Holguín MM, and Ulate E (2008). Neuropeptides in Dental Pulp: The Silent Protagonists. *J Endod* **34**: 773-788.

Chai Y, Jiang X, Ito Y, Bringas P, Jr., Han J, Rowitch DH, Soriano P, McMahon AP, and Sucov HM (2000). Fate of the mammalian cranial neural crest during tooth and mandibular morphogenesis. *Development* **127**: 1671-1679.

Charoenlarp P, Wanachantararak S, Vongsavan N, and Matthews B (2007). Pain and the rate of dentinal fluid flow produced by hydrostatic pressure stimulation of exposed dentine in man. *Arch Oral Biol* **52**: 625-631.

Chaudhary P, Martenson ME, and Baumann TK (2001). Vanilloid receptor expression and capsaicin excitation of rat dental primary afferent neurons. *J Dent Res* **80**: 1518-1523.

Chen E, and Abbott PV (2009). Dental Pulp Testing: A Review %J International Journal of Dentistry. **2009**.

Chen X, Molliver DC, and Gebhart GF (2010). The P2Y2 receptor sensitizes mouse bladder sensory neurons and facilitates purinergic currents. *J Neurosci* **30**: 2365-2372.

Chen Y, Williams SH, McNulty AL, Hong JH, Lee SH, Rothfusz NE, Parekh PK, Moore C, Gereau RWt, Taylor AB, Wang F, Guilak F, and Liedtke W (2013). Temporomandibular joint pain: a critical role for Trpv4 in the trigeminal ganglion. *Pain* **154**: 1295-1304.

Chiang CY, Dostrovsky JO, Iwata K, and Sessle BJ (2011). Role of glia in orofacial pain. *Neuroscientist* **17**: 303-320.

Chiang CY, Park SJ, Kwan CL, Hu JW, and Sessle BJ (1998). NMDA receptor mechanisms contribute to neuroplasticity induced in caudalis nociceptive neurons by tooth pulp stimulation. *J Neurophysiol* **80**: 2621-2631.

Chichorro JG, Porreca F, and Sessle B (2017). Mechanisms of craniofacial pain. *Cephalalgia* **37**: 613-626.

Cho YS, Ryu CH, Won JH, Vang H, Oh SB, Ro JY, and Bae YC (2016). Rat odontoblasts may use glutamate to signal dentin injury. *Neuroscience* **335**: 54-63.

Choi SJ, Song IS, Feng JQ, Gao T, Haruyama N, Gautam P, Robey PG, and Hart TC (2010). Mutant DLX 3 disrupts odontoblast polarization and dentin formation. *Dev Biol* **344**: 682-692.

Chung G, Jung SJ, and Oh SB (2013). Cellular and molecular mechanisms of dental nociception. *J Dent Res* **92**: 948-955.

Chung MK, Jue SS, and Dong X (2012). Projection of Non-peptidergic Afferents to Mouse Tooth Pulp. *J Dent Res* **91**: 777-782.

Chung MK, Lee J, Duraes G, and Ro JY (2011). Lipopolysaccharide-induced Pulpitis Up-regulates TRPV1 in Trigeminal Ganglia. *J Dent Res* **90**: 1103-1107.

Coffey CT, Ingram MJ, and Bjorndal AM (1970). Analysis of human dentinal fluid. *Oral Surgery, Oral Medicine, Oral Pathology* **30**: 835-837.

Contreras JE, Sáez JC, Bukauskas FF, and Bennett MVL (2003). Gating and regulation of connexin 43 (Cx43) hemichannels. *Proceedings of the National Academy of Sciences* **100**: 11388.

Cook SP, Vulchanova L, Hargreaves KM, Elde R, and McCleskey EW (1997). Distinct ATP receptors on pain-sensing and stretch-sensing neurons. *Nature* **387**: 505-508.

Correll CC, Phelps PT, Anthes JC, Umland S, and Greenfeder S (2004). Cloning and pharmacological characterization of mouse TRPV1. *Neurosci Lett* **370**: 55-60.

Couble ML, Farges JC, Bleicher F, Perrat-Mabillon B, Boudeulle M, and Magloire H (2000). Odontoblast differentiation of human dental pulp cells in explant cultures. *Calcif Tissue Int* **66**: 129-138.

Cowan RW, Seidlitz EP, and Singh G (2012). Glutamate Signaling in Healthy and Diseased Bone. *Front Endocrinol (Lausanne)* **3**: 89.

Cox CF, Suzuki K, Yamaguchi H, Ruby JD, Suzuki S, Akimoto N, Maeda N, and Momoi Y (2017). Sensory mechanisms in dentine: A literature review of light microscopy (LM), transmission microscopy (TEM), scanning microscopy (SEM) & electro physiological (EP) tooth sensitivity: Is the ciliary organelle on the odontoblast the elusive primary nociceptor? *Dent Oral Craniofac Res* **4**.

Cuffaro HM, Paakkonen V, and Tjaderhane L (2016). Enzymatic isolation of viable human odontoblasts. *Int Endod J* **49**: 454-461.

D'Souza RN, Aberg T, Gaikwad J, Cavender A, Owen M, Karsenty G, and Thesleff I (1999). Cbfa1 is required for epithelial-mesenchymal interactions regulating tooth development in mice. *Development* **126**: 2911-2920.

D'Souza RN, Cavender A, Sunavala G, Alvarez J, Ohshima T, Kulkarni AB, and MacDougall M (1997). Gene expression patterns of murine dentin matrix protein 1 (Dmp1) and dentin sialophosphoprotein (DSPP) suggest distinct developmental functions in vivo. *J Bone Miner Res* **12**: 2040-2049.

Dababneh RH, Khouri AT, and Addy M (1999). Dentine hypersensitivity - an enigma? A review of terminology, mechanisms, aetiology and management. *Br Dent J* **187**: 606-611; discussion 603.

de la Roche J, Eberhardt MJ, Klinger AB, Stanslowsky N, Wegner F, Koppert W, Reeh PW, Lampert A, Fischer MJ, and Leffler A (2013). The molecular basis for species-specific activation of human TRPA1 protein by protons involves poorly conserved residues within transmembrane domains 5 and 6. *J Biol Chem* **288**: 20280-20292.

de la Roche J, Walther I, Leonow W, Hage A, Eberhardt M, Fischer M, Reeh PW, Sauer S, and Leffler A (2016). Lactate is a potent inhibitor of the capsaicin receptor TRPV1. *Scientific Reports* **6**: 36740.

Diaz R, Mayorga LS, Weidman PJ, Rothman JE, and Stahl PD (1989). Vesicle fusion following receptor-mediated endocytosis requires a protein active in Golgi transport. *Nature* **339**: 398.

Diogenes A, Ferraz CC, Akopian AN, Henry MA, and Hargreaves KM (2011). LPS sensitizes TRPV1 via activation of TLR4 in trigeminal sensory neurons. *J Dent Res* **90**: 759-764.

Dionne RA, Max MB, Gordon SM, Parada S, Sang C, Gracely RH, Sethna NF, and MacLean DB (1998). The substance P receptor antagonist CP-99,994 reduces acute postoperative pain. *Clin Pharmacol Ther* **64**: 562-568.

Djouhri L, and Lawson SN (2004). Aβ-fiber nociceptive primary afferent neurons: a review of incidence and properties in relation to other afferent A-fiber neurons in mammals. *Brain Res Rev* **46**: 131-145.

Docherty RJ, Yeats JC, and Piper AS (1997). Capsazepine block of voltage-activated calcium channels in adult rat dorsal root ganglion neurones in culture. *Br J Pharmacol* **121**: 1461-1467.

Dong WK, Chudler EH, and Martin RF (1985). Physiological properties of intradental mechanoreceptors. *Brain Res* **334**: 389-395.

Dong WK, Shiwaku T, Kawakami Y, and Chudler EH (1993). Static and dynamic responses of periodontal ligament mechanoreceptors and intradental mechanoreceptors. *J Neurophysiol* **69**: 1567-1582.

Durand SH, Flacher V, Romeas A, Carrouel F, Colomb E, Vincent C, Magloire H, Couble ML, Bleicher F, Staquet MJ, Lebecque S, and Farges JC (2006). Lipoteichoic acid increases TLR and functional chemokine expression while reducing dentin formation in in vitro differentiated human odontoblasts. *J Immunol* **176**: 2880-2887.

Edwall L, and Olgart L (1977). A new technique for recording of intradental sensory nerve activity in man. *Pain* **3**: 121-125.

Egbuniwe O, Grover S, Duggal AK, Mavroudis A, Yazdi M, Renton T, Di Silvio L, and Grant AD (2014). TRPA1 and TRPV4 activation in human odontoblasts stimulates ATP release. *J Dent Res* **93**: 911-917.

El-Tayeb A, Qi A, and Muller CE (2006). Synthesis and structure-activity relationships of uracil nucleotide derivatives and analogues as agonists at human P2Y2, P2Y4, and P2Y6 receptors. *J Med Chem* **49**: 7076-7087.

El Karim I, McCrudden MT, Linden GJ, Abdullah H, Curtis TM, McGahon M, About I, Irwin C, and Lundy FT (2015). TNF-alpha-induced p38MAPK activation regulates TRPA1 and TRPV4 activity in odontoblast-like cells. *Am J Pathol* **185**: 2994-3002.

El Karim IA, Linden GJ, Curtis TM, About I, McGahon MK, Irwin CR, and Lundy FT (2011). Human odontoblasts express functional thermo-sensitive TRP channels: implications for dentin sensitivity. *Pain* **152**: 2211-2223.

Ellis A, and Bennett DLH (2013). Neuroinflammation and the generation of neuropathic pain. *British Journal of Anaesthesia* **111**: 26-37.

Erb L, and Weisman GA (2012). Coupling of P2Y receptors to G proteins and other signaling pathways. *Wiley interdisciplinary reviews Membrane transport and signaling* **1**: 789-803.

Eskandari S, Zampighi GA, Leung DW, Wright EM, and Loo DD (2002). Inhibition of gap junction hemichannels by chloride channel blockers. *J Membr Biol* **185**: 93-102.

Eun SY, Jung SJ, Park YK, Kwak J, Kim SJ, and Kim J (2001). Effects of capsaicin on Ca(2+) release from the intracellular Ca(2+) stores in the dorsal root ganglion cells of adult rats. *Biochem Biophys Res Commun* **285**: 1114-1120.

Farahani RM, Simonian M, and Hunter N (2011). Blueprint of an ancestral neurosensory organ revealed in glial networks in human dental pulp. *J Comp Neurol* **519**: 3306-3326.

Farges J-C, Bellanger A, Ducret M, Aubert-Foucher E, Richard B, Alliot-Licht B, Bleicher F, and Carrouel F (2015). Human odontoblast-like cells produce nitric oxide with antibacterial activity upon TLR2 activation. *Frontiers in Physiology* **6**: 185.

Farges JC, Carrouel F, Keller JF, Baudouin C, Msika P, Bleicher F, and Staquet MJ (2011). Cytokine production by human odontoblast-like cells upon Toll-like receptor-2 engagement. *Immunobiology* **216**: 513-517.

Fearnhead RW (1957). Histological evidence for the innervation of human dentine. *Journal of Anatomy* **91**: 267-277.

Featherstone JD, and Lussi A (2006). Understanding the chemistry of dental erosion. *Monogr Oral Sci* **20**: 66-76.

Fehrenbacher JC, Sun XX, Locke EE, Henry MA, and Hargreaves KM (2009). Capsaicin-evoked iCGRP release from human dental pulp: a model system for the study of peripheral neuropeptide secretion in normal healthy tissue. *Pain* **144**: 253-261.

Fen JQ, Zhang J, Dallas SL, Lu Y, Chen S, Tan X, Owen M, Harris SE, and MacDougall M (2002). Dentin matrix protein 1, a target molecule for Cbfa1 in bone, is a unique bone marker gene. *J Bone Miner Res* **17**: 1822-1831.

Feng JQ, Huang H, Lu Y, Ye L, Xie Y, Tsutsui TW, Kunieda T, Castranio T, Scott G, Bonewald LB, and Mishina Y (2003). The Dentin matrix protein 1 (Dmp1) is specifically expressed in mineralized, but not soft, tissues during development. *J Dent Res* **82**: 776-780.

Ferraz CCR, Diógenes A, Henry MA, and Hargreaves KM (2011). LPS from Porphyromonas gingivalis Sensitizes Capsaicin-Sensitive Nociceptors. *J Endod* **37**: 45-48.

Forssell-Ahlberg K, Brannstrom M, and Edwall L (1975). The diameter and number of dentinal tubules in rat, cat, dog and monkey. A comparative scanning electron microscopic study. *Acta Odontol Scand* **33**: 243-250.

Foster BL, Nagatomo KJ, Tso HW, Tran AB, Nociti FH, Narisawa S, Yadav MC, McKee MD, Millán JL, and Somerman MJ (2013). Tooth root dentin mineralization defects in a mouse model of hypophosphatasia. *J Bone Miner Res* **28**: 271-282.

Frank RM (1968). Attachment sites between the odontoblast process and the intradentinal nerve fibre. *Arch Oral Biol* **13**: 833-IN839.

Fried K, Aldskogius H, and Hildebrand C (1988). Proportion of unmyelinated axons in rat molar and incisor tooth pulps following neonatal capsaicin treatment and/or sympathectomy. *Brain Res* **463**: 118-123.

Fried K, Arvidsson J, Robertson B, Brodin E, and Theodorsson E (1989). Combined retrograde tracing and enzyme/immunohistochemistry of trigeminal ganglion cell bodies innervating tooth pulps in the rat. *Neuroscience* **33**: 101-109.

Fried K, and Gibbs JL (2014). Dental Pulp Innervation. In The Dental Pulp: Biology, Pathology, and Regenerative Therapies. ed Goldberg M. Springer Berlin

Heidelberg: Berlin, Heidelberg, pp 75-95. https://doi.org/10.1007/978-3-642-55160-4_6

Fried K, Risling M, Edwall L, and Olgart L (1992). Immuno-electron-microscopic localization of laminin and collagen type IV in normal and denervated tooth pulp of the cat. *Cell Tissue Res* **270**: 157-164.

Fried K, Sessle BJ, and Devor M (2011). The paradox of pain from tooth pulp: low-threshold "algoneurons"? *Pain* **152**: 2685-2689.

Furia TE (1972). Sequestrants in Foods. In CRC Handbook of Food Additives. ed Furia T.E. CRC Press: New York, London.

Galicia JC, Henson BR, Parker JS, and Khan AA (2016). Gene expression profile of pulpitis. *Genes and immunity* **17**: 239-243.

Gans C, and Northcutt RG (1983). Neural crest and the origin of vertebrates: a new head. *Science* **220**: 268-273.

Gao XJ, Fan Y, Kent RL, Van Houte J, and Margolis HC (2001). Association of Caries Activity with the Composition of Dental Plaque Fluid. *J Dent Res* **80**: 1834-1839.

Gavva NR, Treanor JJ, Garami A, Fang L, Surapaneni S, Akrami A, Alvarez F, Bak A, Darling M, Gore A, Jang GR, Kesslak JP, Ni L, Norman MH, Palluconi G, Rose MJ, Salfi M, Tan E, Romanovsky AA, Banfield C, and Davar G (2008). Pharmacological blockade of the vanilloid receptor TRPV1 elicits marked hyperthermia in humans. *Pain* **136**: 202-210.

Geddes DA (1975). Acids produced by human dental plaque metabolism in situ. *Caries Res* **9**: 98-109.

Gees M, Alpizar YA, Boonen B, Sanchez A, Everaerts W, Segal A, Xue F, Janssens A, Owsianik G, Nilius B, Voets T, and Talavera K (2013). Mechanisms of transient receptor potential vanilloid 1 activation and sensitization by allyl isothiocyanate. *Mol Pharmacol* **84**: 325-334.

Geraldeli S, Li Y, Hogan MMB, Tjaderhane LS, Pashley DH, Morgan TA, Zimmerman MB, and Brogden KA (2012). Inflammatory mediators in fluid extracted from the coronal occlusal dentin of trimmed teeth. *Arch Oral Biol* **57**: 264-270.

Gerevich Z, Zadori Z, Müller C, Wirkner K, Schröder W, Rubini P, and Illes P (2007). Metabotropic P2Y receptors inhibit P2X(3) receptor-channels via G protein-dependent facilitation of their desensitization. *Br J Pharmacol* **151**: 226-236.

Ghatak S, and Sikdar SK (2016). Lactate modulates the intracellular pH sensitivity of human TREK1 channels. *Pflügers Archiv - European Journal of Physiology* **468**: 825-836.

Gibbs JL, Melnyk JL, and Basbaum AI (2011). Differential TRPV1 and TRPV2 Channel Expression in Dental Pulp. *J Dent Res* **90**: 765-770.

Goers L, Freemont P, and Polizzi KM (2014). Co-culture systems and technologies: taking synthetic biology to the next level. *Journal of the Royal Society Interface* **11**: 20140065.

Goldberg M (2014). Pulp Anatomy and Characterization of Pulp Cells. In The Dental Pulp: Biology, Pathology, and Regenerative Therapies. ed Goldberg M. Springer Berlin Heidelberg: Berlin, Heidelberg, pp 13-33. https://doi.org/10.1007/978-3-642-55160-4_2

Goldberg M, Kulkarni AB, Young M, and Boskey A (2011). Dentin: Structure, Composition and Mineralization: The role of dentin ECM in dentin formation and mineralization. *Frontiers in Bioscience (Elite Edition)* **3**: 711-735.

Goldberg M, and Smith AJ (2004). Cells and extracellular matrices of dentin and pulp: a biological basis for repair and tissue engineering. *Crit Rev Oral Biol Med* **15**: 13-27.

Goodis HE, Bowles WR, and Hargreaves KM (2000). Prostaglandin E2 enhances bradykinin-evoked iCGRP release in bovine dental pulp. *J Dent Res* **79**: 1604-1607.

Grigoriou M, Tucker AS, Sharpe PT, and Pachnis V (1998). Expression and regulation of Lhx6 and Lhx7, a novel subfamily of LIM homeodomain encoding genes, suggests a role in mammalian head development. *Development* **125**: 2063-2074.

Gronthos S, Mankani M, Brahim J, Robey PG, and Shi S (2000). Postnatal human dental pulp stem cells (DPSCs) in vitro and in vivo. *Proc Natl Acad Sci U S A* **97**: 13625-13630.

Gualdani R, Ceruti S, Magni G, Merli D, Di Cesare Mannelli L, Francesconi O, Richichi B, la Marca G, Ghelardini C, Moncelli MR, and Nativi C (2015). Lipoic-Based TRPA1/TRPV1 Antagonist to Treat Orofacial Pain. *ACS Chemical Neuroscience* **6**: 380-385.

Guler AD, Lee H, Iida T, Shimizu I, Tominaga M, and Caterina M (2002). Heat-evoked activation of the ion channel, TRPV4. *J Neurosci* **22**: 6408-6414.

Gunji T (1982). Morphological research on the sensitivity of dentin. *Arch Histol Jpn* **45**: 45-67.

Guo L, Berry JE, Somerman MJ, and Davidson RM (2000). A novel method to isolate odontoblasts from rat incisor. *Calcif Tissue Int* **66**: 212-216.

Haas ET, Rowland K, and Gautam M (2011). Tooth injury increases expression of the cold sensitive TRP channel TRPA1 in trigeminal neurons. *Arch Oral Biol* **56**: 1604-1609.

Haggard P, and de Boer L (2014). Oral somatosensory awareness. *Neurosci Biobehav Rev* **47**: 469-484.

Hahn CL, and Liewehr FR (2007). Relationships between caries bacteria, host responses, and clinical signs and symptoms of pulpitis. *J Endod* **33**: 213-219.

Hampl M, Cela P, Szabo-Rogers HL, Kunova Bosakova M, Dosedelova H, Krejci P, and Buchtova M (2017). Role of Primary Cilia in Odontogenesis. *J Dent Res* **96**: 965-974.

Hanks CT, Fang D, Sun Z, Edwards CA, and Butler WT (1998). Dentin-specific proteins in MDPC-23 cell line. *Eur J Oral Sci* **106 Suppl 1**: 260-266.

Hanstein R, Hanani M, Scemes E, and Spray DC (2016). Glial pannexin1 contributes to tactile hypersensitivity in a mouse model of orofacial pain. *Scientific Reports* **6**: 38266.

Hao J, Zou B, Narayanan K, and George A (2004). Differential expression patterns of the dentin matrix proteins during mineralized tissue formation. *Bone* **34**: 921-932.

Hargreaves KM (2011). CONGRESS Orofacial Pain. *Pain* **152**: S25-S32.

Harks EG, de Roos AD, Peters PH, de Haan LH, Brouwer A, Ypey DL, van Zoelen EJ, and Theuvenet AP (2001). Fenamates: a novel class of reversible gap junction blockers. *J Pharmacol Exp Ther* **298**: 1033-1041.

Hasan R, Leeson-Payne AT, Jaggar JH, and Zhang X (2017). Calmodulin is responsible for Ca(2+)-dependent regulation of TRPA1 Channels. *Sci Rep* **7**: 45098.

Hasan R, and Zhang X (2018). Ca(2+) Regulation of TRP Ion Channels. *Int J Mol Sci* **19**.

Hasselgren G, and Reit C (1989). Emergency pulpotomy: pain relieving effect with and without the use of sedative dressings. *J Endod* **15**: 254-256.

Hechler B, Vigne P, Leon C, Breittmayer JP, Gachet C, and Frelin C (1998). ATP derivatives are antagonists of the P2Y1 receptor: similarities to the platelet ADP receptor. *Mol Pharmacol* **53**: 727-733.

Henry MA, and Hargreaves KM (2007). Peripheral mechanisms of odontogenic pain. *Dent Clin North Am* **51**: 19-44, v.

Henry MA, Luo S, and Levinson SR (2012). Unmyelinated nerve fibers in the human dental pulp express markers for myelinated fibers and show sodium channel accumulations. *BMC Neurosci* **13**: 29.

Hermanstyne TO, Markowitz K, Fan L, and Gold MS (2008). Mechanotransducers in Rat Pulpal Afferents. *J Dent Res* **87**: 834-838.

Hesselager M, Timmermann DB, and Ahring PK (2004). pH Dependency and desensitization kinetics of heterologously expressed combinations of acid-sensing ion channel subunits. *J Biol Chem* **279**: 11006-11015.

Heyeraas KJ, and Berggreen E (1999). Interstitial fluid pressure in normal and inflamed pulp. *Crit Rev Oral Biol Med* **10**: 328-336.

Heyeraas KJ, Kvinnsland I, Byers MR, and Jacobsen EB (1993). Nerve fibers immunoreactive to protein gene product 9.5, calcitonin gene-related peptide, substance P, and neuropeptide Y in the dental pulp, periodontal ligament, and gingiva in cats. *Acta Odontol Scand* **51**: 207-221.

Hide I, Tanaka M, Inoue A, Nakajima K, Kohsaka S, Inoue K, and Nakata Y (2000). Extracellular ATP triggers tumor necrosis factor-alpha release from rat microglia. *J Neurochem* **75**: 965-972.

Hildebrand C, Fried K, Tuisku F, and Johansson CS (1995). Teeth and tooth nerves. *Prog Neurobiol* **45**: 165-222.

Hinman A, Chuang HH, Bautista DM, and Julius D (2006). TRP channel activation by reversible covalent modification. *Proc Natl Acad Sci U S A* **103**: 19564-19568.

Hirose Y, Yamaguchi M, Kawabata S, Murakami M, Nakashima M, Gotoh M, and Yamamoto T (2016). Effects of Extracellular pH on Dental Pulp Cells In Vitro. *J Endod* **42**: 735-741.

Hirvonen TJ, and Narhi MVO (1986). The Effect of Dentinal Stimulation on Pulp Nerve Function and Pulp Morphology in the Dog. *J Dent Res* **65**: 1290-1293.

Hisamoto M, Goto M, Muto M, Nio-Kobayashi J, Iwanaga T, and Yokoyama A (2016). Developmental changes in primary cilia in the mouse tooth germ and oral cavity. *Biomed Res* **37**: 207-214.

Hofmann T, Schäfer S, Linseisen M, Sytik L, Gudermann T, and Chubanov V (2014). Activation of TRPM7 channels by small molecules under physiological conditions. *Pflügers Archiv - European Journal of Physiology* **466**: 2177-2189.

Hojo S, Komatsu M, Okuda R, Takahashi N, and Yamada T (1994). Acid profiles and pH of carious dentin in active and arrested lesions. *J Dent Res* **73**: 1853-1857.

Honma S, Kadono K, Kawano A, and Wakisaka S (2017). Immunohistochemical localization of SNARE core proteins in intrapulpal and intradentinal nerve fibers of rat molar teeth. *Arch Oral Biol* **73**: 248-252.

Horn RS, and Haugaard N (1966). Inhibition of carbohydrate metabolism by oxygen and N-ethylmaleimide in rat heart homogenates. *J Biol Chem* **241**: 3078-3082.

Horst OV, Horst JA, Samudrala R, and Dale BA (2011). Caries induced cytokine network in the odontoblast layer of human teeth. *BMC Immunology* **12**: 9.

Hotton D, Mauro N, Lezot F, Forest N, and Berdal A (1999). Differential expression and activity of tissue-nonspecific alkaline phosphatase (TNAP) in rat odontogenic cells in vivo. *J Histochem Cytochem* **47**: 1541-1552.

Huang GT, Shagramanova K, and Chan SW (2006). Formation of odontoblast-like cells from cultured human dental pulp cells on dentin in vitro. *J Endod* **32**: 1066-1073.

Hucho T, and Levine JD (2007). Signaling pathways in sensitization: toward a nociceptor cell biology. *Neuron* **55**: 365-376.

Huff T, and Daly DT (2018). Neuroanatomy, Cranial Nerve 5, Trigeminal (CN V). In StatPearls. StatPearls Publishing LLC.: Treasure Island (FL). https://www.ncbi.nlm.nih.gov/books/NBK482283/

Ibuki T, Kido MA, Kiyoshima T, Terada Y, and Tanaka T (1996). An ultrastructural study of the relationship between sensory trigeminal nerves and odontoblasts in rat dentin/pulp as demonstrated by the anterograde transport of wheat germ agglutinin-horseradish peroxidase (WGA-HRP). *J Dent Res* **75**: 1963-1970.

Ichikawa H, Deguchi T, Nakago T, Jacobowitz DM, and Sugimoto T (1995). Parvalbumin- and calretinin-immunoreactive trigeminal neurons innervating the rat molar tooth pulp. *Brain Res* **679**: 205-211.

Ichikawa H, Kim HJ, Shuprisha A, Shikano T, Tsumura M, Shibukawa Y, and Tazaki M (2012). Voltage-dependent sodium channels and calcium-activated potassium channels in human odontoblasts in vitro. *J Endod* **38**: 1355-1362.

Ikeda E, Goto T, Gunjigake K, Kuroishi K, Ueda M, Kataoka S, Toyono T, Nakatomi M, Seta Y, Kitamura C, Nishihara T, and Kawamoto T (2016). Expression of Vesicular Nucleotide Transporter in Rat Odontoblasts. *Acta Histochem Cytochem* **49**: 21-28.

Ikeda H, and Suda H (2013). Odontoblastic syncytium through electrical coupling in the human dental pulp. *J Dent Res* **92**: 371-375.

Immke DC, and McCleskey EW (2001). Lactate enhances the acid-sensing Na+ channel on ischemia-sensing neurons. *Nature neuroscience* **4**: 869.

Iwata K, Takeda M, Oh SB, and Shinoda M (2017). Neurophysiology of Orofacial Pain. In Contemporary Oral Medicine. eds Farah C.S., Balasubramaniam R., & McCullough M.J. Springer International Publishing: Cham, pp 1-23. https://doi.org/10.1007/978-3-319-28100-1_8-1

Jacinto RC, Gomes BP, Shah HN, Ferraz CC, Zaia AA, and Souza-Filho FJ (2005). Quantification of endotoxins in necrotic root canals from symptomatic and asymptomatic teeth. *J Med Microbiol* **54**: 777-783.

Jacinto RC, Gomes BP, Shah HN, Ferraz CC, Zaia AA, and Souza-Filho FJ (2006). Incidence and antimicrobial susceptibility of Porphyromonas gingivalis isolated from mixed endodontic infections. *Int Endod J* **39**: 62-70.

Jacobsen EB, and Heyeraas KJ (1996). Effect of capsaicin treatment or inferior alveolar nerve resection on dentine formation and calcitonin gene-related peptide- and substance P-immunoreactive nerve fibres in rat molar pulp. *Arch Oral Biol* **41**: 1121-1131.

Jerman S, Ward HH, Lee R, Lopes CAM, Fry AM, MacDougall M, and Wandinger-Ness A (2014). OFD1 and Flotillins Are Integral Components of a Ciliary Signaling Protein Complex Organized by Polycystins in Renal Epithelia and Odontoblasts. *PLoS One* **9**: e106330.

Jiang HW, Zhang W, Ren BP, Zeng JF, and Ling JQ (2006). Expression of toll like receptor 4 in normal human odontoblasts and dental pulp tissue. *J Endod* **32**: 747-751.

Jiang J, and Gu J (2002). Expression of adenosine triphosphate P2X3 receptors in rat molar pulp and trigeminal ganglia. *Oral Surg Oral Med Oral Pathol Oral Radiol Endod* **94**: 622-626.

Jin Y (2015). La(3+) Alters the Response Properties of Neurons in the Mouse Primary Somatosensory Cortex to Low-Temperature Noxious Stimulation of the Dental Pulp. *Biochemistry Insights* **8**: 9-20.

Johansson CS, Hildebrand C, and Povlsen B (1992). Anatomy and developmental chronology of the rat inferior alveolar nerve. *Anat Rec* **234**: 144-152.

Johnsen D, and Johns S (1978). Quantitation of nerve fibres in the primary and permanent canine and incisor teeth in man. *Arch Oral Biol* **23**: 825-829.

Johnson G, and Brannstrom M (1974). The sensitivity of dentin. Changes in relation to conditions at exposed tubule apertures. *Acta Odontol Scand* **32**: 29-38.

Jordt SE, Bautista DM, Chuang HH, McKemy DD, Zygmunt PM, Hogestatt ED, Meng ID, and Julius D (2004). Mustard oils and cannabinoids excite sensory nerve fibres through the TRP channel ANKTM1. *Nature* **427**: 260-265.

Joury E, Bernabe E, Gallagher JE, and Marcenes W (2018). Burden of orofacial pain in a socially deprived and culturally diverse area of the United Kingdom. *Pain* **159**: 1235-1243.

Julius D, and Basbaum AI (2001). Molecular mechanisms of nociception. *Nature* **413**: 203-210.

Jyvasjarvi E, and Kniffki KD (1987). Cold stimulation of teeth: a comparison between the responses of cat intradental A delta and C fibres and human sensation. *J Physiol* **391**: 193-207.

Kadala A, Sotelo-Hitschfeld P, Ahmad Z, Tripal P, Schmid B, Mueller A, Bernal L, Winter Z, Brauchi S, Lohbauer U, Messlinger K, Lennerz JK, and Zimmermann K (2018). Fluorescent Labeling and 2-Photon Imaging of Mouse Tooth Pulp Nociceptors. *J Dent Res* **97**: 460-466.

Kadkova A, Synytsya V, Krusek J, Zimova L, and Vlachova V (2017). Molecular basis of TRPA1 regulation in nociceptive neurons. A review. *Physiol Res* **66**: 425-439.

Kakehashi S, Stanley HR, and Fitzgerald RJ (1965). The effects of surgical exposures of dental pulps in germ-free and conventional laboratory rays. *Oral Surg Oral Med Oral Pathol* **20**: 340-349.

Kassebaum NJ, Bernabe E, Dahiya M, Bhandari B, Murray CJ, and Marcenes W (2015). Global burden of untreated caries: a systematic review and metaregression. *J Dent Res* **94**: 650-658.

Kawaguchi H, Yamanaka A, Uchida K, Shibasaki K, Sokabe T, Maruyama Y, Yanagawa Y, Murakami S, and Tominaga M (2010). Activation of Polycystic Kidney Disease-2-like 1 (PKD2L1)-PKD1L3 Complex by Acid in Mouse Taste Cells. *J Biol Chem* **285**: 17277-17281.

Kawashima N, and Okiji T (2016). Odontoblasts: Specialized hard-tissue-forming cells in the dentin-pulp complex. *Congenit Anom (Kyoto)* **56**: 144-153.

Keller JF, Carrouel F, Colomb E, Durand SH, Baudouin C, Msika P, Bleicher F, Vincent C, Staquet MJ, and Farges JC (2010). Toll-like receptor 2 activation by lipoteichoic acid induces differential production of pro-inflammatory cytokines in human odontoblasts, dental pulp fibroblasts and immature dendritic cells. *Immunobiology* **215**: 53-59.

Keller L, Kuchler-Bopp S, Mendoza SA, Poliard A, and Lesot H (2011). Tooth engineering: searching for dental mesenchymal cells sources. *Front Physiol* **2**: 7.

Khabbaz MG, Anastasiadis PL, and Sykaras SN (2000). Determination of endotoxins in caries: association with pulpal pain. *Int Endod J* **33**: 132-137.

Khan AA, Diogenes A, Jeske NA, Henry MA, Akopian A, and Hargreaves KM (2008). Tumor necrosis factor alpha enhances the sensitivity of rat trigeminal neurons to capsaicin. *Neuroscience* **155**: 503-509.

Khatibi Shahidi M, Krivanek J, Kaukua N, Ernfors P, Hladik L, Kostal V, Masich S, Hampl A, Chubanov V, Gudermann T, Romanov RA, Harkany T, Adameyko I, and Fried K (2015). Three-dimensional Imaging Reveals New Compartments and Structural Adaptations in Odontoblasts. *J Dent Res* **94**: 945-954.

Kim HY, Chung G, Jo HJ, Kim YS, Bae YC, Jung SJ, Kim JS, and Oh SB (2011). Characterization of dental nociceptive neurons. *J Dent Res* **90**: 771-776.

Kim S (1990). Neurovascular interactions in the dental pulp in health and inflammation. *J Endod* **16**: 48-53.

Kim S, Barry DM, Liu XY, Yin S, Munanairi A, Meng QT, Cheng W, Mo P, Wan L, Liu SB, Ratnayake K, Zhao ZQ, Gautam N, Zheng J, Karunarathne WK, and Chen ZF (2016). Facilitation of TRPV4 by TRPV1 is required for itch transmission in some sensory neuron populations. *Sci Signal* **9**: ra71.

Kim YS, Jung HK, Kwon TK, Kim CS, Cho JH, Ahn DK, and Bae YC (2012). Expression of transient receptor potential ankyrin 1 in human dental pulp. *J Endod* **38**: 1087-1092.

Kim YS, Kim YJ, Paik SK, Cho YS, Kwon TG, Ahn DK, Kim SK, Yoshida A, and Bae YC (2009). Expression of metabotropic glutamate receptor mGluR5 in human dental pulp. *J Endod* **35**: 690-694.

Kimura M, Sase T, Higashikawa A, Sato M, Sato T, Tazaki M, and Shibukawa Y (2016). High pH-Sensitive TRPA1 Activation in Odontoblasts Regulates Mineralization. *J Dent Res* **95**: 1057-1064.

Kojima Y, Higashikawa A, Kimura M, Sato M, Mochizuki H, Ogura K, Sase T, Shinya A, Kobune K, Furuya T, Sato T, Shibukawa Y, and Tazaki M (2015). Depolarization-induced Intracellular Free Calcium Concentration Increases Show No Desensitizing Effect in Rat Odontoblasts. *Bull Tokyo Dent Coll* **56**: 131-134.

Kojima Y, Kimura M, Higashikawa A, Kono K, Ando M, Tazaki M, and Shibukawa Y (2017). Potassium Currents Activated by Depolarization in Odontoblasts. *Frontiers in Physiology* **8**: 1078.

Kokkas AB, Goulas A, Varsamidis K, Mirtsou V, and Tziafas D (2007). Irreversible but not reversible pulpitis is associated with up-regulation of tumour necrosis factor-alpha gene expression in human pulp. *Int Endod J* **40**: 198-203.

Komori T (2010). Regulation of bone development and extracellular matrix protein genes by RUNX2. *Cell Tissue Res* **339**: 189-195.

Kontakiotis EG, Tsatsoulis IN, Filippatos CG, and Agrafioti A (2015). A quantitative and diametral analysis of human dentinal tubules at pulp chamber ceiling and floor under scanning electron microscopy. *Aust Endod J* **41**: 29-34.

Kovacic U, Tesovnik B, Molnar N, Cor A, Skaleric U, and Gaspersic R (2013). Dental pulp and gingivomucosa in rats are innervated by two morphologically and neurochemically different populations of nociceptors. *Arch Oral Biol* **58**: 788-795.

Kubo K, Shibukawa Y, Shintani M, Suzuki T, Ichinohe T, and Kaneko Y (2008). Cortical representation area of human dental pulp. *J Dent Res* **87**: 358-362.

Kung LH, Gong K, Adedoyin M, Ng J, Bhargava A, Ohara PT, and Jasmin L (2013). Evidence for glutamate as a neuroglial transmitter within sensory ganglia. *PLoS One* **8**: e68312.

Kuribayashi M, Kitasako Y, Matin K, Sadr A, Shida K, and Tagami J (2012). Intraoral pH measurement of carious lesions with qPCR of cariogenic bacteria to differentiate caries activity. *J Dent* **40**: 222-228.

Kvinnsland IH, Luukko K, Fristad I, Kettunen P, Jackson DL, Fjeld K, von Bartheld CS, and Byers MR (2004). Glial cell line-derived neurotrophic factor (GDNF) from adult rat tooth serves a distinct population of large-sized trigeminal neurons. *Eur J Neurosci* **19**: 2089-2098.

Kwon M, Baek SH, Park CK, Chung G, and Oh SB (2014). Single-cell RT-PCR and immunocytochemical detection of mechanosensitive transient receptor potential channels in acutely isolated rat odontoblasts. *Arch Oral Biol* **59**: 1266-1271.

Lacerda-Pinheiro S, Marchadier A, Donãs P, Septier D, Benhamou L, Kellermann O, Goldberg M, and Poliard A (2008). An In vivo Model for Short-Term Evaluation of the Implantation Effects of Biomolecules or Stem Cells in the Dental Pulp. *The Open Dentistry Journal* **2**: 67-72.

Lakshmi S, and Joshi PG (2005). Co-activation of P2Y2 receptor and TRPV channel by ATP: implications for ATP induced pain. *Cell Mol Neurobiol* **25**: 819-832.

Larmas M (2001). Odontoblast function seen as the response of dentinal tissue to dental caries. *Adv Dent Res* **15**: 68-71.

Larmas M, and Thesleff I (1980). Biochemical study of changes in non-specific alkaline phosphomonoesterase activity during mouse tooth ontogeny. *Arch Oral Biol* **25**: 791-797.

Larsson PA, Howell DS, Pita JC, and Blanco LN (1988). Aspiration and Characterization of Predentin Fluid in Developing Rat Teeth by means of a Micropuncture and Micro-analytical Technique. *J Dent Res* **67**: 870-875.

Lawson SN (2002). Phenotype and Function of Somatic Primary Afferent Nociceptive Neurones with C-, Adelta- or Aalpha/beta-Fibres. *Exp Physiol* **87**: 239-244.

Lazarov NE (2007). Neurobiology of orofacial proprioception. *Brain Res Rev* **56**: 362-383.

Lazarowski ER, Watt WC, Stutts MJ, Boucher RC, and Harden TK (1995). Pharmacological selectivity of the cloned human P2U-purinoceptor: potent activation by diadenosine tetraphosphate. *Br J Pharmacol* **116**: 1619-1627.

Lechner SG, and Boehm S (2004). Regulation of neuronal ion channels via P2Y receptors. *Purinergic Signal* **1**: 31-41.

Lee BM, Jo H, Park G, Kim YH, Park CK, Jung SJ, Chung G, and Oh SB (2017). Extracellular ATP Induces Calcium Signaling in Odontoblasts. *J Dent Res* **96**: 200-207.

Lepinski AM, Hargreaves KM, Goodis HE, and Bowles WR (2000). Bradykinin Levels in Dental Pulp by Microdialysis. *J Endod* **26**: 744-747.

Lesot H, Osman M, and Ruch JV (1981). Immunofluorescent localization of collagens, fibronectin, and laminin during terminal differentiation of odontoblasts. *Developmental Biology* **82**: 371-381.

Lewis C, Neidhart S, Holy C, North RA, Buell G, and Surprenant A (1995). Coexpression of P2X2 and P2X3 receptor subunits can account for ATP-gated currents in sensory neurons. *Nature* **377**: 432-435.

Li C, Jing Y, Wang K, Ren Y, Liu X, Wang X, Wang Z, Zhao H, and Feng JQ (2018). Dentinal mineralization is not limited in the mineralization front but occurs along with the entire odontoblast process. *International Journal of Biological Sciences* **14**: 693-704.

Lide DR (2009) *CRC Handbook of Chemistry and Physics, 89th Edition (Internet Version)*. CRC Press/Taylor and Francis: Boca Raton, FL.

Lillesaar C, Eriksson C, and Fried K (2001). Rat tooth pulp cells elicit neurite growth from trigeminal neurones and express mRNAs for neurotrophic factors in vitro. *Neurosci Lett* **308**: 161-164.

Lillesaar C, Eriksson C, Johansson CS, Fried K, and Hildebrand C (1999). Tooth pulp tissue promotes neurite outgrowth from rat trigeminal ganglia in vitro. *J Neurocytol* **28**: 663-670.

Lillesaar C, and Fried K (2004). Neurites from trigeminal ganglion explants grown in vitro are repelled or attracted by tooth-related tissues depending on developmental stage. *Neuroscience* **125**: 149-161.

Lin M, Genin GM, Xu F, and Lu T (2014). Thermal Pain in Teeth: Electrophysiology Governed by Thermomechanics. *Applied Mechanics Reviews* **66**: 0308011-03080114.

Lin M, Liu F, Liu S, Ji C, Li A, Lu TJ, and Xu F (2017). The race to the nociceptor: mechanical versus temperature effects in thermal pain of dental neurons. *Acta Mechanica Sinica* **33**: 260-266.

Lin M, Liu QD, Kim T, Xu F, Bai BF, and Lu TJ (2010). A new method for characterization of thermal properties of human enamel and dentine: Influence of microstructure. *Infrared Physics & Technology* **53**: 457-463.

Lin M, Luo ZY, Bai BF, Xu F, and Lu TJ (2011). Fluid Mechanics in Dentinal Microtubules Provides Mechanistic Insights into the Difference between Hot and Cold Dental Pain. *PLoS One* **6**: e18068.

Linde A, and Goldberg M (1993). Dentinogenesis. *Critical Reviews in Oral Biology & Medicine* **4**: 679-728.

Lingueglia E, and Lazdunski M (2013). Pharmacology of ASIC channels. *Wiley Interdisciplinary Reviews: Membrane Transport and Signaling* **2**: 155-171.

Linsuwanont P, Versluis A, Palamara JE, and Messer HH (2008). Thermal stimulation causes tooth deformation: A possible alternative to the hydrodynamic theory? *Arch Oral Biol* **53**: 261-272.

Lisney SJ (1978). Some anatomical and electrophysiological properties of tooth-pulp afferents in the cat. *J Physiol* **284**: 19-36.

Liu X, Wang C, Fujita T, Malmstrom HS, Nedergaard M, Ren YF, and Dirksen RT (2015). External Dentin Stimulation Induces ATP Release in Human Teeth. *J Dent Res* **94**: 1259-1266.

Liu X, Yu L, Wang Q, Pelletier J, Fausther M, Sévigny J, Malmström HS, Dirksen RT, and Ren YF (2012). Expression of Ecto-ATPase NTPDase2 in Human Dental Pulp. *J Dent Res* **91**: 261-267.

Loeser JD, and Treede RD (2008). The Kyoto protocol of IASP Basic Pain Terminology. *Pain* **137**: 473-477.

Lolignier S, Gkika D, Andersson D, Leipold E, Vetter I, Viana F, Noel J, and Busserolles J (2016). New Insight in Cold Pain: Role of Ion Channels, Modulation, and Clinical Perspectives. *J Neurosci* **36**: 11435-11439.

Lopes DM, Denk F, and McMahon SB (2017). The Molecular Fingerprint of Dorsal Root and Trigeminal Ganglion Neurons. *Front Mol Neurosci* **10**: 304.

Love RM, and Jenkinson HF (2002). Invasion of dentinal tubules by oral bacteria. *Crit Rev Oral Biol Med* **13**: 171-183.

Lundbaek JA, Birn P, Tape SE, Toombes GE, Sogaard R, Koeppe RE, 2nd, Gruner SM, Hansen AJ, and Andersen OS (2005). Capsaicin regulates voltage-dependent sodium channels by altering lipid bilayer elasticity. *Mol Pharmacol* **68**: 680-689.

Lundgren T, Nannmark U, and Linde A (1992). Calcium ion activity and pH in the odontoblast-predentin region: Ion-selective microelectrode measurements. *Calcif Tissue Int* **50**: 134-136.

Luukko K, Moe K, Sijaona A, Furmanek T, Hals Kvinnsland I, Midtbø M, and Kettunen P (2008). Secondary induction and the development of tooth nerve supply. *Annals of Anatomy - Anatomischer Anzeiger* **190**: 178-187.

Lyall V, Alam RI, Phan DQ, Ereso GL, Phan TH, Malik SA, Montrose MH, Chu S, Heck GL, Feldman GM, and DeSimone JA (2001). Decrease in rat taste receptor cell intracellular pH is the proximate stimulus in sour taste transduction. *Am J Physiol Cell Physiol* **281**: C1005-1013.

Ma W, Hui H, Pelegrin P, and Surprenant A (2009). Pharmacological characterization of pannexin-1 currents expressed in mammalian cells. *J Pharmacol Exp Ther* **328**: 409-418.

Ma Z, Siebert AP, Cheung K-H, Lee RJ, Johnson B, Cohen AS, Vingtdeux V, Marambaud P, and Foskett JK (2012). Calcium homeostasis modulator 1 (CALHM1) is the pore-forming subunit of an ion channel that mediates extracellular Ca(2+) regulation of neuronal excitability. *Proc Natl Acad Sci U S A* **109**: E1963-E1971.

MacDougall M, Simmons D, Luan X, Nydegger J, Feng J, and Gu TT (1997). Dentin phosphoprotein and dentin sialoprotein are cleavage products expressed from a single transcript coded by a gene on human chromosome 4. Dentin phosphoprotein DNA sequence determination. *J Biol Chem* **272**: 835-842.

Macfarlane TV, Blinkhorn AS, Davies RM, Kincey J, and Worthington HV (2002). Oro-facial pain in the community: prevalence and associated impact. *Community Dent Oral Epidemiol* **30**: 52-60.

Macpherson LJ, Geierstanger BH, Viswanath V, Bandell M, Eid SR, Hwang S, and Patapoutian A (2005). The pungency of garlic: activation of TRPA1 and TRPV1 in response to allicin. *Curr Biol* **15**: 929-934.

Macpherson LJ, Hwang SW, Miyamoto T, Dubin AE, Patapoutian A, and Story GM (2006). More than cool: promiscuous relationships of menthol and other sensory compounds. *Mol Cell Neurosci* **32**: 335-343.

Magloire H, Couble ML, Romeas A, and Bleicher F (2004). Odontoblast primary cilia: facts and hypotheses. *Cell Biol Int* **28**: 93-99.

Magloire H, Lesage F, Couble ML, Lazdunski M, and Bleicher F (2003). Expression and localization of TREK-1 K+ channels in human odontoblasts. *J Dent Res* **82**: 542-545.

Magloire H, Maurin JC, Couble ML, Shibukawa Y, Tsumura M, Thivichon-Prince B, and Bleicher F (2010). Topical review. Dental pain and odontoblasts: facts and hypotheses. *J Orofac Pain* **24**: 335-349.

Magne D, Bluteau G, Lopez-Cazaux S, Weiss P, Pilet P, Ritchie HH, Daculsi G, and Guicheux J (2004). Development of an odontoblast in vitro model to study dentin mineralization. *Connect Tissue Res* **45**: 101-108.

Maingret F, Patel AJ, Lesage F, Lazdunski M, and Honore E (1999). Mechano- or acid stimulation, two interactive modes of activation of the TREK-1 potassium channel. *J Biol Chem* **274**: 26691-26696.

Malarkey EB, and Parpura V (2008). Mechanisms of glutamate release from astrocytes. *Neurochemistry international* **52**: 142-154.

Malhotra D, and Casey JR (2015). Intracellular pH Measurement. In eLS. John Wiley & Sons, Ltd: Chichester.

https://onlinelibrary.wiley.com/doi/abs/10.1002/9780470015902.a0002643.pub3

Manteniotis S, Lehmann R, Flegel C, Vogel F, Hofreuter A, Schreiner BS, Altmuller J, Becker C, Schobel N, Hatt H, and Gisselmann G (2013). Comprehensive RNA-Seq expression analysis of sensory ganglia with a focus on ion channels and GPCRs in Trigeminal ganglia. *PLoS One* **8**: e79523.

Marfurt CF, and Turner DF (1984). The central projections of tooth pulp afferent neurons in the rat as determined by the transganglionic transport of horseradish peroxidase. *J Comp Neurol* **223**: 535-547.

Margolis HC, and Moreno EC (1994). Composition and cariogenic potential of dental plaque fluid. *Crit Rev Oral Biol Med* **5**: 1-25.

Marion D, Jean A, Hamel H, Kerebel LM, and Kerebel B (1991). Scanning electron microscopic study of odontoblasts and circumpulpal dentin in a human tooth. *Oral Surg Oral Med Oral Pathol* **72**: 473-478.

Marshall SJ, Balooch M, Breunig T, Kinney JH, Tomsia AP, Inai N, Watanabe LG, Wu-Magidi IC, and Marshall GW (1998). Human dentin and the dentin-resin adhesive interface. *Acta Materialia* **46**: 2529-2539.

Matthews B (1977). Responses of intradental nerves to electrical and thermal stimulation of teeth in dogs. *J Physiol* **264**: 641-664.

Matthews B, Baxter J, and Watts S (1976). Sensory and reflex responses to tooth pulp stimulation in man. *Brain Res* **113**: 83-94.

Maurin JC, Couble ML, Didier-Bazes M, Brisson C, Magloire H, and Bleicher F (2004). Expression and localization of reelin in human odontoblasts. *Matrix Biol* **23**: 277-285.

Maurin JC, Couble ML, Staquet MJ, Carrouel F, About I, Avila J, Magloire H, and Bleicher F (2009). Microtubule-associated protein 1b, a neuronal marker involved in odontoblast differentiation. *J Endod* **35**: 992-996.

Maurin JC, Delorme G, Machuca-Gayet I, Couble ML, Magloire H, Jurdic P, and Bleicher F (2005). Odontoblast expression of semaphorin 7A during innervation of human dentin. *Matrix Biol* **24**: 232-238.

McGrath PA, Gracely RH, Dubner R, and Heft MW (1983). Non-pain and pain sensations evoked by tooth pulp stimulation. *Pain* **15**: 377-388.

McGrath PA, Sharav Y, Dubner R, and Gracely RH (1981). Masseter inhibitory periods and sensations evoked by electrical tooth pulp stimulation. *Pain* **10**: 1-17.

McKee MD, and Nanci A (1996). Osteopontin at mineralized tissue interfaces in bone, teeth, and osseointegrated implants: ultrastructural distribution and

implications for mineralized tissue formation, turnover, and repair. *Microsc Res Tech* **33**: 141-164.

Meier ML, de Matos NM, Brugger M, Ettlin DA, Lukic N, Cheetham M, Jancke L, and Lutz K (2014). Equal pain-Unequal fear response: enhanced susceptibility of tooth pain to fear conditioning. *Front Hum Neurosci* **8**: 526.

Melzack R (2001). Pain and the neuromatrix in the brain. *Journal of Dental Education* **65**: 1378.

Meng J, Wang J, Steinhoff M, and Dolly JO (2016). TNFalpha induces co-trafficking of TRPV1/TRPA1 in VAMP1-containing vesicles to the plasmalemma via Munc18-1/syntaxin1/SNAP-25 mediated fusion. *Sci Rep* **6**: 21226.

Mengel MK, Stiefenhofer AE, Jyvasjarvi E, and Kniffki KD (1993). Pain sensation during cold stimulation of the teeth: differential reflection of A delta and C fibre activity? *Pain* **55**: 159-169.

Meseguer V, Alpizar YA, Luis E, Tajada S, Denlinger B, Fajardo O, Manenschijn J-A, Fernández-Peña C, Talavera A, Kichko T, Navia B, Sánchez A, Señarís R, Reeh P, Pérez-García MT, López-López JR, Voets T, Belmonte C, Talavera K, and Viana F (2014). TRPA1 channels mediate acute neurogenic inflammation and pain produced by bacterial endotoxins. *Nature Communications* **5**: 3125.

Michot B, Lee CS, and Gibbs JL (2018). TRPM8 and TRPA1 do not contribute to dental pulp sensitivity to cold. *Sci Rep* **8**: 13198.

Mickle AD, Shepherd AJ, and Mohapatra DP (2016). Nociceptive TRP Channels: Sensory Detectors and Transducers in Multiple Pain Pathologies. *Pharmaceuticals* **9**: 72.

Miletich I, and Sharpe PT (2004). Neural crest contribution to mammalian tooth formation. *Birth Defects Res C Embryo Today* **72**: 200-212.

Miyazaki T, Baba TT, Mori M, Moriishi T, and Komori T (2015). Microtubule-associated protein tau (Mapt) is expressed in terminally differentiated odontoblasts and severely down-regulated in morphologically disturbed odontoblasts of Runx2 transgenic mice. *Cell Tissue Res* **361**: 457-466.

Mizumachi H, Yoshida S, Tomokiyo A, Hasegawa D, Hamano S, Yuda A, Sugii H, Serita S, Mitarai H, Koori K, Wada N, and Maeda H (2017). Calcium-sensing receptor-ERK signaling promotes odontoblastic differentiation of human dental pulp cells. *Bone* **101**: 191-201.

Mo G, Peleshok JC, Cao CQ, Ribeiro-da-Silva A, and Seguela P (2013). Control of P2X3 channel function by metabotropic P2Y2 utp receptors in primary sensory neurons. *Mol Pharmacol* **83**: 640-647.

Mochizuki T, Sokabe T, Araki I, Fujishita K, Shibasaki K, Uchida K, Naruse K, Koizumi S, Takeda M, and Tominaga M (2009). The TRPV4 cation channel

mediates stretch-evoked Ca2+ influx and ATP release in primary urothelial cell cultures. *J Biol Chem* **284**: 21257-21264.

Moehring F, Cowie AM, Menzel AD, Weyer AD, Grzybowski M, Arzua T, Geurts AM, Palygin O, and Stucky CL (2018). Keratinocytes mediate innocuous and noxious touch via ATP-P2X4 signaling. *eLife* **7**: e31684.

Moore PA, Ziegler KM, Lipman RD, Aminoshariae A, Carrasco-Labra A, and Mariotti A (2018). Benefits and harms associated with analgesic medications used in the management of acute dental pain: An overview of systematic reviews. *The Journal of the American Dental Association* **149**: 256-265.e253.

Morgan CR, Rodd HD, Clayton N, Davis JB, and Boissonade FM (2005). Vanilloid receptor 1 expression in human tooth pulp in relation to caries and pain. *J Orofac Pain* **19**: 248-260.

Moriguchi T, Yano K, Nakagawa S, and Kaji F (2003). Elucidation of adsorption mechanism of bone-staining agent alizarin red S on hydroxyapatite by FT-IR microspectroscopy. *J Colloid Interface Sci* **260**: 19-25.

Mosconi T, Snider WD, and Jacquin MF (2001). Neurotrophin receptor expression in retrogradely labeled trigeminal nociceptors--comparisons with spinal nociceptors. *Somatosens Mot Res* **18**: 312-321.

Mukohata Y, and Yoshida M (1987). Activation and inhibition of ATP synthesis in cell envelope vesicles of Halobacterium halobium. *J Biochem* **101**: 311-318.

Murakami S, Muramatsu T, and Shimono M (2001). Expression and localization of connexin 43 in rat incisor odontoblasts. *Anat Embryol (Berl)* **203**: 367-374.

Muraki K, Iwata Y, Katanosaka Y, Ito T, Ohya S, Shigekawa M, and Imaizumi Y (2003). TRPV2 is a component of osmotically sensitive cation channels in murine aortic myocytes. *Circ Res* **93**: 829-838.

Nagaoka S, Miyazaki Y, Liu HJ, Iwamoto Y, Kitano M, and Kawagoe M (1995). Bacterial invasion into dentinal tubules of human vital and nonvital teeth. *J Endod* **21**: 70-73.

Nair PN (1995). Neural elements in dental pulp and dentin. *Oral Surg Oral Med Oral Pathol Oral Radiol Endod* **80**: 710-719.

Nair PN, Luder HU, and Schroeder HE (1992). Number and size-spectra of myelinated nerve fibers of human premolars. *Anat Embryol (Berl)* **186**: 563-571.

Nair PN, and Schroeder HE (1995). Number and size spectra of non-myelinated axons of human premolars. *Anat Embryol (Berl)* **192**: 35-41.

Nakanishi T, Matsuo T, and Ebisu S (1995). Quantitative analysis of immunoglobulins and inflammatory factors in human pulpal blood from exposed pulps. *J Endod* **21**: 131-136.

Nakano Y, Le MH, Abduweli D, Ho SP, Ryazanova LV, Hu Z, Ryazanov AG, Den Besten PK, and Zhang Y (2016). A Critical Role of TRPM7 As an Ion Channel Protein in Mediating the Mineralization of the Craniofacial Hard Tissues. *Frontiers in Physiology* **7**: 258.

Narhi M, Jyvasjarvi E, Virtanen A, Huopaniemi T, Ngassapa D, and Hirvonen T (1992). Role of intradental A- and C-type nerve fibres in dental pain mechanisms. *Proc Finn Dent Soc* **88 Suppl 1**: 507-516.

Närhi M, Yamamoto H, Ngassapa D, and Hirvonen T (1994). The neurophysiological basis and the role of inflammatory reactions in dentine hypersensitivity. *Arch Oral Biol* **39**: S23-S30.

Nauli SM, Jin X, AbouAlaiwi WA, El-Jouni W, Su X, and Zhou J (2013). Non-Motile Primary Cilia as Fluid Shear Stress Mechanosensors. *Methods in enzymology* **525**: 1-20.

Neunzehn J, Potschke S, Hannig C, Wiesmann HP, and Weber MT (2017). Odontoblast-like differentiation and mineral formation of pulpsphere derived cells on human root canal dentin in vitro. *Head Face Med* **13**: 23.

Nguyen MQ, Wu Y, Bonilla LS, von Buchholtz LJ, and Ryba NJP (2017). Diversity amongst trigeminal neurons revealed by high throughput single cell sequencing. *PLoS One* **12**: e0185543.

Nielsen TA, Eriksen MA, Gazerani P, and Andersen HH (2018). Psychophysical and vasomotor evidence for interdependency of TRPA1 and TRPV1-evoked nociceptive responses in human skin: an experimental study. *Pain* **159**: 1989-2001.

Nishiyama A, Sato M, Kimura M, Katakura A, Tazaki M, and Shibukawa Y (2016). Intercellular signal communication among odontoblasts and trigeminal ganglion neurons via glutamate. *Cell Calcium* **60**: 341-355.

North RA (2002). Molecular physiology of P2X receptors. *Physiol Rev* **82**: 1013-1067.

Ogata K, Tsumuraya T, Oka K, Shin M, Okamoto F, Kajiya H, Katagiri C, Ozaki M, Matsushita M, and Okabe K (2017). The crucial role of the TRPM7 kinase domain in the early stage of amelogenesis. *Scientific Reports* **7**: 18099.

Ohkura M, Ohkura N, Yoshiba N, Yoshiba K, Ida-Yonemochi H, Ohshima H, Saito I, and Okiji T (2018). Orthodontic force application upregulated pain-associated prostaglandin-I2/PGI2-receptor/TRPV1 pathway-related gene expression in rat molars. *Odontology* **106**: 2-10.

Okumura R, Shima K, Muramatsu T, Nakagawa K, Shimono M, Suzuki T, Magloire H, and Shibukawa Y (2005). The odontoblast as a sensory receptor cell? The expression of TRPV1 (VR-1) channels. *Arch Histol Cytol* **68**: 251-257.

Olszewski J (1950). On the anatomical and functional organization of the spinal trigeminal nucleus. *J Comp Neurol* **92**: 401-413.

Orimo H (2010). The mechanism of mineralization and the role of alkaline phosphatase in health and disease. *J Nippon Med Sch* **77**: 4-12.

Oswald DJ, Lee A, Trinidad M, Chi C, Ren R, Rich CB, and Trinkaus-Randall V (2012). Communication between Corneal Epithelial Cells and Trigeminal Neurons Is Facilitated by Purinergic (P2) and Glutamatergic Receptors. *PLoS One* **7**: e44574.

Paakkonen V, Bleicher F, Carrouel F, Vuoristo JT, Salo T, Wappler I, Couble ML, Magloire H, Peters H, and Tjaderhane L (2009). General expression profiles of human native odontoblasts and pulp-derived cultured odontoblast-like cells are similar but reveal differential neuropeptide expression levels. *Arch Oral Biol* **54**: 55-62.

Pagella P, Neto E, Jiménez-Rojo L, Lamghari M, and Mitsiadis TA (2014). Microfluidics co-culture systems for studying tooth innervation. *Frontiers in Physiology* **5**: 326.

Paik SK, Lee DS, Kim JY, Bae JY, Cho YS, Ahn DK, Yoshida A, and Bae YC (2010). Quantitative ultrastructural analysis of the neurofilament 200-positive axons in the rat dental pulp. *J Endod* **36**: 1638-1642.

Paik SK, Park KP, Lee SK, Ma SK, Cho YS, Kim YK, Rhyu IJ, Ahn DK, Yoshida A, and Bae YC (2009). Light and electron microscopic analysis of the somata and parent axons innervating the rat upper molar and lower incisor pulp. *Neuroscience* **162**: 1279-1286.

Pan Y, Wheeler EF, Bernanke JM, Yang H, and Naftel JP (2003). A model experimental system for monitoring changes in sensory neuron phenotype evoked by tooth injury. *Journal of Neuroscience Methods* **126**: 99-109.

Papagerakis P, Berdal A, Mesbah M, Peuchmaur M, Malaval L, Nydegger J, Simmer J, and Macdougall M (2002). Investigation of osteocalcin, osteonectin, and dentin sialophosphoprotein in developing human teeth. *Bone* **30**: 377-385.

Paphangkorakit J, and Osborn JW (1998). Discrimination of hardness by human teeth apparently not involving periodontal receptors. *Arch Oral Biol* **43**: 1-7.

Paphangkorakit J, and Osborn JW (2000). The effect of normal occlusal forces on fluid movement through human dentine in vitro. *Arch Oral Biol* **45**: 1033-1041.

Paredes RM, Etzler JC, Watts LT, Zheng W, and Lechleiter JD (2008). Chemical calcium indicators. *Methods* **46**: 143-151.

Park CK, Bae JH, Kim HY, Jo HJ, Kim YH, Jung SJ, Kim JS, and Oh SB (2010). Substance P sensitizes P2X3 in nociceptive trigeminal neurons. *J Dent Res* **89**: 1154-1159.

Park CK, Kim MS, Fang Z, Li HY, Jung SJ, Choi SY, Lee SJ, Park K, Kim JS, and Oh SB (2006). Functional expression of thermo-transient receptor potential channels in dental primary afferent neurons: implication for tooth pain. *J Biol Chem* **281**: 17304-17311.

Park U, Vastani N, Guan Y, Raja SN, Koltzenburg M, and Caterina MJ (2011). TRP vanilloid 2 knock-out mice are susceptible to perinatal lethality but display normal thermal and mechanical nociception. *J Neurosci* **31**: 11425-11436.

Pashley DH (1996). Dynamics of the pulpo-dentin complex. *Crit Rev Oral Biol Med* **7**: 104-133.

Pellegatti P, Falzoni S, Pinton P, Rizzuto R, and Di Virgilio F (2005). A Novel Recombinant Plasma Membrane-targeted Luciferase Reveals a New Pathway for ATP Secretion. *Molecular Biology of the Cell* **16**: 3659-3665.

Peng YB, Ringkamp M, Campbell JN, and Meyer RA (1999). Electrophysiological assessment of the cutaneous arborization of Adelta-fiber nociceptors. *J Neurophysiol* **82**: 1164-1177.

Pezelj-Ribaric S, Anic I, Brekalo I, Miletic I, Hasan M, and Simunovic-Soskic M (2002). Detection of tumor necrosis factor alpha in normal and inflamed human dental pulps. *Arch Med Res* **33**: 482-484.

Pfaffl MW (2001). A new mathematical model for relative quantification in real-time RT-PCR. *Nucleic Acids Res* **29**: e45.

Praetorius HA, and Leipziger J (2009). ATP release from non-excitable cells. *Purinergic Signal* **5**: 433-446.

Priam F, Ronco V, Locker M, Bourd K, Bonnefoix M, Duchene T, Bitard J, Wurtz T, Kellermann O, Goldberg M, and Poliard A (2005). New cellular models for tracking the odontoblast phenotype. *Arch Oral Biol* **50**: 271-277.

Punnia-Moorthy A (1987). Evaluation of pH changes in inflammation of the subcutaneous air pouch lining in the rat, induced by carrageenan, dextran and Staphylococcus aureus. *J Oral Pathol* **16**: 36-44.

Qin C, Brunn JC, Cadena E, Ridall A, Tsujigiwa H, Nagatsuka H, Nagai N, and Butler WT (2002). The expression of dentin sialophosphoprotein gene in bone. *J Dent Res* **81**: 392-394.

Qin C, Brunn JC, Jones J, George A, Ramachandran A, Gorski JP, and Butler WT (2001). A comparative study of sialic acid-rich proteins in rat bone and dentin. *Eur J Oral Sci* **109**: 133-141.

Qin C, D'Souza R, and Feng JQ (2007). Dentin matrix protein 1 (DMP1): new and important roles for biomineralization and phosphate homeostasis. *J Dent Res* **86**: 1134-1141.

Qin X, Yue Z, Sun B, Yang W, Xie J, Ni E, Feng Y, Mahmood R, Zhang Y, and Yue L (2013). Sphingosine and FTY720 are potent inhibitors of the transient receptor potential melastatin 7 (TRPM7) channels. *Br J Pharmacol* **168**: 1294-1312.

Quiding H, Jonzon B, Svensson O, Webster L, Reimfelt A, Karin A, Karlsten R, and Segerdahl M (2013). TRPV1 antagonistic analgesic effect: a randomized study of AZD1386 in pain after third molar extraction. *Pain* **154**: 808-812.

Ranade SS, Syeda R, and Patapoutian A (2015). Mechanically Activated Ion Channels. *Neuron* **87**: 1162-1179.

Ranade SS, Woo SH, Dubin AE, Moshourab RA, Wetzel C, Petrus M, Mathur J, Begay V, Coste B, Mainquist J, Wilson AJ, Francisco AG, Reddy K, Qiu Z, Wood JN, Lewin GR, and Patapoutian A (2014). Piezo2 is the major transducer of mechanical forces for touch sensation in mice. *Nature* **516**: 121-125.

Rechenberg D-K, Held U, Burgstaller JM, Bosch G, and Attin T (2016). Pain levels and typical symptoms of acute endodontic infections: a prospective, observational study. *BMC Oral Health* **16**: 61.

Renton T, Yiangou Y, Baecker PA, Ford AP, and Anand P (2003). Capsaicin receptor VR1 and ATP purinoceptor P2X3 in painful and nonpainful human tooth pulp. *J Orofac Pain* **17**: 245-250.

Ricucci D, Loghin S, Lin LM, Spangberg LS, and Tay FR (2014). Is hard tissue formation in the dental pulp after the death of the primary odontoblasts a regenerative or a reparative process? *J Dent* **42**: 1156-1170.

Rimondini L, Baroni C, and Carrassi A (1995). Ultrastructure of hypersensitive and non-sensitive dentine. A study on replica models. *J Clin Periodontol* **22**: 899-902.

Robertson LT, Levy JH, Petrisor D, Lilly DJ, and Dong WK (2003). Vibration perception thresholds of human maxillary and mandibular central incisors. *Arch Oral Biol* **48**: 309-316.

Rodd HD, and Boissonade FM (2000). Substance P expression in human tooth pulp in relation to caries and pain experience. *Eur J Oral Sci* **108**: 467-474.

Rodd HD, and Boissonade FM (2001). Innervation of human tooth pulp in relation to caries and dentition type. *J Dent Res* **80**: 389-393.

Rodd HD, and Boissonade FM (2002). Comparative immunohistochemical analysis of the peptidergic innervation of human primary and permanent tooth pulp. *Arch Oral Biol* **47**: 375-385.

Rodriguez E, Sakurai K, Xu J, Chen Y, Toda K, Zhao S, Han B-X, Ryu D, Yin H, Liedtke W, and Wang F (2017). A craniofacial-specific monosynaptic circuit enables heightened affective pain. *Nature neuroscience* **20**: 1734-1743.

Romanov RA, Rogachevskaja OA, Bystrova MF, Jiang P, Margolskee RF, and Kolesnikov SS (2007). Afferent neurotransmission mediated by hemichannels in mammalian taste cells. *The EMBO Journal* **26**: 657-667.

Ruch JV, Lesot H, and Begue-Kirn C (1995). Odontoblast differentiation. *Int J Dev Biol* **39**: 51-68.

Ryazanova LV, Rondon LJ, Zierler S, Hu Z, Galli J, Yamaguchi TP, Mazur A, Fleig A, and Ryazanov AG (2010). TRPM7 is essential for Mg(2+) homeostasis in mammals. *Nat Commun* **1**: 109.

Sabio G, and Davis RJ (2014). TNF and MAP kinase signaling pathways. *Seminars in immunology* **26**: 237-245.

Sakamoto M, Rocas IN, Siqueira JF, Jr., and Benno Y (2006). Molecular analysis of bacteria in asymptomatic and symptomatic endodontic infections. *Oral Microbiol Immunol* **21**: 112-122.

Saloman JL, Chung MK, and Ro JY (2013). P2X(3) and TRPV1 functionally interact and mediate sensitization of trigeminal sensory neurons. *Neuroscience* **232**: 226-238.

Samways DS, Harkins AB, and Egan TM (2009). Native and recombinant ASIC1a receptors conduct negligible Ca2+ entry. *Cell Calcium* **45**: 319-325.

Sasano T, Shoji N, Kuriwada S, Sanjo D, Izumi H, and Karita K (1995). Absence of parasympathetic vasodilatation in cat dental pulp. *J Dent Res* **74**: 1665-1670.

Sato M, Ogura K, Kimura M, Nishi K, Ando M, Tazaki M, and Shibukawa Y (2018). Activation of Mechanosensitive Transient Receptor Potential/Piezo Channels in Odontoblasts Generates Action Potentials in Cocultured Isolectin B4–negative Medium-sized Trigeminal Ganglion Neurons. *J Endod* **44**: 984-991.e982.

Sato M, Sobhan U, Tsumura M, Kuroda H, Soya M, Masamura A, Nishiyama A, Katakura A, Ichinohe T, Tazaki M, and Shibukawa Y (2013). Hypotonic-induced stretching of plasma membrane activates transient receptor potential vanilloid channels and sodium-calcium exchangers in mouse odontoblasts. *J Endod* **39**: 779-787.

Sattari M, Mozayeni MA, Matloob A, Mozayeni M, and Javaheri HH (2010). Substance P and CGRP expression in dental pulps with irreversible pulpitis. *Aust Endod J* **36**: 59-63.

Schaible H-G, Ebersberger A, and Natura G (2011). Update on peripheral mechanisms of pain: beyond prostaglandins and cytokines. *Arthritis Research & Therapy* **13**: 210-210.

Schilke R, Lisson JA, Bauss O, and Geurtsen W (2000). Comparison of the number and diameter of dentinal tubules in human and bovine dentine by scanning electron microscopic investigation. *Arch Oral Biol* **45**: 355-361.

Schmidt K, Forkmann K, Sinke C, Gratz M, Bitz A, and Bingel U (2016). The differential effect of trigeminal vs. peripheral pain stimulation on visual processing and memory encoding is influenced by pain-related fear. *Neuroimage* **134**: 386-395.

Schmidt K, Schunke O, Forkmann K, and Bingel U (2015). Enhanced short-term sensitization of facial compared with limb heat pain. *J Pain* **16**: 781-790.

Schmitz C, Perraud AL, Johnson CO, Inabe K, Smith MK, Penner R, Kurosaki T, Fleig A, and Scharenberg AM (2003). Regulation of vertebrate cellular Mg2+ homeostasis by TRPM7. *Cell* **114**: 191-200.

Schneider BJ, Freitag-Wolf S, and Kern M (2014). Tactile sensitivity of vital and endodontically treated teeth. *J Dent* **42**: 1422-1427.

Sessle BJ (2000). Acute and chronic craniofacial pain: brainstem mechanisms of nociceptive transmission and neuroplasticity, and their clinical correlates. *Crit Rev Oral Biol Med* **11**: 57-91.

Sessle BJ, Hu JW, Amano N, and Zhong G (1986). Convergence of cutaneous, tooth pulp, visceral, neck and muscle afferents onto nociceptive and non-nociceptive neurones in trigeminal subnucleus caudalis (medullary dorsal horn) and its implications for referred pain. *Pain* **27**: 219-235.

Shabir S, Cross W, Kirkwood LA, Pearson JF, Appleby PA, Walker D, Eardley I, and Southgate J (2013). Functional expression of purinergic P2 receptors and transient receptor potential channels by the human urothelium. *Am J Physiol Renal Physiol* **305**: F396-406.

Shang S, Zhu F, Liu B, Chai Z, Wu Q, Hu M, Wang Y, Huang R, Zhang X, Wu X, Sun L, Wang Y, Wang L, Xu H, Teng S, Liu B, Zheng L, Zhang C, Zhang F, Feng X, Zhu D, Wang C, Liu T, Zhu MX, and Zhou Z (2016). Intracellular TRPA1 mediates Ca(2+) release from lysosomes in dorsal root ganglion neurons. *The Journal of Cell Biology* **215**: 369-381.

Shao M-Y, Fu Z-S, Cheng R, Yang H, Cheng L, Wang F-M, and Hu T (2011). The Presence of Open Dentinal Tubules Affects the Biological Properties of Dental Pulp Cells Ex Vivo. *Molecules and Cells* **31**: 65-71.

Shen B, Wong CO, Lau OC, Woo T, Bai S, Huang Y, and Yao X (2015). Plasma membrane mechanical stress activates TRPC5 channels. *PLoS One* **10**: e0122227.

Shephard MK, Macgregor EA, and Zakrzewska JM (2014). Orofacial pain: a guide for the headache physician. *Headache* **54**: 22-39.

Shibukawa Y, Sato M, Kimura M, Sobhan U, Shimada M, Nishiyama A, Kawaguchi A, Soya M, Kuroda H, Katakura A, Ichinohe T, and Tazaki M (2015). Odontoblasts as sensory receptors: transient receptor potential channels, pannexin-1, and ionotropic ATP receptors mediate intercellular odontoblast-neuron signal transduction. *Pflugers Arch* **467**: 843-863.

Shimizu K, Asano M, Kitagawa J, Ogiso B, Ren K, Oki H, Matsumoto M, and Iwata K (2006). Phosphorylation of Extracellular Signal-Regulated Kinase in medullary and upper cervical cord neurons following noxious tooth pulp stimulation. *Brain Res* **1072**: 99-109.

Shiozaki Y, Sato M, Kimura M, Sato T, Tazaki M, and Shibukawa Y (2017). Ionotropic P2X ATP Receptor Channels Mediate Purinergic Signaling in Mouse Odontoblasts. *Front Physiol* **8**: 3.

Shiromoto M (1984). Ultrastructural relationships between the sensory nerve terminals and the odontoblast process in the human dental pulp. *Kurume Med J* **31**: 185-195.

Silva AC, Faria MR, Fontes A, Campos MS, and Cavalcanti BN (2009). Interleukin-1 beta and interleukin-8 in healthy and inflamed dental pulps. *J Appl Oral Sci* **17**: 527-532.

Silverman W, Locovei S, and Dahl G (2008). Probenecid, a gout remedy, inhibits pannexin 1 channels. *Am J Physiol Cell Physiol* **295**: C761-767.

Simon-Soro A, Belda-Ferre P, Cabrera-Rubio R, Alcaraz LD, and Mira A (2013). A tissue-dependent hypothesis of dental caries. *Caries Res* **47**: 591-600.

Sloan AJ, Shelton RM, Hann AC, Moxham BJ, and Smith AJ (1998). An in vitro approach for the study of dentinogenesis by organ culture of the dentine-pulp complex from rat incisor teeth. *Arch Oral Biol* **43**: 421-430.

Smith AJ, Cassidy N, Perry H, Begue-Kirn C, Ruch JV, and Lesot H (1995). Reactionary dentinogenesis. *Int J Dev Biol* **39**: 273-280.

Solé-Magdalena A, Martínez-Alonso M, Coronado CA, Junquera LM, Cobo J, and Vega JA (2018). Molecular basis of dental sensitivity: The odontoblasts are multisensory cells and express multifunctional ion channels. *Annals of Anatomy - Anatomischer Anzeiger* **215**: 20-29.

Sole-Magdalena A, Revuelta EG, Menenez-Diaz I, Calavia MG, Cobo T, Garcia-Suarez O, Perez-Pinera P, De Carlos F, Cobo J, and Vega JA (2011). Human odontoblasts express transient receptor protein and acid-sensing ion channel mechanosensor proteins. *Microsc Res Tech* **74**: 457-463.

Son AR, Yang YM, Hong JH, Lee SI, Shibukawa Y, and Shin DM (2009). Odontoblast TRP channels and thermo/mechanical transmission. *J Dent Res* **88**: 1014-1019.

Song Z, Chen L, Guo J, Qin W, Wang R, Huang S, Yang X, Tian Y, and Lin Z (2017). The Role of Transient Receptor Potential Cation Channel, Subfamily C, Member 1 in the Odontoblast-like Differentiation of Human Dental Pulp Cells. *J Endod* **43**: 315-320.

Souto R, Andrade AFBd, Uzeda M, and Colombo APV (2006). Prevalence of "non-oral" pathogenic bacteria in subgingival biofilm of subjects with chronic periodontitis %J Brazilian Journal of Microbiology. **37**: 208-215.

Sreenath T, Thyagarajan T, Hall B, Longenecker G, D'Souza R, Hong S, Wright JT, MacDougall M, Sauk J, and Kulkarni AB (2003). Dentin sialophosphoprotein knockout mouse teeth display widened predentin zone and develop defective dentin mineralization similar to human dentinogenesis imperfecta type III. *J Biol Chem* **278**: 24874-24880.

Srinivas M, and Spray DC (2003). Closure of gap junction channels by arylaminobenzoates. *Mol Pharmacol* **63**: 1389-1397.

Staquet MJ, Durand SH, Colomb E, Romeas A, Vincent C, Bleicher F, Lebecque S, and Farges JC (2008). Different roles of odontoblasts and fibroblasts in immunity. *J Dent Res* **87**: 256-261.

Steele J, Pitts N, Fuller E, and Treasure E (2011) *Urgent Conditions - a report from the Adult Dental Health Survey 2009*. NHS Information Centre for Health and Social Care.

Story GM, Peier AM, Reeve AJ, Eid SR, Mosbacher J, Hricik TR, Earley TJ, Hergarden AC, Andersson DA, Hwang SW, McIntyre P, Jegla T, Bevan S, and Patapoutian A (2003). ANKTM1, a TRP-like channel expressed in nociceptive neurons, is activated by cold temperatures. *Cell* **112**: 819-829.

Strotmann R, Harteneck C, Nunnenmacher K, Schultz G, and Plant TD (2000). OTRPC4, a nonselective cation channel that confers sensitivity to extracellular osmolarity. *Nat Cell Biol* **2**: 695-702.

Su KC, Chuang SF, Ng EY, and Chang CH (2014). An investigation of dentinal fluid flow in dental pulp during food mastication: simulation of fluid-structure interaction. *Biomech Model Mechanobiol* **13**: 527-535.

Sugimoto T, Fujiyoshi Y, He Y-F, Xiao C, and Ichikawa H (1997). Trigeminal primary projection to the rat brain stem sensory trigeminal nuclear complex and surrounding structures revealed by anterograde transport of cholera toxin B subunit-conjugated and Bandeiraea simplicifolia isolectin B4-conjugated horseradish peroxidase. *Neuroscience Research* **28**: 361-371.

Sugimoto T, and Takemura M (1993). Tooth pulp primary neurons: cell size analysis, central connection, and carbonic anhydrase activity. *Brain Res Bull* **30**: 221-226.

Suzuki M, Mizuno A, Kodaira K, and Imai M (2003). Impaired pressure sensation in mice lacking TRPV4. *J Biol Chem* **278**: 22664-22668.

Takahashi N, and Nyvad B (2011). The role of bacteria in the caries process: ecological perspectives. *J Dent Res* **90**: 294-303.

Takemura M, Nagase Y, Yoshida A, Yasuda K, Kitamura S, Shigenaga Y, and Matano S (1993). The central projections of the monkey tooth pulp afferent neurons. *Somatosens Mot Res* **10**: 217-227.

Taylor PE, and Byers MR (1990). An immunocytochemical study of the morphological reaction of nerves containing calcitonin gene-related peptide to microabscess formation and healing in rat molars. *Arch Oral Biol* **35**: 629-638.

Taylor PE, Byers MR, and Redd PE (1988). Sprouting of CGRP nerve fibers in response to dentin injury in rat molars. *Brain Res* **461**: 371-376.

Tazawa K, Ikeda H, Kawashima N, and Okiji T (2017). Transient receptor potential melastatin (TRPM) 8 is expressed in freshly isolated native human odontoblasts. *Arch Oral Biol* **75**: 55-61.

Thivichon-Prince B, Couble ML, Giamarchi A, Delmas P, Franco B, Romio L, Struys T, Lambrichts I, Ressnikoff D, Magloire H, and Bleicher F (2009). Primary cilia of odontoblasts: possible role in molar morphogenesis. *J Dent Res* **88**: 910-915.

Tjaderhane L, Palosaari H, Wahlgren J, Larmas M, Sorsa T, and Salo T (2001). Human odontoblast culture method: the expression of collagen and matrix metalloproteinases (MMPs). *Adv Dent Res* **15**: 55-58.

Tokuda M, Fujisawa M, Miyashita K, Kawakami Y, Morimoto-Yamashita Y, and Torii M (2015a). Involvement of TRPV1 and AQP2 in hypertonic stress by xylitol in odontoblast cells. *Connect Tissue Res* **56**: 44-49.

Tokuda M, Tatsuyama S, Fujisawa M, Morimoto-Yamashita Y, Kawakami Y, Shibukawa Y, and Torii M (2015b). Dentin and pulp sense cold stimulus. *Med Hypotheses* **84**: 442-444.

Tominaga M, Caterina MJ, Malmberg AB, Rosen TA, Gilbert H, Skinner K, Raumann BE, Basbaum AI, and Julius D (1998). The Cloned Capsaicin Receptor Integrates Multiple Pain-Producing Stimuli. *Neuron* **21**: 531-543.

Tominaga M, Wada M, and Masu M (2001). Potentiation of capsaicin receptor activity by metabotropic ATP receptors as a possible mechanism for ATP-evoked pain and hyperalgesia. *Proc Natl Acad Sci U S A* **98**: 6951-6956.

Torres-da-Silva KR, Tessarin GWL, Dias CA, Guiati IZ, Ervolino E, Goncalves A, Beneti IM, Lovejoy DA, and Casatti CA (2017). Teneurin-2 presence in rat and human odontoblasts. *PLoS One* **12**: e0184794.

Trulsson M (2006). Sensory-motor function of human periodontal mechanoreceptors. *J Oral Rehabil* **33**: 262-273.

Tsuchiya M, Sasano Y, Kagayama M, and Watanabe M (2002). The extent of odontoblast processes in the dentin is distinct between cusp and cervical regions during development and aging. *Arch Histol Cytol* **65**: 179-188.

Tsuchiya N, Kodama D, Goto S, and Togari A (2015). Shear stress-induced Ca2+ elevation is mediated by autocrine-acting glutamate in osteoblastic MC3T3-E1 cells. *Journal of Pharmacological Sciences* **127**: 311-318.

Tsuda M, Tozaki-Saitoh H, and Inoue K (2010). Pain and purinergic signaling. *Brain Res Rev* **63**: 222-232.

Tsumura M, Sobhan U, Muramatsu T, Sato M, Ichikawa H, Sahara Y, Tazaki M, and Shibukawa Y (2012). TRPV1-mediated calcium signal couples with cannabinoid receptors and sodium-calcium exchangers in rat odontoblasts. *Cell Calcium* **52**: 124-136.

Tsumura M, Sobhan U, Sato M, Shimada M, Nishiyama A, Kawaguchi A, Soya M, Kuroda H, Tazaki M, and Shibukawa Y (2013). Functional expression of TRPM8 and TRPA1 channels in rat odontoblasts. *PLoS One* **8**: e82233.

Turner DF, Marfurt CF, and Sattelberg C (1989). Demonstration of physiological barrier between pulpal odontoblasts and its perturbation following routine restorative procedures: a horseradish peroxidase tracing study in the rat. *J Dent Res* **68**: 1262-1268.

Üçeyler N, Schäfers M, and Sommer C (2009). Mode of action of cytokines on nociceptive neurons. *Experimental Brain Research* **196**: 67-78.

Uddman R, Grunditz T, and Sundler F (1984). Neuropeptide Y: occurrence and distribution in dental pulps. *Acta Odontol Scand* **42**: 361-365.

Urban LA, and Fox AJ (2000). NK1 receptor antagonists--are they really without effect in the pain clinic? *Trends Pharmacol Sci* **21**: 462-464; author reply 465.

Ushiyama J (1989). Gap junctions between odontoblasts revealed by transjunctional flux of fluorescent tracers. *Cell Tissue Res* **258**: 611-616.

Usoskin D, Furlan A, Islam S, Abdo H, Lönnerberg P, Lou D, Hjerling-Leffler J, Haeggström J, Kharchenko O, Kharchenko PV, Linnarsson S, and Ernfors P (2014). Unbiased classification of sensory neuron types by large-scale single-cell RNA sequencing. *Nature neuroscience* **18**: 145.

Utreras E, Prochazkova M, Terse A, Gross J, Keller J, Iadarola MJ, and Kulkarni AB (2013). TGF-β1 sensitizes TRPV1 through Cdk5 signaling in odontoblast-like cells. *Molecular Pain* **9**: 24-24.

Vandewauw I, Owsianik G, and Voets T (2013). Systematic and quantitative mRNA expression analysis of TRP channel genes at the single trigeminal and dorsal root ganglion level in mouse. *BMC Neurosci* **14**: 21.

Vanegas H, and Schaible H-G (2007). NMDA Receptors in Spinal Nociceptive Processing. In Encyclopedia of Pain. eds Schmidt R.F., & Willis W.D. Springer Berlin Heidelberg: Berlin, Heidelberg, pp 1349-1352. https://doi.org/10.1007/978-3-540-29805-2_2732

Veerayutthwilai O, Byers MR, Pham TT, Darveau RP, and Dale BA (2007). Differential regulation of immune responses by odontoblasts. *Oral Microbiol Immunol* **22**: 5-13.

Vertrees RA, Goodwin T, Jordan JM, and Zwischenberger JB (2008). Tissue Culture Models. In Molecular Pathology of Lung Diseases. eds Zander D.S., Popper H.H., Jagirdar J., Haque A.K., Cagle P.T., & Barrios R. Springer New York: New York, NY, pp 150-165. https://doi.org/10.1007/978-0-387-72430-0_15

Vilceanu D, and Stucky CL (2010). TRPA1 Mediates Mechanical Currents in the Plasma Membrane of Mouse Sensory Neurons. *PLoS One* **5**: e12177.

Virtanen AS, Huopaniemi T, Narhi MV, Pertovaara A, and Wallgren K (1987). The effect of temporal parameters on subjective sensations evoked by electrical tooth stimulation. *Pain* **30**: 361-371.

Vongsavan N, and Matthews B (2007). The relationship between the discharge of intradental nerves and the rate of fluid flow through dentine in the cat. *Arch Oral Biol* **52**: 640-647.

Wang YY, Chang RB, Allgood SD, Silver WL, and Liman ER (2011). A TRPA1-dependent mechanism for the pungent sensation of weak acids. *J Gen Physiol* **137**: 493-505.

Wei X, Ling J, Wu L, Liu L, and Xiao Y (2007). Expression of Mineralization Markers in Dental Pulp Cells. *J Endod* **33**: 703-708.

Wemmie JA, Taugher RJ, and Kreple CJ (2013). Acid-sensing ion channels in pain and disease. *Nat Rev Neurosci* **14**: 461-471.

Wen W, Que K, Zang C, Wen J, Sun G, Zhao Z, and Li Y (2017). Expression and distribution of three transient receptor potential vanilloid(TRPV) channel proteins in human odontoblast-like cells. *J Mol Histol* **48**: 367-377.

West NX, Lussi A, Seong J, and Hellwig E (2013). Dentin hypersensitivity: pain mechanisms and aetiology of exposed cervical dentin. *Clinical Oral Investigations* **17**: 9-19.

Wheatley DN, Wang AM, and Strugnell GE (1996). Expression of primary cilia in mammalian cells. *Cell Biol Int* **20**: 73-81.

Wheeler EF, Naftel JP, Pan M, von Bartheld CS, and Byers MR (1998). Neurotrophin receptor expression is induced in a subpopulation of trigeminal neurons that label by retrograde transport of NGF or fluoro-gold following tooth injury. *Brain Res Mol Brain Res* **61**: 23-38.

Won J, Vang H, Kim JH, Lee PR, Kang Y, and Oh SB (2018). TRPM7 Mediates Mechanosensitivity in Adult Rat Odontoblasts. *J Dent Res* **97**: 1039-1046.

Won J, Vang H, Lee PR, Kim YH, Kim HW, Kang Y, and Oh SB (2017). Piezo2 Expression in Mechanosensitive Dental Primary Afferent Neurons. *J Dent Res* **96**: 931-937.

Woo SH, Lukacs V, de Nooij JC, Zaytseva D, Criddle CR, Francisco A, Jessell TM, Wilkinson KA, and Patapoutian A (2015). Piezo2 is the principal mechanotransduction channel for proprioception. *Nat Neurosci* **18**: 1756-1762.

Worsley MA, Clayton NM, Bountra C, and Boissonade FM (2008). The effects of ibuprofen and the neurokinin-1 receptor antagonist GR205171A on Fos expression in the ferret trigeminal nucleus following tooth pulp stimulation. *Eur J Pain* **12**: 385-394.

Xie H, Dubey N, Shim W, Ramachandra CJA, Min KS, Cao T, and Rosa V (2018). Functional Odontoblastic-Like Cells Derived from Human iPSCs. *J Dent Res* **97**: 77-83.

Yamamoto M, Kawashima N, Takashino N, Koizumi Y, Takimoto K, Suzuki N, Saito M, and Suda H (2014). Three-dimensional spheroid culture promotes odonto/osteoblastic differentiation of dental pulp cells. *Arch Oral Biol* **59**: 310-317.

Yang F, Xiao X, Cheng W, Yang W, Yu P, Song Z, Yarov-Yarovoy V, and Zheng J (2015). Structural mechanism underlying capsaicin binding and activation of the TRPV1 ion channel. *Nat Chem Biol* **11**: 518-524.

Yang H, Bernanke JM, and Naftel JP (2006). Immunocytochemical evidence that most sensory neurons of the rat molar pulp express receptors for both glial cell line-derived neurotrophic factor and nerve growth factor. *Arch Oral Biol* **51**: 69-78.

Yang R, Xiong Z, Liu C, and Liu L (2014). Inhibitory effects of capsaicin on voltage-gated potassium channels by TRPV1-independent pathway. *Cellular and molecular neurobiology* **34**: 565-576.

Yang X, Song Z, Chen L, Wang R, Huang S, Qin W, Guo J, and Lin Z (2017). Role of transient receptor potential channel 6 in the odontogenic differentiation of human dental pulp cells. *Experimental and Therapeutic Medicine* **14**: 73-78.

Yeon KY, Chung G, Shin MS, Jung SJ, Kim JS, and Oh SB (2009). Adult rat odontoblasts lack noxious thermal sensitivity. *J Dent Res* **88**: 328-332.

Yoshiba K, Yoshiba N, and Iwaku M (2003). Class II antigen-presenting dendritic cell and nerve fiber responses to cavities, caries, or caries treatment in human teeth. *J Dent Res* **82**: 422-427.

Yousuf A, Klinger F, Schicker K, and Boehm S (2011). Nucleotides control the excitability of sensory neurons via two P2Y receptors and a bifurcated signaling cascade. *Pain* **152**: 1899-1908.

Yu C, and Abbott PV (2007). An overview of the dental pulp: its functions and responses to injury. *Aust Dent J* **52**: S4-16.

Yuan H, Veldman T, Rundell K, and Schlegel R (2002). Simian Virus 40 Small Tumor Antigen Activates AKT and Telomerase and Induces Anchorage-Independent Growth of Human Epithelial Cells. *Journal of Virology* **76**: 10685.

Yuasa K, Fukumoto S, Kamasaki Y, Yamada A, Fukumoto E, Kanaoka K, Saito K, Harada H, Arikawa-Hirasawa E, Miyagoe-Suzuki Y, Takeda S, Okamoto K, Kato Y, and Fujiwara T (2004). Laminin alpha2 is essential for odontoblast differentiation regulating dentin sialoprotein expression. *J Biol Chem* **279**: 10286-10292.

Yumoto H, Hirao K, Hosokawa Y, Kuramoto H, Takegawa D, Nakanishi T, and Matsuo T (2018). The roles of odontoblasts in dental pulp innate immunity. *Japanese Dental Science Review* **54**: 105-117.

Zhang H, Cang CL, Kawasaki Y, Liang LL, Zhang YQ, Ji RR, and Zhao ZQ (2007). Neurokinin-1 receptor enhances TRPV1 activity in primary sensory neurons via PKCepsilon: a novel pathway for heat hyperalgesia. *J Neurosci* **27**: 12067-12077.

Zhang J-M, and An J (2007). Cytokines, Inflammation and Pain. *International anesthesiology clinics* **45**: 27-37.

Zhang Y-R, Du W, Zhou X-D, and Yu H-Y (2014). Review of research on the mechanical properties of the human tooth. *International Journal Of Oral Science* **6**: 61.

Zhou C, Yang G, Chen M, He L, Xiang L, Ricupero C, Mao JJ, and Ling J (2015). Lhx6 and Lhx8: cell fate regulators and beyond. *Faseb j* **29**: 4083-4091.

Zimmermann K, Lennerz JK, Hein A, Link AS, Kaczmarek JS, Delling M, Uysal S, Pfeifer JD, Riccio A, and Clapham DE (2011). Transient receptor potential cation channel, subfamily C, member 5 (TRPC5) is a cold-transducer in the peripheral nervous system. *Proc Natl Acad Sci U S A* **108**: 18114-18119.